

University of Nevada, Reno

Reflective Cracking of Flexible Pavements: Literature Review, Analysis Models, and Testing Methods

A thesis submitted in partial fulfillment of the requirements for the degree of Master Science in Civil Engineering

by

Luis Guillermo Loria-Salazar

Elie Y. Hajj, Ph.D.
Peter E. Sebaaly, Ph.D, P.E
Thesis Advisors

May, 2008

UMI Number: 1453593



UMI Microform 1453593

Copyright 2008 by ProQuest Information and Learning Company.
All rights reserved. This microform edition is protected against
unauthorized copying under Title 17, United States Code.

ProQuest Information and Learning Company
300 North Zeeb Road
P.O. Box 1346
Ann Arbor, MI 48106-1346



THE GRADUATE SCHOOL

We recommend that the thesis
prepared under our supervision by

LUIS GUILLERMO LORIA-SALAZAR

entitled

**Reflective Cracking Of Flexible Pavements: Literature Review, Analysis Models,
And Testing Methods**

be accepted in partial fulfillment of the
requirements for the degree of

MASTER OF SCIENCE

Dr. Peter E. Sebaaly, P.E., Advisor

Dr. Elie Y. Hajj, Committee Member

Dr. Gary Norris, P.E., Committee Member

Dr. George G.C. Fernandez, Graduate School Representative

Marsha H. Read, Ph. D., Associate Dean, Graduate School

May, 2008

Abstract

Hot mixed asphalt (HMA) overlay is one of the commonly used methods for rehabilitating deteriorated pavements. The Nevada Department of Transportation (NDOT) uses HMA overlays as a rehabilitation technique for the majority of the state's flexible pavements. One major type of distress influencing the life of an overlay is reflective cracking. In the past, NDOT has experimented with a number of techniques to reduce the impact of reflective cracking on HMA overlays like cold in-place recycling, reinforced fabrics, stress relief courses, mill and overlay, Portland Cement Concrete (PCC) rubblization, and PCC crack and seat.

In 2006, the Nevada DOT initiated a three-phase research project to identify the promising techniques to mitigate reflective cracking in HMA overlays: a) Phase I: Review of literature and the performance of the various techniques in Nevada, b) Phase II: Identify analysis models and laboratory tests, and c) Phase III: field verification of the selected techniques.

A literature review was conducted for the current and previous efforts outside Nevada on the reflective cracking mitigation techniques in HMA overlays. The standard specifications on the reflective cracking mitigation techniques from all fifty state DOTs were reviewed and summarized. Thirty two states out of fifty have specified a reflective cracking control system in their current standard specifications.

Based on the review of the currently available analytical models to predict the resistance of HMA overlays to reflective cracking, three design methods were identified and summarized:

- Virginia Tech Simplified Overlay Design Model
- Rubber Pavements Association Overlay Design Model
- The New AASHTO model for Reflective Cracking

An overlay design was conducted for three different HMA overlay mixes according to the three identified overlay design methods. In a summary, the Virginia Tech method showed a thinner overlay thickness for the stiffer mix whereas, the Rubber Pavements Association method, which considers both stiffness and fatigue characteristics of the mix, the overlay thickness was dependent on the interaction between the two material properties. On the other hand, a unique and thick overlay thickness was found with the new AASHTO method as it does not consider the material properties of the overlay mix as part of the design.

Additionally, a literature review was performed for the available laboratory tests to evaluate the resistance of HMA mixtures to reflective cracking. None of the reviewed laboratory test methods has undergone field validation except the Texas Transportation Institute (TTI) Overlay Tester which showed consistency between the mixtures' test results and their corresponding field performance. The TTI Overlay Tester results on the cores taken from different highway projects showed that asphalt mixtures performed very well in the field when the reflective cracking life (from the overlay tester) is larger than 300.

Finally, based on the analysis of the various findings it was recommended to:

- Further evaluate the stress relief course as a reflective cracking mitigation technique under Nevada's conditions.
- Use the TTI Upgraded Overlay Tester to evaluate mixtures in the Laboratory for reflective cracking resistance.
- Use the Rubber Pavements Association Overlay Design Model to design the require overlay thickness.

Dedication

The Author dedicates this dissertation to his parents, Luis Guillermo Loria-Meneses and Sandra Salazar-Morales, and to his beloved wife, Belkys Gonzalez Deloria.

Dedication

I would like to express my deep gratitude to Dr. Peter E. Sebaaly and Dr. Elie Hajj for their endorsement, advice and assistance during the research work. Your guidance and supervising are greatly appreciated.

Thanks to Dr. George Fernandez for all the help and cooperation in achieving the statistical analysis.

Thanks to Dr. Norris for his participation in my thesis committee.

I would like to thank my two beloved sisters, Monica and Marcela, who always have encouraged me in any moment of my life.

A special thanks and appreciation to the Nevada Department of Transportation for making resources available and for their support and help.

I would like to acknowledge and thanks my friends at the Pavement Program for all the good times we have had together, I will always have you in my heart: Haissam, Jessa, Mano, Ziad, George, Raghu, Prateep, Thileepan, Bheem Raj, Shiva, Alvaro, Wendy, Aaran, Nathan, Edward, Roy, Tusha and Andrew.

Finally, I would like to thank the good LORD, for always provide me of his mercy and bless.

TABLE OF CONTENTS

Chapter 1- INTRODUCTION	1
Chapter 2- LITERATURE REVIEW	7
2.1 Review of Current and Previous Efforts.....	7
2.1.1 Arizona Department of Transportation.....	7
2.1.2 California Department of Transportation.....	10
2.1.3 Colorado Department of Transportation.....	11
2.1.4 Georgia Department of Transportation.....	13
2.1.5 Illinois Department of Transportation	13
2.1.6 Indiana Department of Transportation.....	16
2.1.7 Louisiana Department of Transportation.....	17
2.1.8 Michigan Department of Transportation	18
2.1.9 Mississippi Department of Transportation.....	19
2.1.10 Pennsylvania Department of Transportation	20
2.1.11 Texas Department of Transportation	22
2.1.12 Virginia Department of Transportation	26
2.1.13 Wisconsin Department of Transportation.....	27
2.1.14 International Practice	30
2.2 DOTs Standard Specifications for Highway Construction.....	33
Chapter 3 – REVIEW AND ANALYSIS OF NDOT REFLECTIVE CRACKING MITIGATIONS TECHNIQUES	34
3.1 Review of Nevada DOT Experience.....	34
3.1.1 Performance Related Data	34
3.2 Performance of Selected NDOT Projects	38
3.2.1 Cold In-Place Recycling (CIR) Projects	39
3.2.2 Reinforced Fabrics (RF) Projects.....	44
3.2.3 Stress Relief Course (SRC) Projects.....	47
3.2.4 Mill and Overlay (MOL) Projects.....	50
3.2.5 Crack and Seat (CS) Projects.....	54
3.2.6 Rubblization (RPCC) Projects	57
3.3 Overall Summary of the Performance of the Selected NDOT Projects.....	60
3.4 Statistical Analysis of the Surface Cracking Data – Principal Component Analysis	63
3.4.1 Overall Ranking of the Performance of Selected NDOT Projects	65
3.4.2 Fixed Qualitative and Qualitative Factorial Analysis.....	71
3.5 Final Analysis from the NDOT Projects.....	75
3.6 Summary of the Phase I Findings	76
Chapter 4 – REVIEW OF REFLECTIVE CRACKING ANALYSIS MODELS	79
4.1 Virginia Tech Simplified Overlay Design Model.....	79
4.1.1 Fundamentals of Reflective Cracking.....	79
4.1.2 Fracture Mechanics Analysis Using Finite Element Method	82

4.1.3	Development of Design Equations	84
4.1.4	Service Life Prediction for Pavements with Potential Reflective Cracking	84
4.1.5	Design Example	86
4.2	Asphalt Rubber Association Overlay Design Model.....	86
4.2.1	Proposed Reflective Cracking Design Method.....	89
4.3	The New AASHTO model for Reflective Cracking.....	94
4.3.1	HMA Overlay of Cracked HMA Pavement Surface	95
4.3.2	HMA Overlay of Crack-free HMA Pavement Surface.....	96
4.4	Design Example Using the Various Analysis Models.....	97
4.4.1	Traffic Data.....	97
4.4.2	HMA Overlay Material Properties.....	98
4.4.3	Overlay Design Using Virginia Tech Simplified Overlay Model	99
4.4.4	Overlay Design Using Asphalt Rubber Association Method	99
4.4.5	Overlay Design Using the New AASHTO Model for Reflective Cracking.....	100
4.4.6	Summary of Design Example	101
Chapter 5	– REVIEW OF REFLECTIVE CRACKING TESTING METHODS	102
5.1	Cracow University of Technology, Cracow, Poland	102
5.2	Technion-Israel Institute of Technology, Haifa, Israel.....	104
5.3	Geo-materials Laboratory, ENTPE, France.....	106
5.4	Technical University of Vienna, Austria	108
5.5	Laboratory of Public Roads of Autum, France.....	111
5.6	University College of Dublin, Ireland	112
5.7	University of Illinois, United States.....	114
5.8	Aeronautical Technological Institute (ATI), Brazil.....	116
5.9	Florida Atlantic University, United States.....	117
5.10	Polytechnic University of Madrid, Spain.....	120
5.11	Regional Laboratory of Ponts et Chaussées, France	121
5.12	Texas Transportation Institute Overlay Tester, United States	122
5.12.1	Variability of Upgraded Overlay Testing	125
5.12.2	Sensitivity of Upgraded Overlay Testing	126
5.12.3	Validation of Upgraded Overlay Tester.....	128
5.13	Federal University of Rio Grande do Sul, Brazil.....	131
5.14	Summary of Laboratory Test Methods	133
Chapter 6	– SUMMARIES AND RECOMMENDATIONS.....	134
6.1	Summary of Phase I Findings.....	134
6.1.1	Recommendations of Phase I.....	134
6.2	Summary of Phase II Findings.....	135
6.2.1	Analysis Models.....	135
6.2.2	Laboratory Tests	138
6.2.3	Recommendations of Phase II	139
6.3	Overall Recommendations.....	139
6.5	Proposed Plan for Phase III.....	153
REFERENCES	155

TABLES	161
FIGURES	191
APPENDIX A – Summary of Various Studies to Mitigate Reflective Cracking.....	267
APPENDIX B – DOTs Standard Specifications for Highway Construction	275
APPENDIX C – PC1 Values Along with Measured Surface Cracks of NDOT Projects.....	282

LIST OF TABLES

Table 3.1 List of Selected NDOT Projects.	162
Table 3.2a Pavement Distresses Summary of Selected NDOT Projects.	163
Table 3.3a Ranking of Selected NDOT Projects Based on Principal Component Analysis.	165
Table 3.4 Statistical Analysis of the Various Treatments Based on the PCA Rankings at One-year.....	167
Before Treatment Construction and One-year After Treatment Construction for Flexible Pavements.	167
Table 3.5 Statistical Analysis of the Various Treatments Based on the PCA Rankings at One-year.....	167
Before Treatment Construction and Three-years After Treatment Construction for Flexible Pavements.	167
Table 3.6 Statistical Analysis of the Various Treatments Based on the PCA Rankings at One-year.....	168
Before Treatment Construction and Five-years After Treatment Construction for Flexible Pavements.	168
Table 3.7 Fixed Qualitative Factorial Analysis Based on the PCA Rankings at One-year After Treatment Construction.	169
Table 3.8 Fixed Qualitative Factorial Analysis Based on the PCA Rankings at Three-years After Treatment Construction.....	170
Table 3.9 Fixed Qualitative Factorial Analysis Based on the PCA Rankings at Five-years After Treatment Construction.	171
Table 3.10 Fixed Qualitative-Quantitative Factorial Analysis Based on the PCA Rankings at One-year After Treatment Construction.	172
Table 3.11 Fixed Qualitative-Quantitative Factorial Analysis Based on the PCA Rankings at Three-years After Treatment Construction.	173
Table 3.12 Fixed Qualitative-Quantitative Factorial Analysis Based on the PCA Rankings at Five-years After Treatment Construction.	174
Table 4.1 Plane Strain Fracture Toughness (K _{Ic}) for Different HMA Mixtures.....	175
Table 4.2 Statistical Coefficients for the ϵ_{VM} Model.....	175
Table 4.3 Minimum and Maximum Values for the Pavement Thicknesses and Moduli.	175
Table 4.4 Traffic Information.	175
Table 4.5 HMA Overlay Dynamic Modulus at 70°F and 10 Hz.	176
Table 4.6 HMA Overlay Thickness Using the New AASHTO Model.	176
Table 5.1 Results of the Bending Test under Repeated load.	177
Table 5.2 Results of the Shearing Test.	177
Table 5.3 Comparison of Different Mitigation Techniques.....	177
Table 5.4 Geogrid effectiveness factor (FEG).....	178
Table 5.5 Three Test Cells of MnRoad: Asphalt Mixture and Cracking Performance.	178
Table 5.6 Summary of Laboratory Testing Methods for Reflective Cracking.	179
Table 6.1 Summary of Literature Review.....	183
Table 6.2 Summary of NDOT Reflective Cracking Mitigation Techniques Review.....	184
Table 6.3 Pavement Layers Material Properties.	185
Table 6.4 Overlay Design Thicknesses for 20 years Design Period.....	185

Table 6.5 ADOT Rubber Gradation for SAMI (Type A).....	185
Table 6.6 Required Properties for the Asphalt-rubber.....	186
Table 6.7 Required Properties for the Mineral Aggregates.....	186
Table 6.8 Laboratory Asphalt Rubber Binder Design Data.....	186
Table 6.9 Requirements for CALTRANS SAMI-R's Construction.....	187
Table 6.10 Gradations for Ground Tire Rubber.....	187
Table 6.11 FDOT Standard Specifications for Asphalt-rubber.....	187
Table 6.12 MDOT Standard Specifications for Asphalt-Rubber Gradation.....	187
Table 6.13 Aggregate Quality Requirements.....	188
Table 6.14 Gradation Requirements for Fine Aggregate.....	188
Table 6.15 Master Gradation Bands and Volumetric Properties.....	188
Table 6.16 Mixture Design Properties.....	189
Table 6.17 Compacted Lift Thickness and Required Core Height.....	189
Table 6.18 Minimum Pavement Surface Temperatures.....	189
Table 6.19 UDOT Specifications for Asphalt Binder.....	189
Table 6.20 Aggregate Gradation for SAMI According to UDOT Specifications.....	190
Table 6.21 UDOT Specifications for SAMI.....	190

LIST OF FIGURES

Figure 3.1: Performance data of contract 2808a on US050 from mileposts 0 to 3.....	192
Figure 3.3: Performance data of contract 2838 on SR396 from mileposts 1.13 to 7.7.....	194
Figure 3.4: Performance data of contract 2935 on SR360 from mileposts 0 to 23.25.....	195
Figure 3.5: Performance data of contract 2819 on US095 from mileposts 6.98 to 14.38	196
Figure 3.6: Performance data of contract 2873 on US095 from mileposts 56.24 to 72.00	197
Figure 3.7: Performance data of contract 2961 on US006 from mileposts 18.87 to 43.99	198
Figure 3.8: Performance data of contract 3013 on US095A from mileposts 24.55 to 44.18	199
Figure 3.9: Performance data of contract 3025a on US093 from mileposts 0 to 11.....	200
Figure 3.10: Performance data of contract 3025b on US093 from mileposts 109.33 to 131.55.....	201
Figure 3.11: Performance data of contract 3025c on US093 from mileposts 147.45 to 172.4.....	202
Figure 3.12: Performance data of contract 2876 on SR208 from mileposts 2.33 to 8.86.....	203
Figure 3.13: Performance data of contract 2761 on SR443 from mileposts 0.00 to 0.87.....	204
Figure 3.14: Performance data of contract 2932 on US095 from mileposts 49.24 to 50.41	205
Figure 3.15: Performance data of contract 2980a on US050 from mileposts 19.4 to 21.14.....	206
Figure 3.16: Performance data of contract 2980b on US095 from mileposts 26.19 to 28.22.....	207
Figure 3.17: Performance data of contract 3006 on IR080 from mileposts 50.0 to 50.23	208
Figure 3.18: Performance data of contract 3008 on SR227 from mileposts 1.39 to 6.56.....	209
Figure 3.19: Performance data of contract 2723 on US095 from mileposts 96.89 to 117.5	210
Figure 3.20: Performance data of contract 3031 on US395 from mileposts 25.21 to 29.24	211
Figure 3.21: Performance data of contract 3048 on SR157 from mileposts 12.47 to 21.1.....	212
Figure 3.22: Performance data of contract 3045 on US050 from mileposts 36.81 to 37.38	213
Figure 3.23: Performance data of contract 3162on US395 from mileposts 17.37 to 19.4	214
Figure 3.24: Performance data of contract 2384a on US095 from mileposts 14.81 to 16.6.....	215
Figure 3.25: Performance data of contract 2384b on US095 from mileposts 0 to 2.74	216
Figure 3.26: Performance data of contract 2432 on SR157 from mileposts 3.41 to 12.18.....	217
Figure 3.27: Performance data of contract 2505 on US095 from mileposts 62.54 to 64.01	218
Figure 3.28: Performance data of contract 2651a on US095 from mileposts 12 to 15.....	219
Figure 3.29: Performance data of contract 2651b on US095 from mileposts 43 to 44.8	220
Figure 3.30: Performance data of contract 2651c on US095 from mileposts 32.88 to 39.....	221
Figure 3.31: Performance data of contract 2679 on US095 from mileposts 19.96 to 32.88	222
Figure 3.32: Performance data of contract 3028 on SR512 from mileposts 0 to 1.38.....	223
Figure 3.33: Performance data of contract 3070 on SR160 from mileposts SR 160.....	224
Figure 3.34: Performance data of contract 2886 on IR080 from mileposts 3.36 to 9.06	225
Figure 3.35: Performance data of contract 2889 on IR080 from mileposts 26.61 to 32	226
Figure 3.36: Performance data of contract 2962 on IR080 from mileposts 117.68 to 132.72.....	227
Figure 3.37: Performance data of contract 2999 on IR080 from mileposts 69.02 to 74.92	228
Figure 3.38: Performance data of contract 3021 on IR080 from mileposts 26.77 to 41.99	229
Figure 3.39: Performance data of contract 2549 on IR080 from mileposts 11.08 to 20	230
Figure 3.40: Performance data of contract 2869 on IR080 from mileposts 1.13 to 7.51	231

Figure 3.41: Performance data of contract 2901 on IR080 from mileposts 11.68 to 17.36	232
Figure 3.42: Performance data of contract 3088 on IR080 from mileposts 18.59 to 26.21	233
Figure 3.43: Performance data of contract 3186a on IR080 from mileposts 60.32 to 61.38.....	234
Figure 3.44: Performance data of contract 3186b on IR080 from mileposts 85.25 to 26.21	235
Figure 3.45: Comparison between the ranking of the various treatments at 1-year before	236
treatment construction and 1-year after treatment construction.	236
Figure 3.46: Comparison between the ranking of the various treatments at 1-year before	236
treatment construction and 3-year after treatment construction.	236
Figure 3.47: Comparison between the ranking of the various treatments at 1-year before	237
treatment construction and 5-year after treatment construction.	237
Figure 4.1 Fracture Modes.....	238
Figure 4.2 Schematic representation of reflective cracking device (RCD)	238
Figure 4.3 (a) Bottom platens of the reflective cracking device.....	238
(b) Reflective cracking device with both (top and bottom) plates.....	238
Figure 4.4 Representation of the overlay zone subjected to the reflective cracking	239
Figure 4.5 Flowchart of the Asphalt Rubber Association overlay design method	240
Figure 4.6 Existing HMA pavement structure.....	241
Figure 4.7 Required overlay thickness according to the Virginia tech method.....	241
Figure 4.8 T2C required overlay thickness according to the asphalt rubber method	242
Figure 4.9 CT required overlay thickness according to the asphalt rubber method	242
Figure 4.10 NRM required overlay thickness according to the asphalt rubber method	243
Figure 4.11 Overlay thickness according to the asphalt rubber method for selected	244
percent cracking.....	244
Figure 4.12 Required overlay thickness according to the new AASHTO method.....	244
Figure 4.13 Required overlay thickness according to the new AASHTO method for 100%	245
reflected cracks	245
Figure 4.14 Required T2C overlay thickness using various analysis models.....	245
Figure 4.15 Required CT overlay thickness using various analysis models.....	246
Figure 4.16 Required NRM overlay thickness using various analysis models.....	246
Figure 5.1 Bending test under static load – Cracow University of Technology.....	247
Figure 5.2 Results of the bending test under static load for HMA beams with and without	247
geotextile at 20°C.....	247
Figure 5.3 Shearing test – Cracow University of Technology.....	248
Figure 5.4 The laboratory wheel-tracking device.....	248
Figure 5.5 Beam specimens for the laboratory wheel-tracking device.....	249
Figure 5.6 Summary of test results under the laboratory wheel-tracking device	250
Figure 5.7 Fissurometer apparatus description	250
Figure 5.7 a. Principal of testing method (Tschegg 1986).....	251
b. Schematic load-deformation curve	251
Figure 5.8 Specimen shapes for the wedge splitting test method (Tschegg 1986).....	251
Figure 5.9 Typical results from the wedge splitting test method.....	251
Figure 5.10 Load-displacement curves for gravel and crushed HMA mixtures.....	252
Figure 5.11 a. Maximum splitting force F_{max} versus test temperature.....	252
b. Specific fracture energy G_f versus test temperature.....	252
Figure 12 Shrinkage-bending test device for reflective cracking resistance	253

Figure 5.13 Test results example for shrinkage-bending test device.....	253
Figure 5.14 Mechanism of cracking of overlay	253
Figure 5.16 Test set-up for top-down cracking tests.....	254
Figure 5.17 Testing equipment for ISAC system	254
Figure 5.18 Strain in HMA overlay as function of test cycles – control section.....	255
Figure 5.19 Strain in HMA overlay as function of test cycles – ISAC section	255
Figure 5.20 Instrumentation of fatigue test.....	256
Figure 5.21 Cracking pattern at the end of test – beam without geogrid.....	256
Figure 5.22 Cracking pattern at the end of test – beam with geogrid.....	257
Figure 5.23 Schematic representation of the test setup.....	257
Figure 5.24 Schematic representation of WRC test.....	258
Figure 5.25 Wheel Reflective Cracking (WRC) equipment.....	258
Figure 5.26 Wheel Reflective Cracking device test specimen in plates of adherence	259
Figure 5.27 Mechanism simulating the relative vertical movement in the WRC.....	259
Figure 5.28 General scheme of the MEFISTO device.....	259
Figure 5.29 Schematic of MEFISTO device and testing sample (one column)	260
Figure 5.30 Typical test results from the MEFISTO device.....	260
Figure 5.31 Concept of TTI overlay tester (after Cleveland et al.....	260
Figure 5.32 Upgraded TTI overlay tester	261
Figure 5.33 Typical TTI overlay tester result (each opening and closing is 10 sec.)	261
Figure 5.34 Upgraded overlay tester SGC sample.....	261
Figure 5.35 Repeatability of overlay testing on TxDOT type D mixture.....	262
Figure 5.36 Relationship between number of specimens and specified tolerance of reflective cracking life for TxDOT type D mixture.....	262
Figure 5.37 Influence of temperature on reflective cracking life	262
Figure 5.38 Influence of opening displacement on reflective cracking life	263
Figure 5.39 Influence of asphalt content on reflective cracking life	263
Figure 5.40 Influence of air voids on reflective cracking life.....	263
Figure 5.41 UFRGS-DAER traffic simulator from Brazil.....	264
Figure 5.42 Test pavement showing cracked areas and instrumentation location.....	264
Figure 5.43 Test pavement sections.....	264
Figure 5.44 Failed HMA layer cracking pattern.....	265
Figure 5.45 Transverse cracks painted in different colors according to their appearance.....	265
Figure 5.46 Cracking severity index evolution in both overlays	265

Chapter 1- INTRODUCTION

Pavement rehabilitation is rapidly becoming one of the most important issues facing many highway departments. Hot mixed asphalt (HMA) overlay is one of the commonly used methods for rehabilitating deteriorated pavements. The Nevada Department of Transportation (NDOT) uses HMA overlays as a rehabilitation technique for the majority of the state's flexible pavements.

One major type of distress influencing the life of an overlay is reflective cracking (1). When asphalt overlays are placed over jointed or severely cracked existing rigid and flexible pavements, cracks will reflect to the surface in a relatively short period of time. Physical tearing of the overlay occurs because of movements under heavy wheel loads at joints and cracks in the underlying pavement layer. Therefore, the long-term performance of the HMA overlays will depend on their ability to resist reflective cracking. Reflective cracking in the overlay allows water to percolate into the pavement structure and weaken the HMA and the supporting layers, hence contributing to many forms of pavement deterioration. Moisture can damage the HMA mix by promoting the stripping of the asphalt binder from the aggregate. It can also significantly reduce the strength of the base and subgrade materials, which would lead to the total failure of the flexible pavement structure.

Numerous previous efforts have been exerted to reduce or prevent reflective cracking of HMA overlays including the increase thickness of HMA overlay, the use of stress absorbing membranes inter-layers, the use of fabrics and geotextiles membranes, and the fracturing of the existing concrete slabs. The basic principle of reflective cracking is that the tensile stresses at the interface of the crack and the new HMA overlay

are significantly increased due to the discontinuity at the tip of the crack. The developed tensile stresses rapidly exceed the tensile strength of the HMA overlay and the crack forms at the interface and quickly propagates to the surface. Combating reflective cracking can be achieved by either one of the two approaches: a) reduce the magnitude of the tensile stresses at the crack-overlay interface or b) increase the tensile strength of the HMA overlay.

The increase of the thickness of the HMA overlay as well as placing a stress absorbing membrane inter-layer follow the approach of reducing the magnitude of the tensile stresses at the crack-overlay interface. The stress absorbing membrane inter-layer usually consists of a single or double chip seal. The chip seal is a highly flexible layer which reduces the magnitude of the tensile stresses before they intersect with the new HMA layer. The ability of the stress absorbing membrane inter-layer to reduce the tensile stresses increases as its thickness increase (i.e. single versus double chip seal), as its binder content increases, and as the flexibility of the binder increases. However, having a thick, rich and highly flexible stress absorbing membrane inter-layer may cause potential rutting and shoving problems under heavy traffic. An optimum design must be established in order to effectively mitigate reflective cracking without negatively impacting the long-term performance of the HMA overlay.

The fabric and geotextile technique follows the approach of increasing the tensile strength of the HMA overlay. These materials have high tensile strengths and if they are effectively bonded to the HMA layer, will improve the tensile strength of the overlay. There are numerous brands of fabrics and geotextiles currently in the market covering a wide range of cost and strength properties. Selecting the best type of fabric or geotextile

requires an in-depth assessment of their relative properties and their long-term performance.

The concept of slab fracturing before overlaying follows the approach of reducing the magnitude of the tensile stresses and resulting strains at the crack-overlay interface by reducing the movement of the cracked or broken concrete slabs beneath the overlay. Methods used to fracture slabs are generally divided into three categories: rubblization, cracking and seating, and breaking and seating. Rubblizing involves reducing the concrete slab into fragments having textural and gradation characteristics similar to a crushed aggregate material. It is usually accomplished with a resonant pavement breaker and has been used on all types of concrete pavements (i.e., jointed plain concrete (JPC), jointed reinforced concrete (JRC), and continuously reinforced concrete (CRC) pavements). Crack/seat and break/seat are fracture techniques intended to produce very short rigid slabs with effective lengths on the order of 12 to 48 inches. The process of cracking or breaking the pavement is usually accomplished with modified pile drivers, guillotines, or spring arm (whip) hammers. A significant distinction between the two techniques exists. Crack/seat is associated with the fractured slab technique conducted solely on JPC pavements. The intent of cracking is to create closely spaced pieces small enough so that vertical and horizontal movement is reduced but full aggregate interlock is maintained to permit load transfer across the crack with little loss of structural capacity. Break/seat, on the other hand, is the process by which JRC slabs are more severely fractured. A significantly higher level of energy is required to accomplish breaking of JRC slabs because of the need to destroy the bond between reinforcing steel and concrete (2).

In addition to the development in construction methods to resist reflective cracking, recent efforts also included the development of pavement design techniques to account for reflective cracking. Three methods were identified and evaluated: The newly developed AASHTO Mechanistic-empirical Pavement Design Guide (MEPDG) method (3), the Rubber Pavements Association (RPA) Overlay Design method and the Virginia Tech Simplified Overlay Design Model. The MEPDG method offers an analysis model for reflective cracking but leaves the selection of the mitigation technique to the agency. The Virginia Tech Simplified method is based on the linear elastic fracture mechanics (LEFM) method and provides a regression equation to predict the number of cycles to failure against the reflective cracking of an HMA overlay using the moduli and the thicknesses of the new and the old pavement layers. The RPA Overlay Design method provides a mathematical model based on statistical analysis and finite element analysis (FEM). All these three methods are used to determine the required overlay thickness to delay the reflective cracking in the new overlay.

Furthermore, recent efforts included the use of laboratory and field tests to evaluate the resistance of HMA mixtures and pavements to reflective cracking. Laboratory tests are typically used to evaluate the resistance of the HMA mixtures to reflective cracking during the mix design stage. Field tests are used to evaluate the performance of the rehabilitation technique used to minimize reflective cracking in HMA pavements.

The research effort documented herein was directed toward identifying an effective method to eliminate the propagation of the cracks from the old surface layer

through the new HMA overlay. As discussed earlier, the propagation of the cracks through the new HMA layer is impacted by various factors such as: treatment of the cracks in the old pavement, the installation of a crack retarding layer, properties of the new HMA mix, traffic loads, and environmental conditions. Traffic loads and environmental conditions are primarily fixed for a given project location, which leaves crack treatment, retarding layer, and the design of the new mix as the three factors that can be optimized. NDOT recognizes that the reflection of these cracks through the newly constructed HMA overlay must be effectively controlled in order to achieve good long-term performance of the overlay.

In 2006, the Nevada Department of Transportation (NDOT) initiated a three-phase research project to identify the most promising techniques to mitigate reflective cracking in HMA overlays: a) Phase I: Review of literature and the performance of the various techniques in Nevada, b) Phase II: Identify analysis models and laboratory tests, and c) Phase III: Field verification of the selected techniques. The research effort presented in this thesis includes the findings of Phase I and Phase II along with recommendations for the Phase III study.

Under Phase I, the current and previous efforts on the mitigation of reflective cracking in HMA overlays were reviewed. Additionally, the reflective cracking techniques that have been used by NDOT were identified and analyzed to assess their effectiveness in mitigating reflective cracking under Nevada's conditions.

Under Phase II of this study, the currently available analytical models to predict the resistance of HMA overlays to reflective cracking were identified and assessed based on their technical merit and their ability to predict the performance of HMA overlays.

Additionally, laboratory and field test methods used to evaluate the resistance of HMA mixtures to reflective cracking were reviewed and summarized.

Chapter 2- LITERATURE REVIEW

This first task of Phase I of the research was to review the current and previous efforts used to mitigate reflective cracking in HMA overlays. An exerted effort was made to identify all the case studies that have been completed to evaluate the effectiveness of the various techniques under actual field conditions. The relevant literature and data were collected from the various studies and analyzed to assess the effectiveness of the various techniques that are currently available in the industry. The following chapter describes the various studies conducted and are summarized in *Appendix A* in the same order listed in the text.

2.1 REVIEW OF CURRENT AND PREVIOUS EFFORTS

2.1.1 Arizona Department of Transportation

The Arizona Department of Transportation (ADOT) has been distinguished as a major leader in the use of Asphalt-Rubber (AR) overlays on Continuously Reinforced Concrete Pavement (CRCP). In 1989, Scofield (4) documented in a research report the history, development, and performance of asphalt rubber in Arizona. In that report the following conclusion was stated, “asphalt rubber has successfully been used as an encapsulating membrane to control pavement distortion due to expansive soils and to reduce reflection cracking in overlays on both rigid and flexible pavements.”

In 1990, ADOT designed and constructed a large scale Asphalt-Rubber test project in Flagstaff, Arizona on the very heavily trafficked Interstate 40 (5,6). The 1999 traffic exceeded 20,000 vehicles per day with 35% heavy trucks. The purpose of the test project was to determine whether a relatively thin overlay with AR could reduce

reflective cracking. AR is a mixture of 80% hot paving grade asphalt and 20% ground tire rubber. This mixture is also commonly referred to as the Asphalt-Rubber wet process or the McDonald process. The overlay project was built on top of a very badly cracked concrete pavement that was in need of reconstruction. The design section included edge drains, crack and seat the concrete pavement, a five inch overlay consisting of a 3-inch conventional dense HMA overlaid by a two inch gap graded asphalt-rubber mix (AR-AC) with a 6.5% binder and a one-half inch AR OGFC with a 9% binder content. It was reported that the AR overlay has performed beyond original expectations. After nine years of service the overlay was still nearly crack-free, with good ride, virtually no rutting or maintenance, and good skid resistance. The benefits of using AR on this project represent about \$18 million in construction savings and four years less construction time. The Strategic Highway Research Program SPS-6 test sections constructed in conjunction with the project further illustrate the very good performance of AR. Results of this project have led to widespread use of AR hot mixes throughout Arizona. On the basis of this work, over 2,000 miles of successfully performing AR pavements have been constructed since 1990 (7).

In 1989, Rahman, et al. (8) documented the results of the installation of three commercial paving fabrics for the reduction of reflective cracking in asphalt overlays in Arizona. The fabrics installed were Paveprep (by PavePrep Corporation), Glassgrid (by Bay Mills Ltd.) and Tapecoat (by Tapecoat Company). The following recommendations were made by the researchers:

- The need for proper tack coat selection based on the expected construction conditions and product selections when paving fabrics are used in pavement rehabilitation.
- The need for additional field testing of Paveprep on milled surfaces.
- Caution regarding the use of Glassgrid on rough surfaces.

In summary, proper installation procedures are critical for optimum performance. Installation of paving fabrics has become more sophisticated in recent years. But it is by no means a closed science in the respect that everything has been learned (9).

In 1996, a study was conducted by the University of Arizona (7,10) to determine the effectiveness of the stress absorbing membrane interlayer (SAMI). Various types of fabric were analyzed and a simple ‘Pull-off’ test was used to measure the bitumen/fabric bond strengths. Fabric structure and rate of spray of emulsion tack-coat were found to be the variables that had the most significant effect. In addition, it was found that absorption and retention of water from the tack-coat was a major factor. A series of samples consisting of fabrics sandwiched between asphalt cores were manufactured and sheared by a direct shear mechanism. Additional samples were tested in a creep shear test. The variables considered included emulsion tack-coat rate, fabric type (i.e., geotextiles, geogrids, geonets, geomembranes, clay liners, geopipes, geofoam, and geomcosites), structure (i.e., woven and non-woven), and fabric orientation. The first two were found to have considerable effect while the latter had virtually no effect.

Additionally, Woodside et al. (11) found that SAMIs can reduce the likelihood of damage and the need for large reconstruction work. The researchers found that the pavement life may be extended by 50% and that of an asphalt overlay by up to 200%.

2.1.2 California Department of Transportation

The California Department of Transportation (Caltrans) evaluated the increase of HMA thickness overlays to minimize reflective cracking. Research conducted by Predoehl (1989) in California showed that 4.8 inches of overlay is required to reduce reflective cracking for 10 years (12).

In 1992, Caltrans decided to evaluate the effectiveness of glassgrid in retarding reflective cracking caused by thermal fatigue (13). From Caltrans' past experience, pavement reinforcing fabrics (PRF) have been minimally effective in areas of high thermal stresses and moisture-related expansion and contraction. Caltrans applied the glassgrid on a section of Highway 89 located in northeastern California through the Sierra Nevada Mountains. The existing pavement consisted of 7 inches of asphalt concrete (AC) over a granular base of volcanic origin. The pavement carries a high volume of logging trucks (average annual daily truck traffic of 512) due to the timber harvesting in the area. The existing asphalt pavement was experiencing bleeding, rutting, alligator and transverse cracks. The maintenance strategy for this area consisted of a 1.5 inch AC overlay on top of the glassgrid mesh to be compared to a control section of a 1.5 inch AC overlay where no glassgrid was applied. Cracks wider than 1/4 inch were filled with an asphalt mix prior to the placement of the glassgrid mesh.

The test site was visited in 1994 and 1995. In 1994, one partial transverse crack was observed on the outer edge of the pavement over a culvert at the north end of the glassgrid section, but no other pavement distress was present. There were no changes in 1995 from the 1994 evaluation. During the 1994 evaluation of the control section, three

partial transverse cracks and approximately 15 feet of longitudinal cracks were observed. In 1995, alligator cracking with associated pumping appeared in the control section. Therefore, the glassgrid has reinforced the AC overlay and retarded reflective cracking in an area of high tensile stress. Based on the findings of this study, Caltrans now considers glassgrid application for the overlay strategy (13).

2.1.3 Colorado Department of Transportation

In 1982, FHWA reported a study on the performance of fabrics in asphalt overlays from Colorado test sections (14). The report revealed that the control section (1.5 inch AC overlay) developed 10% cracking in 1.25 years and 50% within 3.25 years, while the fabric section (1.5 inch AC overlay and fabric) developed less than 2% reflection cracking in 1.25 years and 30% within 3.25 years.

In 2004, an experiment to assess the economics of various types of reflective cracking reduction techniques was conducted on I-25 near Colorado Springs, Colorado (15). The project consisted of rehabilitating approximately four miles of I-25 by milling the surface of the old pavement and replacing it with a new HMA overlay. The responsibility for repairing the new surface course if reflection of the old cracks occurs during the warranty period entailed the contractor to built eighteen test sections within the project to evaluate the most cost effective solution to reduce reflective cracking.

Two experimental sections were constructed. Section 1 consisted of removing 1 inch of the old asphalt pavement surface in the passing lane and shoulders and 2.5 inches in the driving lane by cold milling and replacing with 4 inches of new HMA in the passing lane and shoulders and 5.5 inches in the driving lane. Section 2 was equivalent to

Section 1 except the entire pavement width was milled 1 inch and replaced with 4 inches of new HMA.

Eight different treatments and a control section were installed in each of Sections 1 and 2 to measure the effect on reflection cracking and consisted of:

- Treatment A: 90 lb Geotextile (Petromat).
- Treatment B: 120 lb Geotextile (Petromat).
- Treatment C: reinforced fabric (Petrotac).
- Treatment D: fiberglass tape (ProGuard), each 18 inches wide.
- Treatment E: crack sealer type ASTM D 3405, applied to original cracks after routing to a ½-inch width and depth.
- Treatment F: crack sealer type ASTM D 3405, applied to original cracks without routing.
- Treatment G: crack sealer polymer modified type ASTM D3405, applied to original cracks after routing to a ½-inch width and depth.
- Treatment H: crack sealer polymer modified type ASTM D3405, applied to original cracks without routing.
- Control treatment: consisted of applying the HMA according to the description of Sections 1 and 2, directly over the milled surface.

The rate of crack reflections was measured each year since construction and documented. After 5 years of pavement service the following conclusions were made (15).

- Treatments A, B, C, F, G and H had a lower percentage of reflection cracks than the control section in Test section 1.
- Treatment B, C, D, E, and H had a lower percentage of reflection cracks than the control section in test section 2.
- No treatments performed better than the control in the passing lane.
- The control sections provided the least total cost of construction and repair over the five years of analysis period.
- Treatments B, C, and H have performed better than the control with respect to reduction in reflection cracking in both test sections.

2.1.4 Georgia Department of Transportation

In 1984 and 1985, the evaluation of HMA overlays over deteriorated PCC pavements in Georgia indicated that 20% of cracking area occurred in six years for a 6-inch HMA overlay compared to two years for a 4-inch HMA overlay (16, 17). Reflective cracking appeared almost immediately after construction for a 2-inch overlay.

In 1991, the Georgia Department of Transportation (GDOT) began to evaluate the production and placement of crumb rubber HMA to reduce rutting and reflective cracking in HMA overlays (18). The crumb rubber mix (CRM) used by GDOT was produced by adding ground tire rubber to HMA using the wet process. A test section of CRM was placed on I-75 in Henry County, just south of Atlanta, consisting of a surface mix containing 6% crumb rubber by weight of asphalt cement (AC). The test section was evaluated from 1991 to 1995. The test section indicated that the CRM became very brittle over time, as indicated by a large increase in viscosity and decrease in penetration, and by a large amount of transverse reflective cracking. Compared with the control mix, the CRM did not reduce rutting and was more than twice as expensive to place (18).

2.1.5 Illinois Department of Transportation

In 1981, Mascunana summarized the application of four treatments to reduce reflective cracking on 10 state and local roads resurfacing projects in Illinois (19). Treatments included two commercially available engineering fabrics (Petromat by Phillips Fibers Corporation and Mirafi 140 by Celanese Fibers Marketing Company), a fabricated interlayer membrane (Heavy Duty Bituthene by W. R. Grace & Company), and an asphalt-rubber membrane interlayer. The findings of this study have indicated that the treatment methods were not effective in preventing the development of transverse

reflective cracking on overlays with cement treated bases. However, they controlled longitudinal reflective cracking. In addition, they were generally effective in reducing or retarding both transverse and longitudinal reflective cracking on overlays with bituminous base courses (19, 9).

In 1999, Buttlar et al. evaluated the cost-effectiveness of the Illinois Department of Transportation (IDOT) reflective crack control system consisting of a nonwoven polypropylene paving fabric (20). The study was limited to projects constructed originally as rigid pavements and subsequently rehabilitated with one or more bituminous overlays. The performance of 52 projects across Illinois was assessed through crack mapping and from distress and serviceability data in IDOT's condition rating survey database. The performance monitoring indicated an increase in life spans by 1.1 and 3.6 years for paving fabric strip (over existing cracks) and area applications (over the entire pavement), respectively. Life-cycle analysis indicated that the paving fabric reflective control system was marginally cost-effective in Illinois. Cost saving ranged from a break-even level for small projects (less than 1.6 lane-mile) to about 6.2% for large projects (6 lane-miles). Greater savings were realized where large quantities of paving fabric were used (20, 9).

In 1993, the University of Illinois completed a research project for IDOT on a prototype Interlayer Stress Absorbing Composite (ISAC). A prototype test section was placed on IL 38 near Rochelle, IL in 1993. Other ISAC test sections were placed on five asphalt concrete overlay (ACOL) projects between 1997 and 2000. Some of these ACOL sections contain other reflective cracking control methods, such as Sand Anti-Fracture (SAF) layer, strip, and area-wide reflective cracking control fabric (21).

The ISAC consists of a three-layer system. The top layer is a high strength woven geotextile to resist stresses caused by underlying pavement movements. This layer has the ability to, due to its weaving, expand like a chain link fence. This movement dissipates the stress caused by the movement of the underlying pavement. Typically, this geotextile has a tensile strength greater than 4,000 lb. /in. (700 N/mm) at 5% strain (ASTM D 4595). High strength is needed to ensure that when the geotextile is expanded to its full extent its strength is greater than the strength of the bituminous concrete overlay. The bottom layer is a low strength nonwoven geotextile (meeting AASHTO M-288-92). The middle layer is a modified rubberized asphalt layer to absorb the strain energy and bond the two geotextiles together. The system bridges across the joint or crack and dissipates stresses resulting from opening or closing movements. ISAC is bonded to the existing pavement using a tack coat and then the overlay is placed.

The researchers concluded that the formation of reflective cracks and the subsequent deterioration of these cracks were delayed at ISAC treated joints and cracks. This statement was true for all five test sites. This delay ranged from over one year to close to three years when compared to the untreated and other crack control methods. Of special note, the ISAC areas consistently outperformed the System B products, PavePrep and Roadtac. When compared with SAF, the ISAC delayed reflective cracks by about two years. The two sections performed the same after the cracks were routed and sealed prior to overlay. The cost analysis indicated that the higher the total cost of the project the higher the number of cracks and joints that could be treated with ISAC. The present cost of the ISAC strips being \$10 to \$14 per foot limits the conditions under which it

would be cost effective to use. If asphalt costs are high or the cost of ISAC were to decline more projects could benefit from using ISAC (21).

2.1.6 Indiana Department of Transportation

The Indiana Department of Transportation evaluated cracking and seating before overlay and fiber reinforcement of the overlay mixture as potential methods for reducing pavement cracking on asphalt overlays over concrete pavement (22, 9). The evaluated project on I-74 in Indiana was constructed in 1984 and 1985 and divided into several experimental and control sections. As a performance comparison with the experimental sections, the control sections were overlaid by the conventional method. The study results based on the 7-year pavement performance data indicated that the cracking and seating technique was successful on this project: it delayed most of the transverse cracks for 5 years. The majority of the transverse cracks on the cracked and seated sections were thermal cracks, which were narrower and less severe than the reflective cracks on the control section. It was also found that the type of hammers used for cracking the concrete slabs had strong effects on pavement performance. The use of fibers in the overlay mixture further reduced transverse cracks on cracked and seated sections but did not improve the cracking resistance of the control sections. Fibers improved rutting resistance on both control and cracked and seated sections. However, the sections with fibers exhibited rapid decreases in pavement strength and rideability. Thicker overlays increased the construction costs significantly but did not reduce the transverse crack intensities. According to the pavement performance and the cost analyses, it was recommended that the thickness of asphalt overlay be determined only by the pavement strength requirement and not be increased as a means of cracking control (22, 9).

2.1.7 Louisiana Department of Transportation

In 1991, a project was initiated to evaluate the pavement performance of an alternative pavement design, referred to as stone interlayer or inverted pavement (23). The test section consisted of a 3.5 inch HMA layer on top of a 4 inch stone base layer on top of a 6 inch of in-place cement stabilized base. The control section consisted of a 3.5 inch HMA layer on top of 8.5 inches of cement-stabilized base layer on top of prepared subgrade (standard design). The objective of the study was to evaluate reflective cracking reduction through the asphaltic pavement as well as overall pavement performance. The project took place in Acadia Parish, Route LA-97, near Jennings, Louisiana. LA-97 is considered a low-volume rural highway, with average daily traffic of 2,000 vehicles. The pavement was monitored for 7 years after construction. During the evaluation period, annual crack survey, ride, and deflection measurements were collected. Additionally, as part of the Louisiana Transportation Research Center accelerated pavement testing research program, the same pavement designs were tested to failure using the Accelerated Loading Facility. Results of that investigation showed that the stone interlayer had significantly reduced the amount of reflective cracking. The ride characteristics and structural capacity of both sections were similar during the evaluation period. Accelerated testing results also verified the superior performance of the stone interlayer pavement system. The cost analysis showed initial construction costs for the stone interlayer system may be as high as 20% more than standard design. However, the life of the stone interlayer pavement system is increased to almost five times that of the standard soil cement pavement as tested under accelerated loading (23).

In 1994, the Louisiana Department of Transportation (LODOT) evaluated the effect of GlasGrid in retarding reflective cracking on U.S. Highway 190, a secondary arterial road located between Covington and Baton Rouge, Louisiana (24). A large number of transverse and longitudinal cracks were present in the existing full-depth asphalt and composite pavements. LODOT placed a 1.5-inch thick Type 8 binder course followed by a 1.5-inch thick Type 8 wearing course. GlasGrid 8501 was placed between the two courses, with one area left un-reinforced to serve as a control section. As a result of the monitoring undertaken after construction, the GlasGrid System showed benefits in retarding reflective cracking.

LODOT currently specifies an Asphaltic Surface Treatment (AST) as an interlayer to delay or reduce the occurrence of reflective cracking (25). AST, sometimes referred to as “chip seal”, consists of furnishing properly distributed asphalt material (a specified emulsion applied “cold” or modified asphalt material applied “hot”) followed by a uniform application of aggregate.

2.1.8 Michigan Department of Transportation

In 1989, the Michigan DOT evaluated the performance of the Petrotac Style 4591 which is a unique peel and sticks paving fabric/rubberized asphalt composite membrane (26). Petrotac acts as a moisture barrier as well as a stress absorbing membrane interlayer. It is used in pavement maintenance to treat joints and cracks before overlay placement. Petrotac, used as a stress absorbing membrane interlayer, absorbs stresses from underlying cracks or joints helping to insulate the overlay from reflective cracking. Monitored field performance on high volume roadways demonstrated that pavements with the Petrotac interlayer show considerably less recurrence of reflective cracking.

2.1.9 Mississippi Department of Transportation

In 1990, The Mississippi Department of Transportation (MDOT) conducted a study to evaluate paving fabrics and the asphalt rubber interlayer systems, and to compare them with the use of a single bituminous surface treatment for the purpose of controlling reflective cracking (27). The paving fabric included Amopave (by Amopave Fabrics Company), Fibretex (Crown Zellerbach Corp.), Mirafi (by Mirafi Inc.), and Petromat (by Phillips Fibers Corp.). The findings of this study indicated that the asphalt rubber interlayer, in combination with a thin overlay (about 1.5 inches), reduced and/or delayed reflective cracking over a period of about five years. The study recommended the use of asphalt rubber interlayer to be seriously considered with all thin overlays (9).

In 2005, Amini (9) conducted a survey of the current paving fabric applications (polypropylene, staple fiber, needlepunched, and nonwoven geotextiles) in the state of Mississippi to determine the various practices and performances of the paving fabric systems to reduce reflective cracking. Researcher found that the field performance of overlays using fabric interlayers has generally been successful, although there have been some cases where the paving fabric systems provided little or no improvements. In particular, paving fabrics may not reduce cracking significantly with thin overlays. In one case, at a 25% level of reflection cracking, the inclusion of fabric increased the performances of the 1.5 inch overlays by a factor of 3 (4.5 years versus 1.5 years). In general, fabric interlayers have been most effective when used for load related fatigue distress and have not performed well when used to delay or retard thermal cracking. The study also showed that paving fabrics have been beneficial in the reduction of water entering the pavement; however, documentation showing the derived benefits needs to be

developed through carefully planned field studies. Also, proper construction procedures are critical for optimum performance of paving fabrics. Additionally, the researcher found, in general, that the application of paving fabrics was most effective in warm climates such as southern states. The inclusion of paving fabrics should not be expected to stop the reflection of all thermal cracks. But, the waterproofing effects will help to minimize the freeze/thaw damage and to improve the overall pavement service life (9).

2.1.10 Pennsylvania Department of Transportation

In 1989, Maurer and Malashekik (28, 9) reported the results of early performance and evaluation of six treatments to control reflective cracking. All treatments were compared with each other with a control section not receiving treatment. The treatments included Reepave T-376 paving fabric (by Dupont), Amopave paving fabric (by Amoco), Trevira 1115 paving fabric (by Hoechst Fibers Industries), Mirafi paving fabric (by Mirafi), Fiber Pave reinforced asphalt membrane interlayer (by Hercules Inc.), and Bonifiber reinforced asphalt concrete (by Kapejo Inc.). Treatment comparisons were made based on the construction and maintenance costs, ease of placement, and the ability to prevent or retard reflective cracking. Performance data were evaluated for surveys conducted at 8, 26, and 44 months after construction. All treatments retarded cracks over the evaluation period, although the amount and rate of reduction varied. The Trevira paving fabric and the Bonifiber reinforced asphalt concrete had the highest crack reduction ratios after the 44-month evaluation. On the basis of all factors considered in the evaluation (i.e., cost, ease of construction, and performance relative to distress treated) the Bonifiber reinforced asphalt concrete provided superior performance relative to the other treatments. However, on the basis of the extent of cracking evident after the

44-month survey, and considering current and proposed crack sealing costs in addition to the documented construction costs, none of the treatments used on this project were found to be cost-effective or recommended for use (28, 9).

The performance of 3 paving fabric/geogrid products were also evaluated by the Pennsylvania Department of Transportation (29, 9). These products were evaluated in three test sections with two control sections at two separate locations. The paving fabric types included Petromat, Bit-U-Tex (combination of paving fabric and geogrid), and Glassgrid. This study showed that none of the three paving fabric/geogrid types were found to be effective in preventing or retarding reflective cracking.

In 2004, Morian et al. (30) evaluated the performance of cold in-place recycling (CIR) of existing HMA materials on projects in northwestern Pennsylvania that has been in-service for more than 20 years. A total of 44 pavement sections were available. A subset of these projects was evaluated to determine performance characteristics and cost-effectiveness of the treatment and the material. The treatment is used typically on rehabilitation projects of roadways with 8,000 average daily traffic (ADT) or less but has been used on projects with up to 13,000 ADT. A number of significant conclusions were provided by the researchers.

- CIR provided an effective mean of extending the life of pavement rehabilitation projects for highways with up to 13,000 ADT and 200,000 annual equivalent single axle loads. Projects have been documented to provide service life of up to 160% of the ten-year design life typically provided by conventional mill and resurface projects in the same geographical area.
- CIR provided resistance against reflective cracking between two and three times that exhibited by conventionally resurfaced control sections. This form of recycling has been shown to be very cost effective as a rehabilitation strategy. The cost of CIR is one to two-thirds the cost of conventional HMA material while providing superior performance.

- When good construction process control is implemented, cold in-place recycled material develops stiffness values comparable to those expected for conventional HMA materials. This level of stiffness was identified in several 10-year old projects and in one 15-year old project.
- CIR material appears to typically be a stress sensitive material, providing increased stiffness in response to increased load. This “flexibility” is likely an important factor in the observed good performance of these projects, and the delay in the development of reflective cracking.

2.1.11 Texas Department of Transportation

In 2002, the Texas Transportation Institute (TTI) performed a research project in cooperation with the Texas Department of Transportation (TxDOT) and FHWA to investigate and develop information that will aid in the evaluation of the relative effectiveness of commercially available geosynthetic materials in reducing the severity or delaying the appearance of thermally induced reflective cracking in HMA overlays (31). The researchers conducted an extensive review of literature on studies of geosynthetics for reducing reflective cracking in HMA overlays, along with a formal survey of engineers in each TxDOT district and an informal survey of certain other knowledgeable individuals nationwide. Additionally, mechanistic laboratory testing and analyses were conducted using the TTI Overlay Tester to examine the relative resistance of the three major categories of geosynthetics (fabrics, grids, and composites) in resisting reflection cracking in HMA mixtures. The overlay tester evaluates the laboratory resistance to thermal cracking of a 3×6×20-inch HMA beam sample. Researchers then used fracture mechanics to evaluate the laboratory results and develop a new evaluation methodology termed the “reinforcing factor”. The “reinforcing factor” which is also termed “reduction factor”, is developed to account for the differences between the laboratory measured test value and the desired performance value, in order to convert the lab result into a site-

specific allowable value. Finally, field tests were established in three locations in Texas (Amarillo, Waco, and Pharr Districts) with widely differing climates. These planned field tests will be constructed and all three will be evaluated for several years particularly regarding reflective cracking.

Based on the review of literature and observations made during the fabrication and testing of the HMA specimens the following conclusions were made (31).

- Performance of geosynthetics in addressing reflection cracking in HMA overlays has ranged from highly successful to disastrous failure. Based on literature review, the geosynthetics showed generally marginal cost effectiveness in reducing reflection cracking. Many of the publications reviewed (particularly those related to fabrics) were based on the cost of geosynthetics more than 10 years ago. In recent years, the in-place cost of geosynthetics has become more favorable to paving agencies.
- Generally, the geosynthetics tested in the laboratory consistently increased the number of cycles to failure in the TTI overlay tester.
- Quality assurance tests performed on selected laboratory test beams were compared to the TxDOT job-mix formula (JMF). Extraction revealed asphalt contents between 4.1 and 4.6 percent as compared to the optimum asphalt content of 5.0 percent. Insufficient asphalt cement produces inadequate film thickness around aggregate particles and decreases the tensile properties of the mixture. The mixture for this investigation was sampled at a production plant and stored in metal containers. Re-heating of the mixture for beam fabrication was necessary which, of course, further oxidized these thin films. These findings are considered the major causes for the relatively low number of cycles to failure recorded during this investigation. The remainder of the quality assurance tests were within acceptable ranges of the JMF.
- Control beams were fabricated with and without an asphalt tack coat (0.05 gal/yd²) between the overlay and leveling course. The comparison of the number of load cycles to failure for these specimens indicated that the thin tack coat increased the number of load cycles by 131 percent (from an average of 2.6 load cycles to 6.0). Therefore, in typical overlay construction, researchers concluded that the simple addition of a thin asphalt cement tack coat will increase the life of the overlay.
- Limited experimentation indicated that the use of emulsified asphalt as a tack coat for geosynthetics produced a plane of weak shear, which could promote slippage during overlay construction and service.

As a result of this study, researchers prepared comprehensive guidelines for using geosynthetics with HMA overlays to reduce reflection cracking and made the following recommendations (31):

- Emulsified asphalt should not normally be used as tack for geosynthetics installed to address reflection cracking in HMA overlays. Proper construction methods should be employed and care should be taken when emulsified asphalts are used as a tack coat. Sufficient time should be allotted for breaking and curing of the emulsion.
- When placing a self-adhesive grid to address reflective cracking in an HMA overlay, a tack coat should be applied on top of the grid (i.e., after grid application). The appropriate quantity of tack is that normally used without a grid. Type of tack should be hot applied asphalt cement (not emulsion) of the same grade as that determined for the HMA overlay. Placing any thin overlay without a tack coat could invite delamination from the underlying pavement.
- When ordering geosynthetics, the contractor should specify the desired roll width and length to minimize construction joints and maximize efficiency. The contractor should also consider the maximum roll weight that his application equipment can handle.
- During laboratory testing, cracking patterns occurred in an irregular fashion, due to breaking of cohesive bonds within the HMA, and crack lengths at multiple locations were often difficult to record. Video taping devices should be installed near the specimen to record cracking. This information could be used to monitor and review cracking patterns and could be stored as a permanent record for future review and/or analysis.
- Volumetric properties of the unreinforced HMA mixture should be determined.
- Research needs to be performed to determine the ability of asphalt-impregnated fabrics or composites to reduce intrusion of surface water into a pavement after reflection cracks appear and quantify the benefits, if any, toward preserving pavement structural integrity and smoothness.

In 2004, Darling et al. (32) conducted a study describing the performance of geogrids used in two dissimilar North America climatic zones: Zone I – wet, no freeze; Zone VI – Dry, hard freeze, spring thaw. The two study sites in Zone I are: US Federal Highway 190 located in Hammond, Louisiana and US Federal Highway 96 located in Lumberton, Texas. The study site in Zone VI is Highway 513:02 located in the Municipal District of Taber, Alberta, Canada. On all three projects, varying design

approaches and remedial repairs were carried out in conjunction with utilizing two different strengths reinforcing geogrids. Using visual surveys and quantitative analyses, the performances of the sites were evaluated after 2.5 and 6 years in service. The study showed that the fiberglass reinforcements, which were used on these three sites, can extend the life of the overlay by 2 to 3 times that of the same non-reinforced section of roadway. On all three sites, the fiberglass reinforced pavement has out performed the non-reinforced control sections in terms of retarding reflective cracking. Fiberglass reinforcements, such as 8501 & 8502, are extremely strong and experience low elongations at ultimate strength and are able to reduce the rate of crack reflections significantly to that of non-reinforced overlays. Ultimately, fewer cracks can lead to lower maintenance costs and extend the projected design life (32).

In 2006, Chen et al. (33) published a study on the performance of several different rehabilitation strategies used in the past 10 years in Texas. Reflective cracking of HMA overlays on jointed concrete pavements has been a persistent problem in Texas. The long-term field performances of the various treatments are summarized as follows.

- The crack retarding grid (plastic geosynthetics) did not perform well in retarding reflective cracks. Only one project realized a benefit of the crack retarding grid, where the reflective cracking was delayed by about 1 year. The small openings in the used crack retarding grid and the lack of an effective bond might have caused the separation of the layer.
- A proprietary crack-retarding asphalt material (Strata) performed well over two years of monitoring. Strata is an asphalt-rich, polymer modified binder and fine aggregate hot mix. In one experimental project, 100% of the cracks reflected through conventional overlay material in the first year. Both Petromat fabric underseal and Strata have been performing satisfactorily to retard reflective cracking. However, there is a large cost difference between these two treatments (cost of strata 10 to 20 times higher than the Petromat fabric underseal).
- Seven experimental treatments on a major section of US 59 were evaluated. The worst-performing section on the US 59 project was the break and seat method, which failed due to weak subgrade support. The weak subgrade is unable to

support the cracked concrete, which leads to a rocking action under traffic loads. It was recommended that for future projects, the break and seat method should not be applied on subgrade with a dynamic cone penetrometer penetration rate exceeding 25 mm per blow.

- The flexible base overlay with thin asphalt surfacing has performed well. The flexible base overlay involves placing high-quality crushed limestone directly over the JCP followed by an underseal and thin asphalt overlay. Flexible base overlays were able to absorb the joint movement and eliminate the reflective cracking. The flexible base should be of top quality material with very low moisture susceptibility. In Texas, this involves specifying a Texas triaxial Class 1 material with classification of “good” in the suction/dielectric test. It is also critical to provide an effective seal for the flexible base. A chip seal followed by a thin 75-mm hot mix layer is recommended.
- The Arkansas open graded large stone AC interlayer mix has performed well. The Arkansas mix is the old TxDOT Type G mix.

2.1.12 Virginia Department of Transportation

Like other state highway agencies, the Virginia Department of Transportation (VDOT) in recent years has more frequently used asphalt overlays to rehabilitate severely distressed Portland cement concrete pavements (PCCP). Unfortunately, reflective cracks that form above joints and cracks in the underlying PCCP drastically reduce the useful lives of the HMA overlays. During the past 15 years, the fractured slab approach has gained increased acceptance as a means of retarding the formation of reflective cracks.

In 2002, the Virginia Transportation Research Council conducted a research study to evaluate the concrete slab fracturing technique as a mean of arresting or retarding reflective cracking through asphalt overlays placed over severely distressed PCC pavements in Virginia (34). The study involved monitoring the performance of five pavement rehabilitation projects over a period of up to 8 years. Two of the projects were jointed plain concrete pavements, and the other three were jointed reinforced concrete pavements. The test sections were fractured with a guillotine drop hammer and then

seated with a 50-ton pneumatic tire roller. For comparative purposes, control sections, which were not fractured prior to placement of the asphalt overlay, were constructed just beyond the bounds of three of the fractured test sections.

Detailed visual condition surveys were conducted annually on all sites. For each survey, the number of occurrences of reflective cracks that formed in the fractured sections was directly compared to the number of cracks observed in the control sections to quantify the tendency of slab fracturing to retard or arrest the formation of reflective cracks. The results of this study show that fracturing and seating distressed concrete pavements appear to be an effective mean of retarding the formation of reflective cracking through asphalt overlays on jointed plain concrete pavements. In the case of reinforced concrete pavements, however, the fracturing technique was somewhat less successful in that the formation of reflective cracks appeared to be delayed for only about 3 years. Beyond that point in time, the fractured reinforced sections exhibited approximately the same amount of reflective cracking as the control section.

The researcher concluded that any observed benefit in terms of extended pavement service life or enhanced ride quality resulting from even a slight delay in reflective crack propagation would likely offset the rather nominal cost of the fracturing and seating operation itself (34).

2.1.13 Wisconsin Department of Transportation

In 1989 the Wisconsin DOT initiated a project to evaluate the performance of GlasGrid and a glass fiber mesh pavement reinforcement geotextile in prohibiting or controlling the incidence of reflective cracking (35). In the summer of 1990, test sections examining two different types of the product, a single strand grid and a double strand

grid, were constructed on STH 57 in Sheboygan County. The glassgrid were placed between the 1.5 inch bottom and top lifts of an HMA overlay over a jointed plain PCC pavement that was constructed in 1957. The GlasGrid was only installed across the transverse joints and cracks of the underlying PCC pavement.

Reflective cracks appeared in the test sections within six months of construction. By the end of the fourth year, the percentage of reflective cracking that occurred in the double strand test sections surpassed that of the control sections, which had no GlasGrid. The reflective cracks in the GlasGrid test sections were wider than the reflective cracks in the control section. Annual crack surveys were completed at the test site during the first five years and after ten years. A final field review was completed in April of 2002. The results of these surveys showed that both the single strand grid and double strand grid variations of the GlasGrid product performed unsatisfactorily and were unable to prohibit or control reflective cracking effectively. Based on the results of this study, it was recommended that WisDOT not use GlasGrid fiberglass mesh reinforcement as a method of reducing reflective cracking of an asphaltic concrete overlay or for extending the life of an asphaltic concrete overlay placed on a PCC pavement (35).

In 2004, an experimental project was conducted to evaluate the Interlayer Stress-Absorbing Composite (ISAC) (36). According to the manufacturer, the ISAC should extend the life of a HMA overlay placed over a PCC pavement by retarding reflective cracking. The scope of this project included milling 2 inches from the PCC pavement and replacing it with a 2-inch HMA overlay. The ISAC material was placed over the cleaned and sealed transverse joints prior to placement of the HMA overlay. Immediately after construction a bump was visible in the HMA overlay along the

transverse edge of the ISAC fabric. Due to the transverse bumps in the overlay, the overlay and the ISAC fabric were removed and the test section was repaved without the ISAC. The manufacturer explained that the likely cause of this problem was due to the old age of the ISAC material used. The age of the ISAC was almost three years, which caused the ISAC to wrinkle. According to the manufacturer, they usually don't sell any of the ISAC products beyond thirty days old. Due to the removal of the ISAC system, an in-situ performance evaluation was not possible and this study was canceled (36).

The WisDOT and the City of Milwaukee tried a fine-aggregate, asphalt-rich, polymer-modified asphalt mix interlayer to absorb joint movements, delay reflective cracking, and protect the existing pavement (37). Four Wisconsin projects were constructed using this technique. In the first project, constructed in 1996, the interlayer showed no impact on delaying reflection cracking within the first 3 years. Later projects, however, included specifications for performance related design tests for flexural beam fatigue and Hveem stability and were overlaid with improved mixtures to complement the flexible interlayer. The later projects showed an average 42% improvement in the time to the appearance of surface cracks compared with the control sections. Furthermore, cores taken from the projects showed that even when the overlay cracked, some of the interlayer samples did not, even under severe conditions, thus further protecting the underlying pavement structure. Other major factors contributing to the cracking delay included the type of concrete pavement, concrete patches, and climate (37).

2.1.14 International Practice

Belgium Experience

A study was conducted by the Belgian Road Research Center in Brussels, to evaluate the performance of different interface systems used on various sites in Belgium for preventing reflective cracking. Vanelstraete and Visscher described the results of the long term evaluation of two experimental roads and five individual projects of HMA overlays over PCC pavements where different interface systems were used for prevention of reflective cracking (38). The following treatments were used on the experimental roads:

- SAMI: 1.5 kg/m² elastomeric binder, 9 kg/m² 7/10 pre-coated chippings, and dense graded HMA overlay.
- Non-woven fabric: 1.2 kg/m² elastomeric binder, Non-woven fabric, and dense graded HMA overlay.
- Geogrid: 0.25 kg/m² tack coat, geogrid, 1.2 kg/m² elastomeric binder, 6 kg/m² 7/10 pre-coated chippings, and dense graded HMA overlay.
- Steel nettings: 0.15 kg/m² tack coat, steel netting, 16 kg/m² slurry seal with elastomeric binder, 0.2 kg/m² tack coat, and dense graded HMA overlay.
- No interface: 0.20 kg/m² tack coat and dense graded HMA overlay.

The findings from the experimental roads are as follows.

- The long term evaluation of an experimental road for 8 years showed that crack and seat and steel reinforcing nettings are both effective against reflective cracking. Steel reinforcing nettings treatment consists of placing 0.15 kg/m² tack coat, steel netting, 16 kg/m² slurry seal with elastomeric binder, 0.2 kg/m² tack coat, and overlaid by HMA.
- The long term evaluation of an experimental road for 5 years showed that less reflective cracks were developed on sections with interface systems (SAMI, non-woven, grid, steel reinforcing nettings) when compared to the control section where no interface system was applied.

A follow up of several individual projects with the following interface systems were constructed.

- Nailed steel reinforcement netting, 3 inches dense graded HMA, and asphalt surfacing.
- Nailed steel reinforcement netting, 3 inches dense graded HMA, and 1.5 inches porous mix.
- Steel reinforcement netting and slurry, and 1.5 inches porous mix.
- Steel reinforcement netting and slurry, and 3.5 inches dense graded HMA mix.
- Non-woven polyester, 1.5 kg/m² modified binder, 1.5 inches ultrathin HMA layer.

The field performances of the individual projects with the interface systems confirmed the earlier observations and are summarized as follows.

- The overlay thickness remains one of the predominant factors affecting reflective cracking, even with the use of an interface system.
- Crack and seat of the PCC pavement before placing the overlay system showed to be highly efficient.
- The projects with steel reinforcing nettings performed very well even after more than ten years of repair.

Canadian Experience

In 2003 Tighe et al. reported on the economic benefits of reducing and treating reflection cracking of HMA overlays (39). In fact the Canadian Strategic Highway Research Program's (C-SHRP) Long Term Pavement Performance Study (LTPP) is entirely directed to overlays. The overall goal of the C-LTPP project is to increase pavement life and serviceability through the development of cost-effective rehabilitation strategies, based on a systematic observation of in-service pavement performance. Researchers found that measuring and treating cracking accordingly can yield significant benefits. Proper and timely crack treatment (routing and sealing) can result in extending life by 2 years and cost savings in the order of \$7,000 per lane-km.

Finland Experience

Transverse thermal cracks are a difficult problem on the Finnish road network. Very often, transverse cracks reflect through the HMA overlay in 2 years after

construction. In July 2000 a field test was performed to identify the best method of repairing cracks prior overlay (40). On the main road 1, altogether 49 transverse cracks were repaired by eight different methods and the location of every crack was determined carefully. Four of the methods were based on fiber grids (Glassgrid Geogrid 8511) and the other four were more traditional methods. After the repair work a new SMA overlay was constructed. The repair methods were as follows.

- Leveling the old surface, hot milling and asphalt surfacing.
- Milling the form of a box, 1.5 m wide grid, leveling the old surface, hot milling and asphalt surfacing.
- Milling the form of a box, 0.75 m wide grid, leveling the old surface, hot milling and asphalt surfacing.
- Sawing a crack, filling the crack with hot modified bitumen, leveling the old surface, hot milling and asphalt surfacing.
- Sawing a crack, filling the crack with a band of modified bitumen, leveling the old surface, hot milling and asphalt surfacing.
- Hot milling, apply 1.5 m wide grid, and asphalt surfacing.
- Hot milling, apply 0.75 m wide grid, and asphalt surfacing.
- Hot milling and asphalt surfacing.

As a result of the test area examination in the following spring 2001, not even one of the cracks repaired with grids had occurred again. Traditional methods (crack filling and HMA overlay or mill and HMA overlay) had not been as successful; some cracks were already visible. After two winters, in spring 2002, the difference between grids and traditional methods was even more significant. Then it seemed as if there is a difference also whether the grid has been laid directly on heated remixed surface or on a "milled box". The spring 2003 showed the final order of the tested repair methods. It was found that the best promising method to prevent the reflection of transverse cracks is to lay a grid on a "milled box" (40).

2.2 DOTS STANDARD SPECIFICATIONS FOR HIGHWAY CONSTRUCTION

This section of the thesis summarizes the current standard specifications on the reflective cracking mitigation techniques. The specifications from all fifty state DOTs were reviewed and are summarized in *Appendix B*. Thirty two states out of fifty have specified a reflective cracking control system in their current standard specifications. The reflective cracking control systems varied between simple crack and joints sealing to the application of geotextile and geosynthetics, geogrids, paving and reinforcing fabrics, asphalt rubber stress absorbing membrane, and fiberized asphalt membrane.

Chapter 3 – REVIEW AND ANALYSIS OF NDOT REFLECTIVE CRACKING MITIGATIONS TECHNIQUES

This chapter describes in detail the NDOT's experience applying various techniques to delay the reflective cracking. Such techniques are cold in-place recycling, reinforced fabrics, stress relief courses, mill and overlay for flexible pavements, and crack and seat of PCCP and Rubblization of PCCP for rigid pavements. For this purpose, forty-eight projects to mitigate reflective were selected from the NDOT's Pavement Management System (PMS) inventory. The performance of the various projects is analyzed before and after the treatment applications.

3.1 REVIEW OF NEVADA DOT EXPERIENCE

In the past, NDOT has used several techniques to reduce the impact of reflective cracking on HMA overlays. This second task of Phase I identified all field projects where NDOT has implemented reflective cracking mitigation techniques. The design, construction, and traffic details of these projects were collected along with their corresponding long-term field performance. The information was analyzed to assess the effectiveness of the various techniques in mitigating reflective cracking under Nevada's conditions.

3.1.1 Performance Related Data

Pavement performance data, collected over time, provides the basis for assessing the actual performance of a pavement technology. Pavement roughness, rutting, and cracking represent the major components of NDOT's pavement conditions survey program.

NDOT's philosophy on pavement performance can be summarized as: A "good" pavement provides a comfort ride to its users, does not require extensive maintenance for the repair of distresses, it is structurally adequate for the traffic loads, and provides sufficient friction to avoid accidents.

The present serviceability index (PSI), surface cracking, and rut depth will be used to assess the long term performance of the various reflective cracking techniques that have been implemented by NDOT.

3.1.1.a Present Serviceability Index (PSI)

The PSI is based on the original AASHO Road Test Present Serviceability Rating (PSR). The PSR relate the ride conditions of the road to the opinion of the user which required a panel of observers to actually ride in an automobile over the pavement in question. Since this type of rating is not practical for large-scale pavement networks, a transition to a non-panel based system was needed.

To transition from a PSR serviceability measure (panel developed) to a PSI serviceability measure (no panel required), a panel of raters from 1958 to 1960 rated various roads in the states of Illinois, Minnesota, and Indiana for PSR. This information was then correlated to various pavement measurements (such as slope variance or profile, cracking, etc.) to develop PSI equations. Further, the raters were asked to provide an opinion as to whether a specific pavement assessed for PSR was "acceptable" or "unacceptable" as a primary highway. Thus, although PSI is based on the same 5-point rating system as PSR it goes beyond a simple assessment of ride quality. About one-half of the panel of raters found a PSR of 3.0 acceptable and a PSR of 2.5 unacceptable. Such

information was useful in selecting a "terminal" (or failure) serviceability (PSI) design input for empirical structural design equations.

The original PSI equation has been modified throughout the years by state highway agencies in order to better describe the local conditions. Currently NDOT uses the following PSI equation for flexible pavements:

$$PSI = 5e^{(-0.0041 \times IRI)} - 1.38 \times RD^2 - 0.03 \times (C+P)^{1/2} \quad (3.1)$$

If $PSI < 0$ then $PSI = 0.10$

where, IRI = international roughness index (in/mile)

RD = rut depth (in)

C = cracking ($ft^2/1000ft^2$)

P = patching ($ft^2/1000ft^2$)

The international roughness index (IRI) is the first widely used profile index where the analysis method is intended to work with different types of profilers. It is defined as a property of the true profile, and therefore it can be measured with any valid profilometer. The analysis equations were developed and tested to minimize the effects of some profilometer measurement parameters such as sampling rate.

Prior to 1992, NDOT used the slope variance to measure road roughness, then the ultrasonic profilometer was used until 2000 followed by the laser profilometer thereafter.

NDOT conduct roughness measurements on an annual basis for all the interstates, many of the US routes and some of the state routes, and on a biannual basis for all others. The profilometer measurement is continuous, but an average roughness value for every mile is recorded unless otherwise specified.

3.1.1.b Surface Cracking

For the purpose of this research, fatigue cracking, non-wheelpath longitudinal cracking, transverse cracking, and block cracking monitored over the service life of the pavement were utilized. The cracking classes, extent and severity are defined in the NDOT Flexible Pavements Distress Identification Manual (41) and are summarized here.

- ***Fatigue Cracking:*** Fatigue cracking is caused by repeated traffic loading of the pavement. These cracks initiate at the bottom of the HMA layer and slowly work their way to the surface. Fatigue cracking usually starts as a longitudinal crack in the wheelpath (Type A). Further weakening of the HMA and base layers coupled with repeated traffic loading leads to the progression of the longitudinal crack and the formation of interconnected cracks referred to as alligator cracking since they resemble the shape of an alligator skin (Type B). An unstable base, inadequate drainage, insufficient pavement thickness, degradation/stripping in the HMA combined with traffic loadings will accelerate this type of distress. The extent of type A fatigue cracking is measured as the total linear feet of this type of cracking in the wheelpath of the pavement area being surveyed. The extent of type B fatigue cracking is measured as the total area in square feet of this type of cracking in the wheelpath of the pavement being surveyed (i.e., 10 by 100 foot area at every milepost).
- ***Transverse Cracking:*** This type of cracking is primarily caused by the contraction of the HMA layer due to temperature changes. Other causes include: age hardening, reflection cracking from PCC pavement joints below, and reflection cracking from transverse cracks below. The extent is measured as the total linear feet of cracking throughout the pavement area being surveyed (i.e., 10 by 100 foot area at every milepost).
- ***Block Cracking:*** Block cracking starts as a combination of transverse and non-wheelpath longitudinal cracking (Type A). It is caused by age hardening and shrinkage of the HMA layer. Although traffic loading is not the primary cause of this type of distress, continued loading on the brittle surface will accelerate this distress and break the larger pieces into smaller pieces progressing to Type B, and finally to Type C. The extent of type A is measured as the total linear feet of this type of cracking throughout the pavement area being surveyed. The extent of type B and C is measured as the total area in square feet of this type of cracking throughout the pavement area being surveyed.

3.1.1.c Rutting

Rutting is a load-related failure of the pavement. Ruts are described as longitudinal surface depressions in the wheelpaths as a result of pavement densification or wear. Pavement uplift may occur along the sides of the ruts. Anyone, or combination of the following factors may cause rutting:

- Soft pavement due to poor quality HMA mix
- Insufficient pavement thickness
- Unstable HMA mix
- Insufficient compaction during construction
- Stripping of the HMA mix
- Pavement wear or loss due to abrasive action of traffic

3.2 PERFORMANCE OF SELECTED NDOT PROJECTS

This task documents Nevada's experience with reflective cracking mitigation techniques within the past 15 years. The following list represents a summary of the various techniques that NDOT has evaluated.

- Cold in-place recycling (CIR)
- Reinforced fabrics (RF)
- Stress relief course (SRC)
- Mill and overlay (MOL)
- Crack and seat of PCCP (CS)
- Rubblization of PCCP (RPCC)

A number of projects were constructed under each category. A total of forty four projects were reviewed in this research. The projects were located either in the northern part or the southern part of the state of Nevada covering different environmental and traffic conditions. Table 3.1 summarizes the projects contract number, projects location, applied reflective cracking technique, date of construction (DOC), and the 2005 annual average daily traffic (AADT). A detailed description of each of the projects along with

their long term performance is provided in the following paragraphs. The projects DOC varied between 1990 and 2005. No condition surveys of any of the sections were conducted as part of or specifically for this study. All of the long-term field performance characteristics were obtained from the NDOT pavement management system (PMS).

3.2.1 Cold In-Place Recycling (CIR) Projects

Cold in-place recycling is carried out using specialized recycling machines, the heart of which is a milling drum equipped with a large number of hardened steel teeth. The drum rotates upwards, milling the material in the existing road. As the milling process is taking place, water from a water tanker that is pushed ahead of the recycler is delivered through a flexible hose and is sprayed into the mixing chamber. The water, which is metered accurately by the microprocessor controlled pumping system, is mixed thoroughly with the milled material to bring the material up to its optimum compaction moisture content (42).

In general, the CIR technology is used to build a strong flexible base course. The CIR is believed to strengthen the existing pavement by treating many types and degrees of distresses. Originally, the CIR projects were located on low traffic volume roads ranging from 30 to 300 daily ESALs. However, some agencies, including NDOT, currently apply this treatment to roads with traffic varying from 1000 to even 10000 AADT.

A total of twelve NDOT CIR projects constructed between 1990 and 2001 were analyzed in this study. The following is a description of the various CIR projects.

Contract 2808a

This contract was constructed in 1998 on US050 in White Pine county over 3.0 miles. The construction consisted of CIR the top 2.0” of the existing HMA layer and overlaying it with 2.5” dense graded HMA and 0.75” OGFC.

Figure 3.1 shows the performance related data for contract 2808a. Prior to CIR the pavement exhibited fair PSI (2.3) and moderate transverse cracks and Type A fatigue cracking. After the CIR process, the pavement maintained a PSI value above 4.0 until 2005. Only minor transverse cracks showed up 4 years after construction.

Contract 2808b

This contract was constructed in 1997 on US050 in Eureka county over 9.35 miles. The construction consisted of CIR the top 2.0” of the existing HMA layer and overlaying it with 2.5” dense graded HMA and 0.75” OGFC.

Figure 3.2 shows the performance related data for contract 2808b. Prior to CIR the pavement exhibited a low PSI (1.2) and transverse and fatigue cracking. After the CIR process, the pavement maintained a PSI value above 4.0 until 2005. Three years after construction some transverse cracking start showing up.

Contract 2838

This contract was constructed in 1999 on SR396 in Pershing county over 6.57 miles. The construction consisted of CIR the top 2.0” of the existing HMA layer and overlaying it with 2.5” dense graded HMA and 0.75” OGFC.

Figure 3.3 shows the performance related data for contract 2838. Prior to CIR the pavement exhibited a low PSI (1.4), block cracking, and a rut depth of 0.25 inch. After the CIR process, the pavement maintained a PSI value of 3.7 until 2005. Two years after construction severe fatigue and block cracking showed up at the pavement surface.

Contract 2935

This contract was constructed in 1999 on SR360 in Mineral county over 23.25 miles. The construction consisted of CIR the top 2.0” of the existing HMA layer and overlaying it with 2.5” dense graded HMA and 0.75” OGFC.

Figure 3.4 shows the performance related data for contract 2935. Prior to CIR the pavement exhibited a fair PSI (2.8), and minor transverse and block cracking. After the CIR process, the pavement maintained a PSI value of 4.0 until 2005. No surface cracks showed up after construction.

Contract 2819

This contract was constructed in 1998 on US095 in Nye county over 7.40 miles. The construction consisted of CIR the top 3.0” of the existing HMA layer and overlaying it with 3.0” dense graded HMA and 0.75” OGFC.

Figure 3.5 shows the performance related data for contract 2819. Prior to CIR the pavement exhibited a moderate PSI (3.3), and minor transverse and fatigue cracking. After the CIR process, the pavement maintained a PSI value of 4.0 until 2005. Two years after construction moderate transverse cracks and minor Type A fatigue cracking showed up at the pavement surface.

Contract 2873

This contract was constructed in 1999 on US095 in Nye county over 15.76 miles. The construction consisted of CIR the top 3.0” of the existing HMA layer and overlaying it with 3.0” dense graded HMA and 0.75” OGFC.

Figure 3.6 shows the performance related data for contract 2873. Prior to CIR the pavement exhibited a fair PSI (2.7), minor transverse cracking, and moderate fatigue

cracking. After the CIR process, the pavement maintained a PSI value of 4.0 until 2005. No surface cracks showed up after construction until year of 2005 where minor transverse cracks and Type A fatigue cracking start showing at the pavement surface.

Contract 2961

This contract was constructed in 1999 on US006 in Esmeralda county over 25.12 miles. The construction consisted of CIR the top 3.0” of the existing HMA layer and overlaying it with 3.0” dense graded HMA and 0.75” OGFC.

Figure 3.7 shows the performance related data for contract 2961. Prior to CIR the pavement exhibited a fair PSI (2.8), moderate transverse cracking, and severe Type B and C block cracking. After the CIR process, the pavement maintained a PSI value of 4.0 until 2005. No surface cracks showed up after construction.

Contract 3013

This contract was constructed in 2003 on US095A in Lyon county over 19.63 miles. The construction consisted of CIR the top 3.0” of the existing HMA layer and overlaying it with 3.0” dense graded HMA (AC-20P) and 0.75” OGFC.

Figure 3.8 shows the performance related data for contract 3013. Prior to CIR the pavement exhibited a good PSI (3.5), and minor block cracking. Prior to 2003 the pavement experienced some transverse cracks. After the CIR process, the pavement maintained a PSI value of 4.3 until 2005. No surface cracks showed up after construction. In 2005, very minor transverse cracks showed up at the pavement surface.

Contract 3025a

This contract was constructed in 2001 on US093 in White Pine county over 11.0 miles. The construction consisted of CIR the top 2.0” of the existing HMA layer and

overlaying it with 2.0” dense graded HMA (AC-20P) followed by a chip seal surface treatment.

Figure 3.9 shows the performance related data for contract 3025a. Prior to CIR the pavement exhibited a fair PSI (2.5), and minor transverse and fatigue Type B cracking. After the CIR process, the pavement maintained a PSI value of 3.9 until 2005. The pavement started showing transverse cracks one year after construction.

Contract 3025b

This contract was constructed in 2001 on US093 in Lincoln county over 22.22 miles. The construction consisted of CIR the top 2.0” of the existing HMA layer and overlaying it with 2.0” dense graded HMA (AC-20P) followed by a chip seal surface treatment.

Figure 3.10 shows the performance related data for contract 3025b. Prior to CIR the pavement exhibited a fair PSI (2.5), and some transverse cracking. After the CIR process, the pavement maintained a PSI value of 3.7 until 2005. No surface cracks showed up after construction.

Contract 3025c

This contract was constructed in 2001 on US093 in Lander county over 22.22 miles. The construction consisted of CIR the top 2.0” of the existing HMA layer and overlaying it with 2.0” dense graded HMA (AC-20P) followed by a chip seal surface treatment.

Figure 3.11 shows the performance related data for contract 3025c. Prior to CIR the pavement exhibited a fair PSI (2.5), and some transverse cracking and block cracking.

After the CIR process, the pavement maintained a PSI value of 3.8 until 2005. The pavement started showing transverse cracks one year after construction.

Contract 2876

This contract was constructed in 2001 on SR208 in Lander county over 6.53 miles. The construction consisted of CIR the top 2.0” of the existing HMA layer and overlaying it with 2.0” dense graded HMA and 0.75” OGFC.

Figure 3.12 shows the performance related data for contract 2876. Prior to CIR the pavement exhibited a fair PSI (2.6), and transverse cracks. After the CIR process, the pavement maintained a PSI value of 3.8 until 2005. The pavement started showing transverse cracks one year after construction.

3.2.2 Reinforced Fabrics (RF) Projects

Paving fabrics are a special class of geosynthetic that provide the generally acknowledged functions of a stress-absorbing interlayer and a waterproofing membrane. The stress-related performance has been easily verified by the observed reductions of cracking in pavement overlays. Paving fabric interlayer systems have been used in more than 142,000 lane-miles of pavement in the U.S (31).

A total of six NDOT projects with paving fabrics constructed between 1999 and 2001 were analyzed in this study. The construction consisted of cold milling 2.0” of the existing HMA layer, placing fiberglass yarns, and overlaying with 2.0” Type II (1 inch maximum size) dense graded HMA and 0.75” OGFC.

Contract 2761

This contract was constructed in 1999 on SR443 in Washoe county over 0.87 miles. The construction consisted of cold milling 2.0” of the existing HMA layer,

placing fiberglass yarns, and overlaying with 2.0" Type II dense graded HMA (AC-20P) and 0.75" OGFC.

Figure 3.13 shows the performance related data for contract 2761. Prior to construction the pavement was experiencing a PSI of 2.2 along with several surface cracks. After construction, the pavement experienced an increase in PSI value to 3.5 which kept on decreasing with time to reach a value of 2.8 in 2005. The pavement started showing minor transverse cracks one year after construction.

Contract 2932

This contract was constructed in 1999 on US095 in Mineral county over 1.17 miles. The construction consisted of cold milling 2.0" of the existing HMA layer, placing fiberglass yarns, and overlaying with 2.0" Type II dense graded HMA (AC-20P) and 0.75" OGFC.

Figure 3.14 shows the performance related data for contract 2932. Prior to construction the pavement exhibited a PSI of 2.4 along with severe transverse cracks. After construction, the pavement experienced an increase in PSI value to 3.9 and maintained a constant PSI level for 3 years after which it started decreasing with time. No surface cracks were observed since construction until 2005. In 2005, the pavement showed minor rut depth of 0.1 inch.

Contract 2980a

This contract was constructed in 2000 on US050 in Churchill county over 1.74 miles. The construction consisted of cold milling 2.0" of the existing HMA layer, placing fiberglass yarns, and overlaying with 2.0" Type II dense graded HMA (AC-20P) and 0.75" OGFC.

Figure 3.15 shows the performance related data for contract 2980a. Prior to construction the pavement exhibited a PSI of 2.3 along with moderate transverse cracks. After construction, the pavement experienced an increase in PSI value to 3.8 and maintained a steady PSI level until 2005. No surface cracks were observed since construction until 2005. In 2005, the pavement showed a rut depth of 0.14 inch.

Contract 2980b

This contract was constructed in 2000 on US095 in Churchill county over 2.03 miles. The construction consisted of cold milling 2.0” of the existing HMA layer, placing fiberglass yarns, and overlaying with 2.0” Type II dense graded HMA (AC-20P) and 0.75” OGFC.

Figure 3.16 shows the performance related data for contract 2980b. Prior to construction the pavement exhibited a PSI of 2.8 along with moderate transverse cracks. After construction, the pavement experienced a significant increase in PSI value to 4.2 and maintained a steady PSI level until 2005. Some minor transverse cracks started to reflect 2 years after construction at which a maximum rut depth of 0.2 inch was also observed. At the end of year 2005, the pavement showed a decrease in the rut depth to 0.03 inch.

Contract 3006

This contract was constructed in 2001 on IR080 in Humboldt county over 0.23 miles. The construction consisted of cold milling 2.0” of the existing HMA layer, placing fiberglass yarns, and overlaying with 2.0” Type II dense graded HMA (AC-20P) and 0.75” OGFC.

Figure 3.17 shows the performance related data for contract 3006. Prior to construction the pavement exhibited a PSI of 3.5 along with minor transverse and fatigue cracking. After construction, the pavement experienced an increase in PSI value to 4.2 and maintained a steady PSI level until 2005. No surface cracks were observed until 2005. The pavement showed rut depths of 0.2 and 0.1 inch in years 2003 and 2005, respectively.

Contract 3008

This contract was constructed in 2001 on IR080 in Elko county over 5.17 miles. The construction consisted of cold milling 2.0” of the existing HMA layer, placing fiberglass yarns, and overlaying with 2.0” Type II dense graded HMA (AC-20P) and 0.75” OGFC.

Figure 3.18 shows the performance related data for contract 3008. Prior to construction the pavement exhibited a PSI of 3.8 along with minor transverse and fatigue cracking. After construction, the pavement experienced an increase in PSI value to 4.1 and maintained a steady PSI level for 3 years after construction after which the PSI dropped down to 3.9. Reflective transverse cracks were observed one year after construction. The pavement showed rut depths of 0.2 and 0.1 inch in years 2003 and 2005, respectively.

3.2.3 Stress Relief Course (SRC) Projects

The stress relief course consists of a NDOT Type III (0.5 inch maximum size) dense graded HMA layer. The stress relieve course is placed between the existing pavement and the overlay layer and is intended to act as a separation layer between the cracked surface and the overlay. A total of five NDOT projects with a stress relief course

constructed between 1997 and 2003 were analyzed in this study. The SRC treatment consisted of cold milling 2.0” of the existing HMA layer, placing a 1” stress relief course and overlaying with 2.0” Type II (1 inch maximum size) dense graded HMA and 0.75” OGFC.

Contract 2723

This contract was constructed in 1997 on US095 in Clark county over 20.61 miles. The construction consisted of cold milling 2.0” of the existing HMA layer, placing a 1” stress relief course (AC-20P), and overlaying with 2.0” Type II dense graded HMA (AC-30) and 0.375” OGFC.

Figure 3.19 shows the performance related data for contract 2723. Prior to construction the pavement exhibited a fair PSI of 2.7 along with transverse cracking and severe fatigue cracking. After construction, the pavement experienced an increase in PSI value to 4.2 and maintained a steady PSI level. No surface cracks were observed since construction until 2005. In 2005, the pavement showed a rut depth of 0.1 inch.

Contract 3031

This contract was constructed in 2000 on US395 in Washoe county over 4.03 miles. The construction consisted of cold milling 2.0” of the existing HMA layer, placing a 1” stress relief course (AC-20P), and overlaying with 2.0” Type II dense graded HMA and 0.375” OGFC.

Figure 3.20 shows the performance related data for contract 3031. Prior to construction the pavement exhibited a moderate PSI of 3.1 along with moderate transverse cracking and Type A block cracking. After construction, the pavement

experienced an increase in PSI value to 3.8 and maintained a steady PSI level for 4 years to drop to a level of 3.5 in 2005 when transverse cracks reflected to the pavement surface.

Contract 3048

This contract was constructed in 2000 on SR157 in Clark county over 8.63 miles. The construction consisted of cold milling 2.0” of the existing HMA layer, placing a 1” stress relief course (AC-20P), and overlaying with 2.0” Type II dense graded HMA (AC-30) and 0.375” OGFC.

Figure 3.21 shows the performance related data for contract 3048. Prior to construction the pavement exhibited a PSI of 3.4 along with moderate transverse cracking and Type A fatigue cracking. After construction, the pavement experienced an increase in PSI value to 4.3 and maintained a steady PSI level for 5 years. No serious surface cracks were observed since construction until 2005.

Contract 3045

This contract was constructed in 2001 on US050 in Eureka county over 0.57 miles. The construction consisted of cold milling 2.0” of the existing HMA layer, placing a 1” stress relief course (AC-20P), and overlaying with 2.0” Type II dense graded HMA (AC-30) and 0.375” OGFC.

Figure 3.22 shows the performance related data for contract 3045. Prior to construction the pavement exhibited a PSI of 3.8 along with minor transverse cracking and major Type B fatigue cracking. After construction, the pavement experienced an increase in PSI value to an average value of 4.2 and maintained a steady PSI level for 4 years. No surface cracks were observed since construction until 2005.

Contract 3162

This contract was constructed in 2003 on US395 in Washoe county over 2.03 miles. The construction consisted of cold milling 2.0” of the existing HMA layer, placing a 1” stress relief course (PG64-28NV), and overlaying with 2.0” Type II dense graded HMA and 0.375” OGFC.

Figure 3.23 shows the performance related data for contract 3162. Prior to construction the pavement exhibited a PSI of 3.4 along with minor transverse cracking and a rut depth of 0.27 inch. After construction, the pavement did not experience an increase in the PSI value and maintained a steady PSI level of 3.5 for 2 years. No surface cracks were observed since construction.

3.2.4 Mill and Overlay (MOL) Projects

This technique consists of cold milling up to 2 inches of the existing HMA layer and replacing it with a HMA overlay. The intention is to reduce reflective cracking by eliminating surface cracks through cold milling and replacing with new HMA material. A total of ten NDOT projects constructed between 1990 and 2003 were analyzed in this study.

Contract 2384a

This contract was constructed in 1990 on US095 in Carson City over 1.79 miles. The construction consisted of cold milling 1.0” of the existing HMA layer and overlaying with 1.0” Type III dense graded HMA (AC-10) and 0.75” OGFC.

Figure 3.24 shows the performance related data for contract 2384a. Prior to construction the pavement exhibited a fair PSI of 2.8 along with minor transverse cracking and severe Type B fatigue cracking. After construction, the pavement experienced a minor increase

in the PSI value to 3.2 and kept on decreasing with time to reach a value of 2.8 in 1995. Reflected transverse and fatigue cracking showed up one year after construction.

Contract 2384b

This contract was constructed in 1993 on US095 in Lyon county over 2.74 miles. The construction consisted of cold milling 1.0” of the existing HMA layer and overlaying with 1.0” Type III dense graded HMA (AC-10) and 0.75” OGFC.

Figure 3.25 shows the performance related data for contract 2384b. Prior to construction the pavement exhibited a PSI of 2.4 along with transverse cracking and fatigue cracking. After construction, the pavement experienced an increase in the PSI value to 3.7 and kept steady for 2 years and then started decreasing with time to reach a value of 3.3 in 2000. Reflected transverse cracks showed up two years after construction.

Contract 2432

This contract was constructed in 1993 on SR157 in Clark county over 8.77 miles. The construction consisted of cold milling 1.0” of the existing HMA layer and overlaying with 1.0” Type III dense graded HMA (AC-20) and 0.75” OGFC.

Figure 3.26 shows the performance related data for contract 2432. Prior to construction the pavement exhibited a moderate PSI of 3.0 along with severe transverse cracks. After construction, the pavement experienced an increase in the PSI value to 3.8 and started decreasing with time. Reflected transverse cracks showed up five years after construction.

Contract 2505

This contract was constructed in 1993 on US095 in Mineral county over 1.47 miles. The construction consisted of cold milling 1.0” of the existing HMA layer and overlaying with 1.0” Type III dense graded HMA (AC-20) and 0.75” OGFC.

Figure 3.27 shows the performance related data for contract 2505. Prior to construction the pavement exhibited a fair PSI of 2.7 along with fatigue and block cracking. After construction, the pavement experienced an increase in the PSI value to 3.7 and started decreasing with time. No surface cracks showed up after construction.

Contract 2651a

This contract was constructed in 1995 on US095 in Esmeralda county over 3.0 miles. The construction consisted of cold milling 1.5” of the existing HMA layer and overlaying with 1.5” Type II dense graded HMA (AC-20P) and 0.75” OGFC.

Figure 3.28 shows the performance related data for contract 2651a. Prior to construction the pavement exhibited a fair PSI of 2.8 along with moderate fatigue and block cracking. After construction, the pavement experienced an increase in the PSI value to 3.9 and started decreasing with time. Block cracking Type A was observed 5 years after construction.

Contract 2651b

This contract was constructed in 1996 on US095 in Esmeralda county over 6.12 miles. The construction consisted of cold milling 1.5” of the existing HMA layer and overlaying with 1.5” Type II dense graded HMA (AC-20P) and 0.75” OGFC.

Figure 3.29 shows the performance related data for contract 2651b. Prior to construction the pavement exhibited a moderate PSI of 3.0 along with severe block

cracking. After construction, the pavement experienced an increase in the PSI value to 3.9 and started decreasing with time. Minor transverse cracks were observed 5 years after construction.

Contract 2651c

This contract was constructed in 1996 on US095 in Esmeralda county over 3.0 miles. The construction consisted of cold milling 1.5” of the existing HMA layer and overlaying with 1.5” Type II dense graded HMA (AC-20P) and 0.75” OGFC.

Figure 3.30 shows the performance related data for contract 2651c. Prior to construction the pavement exhibited a moderate PSI of 3.1 along with moderate to severe surface cracks. After construction, the pavement experienced an increase in the PSI value to 4.0 and started decreasing with time. Minor transverse cracks and fatigue cracking were observed 5 years and 3 years after construction, respectively.

Contract 2679

This contract was constructed in 1997 on US095 in Esmeralda county over 12.92 miles. The construction consisted of cold milling 1.5” of the existing HMA layer and overlaying with 1.5” Type II dense graded HMA (AC-20P) and 0.75” OGFC.

Figure 3.31 shows the performance related data for contract 2679. Prior to construction the pavement exhibited a fair PSI of 2.7 along with severe transverse cracks and minor block and fatigue cracking. After construction, the pavement experienced an increase in the PSI value to 3.9 and started decreasing with time. Reflected transverse cracks were observed 5 years after construction.

Contract 3028

This contract was constructed in 2000 on SR512 in Carson City over 1.38 miles. The construction consisted of cold milling 1.0" of the existing HMA layer and overlaying with 1.0" Type III dense graded HMA (AC-20P) and 0.75" OGFC.

Figure 3.32 shows the performance related data for contract 3028. Prior to construction the pavement exhibited a moderate PSI of 3.1 along with moderate transverse cracks. After construction, the pavement experienced an increase in the PSI value to 3.8 and stayed steady for 2 years and started decreasing with time to reach a value of 3.4 in 2005. Reflected transverse cracks were observed 3 years after construction.

Contract 3070

This contract was constructed in 2003 on SR160 in Nye county over 3.56 miles. The construction consisted of cold milling 1.5" of the existing HMA layer and overlaying with 1.5" Type II dense graded HMA (AC-20P) and 0.75" OGFC.

Figure 3.33 shows the performance related data for contract 2651c. Prior to construction the pavement exhibited a moderate PSI of 3.1 along with moderate surface cracks. After construction, the pavement experienced an increase in the PSI value to 4.3 and maintained a steady value. No surface cracks were observed two years after construction.

3.2.5 Crack and Seat (CS) Projects

The main concern with overlaying rigid pavements with HMA overlays is reflective cracking at the joints and cracks propagating through the HMA layer. The crack and seat technique is used in attempt to eliminate or retard reflective cracking in the

HMA overlay over concrete pavements. Cracking the existing slab into large pieces of 1 to 3 feet in length is intended to produce tight cracks that permit load transfer with little loss of structural value. Seating the cracked concrete slab is intended to reestablish full contact with the foundation. A total of five NDOT projects with the crack and seat technique constructed between 1998 and 2001 were analyzed in this study.

Contract 2886

This contract was constructed in 1998 on IR080 in Lander county over 5.70 miles. The construction consisted of cracking and seating the existing 8-inch slabs, placing a leveling course of 1.5", and overlaying with 4.5" Type II dense graded HMA (AC-20P) and 0.375" OGFC.

Figure 3.34 shows the performance related data for contract 2886. Prior to construction the pavement exhibited a fair PSI of 2.8. No surface cracks were observed before construction. After construction, the pavement experienced an increase in the PSI value to 4.1 and maintained a steady value for 4 years after which reflected transverse cracks start to show up resulting in a reduction of the PSI value as a function of time.

Contract 2889

This contract was constructed in 1999 on IR080 in Elko county over 5.39 miles. The construction consisted of cracking and seating the existing 8-inch slabs, placing a leveling course of 1.5", and overlaying with 3.5" Type II dense graded HMA (AC-20P) and 0.375" OGFC.

Figure 3.35 shows the performance related data for contract 2889. Prior to construction the pavement exhibited a fair PSI of 2.9. No surface cracks were observed before construction. After construction, the pavement experienced an increase in the PSI

value to 4.0 and maintained a steady value. Minor fatigue cracking were observed 4 years after construction.

Contract 2962

This contract was constructed in 1999 on IR080 in Elko county over 15.04 miles. The construction consisted of cracking and seating the existing 8-inch slabs, placing a leveling course of 1.5", and overlaying with 4.75" Type II dense graded HMA (AC-20P) and 0.375" OGFC.

Figure 3.36 shows the performance related data for contract 2962. Prior to construction the pavement exhibited a fair PSI of 2.7 along with minor transverse cracks. After construction, the pavement experienced an increase in the PSI value to 4.3 and maintained a steady value. Minor fatigue cracking were observed 6 years after construction.

Contract 2999

This contract was constructed in 2001 on IR080 in Elko county over 5.90 miles. The construction consisted of cracking and seating the existing 8-inch slabs, placing a leveling course of 1.5", and overlaying with 3.5" Type II dense graded HMA (AC-20P) and 0.375" OGFC.

Figure 3.37 shows the performance related data for contract 2999. Prior to construction the pavement exhibited a good PSI of 3.6. No surface cracks were observed before construction. After construction, the pavement experienced an increase in the PSI value to 4.1 and maintained a steady value. Minor fatigue cracking were observed 4 years after construction.

Contract 3021

This contract was constructed in 2001 on IR080 in Elko county over 14.72 miles. The construction consisted of cracking and seating the existing 6-inch slabs, placing a leveling course of 1.5", and overlaying with 3.5" Type II dense graded HMA (AC-20P) and 0.375" OGFC.

Figure 3.38 shows the performance related data for contract 3021. Prior to construction the pavement exhibited a fair PSI of 2.9. No surface cracks were observed before construction. After construction, the pavement experienced an increase in the PSI value to 4.3 and started slightly decreasing with time. Minor Type A fatigue cracking were observed 4 years after construction.

3.2.6 Rubblization (RPCC) Projects

The rubblization provides a total destruction of the existing slabs. A total of six NDOT projects with the rubblization technique constructed between 1996 and 2005 were analyzed in this study.

Contract 2549

This contract was constructed in 1996 on IR080 in Elko county over 8.92 miles. The construction consisted of rubblizing the existing concrete slabs, placing a leveling course of 1.5", and overlaying with 5.0" Type II dense graded HMA and 0.375" OGFC.

Figure 3.39 shows the performance related data for contract 2549. Prior to construction the pavement exhibited a fair PSI of 2.9 along with minor transverse cracks. After construction, the pavement experienced an increase in the PSI value to 4.0 and maintained a steady value. Minor fatigue cracking were observed 5 years after construction.

Contract 2869

This contract was constructed in 1999 on IR080 in Elko county over 6.38 miles. The construction consisted of rubblizing the existing concrete slabs, placing a leveling course of 1.5", and overlaying with 5.0" Type II dense graded HMA and 0.375" OGFC.

Figure 3.40 shows the performance related data for contract 2869. Prior to construction the pavement exhibited a low PSI of 1.9. No surface cracks were observed before construction. After construction, the pavement experienced an increase in the PSI value to 4.2 and started slightly decreasing with time. Fatigue cracking was observed 4 years after construction.

Contract 2901

This contract was constructed in 1999 on IR080 in Humboldt county over 5.68 miles. The construction consisted of rubblizing the existing concrete slabs, placing a leveling course of 1.5", and overlaying with 7.0" Type II dense graded HMA (AC-20P) and 0.375" OGFC.

Figure 3.41 shows the performance related data for contract 2901. Prior to construction the pavement exhibited a fair PSI of 2.7. No surface cracks were observed before construction. After construction, the pavement experienced an increase in the PSI value to 3.8 and maintained a steady value with time. Minor fatigue cracking were observed 6 years after construction.

Contract 3088

This contract was constructed in 2002 on IR080 in Pershing county over 7.62 miles. The construction consisted of rubblizing the existing concrete slabs, placing a

reinforced fabric and non-woven geotextile, placing a leveling course of 1.5", and overlaying with 5.0" Type II dense graded HMA (AC-20P) and 0.375" OGFC.

Figure 3.42 shows the performance related data for contract 3088. Prior to construction the pavement exhibited a moderate PSI of 3.2 along with moderate transverse cracks. After construction, the pavement experienced an increase in the PSI value to 4.2 and maintained a steady value with time. No surface cracks were observed 3 years after construction.

Contract 3186a

This contract was constructed in 2005 on IR080 in Humboldt county over 1.06 miles. The construction consisted of rubblizing the existing concrete slabs, placing a leveling course of 2.0", and overlaying with 4.5" Type II dense graded HMA (AC-20P) and 0.375" OGFC.

Figure 3.43 shows the performance related data for contract 3186a. Prior to construction the pavement exhibited a PSI of 3.5. No surface cracks were observed before construction. After construction, the pavement experienced an increase in the PSI value to 4.2. No PMS data exist for this project at the time of writing this thesis.

Contract 3186b

This contract was constructed in 2005 on IR080 in Lander county over 1.06 miles. The construction consisted of rubblizing the existing concrete slabs, placing a leveling course of 2.0", and overlaying with 4.5" Type II dense graded HMA (AC-20P) and 0.375" OGFC.

Figure 3.44 shows the performance related data for contract 3186b. Prior to construction the pavement exhibited a PSI of 3.6. No surface cracks were observed

before construction. After construction, the pavement experienced an increase in the PSI value to 3.9. No PMS data exist for this project at the time of writing this thesis.

3.3 OVERALL SUMMARY OF THE PERFORMANCE OF THE SELECTED NDOT PROJECTS

The pavement distresses in terms of surface cracks before and after the application of the treatment are summarized in Table 3.2 for each project. Additionally, Table 3.2 shows for each project, the severity of each type of distress considered along with the number of years after construction that each type of cracks appeared on pavement surface. The column labeled “treatment life” in the tables indicates the number of years after construction when cracks first appeared on pavement surface. In general, all projects experienced pre-rehabilitation surface cracks ranging from minor to severe.

Based on the review of the treatment types and applications, all forty four NDOT projects were grouped into sub-treatments with similar characteristics.

CIR treatments

- CIR-A: Contracts 2808a, 2808b, 2838 and 2935. CIR the top 2.0” of the existing HMA layer and overlaying it with 2.5” dense graded HMA and 0.75” open graded friction course (OGFC).
- CIR-B: Contracts 2819, 2873, 2961, and 3013. CIR the top 3.0” of the existing HMA layer and overlaying it with 3.0” dense graded HMA and 0.75” OGFC.
- CIR-C: Contracts 3025a, 3025b, 3025c and 2876. CIR the top 2.0” of the existing HMA layer and overlaying it with 2.0” dense graded HMA and 0.75” OGFC.

RF treatments

- RF: Contracts 2761, 2932, 2980a, 2980b, 3006, and 3008. Cold milling the top 2.0” of the existing HMA layer, placing fiberglass yarns, and overlaying with 2.0” Type II dense graded HMA and 0.75” OGFC.

SRC treatments

- SRC: Contracts 2723, 3031, 3048, 3045, and 3162. Cold milling the top 2.0” of the existing HMA layer, placing a 1” stress relief course and overlaying with 2.0” Type II dense graded HMA and 0.75” OGFC.

MOL treatments

- MOL-A: Contracts 2384a, 2384b. Cold milling 1.0” of the existing HMA layer and overlaying with 1.0” Type III dense graded HMA (AC-10) and 0.75” OGFC.
- MOL-B: Contracts 2432, 2505, and 3208. Cold milling 1.0” of the existing HMA layer and overlaying with 1.0” Type III dense graded HMA (AC-20 or AC-20P) and 0.75” OGFC.
- MOL-C: Contracts 2651a, 2651b, 2651c and 2679 and 3070. Cold milling 1.5” of the existing HMA layer and overlaying with 1.5” Type II dense graded HMA (AC-20P) and 0.75” OGFC.

CS treatments

- CS: Contracts 2886, 2889, 2962, 2999, and 3021. Cracking and seating the existing slabs, placing a leveling course of 1.5”, and overlaying with Type II dense graded HMA (AC-20P) and 0.375” OGFC.

RPCC treatments

- RPCC: Contracts 2549, 2869, 2901, 3088, 3186a, and 3186b. Rubblizing the existing concrete slabs, placing a leveling course of 1.5 or 2.0”, and overlaying with Type II dense graded HMA and 0.375” OGFC.

The CIR treatment was mainly used on roadways with an AADT less than 6,000 except one project on US95 with 14,500 AADT. The performance data in Table 3.2 indicate the following trends for the CIR projects:

- The CIR project with the lowest AADT (CIR-A-4) did not experience any distresses after 6 years in service. On the other hand the CIR project with the highest AADT (CIR-B-4) was among the best performers after 6 years in service.
- Reflective transverse cracking was the most common type of distress on CIR projects. Seven CIR projects experienced reflective transverse cracking 1 to 2 years after construction. Three CIR projects experienced reflective transverse cracking 6 to 7 years after construction.
- Two CIR projects with medium AADT (CIR-B-1 and CIR-B-2) experienced fatigue cracking after 3 and 7 years in service, respectively.
- All the CIR-C projects (CIR 2.0”, HMA overlay 2”) experienced reflective transverse cracking 1 year after construction.

The reinforced fabric treatment was used on roadways with AADT between 1,000 and 10,000. The performance data in Table 3.2 indicate the following trends for the RF projects:

- Three out of the six RF projects did not experience any distresses after 4 to 6 years in service.
- Reflective transverse cracking was the most common type of distress on the RF projects. Three out of six RF projects experienced reflective transverse cracking after 1 to 3 years in service.
- The two RF projects with the highest AADT (RF-1 and RF-6) were among the worst performers.

The 1-inch stress relief course after cold milling and before application of overlay was used on roadways with AADT between 1,900 and 40,000. The performance data in Table 3.2 indicate the following trends for the SRC projects:

- Three out of the five SRC projects did not experience any distresses. One of these projects is 8 years old and has the highest AADT (SRC-1) while the other two are 4 and 2 years old.
- Two out of the five SRC projects experienced reflective transverse cracking after 5 years in service.

The mill and overlay treatment was used on roadways with AADT between 1,700 and 40,000. The performance data in Table 3.2 indicate the following trends for the HMA projects:

- One mill and overlay project did not experience any distresses after 12 years in service (MOL-B-2).
- Reflective transverse cracking was the most common type of distress on the mill and overlay projects. The length of time after construction for the transverse cracking to reflect to the surface ranged from 1 to 5 years.
- The mill and overlay projects were the only ones that experienced block cracking after 5 to 6 years in service.
- The worst performing mill and overlay project was the one that had the highest AADT (MOL-A-1) which experienced moderate reflective fatigue and transverse cracking after 1 year in service.

The crack and seat treatment was used on PCC rehabilitation projects of roadways with AADT between 4700 and 23000. The treatment existed for a period of four to seven in-service years. The performance data in Table 3.2 indicate the following trends for the crack and seat projects:

- Before rehabilitation, the PCC pavements did not show any type of surface cracks for four CS projects out of five. Only project CS-3 had minor transverse cracking before treatment application.
- Fatigue cracking was the most common type of distress on the crack and seat projects. The crack and seat projects experienced fatigue cracking in the HMA overlay after 4 to 6 years in service.
- Only project CS-1 out of the five CS projects experienced reflective transverse cracking after 4 years in service.
- All CS projects with 3.5” overlay experienced fatigue cracking four years after construction whereas CS projects with more than 4.5 inches overlay experienced fatigue cracking six years after construction.

The rubblization treatment was used on PCC rehabilitation projects of roadways with AADT between 6300 and 7700. The treatment existed for a period of maximum nine in-service years. The performance data in Table 3.2 indicate the following trends for the rubblization projects:

- Before rehabilitation, the PCC pavements did not show any type of surface cracks for five RPCC projects out of six. Only project RPCC-1 had minor transverse cracking before treatment application.
- Fatigue cracking was the type of distress on the rubblized projects. The rubblized projects experienced fatigue cracking in the HMA overlay after 4 to 6 years in service.
- The rubblized project RPCC-4 constructed in 2002 and after 3 years in service did not experience any type of surface cracks.
- No performance data exists for the projects RPCC-5 and RPCC-6 that were constructed in 2005.

3.4 STATISTICAL ANALYSIS OF THE SURFACE CRACKING DATA – PRINCIPAL COMPONENT ANALYSIS

In order to objectively evaluate the overall performance of the various treatments, and in order to relatively compare the performance of the treatments to each others the

statistical technique called Principal Component Analysis (PCA) was used as a tool to determine an overall performance indicator. The PCA indicator combines the simultaneous effects of cracking occurrence and severity. Therefore, the PCA works as an indicator of the ability of each treatment to delay the reflective cracking. A detailed explanation of the PCA statistical tool is discussed in the following paragraphs.

The Principal Components Analysis (PCA) is a way of identifying patterns in data, and expressing them in such a way as to highlight their similarities and differences. A formal definition indicates that PCA is a method that reduces data dimensionality by performing a covariance analysis among factors. As such, it is suitable for data sets in multiple dimensions, such as a large data set of pavement distresses. The main applications of PCA are: (1) to *reduce* the number of variables and (2) to *detect structure* in the relationships among variables, that is to *rank variables*.

An example to understand the PCA analysis is provided here for combining two variables into a single factor. Typically, the correlation between two variables can be presented in a scatter-plot. A regression line can then be fitted that represents the "best" summary of the linear relationship between the variables. If we could define a factor that would approximate the regression line in such a plot, then that factor would capture most of the "essence" of the two variables. Therefore, single scores on that new factor, represented by the regression line, could then be used in future data analyses to represent the essence of the two items. In a sense, we have reduced the two variables to one factor. Note that the new factor is actually a linear combination of the two variables.

The example described above, combining two correlated variables into one factor, illustrates the basic idea of PCA. If we extend the two-variable example to multiple

variables, then the computations become more involved, but the basic principle of expressing two or more variables by a single factor remains the same.

The most valuable product obtained from PCA is a linear parameter estimated from a linear combination of the original variables. The objective of the PCA is to reduce dimensionality by extracting the smallest number of variables (factors) that account for most of the variation in the original multivariate data and to summarize the data with little loss of information. In our case, the multivariate data corresponds to the NDOT cracking surveys for each year while the dimensionality represents the extent, severity, and years of occurrence of the various types of cracking. Therefore, in the case of cracking, the PCA tries to provide a combined indicator or a factor that interprets the simultaneous effects of fatigue, transverse, and block cracking in terms of their extent, severity, and time of occurrence (years).

3.4.1 Overall Ranking of the Performance of Selected NDOT Projects

The PCA analysis was conducted on all projects combined at one year before rehabilitation (-1) and at one (+1), three (+3), and five years (+5) after treatment application based on their measured surface cracks (fatigue, transverse, and block cracking). In other words, the PCA scores are used for ranking the combined projects based on their performance at year -1 and +1, at year -1 and +3, and at year -1 and +5. Conducting the PCA ranking of the projects at pre-rehabilitation and after construction at the same time is a good indication of the relative effectiveness of the various treatments taking into consideration pre-construction pavement conditions and allowing for a direct comparison of the condition of the pavement after construction to its condition before rehabilitation. The CIR, RF, SRC, and MOL projects are analyzed separately from the

CS and RPCC projects which consisted of HMA overlays over PCC pavements. The SAS Macro called “factor” was used to perform the PCA analysis (43). Such macro was developed by Dr. George Fernandez. Appendix C shows the various PCA values calculated for each year.

Table 3.3 shows the ranking of the various treatments based on the PCA analysis of the cracking data of the various projects. As stated before, the analysis for the flexible pavement techniques was conducted separately from the analysis for the rigid pavement techniques and hence separate rankings were assigned. Additionally an “NA” was assigned if the project life was younger than the indicated long-performance analysis year.

In the case of the flexible pavement techniques (i.e., CIR, RF, SRC, and MOL), first all thirty three projects at their pre-treatment conditions (-1) and their condition at one year (+1) after treatment application were ranked between 1 and 66 with a rank of “1” indicating the best conditions project and a rank of “66” indicating the worst conditions project. However, the data in Table 3.3 show that the maximum ranking is “38” instead of “66”, this occurred because some projects ranked the same indicating that the conditions of the similarly ranked projects are statistically the same. For example projects CIR-C-2, CIR-C-3, and CIR-C-4 were all ranked at (+1) as “5” indicating statistically the same pavements’ condition.

Then, the projects were ranked at +3 and +5 years after treatment application by re-conducting the PCA analysis at both the -1 and the analysis year (i.e., +3 or +5) excluding the projects that were younger than the indicated long-performance year. Subsequently, the ranking was based on the same total number of projects before (-1) and

after treatment application (+3 or +5). At -1 and +3 years, a total of thirty projects were ranked between 1 and 60 with a maximum ranking of “39”. At -1 and +5 years, a total of 24 projects were ranked between 1 and 48 with a maximum ranking of “36”.

In the case of the ranking of projects at the +1, +3, and +5 years, there are several occasions where several projects are given the same rank. This occurred due to the statistically similar performance of these projects. For example in the case of ranking based on (-1) and (+1) years in Table 3.3, a ranking of “1” is assigned to each project that did not experience any cracking 1 year after construction. On the other hand if two projects showed cracking 1 year after construction, the extent and severity of the cracking would then play a role in the ranking. For example, projects CIR-C-1 and CIR-C-2 both showed minor transverse cracking in year 1 but the PCA analysis assigned a ranking of “3” and “5”, respectively. The reason for the worse ranking of project CIR-C-2 is that the extents of the minor transverse cracking of project CIR-C-2 is higher than the extent of the minor transverse cracking on project CIR-C-1. In summary, the projects are first ranked based on the year of cracking occurrence, followed by the severity of the cracking, and finally by the extent of the cracking. In the cases where all three factors are the same, then the projects are assigned similar ranks.

The same process was followed for ranking all eleven projects for the rigid pavement techniques (i.e., CS and RPCC). All eleven projects at -1 and +1, and at -1 and +3 years were ranked between 1 and 11 with a maximum ranking of “3.” All projects ranked as “1” except the CS-3 and RPCC-1 projects that were ranked as “2” and “3” at year -1 because of the minor transverse cracks that existed before the application of the treatment.

By examining the data presented in Table 3.3, the following observations can be made:

- One year after construction a total of five CIR projects out of twelve performed among the worst projects. Four out of these worst performing five CIR projects (CIR-C-1, -2, -3, and -4) consisted of milling the top 2.0” of the existing layer and overlaying it with 2.0” dense grade HMA. Only one RF project (RF-1) out of six ranked among the worst projects. The RF-1 project experienced severe alligator cracking (Type B) prior to the construction of the treatment. All of the SRC projects ranked among the best performing projects. Two MOL projects (MOL-A-1, C-4) ranked among the worst performing projects with MOL-C-4 pavement condition 1 year after construction worse than its condition 1 year before construction. In the case of rehabilitation techniques for rigid pavements all treatments (i.e., CS and RPCC) ranked best with no difference in performance.
- Three years after construction, additional two CIR, RF, and MOL projects performed among the worst projects whereas the SRC projects still outperformed the other treatments. Evidently the MOL-C-4 pavement condition 3 year after construction was worse than its condition 1 year before construction. In the case of rehabilitation techniques for rigid pavements all treatments (i.e., CS and RPCC) ranked best with no difference in performance.
- Five years after construction, five CIR projects out of eight performed among the best projects. The five CIR projects included three out of the four CIR-B projects. The CIR-B treatment consists of milling the top 3.0” of the existing HMA layer and overlaying it with 3.0” dense graded HMA. Only two RF projects out of four, two SRC projects out of three, and one MOL project out of nine ranked among the best performing projects. In the case of rehabilitation techniques for rigid pavements only one CS project out of five and one RPCC project out of three ranked best with no surface cracks five years after construction. Two RPCC treatments out of three ranked among the worst performing treatments.

A close examination of the performance data summarized in Table 3.3 show that five out of the seven projects that experienced severe alligator cracking (Type B) prior to the construction of the CIR, RF, SRC, and MOL treatments ranked among the worst projects five years after construction. Out of these five projects, two are CIR projects (CIR-A-2 and CIR-B-1), one is RF project (RF-1), and two are MOL projects (MOL-A-1 and MOL-A-2). This indicates the ineffectiveness of the CIR, RF, and MOL-A treatments on a pavement with severe alligator cracking, and the effectiveness of the SRC

treatment on a pavement with severe alligator cracking and high volume traffic (40,000 AADT).

Figures 3.45, 3.46, and 3.47 show a comparison between the ranking of the various treatments at one year before construction versus the ranking at one, three and five years after construction. The objective of these plots is to be able to assess the effectiveness of the various treatments by comparing their historical performance as they relate to the conditions of the pavement prior to rehabilitation. In other words, a treatment that was applied to badly deteriorated pavements but still maintained good performance would be more effective than a treatment that was applied to a less deteriorated pavement that maintained good performance.

Additionally, Figures 3.45-3.47 show the mean, minimum, and maximum rank in each treatment. This analysis was conducted on all projects having data on the analysis performance year and excluding the projects considered as outliers ranked statistically significantly different than the overall average rank of the same treatment. An outlier rank in a treatment can considerably change the average rank and consequently skew and bias the results. The statistical analysis tool called simple descriptive statistics and exploratory graphical analysis using the SAS Macro called “univar” (43) was used to identify the projects with an outlier rank in a specific treatment. These projects are identified in Table 3.3. The total numbers of projects analyzed in each treatment are shown in Tables 3.4-3.6.

By examining the data presented in Figures 3.45-3.47, the following observations can be made:

- The SRC and MOL-B and -C treatments were applied on flexible pavements that experienced the widest range of pre-treatment (-1) performance. The CIR-C and MOL-A were applied on flexible pavements that experienced the narrowest range of pre-treatment performance.
- The CIR projects before treatment (-1) were among the worst performing projects.
- After one year (+1) from the treatment construction (Figure 3.45), all treatments showed similar performance except the CIR-C and the MOL-A treatments showed worse performance.
- After three years (+3) from the treatment construction (Figure 3.46), the CIR-A, CIR-B, SRC, MOL-C treatments showed similar and best performance followed by RF and MOL-B treatments. The CIR-C and the MOL-A treatments still showed significantly worse performance.
- After five years (+5) from the treatments construction (Figure 3.47), the CIR-B treatment performed the best followed by the CIR-A and RF treatments which performed similarly. The performance of the SRC treatment became similar to the MOL treatments. It should be noted that the worst performing CIR-C projects based on the (+1) and (+3) analysis were not included in the (+5) analysis due to the lack of the 5-years performance data from these projects.

Another way of looking at the effectiveness of the various treatments is to examine the means and standard deviations of their relative rankings at the pre-treatment and the 1, 3, and 5-years stages along with the change in their mean relative ranking. Tables 3.4 through 3.6 summarize the means and standard deviation data of the various projects along with the change in the mean relative ranking. An effective treatment would be one that has high mean and low standard deviation for pre-treatment performance and low mean and low standard deviation for the 1, 3, and 5 year performances coupled with the highest change in the mean ranking. Based on this criteria, the evaluated treatments for mitigating reflective cracking under Nevada's conditions are ranked from best to worst after 1, 3, and 5 year from the construction as follows:

<i>After 1 year from construction</i>	<i>After 3 years from construction</i>	<i>After 5 years from construction</i>
CIR-A, CIR-B, MOL-C	CIR-A, CIR-B, MOL-C	CIR-A, CIR-B
SRC, MOL-B	SRC, MOL-B	RF
CIR-C	CIR-C	SRC, MOL-B
RF	RF	MOL-C
MOL-A	MOL-A	MOL-A

3.4.2 Fixed Qualitative and Qualitative Factorial Analysis

The objective of this analysis was to statistically determine the impact of traffic level and project location on the long-term performance of the reflective cracking mitigation techniques experienced by NDOT. The reflective cracking treatments (or mitigation techniques) were: Cold in-place recycling, reinforced fabrics, stress-relief course, mill and overlay, PCC rubblization, and PCC crack and seat. Three levels for traffic (low: 0-3000 AADT; intermediate: 3000-7000 AADT; and high: >7000 AADT) and two levels for project location (north of south) along with their interaction were considered in this analysis. To this end, a fixed qualitative factorial analysis was applied using the SAS macro-call `fixqlql.sas` written by Dr. G. Fernandez of the University of Nevada (43). The analysis was based on the PCA values of the various projects after accounting for traffic level and project location. The comparison for the various PCA values was performed at +1, +3 and +5 years after treatment application. This factorial treatment design is performed to investigate the relationships among the indicated factors (reflective cracking mitigation technique, traffic, and location) and the response variable (PCA value as a pavement performance indicator). This technique allows to provide statistical information on the impact of the evaluated factors and the long-term pavement performance. For example, for a given traffic level (i.e., low: 0-3000 AADT), the impact

of project location (i.e., north vs south) on the long term performance of a given reflective cracking treatment is evaluated by analyzing the PCA values at +1, +3 and +5 years. Additionally, the analysis will allow for detection of any interaction among the various evaluated factors, thus, if any interaction exists between the traffic level and the project location then both factors are dependent of one another and any conclusion that needs to be drawn at the end will be a function of both traffic and project location levels (44).

As with any analysis of variance (ANOVA), the assumptions that random experimental errors are independent and normally distributed with zero mean and a common variance for all treatments should not be violated.

All the analyses were performed at a 0.05 significance level ($p\text{-value} = 0.05$), which mean that for each comparison reported as being significantly different, there is only a 5% chance that this is not true. The significance level (i.e., $p\text{-value} \leq 0.05$) of any experiment is the probability that a given treatment (i.e., mitigation technique, traffic level, and project location) has a significant effect on the response variable (i.e., PCA at +1, +3 and +5 years. The treatment is considered as highly significant if the $p\text{-value}$ is equal or lower than 0.0001. A change in a highly significant treatment produces a highly significant change in the response variable.

Tables 3.7, 3.8 and 3.9 show the general statistical analysis at +1, +3 and +5 years after treatment construction. The statistical results indicate that the reflective cracking mitigation technique, the traffic level, and the project location have highly significant effects on the pavement performance at +1, +3 and +5 years after treatment construction. In other words, there is enough statistic evidence to conclude that these factors are highly

significant up to 5 years after treatment construction. It means that any change in one of those factors is going to affect the long-term pavement performance. Additionally, the interaction among these factors was found to be highly significant. Therefore, the analysis of the performance of any project should consider simultaneously the combination of the three factors evaluated: reflective cracking mitigation technique, traffic level and project location. It implies that any consideration regarding the pavement performance should include the type of treatment applied, the traffic level and the location of the project because the combination of those factors will affect the pavement condition. Unfortunately, although the three studied factors were found highly significant as well as their interaction, it was not possible to find out any trend to conclude under what conditions of traffic level and project location a reflective cracking technique performed better. This may be related to the lack of number of replicates for the various evaluated factors.

Additionally, a fixed quantitative factorial analysis was used to assess the effect of the project condition before the treatment application on the long-term performance of the applied reflective cracking treatment. The applied reflective cracking mitigation technique was considered as the qualitative factor and the PCA value of the evaluated projects before treatment application (PCA-1) was considered as quantitative factor. The response variable selected was the current PCA value for the project at the corresponding year. The quantitative factor (i.e., PCA-1) can have either a linear or a quadratic effect on the response variable (i.e., PCA values at +1, +3, and +5 years). The analysis was performed at years +1, +3 and +5 after treatment application. A fixed qualitative-quantitative factorial analysis was applied using the SAS macro-call `fixqlqt.sas` written by

Dr. G. Fernandez of the University of Nevada (43). The significance p-value is also applied here, in the same manner that it was explained before. Also, the interaction was considered into the analysis. Additionally, the regression coefficient (R-square) was included in the analysis. The multiple regression correlation coefficient, R-square, is a measure of the proportion of the variability explained by the statistical model. It is a number between zero and one and a value close to zero suggests a poor model. In general, values of R-square higher than 0.7 are acceptable for field-related experiments and indicate that the experiment is valid.

The results of this analysis are shown in Tables 3.10, 3.11 and 3.12. The data show that the reflective cracking mitigation technique and the pavement condition before the treatment application are highly significant at +1, +3 and +5 years after treatment application. It means that any variation in those factors will significantly affect the pavement performance. Therefore, the long-term performance of the project is highly related to its previous condition before the treatment application and the type of reflective cracking mitigation technique applied. Additionally, the interaction among such factors was also found significant. Due to the interaction effect, the long-term performance of the project will be affected by both the applied type of reflective cracking mitigation technique and the pavement condition before treatment application. Unfortunately, due to the lack of number of replicates, it was not possible to determine under what conditions a better performance is expected.

The R-square for the three studied years was found to have an acceptable value higher than 0.7. Therefore, the analyzed data and the performed statistical analysis

accounts for most of the variability of the experiment and the conclusions can be accepted as valid.

3.5 FINAL ANALYSIS FROM THE NDOT PROJECTS

The following general conclusions regarding the performance of reflective cracking treatments in Nevada are based on the combined analyses of the distress data and the PCA analysis.

- The PCA analysis was conducted to identify any reflective cracking treatment that may be able to provide good long-term performance regardless of the conditions of the pavement prior to its application. Based on the results of the PCA presented in Figures 3.45 through 3.47, this goal was not achieved. In general, the performance of the reflective cracking treatment is highly dependent on the conditions of the pavement prior to the construction of the treatment. This is supported by the data shown in Figure 3.47 where the CIR and MOL were applied to pavements having lower performance than the pavement where the RF and SRC were applied and showed worse performance after 5 years in service.
- The PCA ranking data in Table 3.3 showed that the CIR-A (CIR 2" and overlay 2.5") and CIR-B (CIR 3.0" and overlay 3.0") treatments regardless of the traffic level are generally effective in stopping reflective cracking for 3 years and retarding reflective cracking for 5 years as long as the existing pavement does not show severe alligator cracking prior to the application of these treatments. On the other hand the CIR-C (CIR 2" and overlay 2") treatment is ineffective in resisting reflective cracking for even a traffic level as low as 1000 AADT.
- The RF treatment showed marginal performance after 3 and 5 years of construction. The RF treatment was able to retard reflective cracking for at least 3 years. The RF treatment was ineffective when applied on a pavement with severe alligator cracking prior to the application of the treatment and/or a traffic level above 3000 AADT.
- The SRC treatment showed excellent performance up to 3 years after construction regardless of the traffic level and the existing pavement condition. However 5 years after construction, reflective transverse cracking showed up on the pavement surface.
- The MOL-A (cold milling 1" and AC-10 overlay 1") treatment was ineffective in resisting reflective cracking of pavements with severe alligator cracking prior to the construction of the treatment. The MOL-B and MOL-C treatments were effective in stopping reflective cracking up to 3 years after construction for

projects with AADT lower than 4000. After 5 years of construction the MOL-B and MOL-C treatments showed minor reflected transverse cracks.

- The CS treatment showed excellent performance up to 3 years after construction for rigid pavements with no or minor surface cracks prior construction. The CS projects experienced fatigue cracking in the HMA overlay after 4 to 6 years in service. The CS treatment with 3.5” HMA overlay retarded fatigue cracking for 4 years after construction whereas CS treatment with more than 4.5” HMA overlay retarded fatigue cracking for 6 years after construction.
- The RPCC treatment showed excellent performance up to 3 years after construction for rigid pavements with no or minor surface cracks prior construction and AADT around 7000. The RPCC projects experienced fatigue cracking in the HMA overlay after 4 to 6 years in service. The RPCC treatment with 5” HMA overlay retarded fatigue cracking for 4 to 5 years after construction whereas RPCC treatment with 7” HMA overlay retarded fatigue cracking for 6 years after construction.
- In general, the long-term effectiveness of the treatments was significantly reduced by the existence of severe alligator cracking on the projects prior to the application of these treatments. Therefore, it is recommended that projects experiencing severe alligator cracking as classified by the NDOT pavement distress manual should be subjected to either re-construction or full depth reclamation.

3.6 SUMMARY OF THE PHASE I FINDINGS

The gathered information and conducted analyses in the various tasks of the Phase I study of the research were used to identify the promising techniques to mitigate reflective cracking in HMA overlays.

Based on the literature review of the current and previous efforts outside Nevada on the mitigation of reflective cracking in HMA overlays, the following general conclusions concerning the performance of reflective cracking treatments can be made.

- Performance of crumb rubber overlay mixtures produced by adding ground tire rubber to HMA using the wet process in addressing reflection cracking in HMA overlays has ranged from successful to devastating failures depending on the percent of crumb rubber in the mix.
- Asphalt rubber interlayer with a combination of a thin overlay (about 1.5 inch) reduced and/or delayed reflective cracking over a period of five years.

- In general, performance of geosynthetics in addressing reflection cracking in HMA overlays has ranged from highly successful to devastating failures.
- Fabric interlayers have been most effective when used for load-related fatigue distress and have not performed well when used to delay or retard thermal cracking. Proper construction procedures are critical for optimum performance of paving fabrics.
- In general, glassgrid showed benefits in retarding reflective cracking and reducing the rate of crack reflections specifically in an area of high tensile stress.
- Cold in-place recycling (CIR) of existing HMA materials provided an effective mean of extending the life of pavement rehabilitation projects for highways with up to 13,000 ADT and 200,000 annual equivalent single axle loads. CIR provided resistance against reflective cracking between two and three times that exhibited by conventionally resurfaced control sections.
- Interlayer stress-absorbing composite (ISAC) delayed reflective cracking at treated joints and cracks from one year to three years when compared to the untreated and other crack control methods. The ISAC consists of a three-layer system. The top layer is a high strength woven geotextiles to resist stresses caused by underlying pavement movements. The bottom layer is a low strength nonwoven geotextile (meeting AASHTO M-288-92). The middle layer is a modified rubberized asphalt layer to absorb the strain energy and bond the two geotextiles together. Based on the local Illinois distributor of ISAC the typical installation costs of ISAC range from \$10 to \$14 per foot depending on the quantity purchased. The larger the quantity purchased, the lower the cost/foot of ISAC.
- SAMI layers can reduce the likelihood of damage and the need for large reconstruction work. They were successfully used to reduce the rate of reflective cracking when the crack spacing and widths were small.
- In general, cracking and seating concrete pavements delayed reflected cracks for five years. The use of fibers in the overlay mixture further reduced transverse cracks.
- Fracturing technique of concrete pavement is somewhat less successful than the crack and seat technique to retard reflective cracking in reinforced concrete pavements. Formation of reflective cracks appeared to be delayed for only about three years.

Based on the review of the long-term field performance of NDOT projects with techniques to reduce the impact of reflective cracking on HMA overlays, the following general conclusions can be made.

- Cold in-place recycling (CIR) of minimum 2” of the existing HMA materials and overlaying it with a minimum 2.5” dense graded HMA mixture with a traffic level up to 14,000 AADT provided an effective mean of stopping reflective cracking

for 5 years after construction as long as the recycled pavement does not show any severe alligator cracking.

- The reinforced fabrics (RF) treatment retarded reflective cracking for at least 3 years after construction and reduced the rate of reflected transverse cracks 5 years after construction. The RF treatment was ineffective when applied on a pavement with severe alligator cracking prior to the application of the treatment.
- The 1" stress relief course (SRC) treatment showed excellent performance up to 3 years after construction regardless of the traffic level (up to 40,000 AADT) and the pre-rehabilitation condition of the pavement. However, the rate of the reflected transverse cracks was accelerated 5 years after construction.
- The mill and overlay (MOL) treatment by cold milling 1" of the existing HMA pavement and overlaying it by a 1" HMA mixture manufactured with an AC-10 asphalt binder was ineffective in resisting reflective cracking of pavements with severe alligator cracking prior to the treatment construction.
- The mill and overlay (MOL) treatment by cold milling 1" of the existing HMA pavement and overlaying it by a 1" HMA mixture manufactured with an AC-20P polymer modified binder provided an effective mean of stopping reflective cracking for 3 years after construction and a traffic level up to 4000 AADT. After 5 years of construction the treatment showed minor reflected transverse cracks.
- The mill and overlay (MOL) treatment by cold milling 1.5" of the existing HMA pavement and overlaying it by a 1.5" HMA mixture manufactured with an AC-20P polymer modified binder provided an effective mean of stopping reflective cracking for 3 years after construction and a traffic level up to 2000 AADT. After 5 years of construction the treatment showed reflected transverse cracks. It should be emphasized that this treatment was placed on pavements with a condition worse than the condition of the pavements where the other two mill and overlay treatments were applied.
- The crack and seat (CS) of concrete pavements with no or minor surface cracks prior to overlay, showed excellent performance for 3 years after construction. Fatigue cracking was experienced in the HMA overlay after 4 to 6 years in service. The 3.5" HMA overlay retarded fatigue cracking for four years after construction whereas the 4.5" and 4.75" HMA overlay retarded fatigue cracking for six years after construction.
- The rubblization (RPCC) of concrete pavements with no or minor surface cracks prior construction and a traffic level of 7000 AADT showed excellent performance for 3 years after construction. Fatigue cracking was experienced in the HMA overlay after 4 to 6 years in service. The 5" HMA overlay retarded fatigue cracking for four to five years after construction whereas the 7" HMA overlay retarded fatigue cracking for six years after construction.
- In general, the long-term effectiveness of the treatments was significantly hampered by the existence of severe alligator cracking on the projects prior to the application of these treatments. Therefore, it is recommended that projects experiencing severe alligator cracking as classified by the NDOT pavement distress manual should be subjected to either re-construction or full depth reclamation.

Chapter 4 – REVIEW OF REFLECTIVE CRACKING ANALYSIS MODELS

The main objective of this chapter was to review and evaluate the currently available analytical models that can be used to predict the resistance of HMA overlays to reflective cracking. Based on the review of the available literatures, three design methods were identified and are summarized in this chapter.

- Virginia Tech Simplified Overlay Design Model
- Asphalt Rubber Association Overlay Design Model
- The New AASHTO model for Reflective Cracking

The identified models are assessed based on their technical merit and their ability to predict the performance of HMA overlays subjected to reflective cracking.

4.1 VIRGINIA TECH SIMPLIFIED OVERLAY DESIGN MODEL

In 2003, Elseifi and Al-Qadi (45) developed an overlay design procedure to predict the service life of rehabilitated flexible pavement structures against reflective cracking. The researchers used the linear elastic fracture mechanics (LEFM) principles to derive a simple equation based on three-dimensional (3D) finite element (FE) models that can be used to predict the number of cycles to failure against reflective cracking for rehabilitated flexible pavements.

4.1.1 Fundamentals of Reflective Cracking

In 1996, Jacobs et al. (46) evaluated the application of fracture mechanics principles to the discontinuous crack growth of HMA layers by comparing FE models simulation (continuous crack growth) to experimental crack growth of HMA (discontinuous crack growth). The researchers found that crack growth process in HMA

might be accurately described using the fracture mechanics theory with a better accuracy for mixes with small aggregate size.

In general, a cracked pavement system can be loaded in any one or a combination of the three following fracture modes (45).

- Mode I loading (opening mode, KI) also called strain mode, results from loads that are applied normally to the crack plane (thermal and traffic loading) (Figure 4.1.a).
- Mode II loading (sliding mode, KII) also called vertical shear strength mode, results from in-plane shear loading, which leads to crack faces sliding against each other normal to the leading edge of the crack (traffic loading) (Figure 4.1.b).
- Mode III loading (tearing mode, KIII) also called horizontal shear strength mode, results from out-of-plane shear loading, which causes sliding of the crack faces parallel to the crack leading edge (Figure 4.1.c). This mode of loading is negligible for pavements.

By neglecting the ultimate failure stage in which the crack growth rate increases rapidly as global instability is approached, two distinct phases are considered in the cracking process of pavement systems and are described as follows (45).

The crack initiation phase: This phase consists of two distinct phases of microcracking and formation of macrocracks, and is defined by the necessary number of load applications to form a visible damaged zone at the bottom of the overlay (47). In case of reflective cracking induced by Mode II loading, the number of cycles of a specific load for crack initiation in the HMA layer may be determined using the Belgian Road Research Center (BRCC) equation (48).

$$N = 4.856 \times 10^{-16} \varepsilon_{zx}^{-4.73} \quad (4.1)$$

where, N = number of cycles before crack initiation

ε_{zx} = shear strains 0.4 inch (10 mm) above the existing crack.

The crack propagation phase: This phase represents the stage where the crack propagates to the surface through the entire thickness of the HMA overlay. The Paris power law may be used to describe the crack propagation phase in flexible pavements (45, 49).

$$\frac{dC}{dN} = A(\Delta K^n) \quad (4.2)$$

where, C = crack length

N = number of loading cycles

A and n = fracture parameters of the material

ΔK = stress intensity factor amplitude.

Elseifi and Al-Qadi (45) used the Paris' law approach in their study which is only valid under the following assumptions:

- Since no exact definition of the stress intensity factor for a multi-layer pavement system was available, a regression analysis was performed to define the stress intensity factor as a function of the crack length (C) for each considered design. The developed regression models are dependent on the assumed stiffness for the pavement layers and the crack propagation resistance of the mix.
- The computed number of cycles is highly sensitive to the assumed values of the fracture parameters (i.e., A and n). The correct way to determine the fracture parameters of a material is to examine the stable crack growth of HMA beam samples under repeated loading conditions, which is a tedious and expensive operation.
- Since no direct measurements of the fracture parameters (A and n) were feasible in this study, and since such testing is not expected to be conducted in a routine overlay design, theoretical relations between the fracture parameters of the material and the mix properties were suggested. The first fracture parameter (n) of the material was related to its creep properties and the second fracture parameter (A) was determined by means of the volumetrics and modulus of the mix (Equation 4.3).

$$n = \frac{2}{m} \quad (4.3a)$$

$$\log A = -2.605104 + 0.184408AV - 4.704209 \log AC - 0.00000066F \quad (4.3b)$$

where, m = slope of the log creep compliance versus log time curve

AV = air-voids (%)

AC = asphalt content (%)

E = resilient modulus of the mixture (in psi).

Based on this concept, and using results of conventional creep testing performed on three types of HMA mixtures, three levels were established for the fracture characteristics of the overlay:

- Type I: $n = 3.40$ and $A = 1.37 \times 10^{-6}$ (rich-binder mix)
- Type II: $n = 3.85$ and $A = 1.67 \times 10^{-6}$
- Type III: $n = 4.50$ and $A = 2.33 \times 10^{-6}$ (high air-voids mix)

The stress intensity factor (ΔK) was determined using FE for different locations of the crack. The following section explains the stress intensity factor concept, and how the stress intensity factor was determined using FE.

4.1.2 Fracture Mechanics Analysis Using Finite Element Method

The stress intensity factor (K) was utilized to measure the severity and stability of a crack in a pavement layer. The stress intensity factor is a scale factor that is used to define the magnitude of the crack tip stress field and is predicted using Equation 4.4.

$$K = \sigma \sqrt{\pi a} \times f(a) \quad (4.4)$$

where, σ = boundary stress

a = crack length

$f(a)$ = geometry depending function.

A given material can resist propagation of a crack as long as the stress intensity factor is below the fracture toughness (K_c) of the material. In contrast to the stress

intensity factor, the fracture toughness is a quantity that is independent of the crack geometry, and the loading imposed on the structure. Although the fracture toughness has not been well defined for HMA, in 1997 Mobasher et al. (50) reported the plane strain fracture toughness (K_{Ic}) for different HMA mixes and at different binder contents as shown in Table 4.1.

Elseifi and Al-Qadi (45) used the commercial software ABAQUS 5.8-1 to indirectly calculate the stress intensity factor using the path independent integral, called J-integral. The J-integral is defined as the change in mechanical energy per unit area of new crack surface. For plane strain condition, the J-integral is given by Equation 4.5 which is function of the Poisson's ratio (ν), elastic modulus (E), and stress intensity factor (K) of the HMA (51).

$$J = \frac{1-\nu^2}{E}(K^2) \quad (4.5)$$

The developed FE models represented a variety of three-layer systems that are regularly encountered in typical HMA pavement overlay applications. A total of 216 different pavement designs were analyzed to develop the suggested design equation. The pavement structure consisted of an HMA overlay with variable thicknesses (2 to 6 inches) applied on top of a cracked HMA layer, a base layer, and a subgrade. The crack initiation and propagation phases were investigated using dynamic three-dimensional models developed for different location of the cracks. Elastic foundations were used to simulate the support provided by the subgrade (non-linear springs). The contact between layers was assumed as fully-bonded. A crack was induced in the existing HMA layer and the pavement structure was subjected to a quasi-static load with an amplitude function

that was obtained based on actual vertical stress measurements in the flexible pavement at the Virginia smart Road.

4.1.3 Development of Design Equations

The total number of load repetitions to produce the crack reflection to the pavement surface was defined as the sum of the number of load repetitions for crack initiation and the number of load repetitions for crack propagation. Global instability in the HMA layer was assumed to be reached when the crack front is at 0.5 inch (12.7 mm) from the pavement surface.

$$N_{total} = N_{initiation} + N_{propagation} \quad (4.6)$$

where, N_{total} = total number of cycles before the crack reach 0.5 inch (12.7 mm) from the surface of the overlay

$N_{initiation}$ = Number of cycles for crack initiation at the bottom of the overlay.

$N_{propagation}$ = Number of cycles for the crack to propagate from the bottom of the overlay to 0.5 inch (12.7 mm) from the surface of the overlay.

The number of cycles for crack initiation ($N_{initiation}$) was determined for each of the pavement structures considered in this study using Equation 4.1 and FE to calculate the maximum shear strain in the vicinity of the crack tip. A shift factor of nine was used in all calculations to adjust the number of cycles for the difference between laboratory and field conditions (e.g., load distribution in the wander area, state of stresses, and rest periods).

The number of cycles for crack propagation ($N_{propagation}$) was determined using Equation 4.2. The stress intensity factor (K) was computed using Equation 4.5 and the J-integral that was obtained using FE for different locations of the crack in the HMA overlay.

4.1.4 Service Life Prediction for Pavements with Potential Reflective Cracking

In order to avoid the time consuming FE analyses, the researchers developed a regression model to predict the number of cycles in ESALs as a function of the significant variables. The developed design equation was based on the results of all the considered cases in this study.

$$\log W_{t80} = \frac{1}{10^4} (255H_{overlay} + 2.08E_{overlay} + 45.3H_{HMA} + 8.73E_{HMA} + 1.37H_{Base} + 6.93E_{Base} + 1.49E_{subgrade}) \quad (4.7)$$

where, W_{t80} = total number of 80-kN single-axle load applications

$H_{overlay}$ = thickness of HMA overlay (mm)

$E_{overlay}$ = resilient modulus of HMA overlay (MPa)

H_{HMA} = thickness of existing HMA layer (mm)

E_{HMA} = resilient modulus of existing HMA layer (MPa)

H_{base} = thickness of base layer (mm)

E_{base} = resilient modulus of base layer (MPa)

$E_{subgrade}$ = resilient modulus of subgrade (MPa).

The interaction between the different variables was also considered, but was found statistically insignificant. It is interesting to notice from this equation that the overlay thickness is undoubtedly the major factor in dictating the overlay performance against reflective cracking failure, followed by the thickness of the existing HMA layer. Additionally, it appears that the base thickness and subgrade modulus has the least effect on the overlay performance.

Although this model was exclusively developed based on a variety of three-layer pavement structures, it may be easily extended to cover a broader number of cases using the Odemark's method. For example, if a subbase was used, it may be converted to an equivalent base thickness using Equation 4.8 as follows (52).

$$h_e = h_{sub} \left[\frac{E_{sub}(1 - \nu_{base}^2)}{E_{base}(1 - \nu_{sub}^2)} \right]^{1/3} \quad (4.8)$$

where, h_e = equivalent base thickness

h_{sub} = original subbase thickness

ν_{base} = base material Poisson's ratio

$\nu_{subbase}$ = base material Poisson's ratio.

4.1.5 Design Example (45)

Consider a pavement structure consisting of a 150 mm HMA layer ($E_{HMA} = 2500$ MPa, $\nu = 0.25$), 150 mm base layer ($E_{base} = 275$ MPa, $\nu = 0.35$), 300 mm subbase layer ($E_{subbase} = 135$ MPa, $\nu = 0.35$), on top of a subgrade ($E_{subgrade} = 68$ MPa, $\nu = 0.40$). Using the Odemark's method, the subbase layer may be transformed to an equivalent base layer resulting in a total base thickness of 385 mm. The designer estimates a total accumulative traffic (80-kN repetitions) of 9.0×10^5 over the service life of the overlay. Using Equation 4.7, the required overlay thickness is 75 mm ($E_{overlay} = 4480$ MPa, $\nu = 0.25$) to sustain the estimated traffic. Depending on fund availability, the designer may then decide to use a multi-stage construction strategy, a reinforcing interlayer system, or any other rehabilitation alternatives to maximize the benefit-cost ratio.

4.2 ASPHALT RUBBER ASSOCIATION OVERLAY DESIGN MODEL

In 1999, the Rubber Pavements Association (RPA) contracted with Consulpav to develop a mechanistic overlay design method for reflective cracking in HMA overlays that are applied to existing cracked HMA pavements (53). The research project involved the development of mathematical and statistical models based upon 3D finite element method (FEM) to determine the stresses and strains in the HMA overlay above the crack. The FEM approach was selected since it is the most sensible way to address the unusual

stress and strain patterns and contours generated by a truck load moving over an overlay placed upon a cracked pavement. The SAP2000 finite element program with linear elastic ASOLID element under the plain strain mode was used in the analyses to model the subgrade layer, the base layer, the cracked bituminous layer, the HMA overlay, and the crack and the zone above the crack. The FEM modeled crack movements were calibrated using actual field measurements with a crack activity meter (CAM) and a Falling Weight Deflectometer (FWD) conducted in Portugal, Arizona and California. The vast majority of this field testing was conducted on cracked Interstate pavements in Arizona. The results of these experiments helped to calibrate the FEM statistically derived model and showed that the CAM correlated very well crack movements and deflections produced by the FWD in the pavement. The “Von Misses strain” was recommended as the statistical factor to determine the development of the crack.

The next phase of this research involved laboratory testing that simulated the observed field crack movements and measured stresses and strains on test specimens similar to the actual field mixes. Two typical mixes using a good quality Portuguese granite aggregate similar to Watsonville granite were prepared and tested in Portugal. One mix consisted of a dense gradation like that used in Arizona and California. Five percent PG70-10 asphalt binder was added to the dense graded aggregate and compacted using the rolling wheel compactor to various levels of air voids (HMA-DG). The second mix (AR-HMA-GG) consisted of an eight percent asphalt rubber (AR) gap graded mix similar to that used in Arizona and California. The AR binder consisted of 80% PG64-16 (Penetration 35/50) base asphalt and 20% ground tire rubber.

These two HMA mixes represented the basis of the mechanistic design method.

Cores and beams were sawed from the rolling wheel compacted slabs. The six inch (150 mm) diameter by two inch (50 mm) high cores were tested with a Reflective Crack Testing device (RCD) specifically built for this research. The RCD is composed by two U-shaped pieces where the specimen is fitted. The base of the device represents the existing pavement and the opening between the U-shaped pieces represents the crack width. The bottom of the specimen is glued to the base of the device and pressed by pistons existing at the top of the device in such a way that either a horizontal or vertical movement can be imposed on the core. Sensors on the core record stresses and strains of the core immediately over the crack.

Figures 4.2 and 4.3 show the RCD with each of the U-shaped pieces connected to a horizontal and a vertical actuator to apply displacements to the specimen. The device was used to apply the displacements measured in the road with the crack activity meter. The RCD simulates the zone above the existing crack of the old pavement which is the zone of the overlay layer that is subjected to reflective cracking (Figure 4.4).

In addition, beams from both mixtures were tested with the four point bending beam fatigue test developed during the Strategic Highway Research Program (SHRP). Results of these tests indicated that the beam fatigue test could be used in place of the reflective crack test (RCD) to derive the necessary input parameters to the FEM model.

The data and test results from the two phases of this research served in the determination of the parameters that best fit the FEM reflective cracking statistical simulation as a function of truck traffic. The model predicts how many truck loading and their corresponding stresses and strains will be needed to bring about a reflective crack.

This mathematical-statistical model was converted into a practical pavement

design method for reflective cracking by reviewing considerable actual field cracking data and material layer properties. First, the estimated traffic to a reflective crack was calculated from the layer thickness and layer modulus and then compared to the actual observed number of truck loading and percent cracking. As long as the ratio of the estimated traffic to the actual traffic stays below 1.0 no cracking would occur. For ratios above 1.0 the different levels of percent cracking would be observed. Aging and temperature adjustment factors were also introduced to this approach.

The final product of this research was an EXCEL spreadsheet that estimates the thickness of a PG70-10 or an AR HMA overlay mix for the specified level of reflective cracking for a wide range of truck traffic loading. The expected design level of cracking, the thicknesses and the elastic moduli of the existing pavement layers, and the modulus of the HMA overlay are inputs for the EXCEL spreadsheet. The moduli may be backcalculated or determined in any reasonable manner, as long as they represent the in situ conditions in the field.

The proposed solution is reliable for these two analyzed mixes (i.e., PG70-10 HMA and AR-HMA) and for climatic conditions similar to those encountered in the (mainly) desert southwest (i.e., Arizona and California). With additional research, curves could be developed for additional mixes, other climates and other field observed historical reflective cracking levels.

4.2.1 Proposed Reflective Cracking Design Method

The method consists of the seven steps presented below (53). Currently the model has been calibrated for only two materials: Dense graded mixes with PG70-10 binders (HMA-DG) and gap graded mixes with asphalt rubber modified binders (AR-

HMA-GG). The asphalt rubber binder must be produced using the “wet” process and it must contain approximately 19-20% crumb rubber.

Step 1: Determination of the moduli and thicknesses of the pavement section layers

This can be accomplished using FWD backcalculation methods or other forms of estimating cracked pavement section moduli. Care must be taken in the selection of modulus representative of the most damaged sections. As such, the 90th or 95th percentile of deflections (or backcalculated moduli) should be selected. Coring for determination of layer thicknesses should be carried out as close to the locations where the 90-95th percentile FWD test points were selected.

Step 2: Determination of representative air temperatures

The maximum and minimum air temperature determined with the desired reliability should be obtained for the location where the pavement is to be overlaid. Furthermore, it is necessary to compute the weighted mean annual air temperature (*w*-MAAT) as proposed by the Shell design method and provided by Equation 4.9 (54).

$$w - MAAT = 7.7068 \times \ln(w - factor) + 20.275 \quad (4.9)$$

where the *w-factor* is a function of the mean monthly air temperature (MMAT) and can be determined using Shell Equation 4.10. The *w-factor* in Equation 4.9 is the average of *w-factors* calculated for all 12 months of the year.

$$w - factor = 0.0723 \times e^{0.1296 \times MMAT} \quad (4.10)$$

Step 3: Selection of design cracking percentage

The design cracking percentage value selected should be in keeping with an

agencies overlay policy. ADOT generally has observed less than five percent cracking over a period of ten years when an asphalt rubber surface mix is used.

Step 4: Determination of adjustment factors

Several adjustment factors must be calculated for the location where the overlay will be placed and for the desired cracking level at the end of the overlay's design life.

Aging Adjustment Factor

The Aging Adjustment Factor (*AAF*) is determined from the maximum air temperature (T_{max}) using Equation 4.11 for conventional PG70-10 mixes (i.e., HMA-DG), and using Equation 4.12 for asphalt rubber mixed with the gap-graded wet process at 19 – 20% crumb binder (i.e., AR-HMA-GG).

$$AAF = 0.0363 \times T_{(\max\ air)} + 0.3000 \quad (4.11)$$

$$AAF = 0.0088 \times T_{(\max\ air)} + 0.8800 \quad (4.12)$$

The *AAF* was introduced to capture the effect of aging in the overlay as a function of the maximum air temperature. Aging will stiffen the HMA overlay as a function of time and temperature. The above relationships are applicable for maximum air temperatures (T_{max}) between 35 and 50°C. Further improvements in the relationships are still needed.

Temperature Adjustment Factor

The temperature adjustment factor was included in the analysis to take into consideration the combined action of the two important variables in reflective cracking: the wheel loads on a daily basis above (or near) the crack and the overlay material above

the crack being under tension due to rapidly decreasing or low temperatures. Those factors have been identified as the most likely causes of high states of stress and strain above the crack.

The Temperature Adjustment Factor (TAF) is determined from Equation 4.13 for HMA-DG mixes and Equation 4.14 for AR-HMA-GG mixes (wet process only). This method is applicable for Reflective Cracking Temperatures (RCTs) between -10°C and $+10^{\circ}\text{C}$. The RCTs corresponds to the typical range of temperatures when the reflective cracking is expected to occur.

$$TAF = -0.09 \times RCT + 2.55 \quad (4.13)$$

$$TAF = -0.072 \times RCT + 1.7448 \quad (4.14)$$

$$RCT = T_{(\min \text{ air})} + 0.5 \times (T_{(\text{average air mean monthly})} - T_{(\min \text{ air})}) \quad (4.15)$$

Field Adjustment Factor

The Field Adjustment Factor (*FAF*) was introduced to relate the predictions obtained using the empirical-mechanistic reflective cracking model with the actual (reported and observed) field performance. The *FAF* is computed from the actual percent cracking (PC) using Equation 4.16. Cracking is only expected when *FAF* is greater than 1.

$$FAF = e^{0.2303 \times PC} \quad (4.16)$$

Step 5: Selection of overlay material modulus

Two types of materials for the overlay may be selected: Conventional HMA-DG or AR-HMA-GG, with the rubberized binder prepared through the wet process at 19-20%

crumb rubber in the binder. For these materials, the modulus and flexural fatigue life are obtained through flexural fatigue tests (AASHTO T321). Other moduli can be computed and introduced in the method based on actual tests performed on other types of materials. However, it must be assumed that the Temperature Adjustment Factor (*TAF*) or the Aging Adjustment Factor (*AAF*) will either be identical to that of the HMA-DG material or the AR-HMA-GG material.

Step 6: Determination of the design value “Von Mises” strain

The modulus of the overlay must be multiplied by the computed Aging Adjustment Factor. Then, the modulus of the existing and overlay HMA must be adjusted to the *w-MAAT* temperature. With the modulus and thickness for each layer, the “Von Mises” strain (ε_{VM}) value for the overlay is determined using Equations 4.17, 4.18, and 4.19. The ε_{VM} value obtained through these equations must be multiplied by 86/132 to convert ε_{VM} from 130 kN to 80 kN axle loads, and also by the Temperature Adjustment Factor (*TAF*). Such factor was included because the “Von Mises” Strain was originally computed for 130 kN axles, and it was then adjusted proportionally for the 86 kN axles. The value obtained in this process is thus the design ε_{VM} .

$$\varepsilon_{VM} (1 \times 10^{-6}) = a [\text{Overlay thickness}(m)]^b \quad (4.17)$$

$$a = \prod_{i=6}^6 [a_{1i} * \ln(X_i) + a_{2i}] \quad (4.18)$$

$$b = \prod_{i=6}^6 [b_{1i} * \ln(X_i) + b_{2i}] \quad (4.19)$$

where ε_{VM} is in 1×10^{-6} m/m, overlay thickness in meter, a_{1i} and b_{1i} are coefficients given

in Table 4.2, and the variables X_i represent the pavement properties of thicknesses and moduli with $i = 1$ for thickness of the cracked HMA; $i = 2$ for thickness of the granular base; $i = 3$ for HMA overlay modulus; $i = 4$ for cracked HMA modulus; $i = 5$ for granular base modulus; and $i = 6$ for subgrade modulus. Table 4.3 shows the order introduced for the X_i values along with the minimum and maximum limits for each variable used in the definition of the model.

Step 7: Determination of design equivalent single axle load (ESAL's)

The last step of this process, determines the number of ESALs that can be withstood by the overlay prior to the onset of reflective cracking using the flexural fatigue Equation 4.20 for the HMA-DG mix with PG70-10 binder or Equation 4.21 for the AR-HMA-GG mix with the asphalt rubber binder binders derived through the wet process, with a 19-20% crumb rubber. ε_{VM} is in 1×10^{-6} m/m.

$$ESALs = 4.1245 \times 10^{19} \times \varepsilon_{VM} (1 \times 10^{-6})^{4.9761} \quad (4.20)$$

$$ESALs = 6.4467 \times 10^{19} \times \varepsilon_{VM} (1 \times 10^{-6})^{-5.93} \quad (4.21)$$

The design ESALs need to be multiplied by the FAF computed in *Step 4*. The resulting number should represent the number of ESALs required for the overlay to reach the selected percentage of cracking. Other fatigue curves can be determined and used by this method, based on actual flexural fatigue tests performed on the specific asphalt (whether conventional or modified) material type proposed with due consideration to all adjustment factors. Figure 4.5 shows a flowchart of the proposed design method.

4.3 THE NEW AASHTO MODEL FOR REFLECTIVE CRACKING

In the new AASHTO Mechanistic-Empirical Pavement Design Guide (MEPDG),

the design procedure for HMA overlays of existing HMA surfaced pavements considers distresses developing in the overlay as well as the continuation of damage in the existing pavement structure. However, it should be noted that the reflective cracking models incorporated in the MEPDG were based strictly on empirical observations and were not a result of rigorous mechanistic-empirical analysis (55).

An active NCHRP 01-41 research study is undergoing to address the issues associated with reflection cracking and to develop mechanistic-based models for use in mechanistic-empirical procedures for the analysis and design of HMA overlays. The objective of the research is to identify or develop mechanistic-based models for predicting reflection cracking in HMA overlays of flexible and rigid pavements and associated computational software for use in mechanistic-empirical procedures for overlay design and analysis.

The proposed MEPDG overlay design procedure allows the designer to consider two types of reflective cracks: a) reflective cracks that exist on the surface prior to overlay placement and b) those that develop in the existing surface after overlay placement.

4.3.1 HMA Overlay of Cracked HMA Pavement Surface

The percentage of reflective cracks through the overlay is predicted as a function of time using the sigmoidal function shown in Equation 4.21.

$$RC = \frac{100}{1 + e^{a+bt}} \quad (4.21)$$

where, RC = Percent of cracks reflected
 t = Time in years

$$a = 3.5 + 0.75 \times h_{ac}$$

$$b = -0.688584 - 3.37302 \times (h_{ac})^{-0.915469}$$

$$h_{ac} = \text{HMA overlay thickness in inches.}$$

The a and b fitting parameters are function of the HMA overlay thickness and are hard coded in the MEPDG software. The designer cannot directly alter these parameters as inputs, but can change them in the software. It is recommended that an agency use historical data to develop a local reflection cracking model.

Additionally, the MEPDG approach assumes that a properly installed fabric is equivalent to 2 inch of HMA overlay. This is purely based on empirical considerations. A Minimum of 2 inches is recommended for the HMA overlay thickness (h_{ac}) of flexible pavements.

4.3.2 HMA Overlay of Crack-free HMA Pavement Surface

Even after overlay placement, the underlying bound layers (including all asphalt bound and chemically stabilized layers) undergo additional fatigue damage with continued traffic loading, and will eventually crack. The continual fatigue damage accumulation of these layers is considered in the overlay analysis procedures of the MEPDG. For any given month m , the total fatigue damage is estimated by Equation 4.22.

$$D_m = \sum_{i=1}^m \Delta D_i \quad (4.22)$$

where, D_m = Damage for month m
 ΔD_i = Increment of damage in month i .

The area of fatigue cracking for the underlying layer at month m (CA_m) is given

by Equation 4.23.

$$CA_m = \frac{100}{1 + e^{6-6 \times D_m}} \quad (4.23)$$

For each month i , there will be an increment of damage ΔD_i which will cause an increment of cracking area ΔCA_i to the stabilized layer. To estimate the amount of cracking reflected from the stabilized layer to the surface of the pavement for month m , the reflective cracking model is applied incrementally, as follows:

$$TRA_m = \sum_{i=1}^m RC_{m-i} \times \Delta CA_i \quad (4.24)$$

where, TRA = Total reflected area for month m

RC_{m-i} = Percent cracking reflected for age $m - i$ (age in years)

ΔCA_i = Increment of fatigue cracking for month i .

The reflective cracking model is applied to each increment of fatigue cracking area because the time elapsed for each of these increments is different. The model included in the MEPDG is based on engineering judgment and a limited amount of published data.

4.4 DESIGN EXAMPLE USING THE VARIOUS ANALYSIS MODELS

In this example, an HMA overlay was designed for a typical flexible pavement section (Figure 4.6) using the various analysis models described before. The existing pavement structure consists of a 4.0 inch (100 mm) HMA layer with a modulus of 360 ksi ($E_{HMA} = 2500$ MPa) and a 10 inch (250 mm) base layer with a modulus of 30 ksi ($E_{base} = 210$ MPa) on top of a subgrade with a modulus of 12 ksi ($E_{subgrade} = 83$ MPa).

4.4.1 Traffic Data

The traffic ESALs are estimated as function of years for an annual average daily traffic (AADT) of 30,000 and a truck percentage of 3.84 percent. The traffic information was obtained from the NDOT 2006 annual traffic report for the McCarran Boulevard in Reno Nevada area. Table 4.4 summarizes the design ESALs over the 20 years analysis period.

4.4.2 HMA Overlay Material Properties

The analysis was conducted for three different HMA mixes that were designed using different aggregate gradations from the Sloan pit in Southern Nevada and a PG76-22NV polymer modified asphalt binder. The three mixtures consisted of:

- NDOT Type 2C gradation, designated as T2C.
- Caltrans gradation used for intersection, designated as CT.
- No Rut Mixture gradation, designated as NRM.

All three mixes were designed according to the NDOT Hveem Mix Design Method as outlined in the NDOT Testing Manual. It should be noted that all mixtures were treated with 1.5% of hydrated lime following the NDOT specifications. The dynamic modulus test (AASHTO TP62) was used to develop the dynamic modulus master curve of the various HMA mixtures. Table 4.5 shows the dynamic modulus ($E_{overlay}$) of the various overlay mixtures at a temperature of 70°F and a loading frequency of 10 Hz.

The fatigue characteristics of the HMA mixtures were evaluated using the flexural beam fatigue test “AASHTO T321-03: Determining the Fatigue Life of Compacted Hot-Mix Asphalt Subjected to Repeated Flexural Bending”. The following equations show the fatigue relationship for each of the evaluated mixtures.

$$\text{T2C: } N_f = 1.3740 \times 10^{-5} \times \left(\frac{1}{\varepsilon}\right)^{4.4142} \left(\frac{1}{E_{\text{overlay}}}\right)^{2.0374} \quad (4.25)$$

$$\text{CT: } N_f = 6.5815 \times 10^{-5} \times \left(\frac{1}{\varepsilon}\right)^{4.3172} \left(\frac{1}{E_{\text{overlay}}}\right)^{2.0598} \quad (4.26)$$

$$\text{NRM: } N_f = 6.8745 \times 10^{-5} \times \left(\frac{1}{\varepsilon}\right)^{4.2395} \left(\frac{1}{E_{\text{overlay}}}\right)^{2.1470} \quad (4.27)$$

where, ε is the flexural strain in microns and E_{Overlay} is the stiffness of the HMA mixture in ksi.

4.4.3 Overlay Design Using Virginia Tech Simplified Overlay Model

Using Equation 4.7, the required HMA overlay thickness as a function of the predicted traffic (ESALs) is shown in Figure 4.7 for the various mixtures. Based on the Virginia Tech Simplified Overlay Design method an overlay thickness of 3.25, 4.0, and 4.5 inch is required for the NRM, CT, and T2C mixes to sustain the predicted 20 years design ESALs, respectively. Therefore, the T2C mix exhibited relatively the best resistance to reflective cracking, followed by the CT mix, followed by the NRM mix.

4.4.4 Overlay Design Using Asphalt Rubber Association Method

Currently the AR model has been calibrated for only two materials: dense graded mixes with PG70-10 binders (HMA-DG) or gap graded mixes with asphalt rubber modified binders (AR-HMA-GG). However, still the AR model can be used with the overlay mixture specific fatigue characteristics. Therefore, the various mixtures fatigue curves shown in Equations 4.25-4.27 are used in this method to estimate the traffic in ESALs required for the overlay to reach a selected percentage of cracking.

The maximum, minimum, and mean monthly air temperatures are determined for the Reno area using the LTPPBind (version 3.1) software. A temperature of -16°F (-26.5°C) and 103°F (39.3°C) were determined for the minimum and maximum air temperature where the existing pavement is to be overlaid, respectively. The mean monthly air temperature was found to be 50°F (10°C).

The analysis was conducted for 5, 10, and 15 percent of reflective cracking at the end of the design life. The required HMA overlay thickness as a function of the predicted traffic (ESALs) is shown in Figures 4.8 to 4.10 for the various mixtures.

Figures 4.8-4.10 show that, for the same design ESALs, a thinner overlay thickness is required for the T2C mix followed by the CT mix followed by the NRM mix to reach the same selected percentage of cracking.

An additional analysis was conducted to determine the percentage of cracking in each mix using the previously determined corresponding overlay thickness after 20 years using the Virginia tech method. In other words, the percentage of cracking in the overlay mix was obtained for an overlay thickness of 4.5, 4.0, and 3.25 inches for the T2C, CT, and NRM mixes, respectively.

Figure 4.11 shows that, the 4.5 inch T2C overlay mix exhibits no cracks after 20 years, the 4.0 inch CT overlay mix exhibits 3.5 percent cracking after 20 years, and the 3.25 inch NRM overlay mix exhibits 17 percent cracking after 20 years.

4.4.5 Overlay Design Using the New AASHTO Model for Reflective Cracking

The percentage of reflected cracks (RC) from a cracked HMA pavement surface through the overlay is predicted as a function of time using the sigmoidal function shown in Equation 4.21. The AASHTO method was applied for a 5, 10, 15, and 20 percent of

reflected cracks. Table 4.6 and Figure 4.12 show the required overlay thickness as a function of predicted traffic ESALs. It should be noted that the new AASHTO method is independent of the overlay material properties; hence the same overlay thickness is required for all three mixes (i.e., T2C, CT, and NRM).

It should be noted that RC is the percent of cracks reflected from the existing cracked pavement surface. Therefore, the time for the cracks in the existing pavement to be 100% reflected in the overlay was also determined. Figure 4.13 shows the required overlay thickness as a function of traffic for a 100% reflection of the cracks in the existing pavement. An overlay thickness of 11.25 inch is required to sustain the predicted 20 years design ESALs (i.e., 7,074,390). It should be noted that, the new AASHTO design manual recommend the development of a local reflection cracking model using historical data.

4.4.6 Summary of Design Example

Figures 4.14-4.16 compares the required overlay thickness determined from the Virginia Tech, asphalt rubber, and the new AASHTO analysis methods. The Virginia Tech and the asphalt rubber analysis models resulted in a relatively comparable overlay design thicknesses with the Virginia Tech method being more conservative. On the other hand, the AASHTO method overestimated the overlay thickness compared to the Virginia Tech and the asphalt rubber methods.

Chapter 5 – REVIEW OF REFLECTIVE CRACKING TESTING METHODS

This chapter reviews all the laboratory and field tests that are being used to evaluate the resistance of HMA mixtures and pavements to reflective cracking. Laboratory tests are typically used to evaluate the resistance of the HMA mixtures to reflective cracking during the mix design stage. Field tests are used to evaluate the performance of the rehabilitation technique used to minimize reflective cracking in HMA pavements. In this chapter, the appropriate laboratory and field tests will be identified and assess their potential effectiveness in NDOT's mix design and field evaluation processes. Based on these evaluations, the most promising tests will be recommended.

5.1 CRACOW UNIVERSITY OF TECHNOLOGY, CRACOW, POLAND

In 1993, the University of Technology of Cracow, Poland, evaluated the effectiveness of geosynthetics in HMA overlays for preventing reflective cracking (56). The reflective cracking resistance of an HMA overlay reinforced with a geogrid was assessed with the following three laboratory tests: bending test under a static load, bending test under a repeated load, and the shearing test.

The bending test under a static load was performed to study the resistance of an HMA overlay with and without geotextile reinforcement at the bottom of the HMA under a static load at a constant rate of application. The setup and dimensions of the tested HMA beams are presented in Figure 5.1. The test samples consist of a 12×3×3 inch (30×7.5×7.5 cm) HMA beams compacted in a static manner. The geotextile is placed at 1/3 of the beam height from the bottom. The beam is simply supported at both ends and

loaded uniaxially at the center at a rate of 0.47 in/min (12 mm/min). The samples were tested at a temperature of 20°C.

The test results for the bending test under static load are shown in Figure 5.2. The maximum measured applied force along with the corresponding bending deflection of the beam are used to calculate the bending strength. It was concluded that the bending strength of HMA mixtures was not substantially affected by the presence of the geotextile. The geotextile influenced the behavior of the samples after cracking of the HMA mix by prolonging the integrity of the beams.

The bending test under repeated load was performed to analyze a loading pattern similar to field loading. Tests were performed at 20°C and on beams with the same setup and dimensions of the bending under static load test. The samples were simply supported at both ends and subjected to the vertical repeated loading using a haversine function with a frequency of 5 Hz and an amplitude of 450 lbs (2 kN) resulting in a bending stress at the outer fiber of 193 psi (1.33 MPa). Measurements of the applied force versus the beam deflection were conducted until the cracking of the HMA mix. Table 5.1 summarizes the number of load repetitions to visible crack in the HMA beams with and without geotextile. Researchers concluded that the HMA samples with geotextile exhibited a substantially greater resistance to the crack development than the samples without geotextile (56). Due to the presence of the geotextile, the HMA layer sustained nearly twice the number of loading cycles before the crack appears.

The shearing tests was performed to study the role of geotextile in HMA overlays as a stress-relieving medium diminishing the stress concentrations above the crack in the lower part of a pavement structure. This approach required the examination and

qualitative estimation of the adhesion between the geotextile and the HMA layers. To this end, a method of direct shear test was developed at Cracow University of Technology (56). The samples, in the form of beams were cut into pieces of a length 2.7 to 3.1 inch (68 to 80 mm) and subjected to shear stresses as shown in Figure 5.3. This test consisted of applying a static force on the sample at a loading rate of 4×10^{-2} in/min (1 mm/min). The test was conducted at a temperature of 30°C. At failure, the maximum shear force is determined and used to calculate the maximum shear stress. Table 5.2 summarizes the maximum shear force and stress in the HMA beams with and without geotextile.

The results for the shearing test showed that the presence of the geotextile diminished by more than two times the maximum shear force and the maximum shear stress acting over the HMA sample. This factor is highly significant in reducing the susceptibility to reflective cracking of the HMA overlay.

The results for the shearing test showed that the presence of a geotextile interlayer diminishes by more than 2 times the adhesion between asphalt layers. This phenomenon is advantageous for the prevention of reflective cracking because the geotextile absorbs the part of the crack energy from the lower cracked layers and does not transfer it upwards.

5.2 TECHNION-ISRAEL INSTITUTE OF TECHNOLOGY, HAIFA, ISRAEL

In 1993, Livneh et al. (57) used the wheel tracking device to predict the behavior of asphaltic pre-coated geotextile felts in retarding reflective cracking. The wheel tracking device consisted of a loaded wheel that travels back and forth on top of an HMA beam that is placed over an elastic rubber base simulating the mode I type of fracture.

The Mode I loading (opening mode, KI) is also called strain mode and results from loads that are applied normally to the crack plane (thermal and traffic loading). The HMA beam had a rectangular groove with a starter notch at the bottom of the groove. Figure 5.4 shows a schematic diagram of the wheel tracking device. The crack length along both sides of the HMA slab is visually determined. The device was located in a temperature-controlled room at a constant temperature of 25°C. The tested HMA beam is 27.6 inch long, 4 inch wide and 4 inch thick (70×10×10 cm).

Three different types of beams were prepared for all tests and are shown in Figure 5.5: 1) beam composed of two HMA layers with a welded fabric in between, 2) monolith HMA beam, and 3) beam composed of two HMA layers bonded with a tack-coat. An artificial groove of 1.2 to 2.0 inch (30 to 50 mm) deep and 0.16 inch (4 mm) wide is made at the center of the bottom of the beam samples. The edge of the groove is rounded. Neither the magnitude of the applied load nor the frequency was reported by the Researchers.

For this study, three types of fabrics were examined (3M, 3/250 and 4/180) along with a monolithic HMA sample and an HMA sample compacted in two layers bonded with a tack coat at a rate of 250 g/yd². For all the cases, the HMA was dense graded with an asphalt grade of 60/70.

In addition to the number of wheel loading repetitions to failure, a phenomenon of dual cracking was observed in some of the tests. The phenomenon is characterized by the propagation of a crack which begins at the edge of the artificial groove and the propagation of a crack which begins on the upper surface. This phenomenon was

observed in half of all beams which did not contain fabric and took place in all beams which included membranes of all of the various types

Figure 5.6 shows the fatigue test results under the wheel-tracking device. The results showed that the geotextile fabric type 3/250 significantly outperformed the rest of the treatments. Its resistance to reflective cracking was about 4 times greater than the other treatments. However, it was shown that the resistance to reflective cracking of the monolithic HMA beam and the HMA sample compacted in two layers was greater than the rest of the geotextile felts (the 3M and the 4/180).

Despite its limitations, the researchers concluded that the wheel-tracking testing device adopted and improved in this study can serve as a reliable method for diagnosing the efficiency of the various treatments for reflection cracking retardation.

5.3 GEO-MATERIALS LABORATORY, ENTPE, FRANCE

In 1992, the Geo-materials Laboratory of France conducted a research to study the reflective cracking in a flexible pavement composed of an HMA overlay placed over a cement treated base course (58). A prototype apparatus called “Fissurometer” was proposed to simulate the reflective cracking phenomenon in the laboratory. The fissurometer allows only for the Mode I type of fracture mechanics failure by simulating reflective cracking due to thermal shrinkages of the pavement. The test is run in two steps: monotonic and dynamic modes.

The fissurometer apparatus shown in Figure 5.7 consists of an upper HMA layer placed on top of two steel plates. One of the steel plates is fixed and the other is moved apart by two force transducers that apply a fixed opening and/or closing rate and subjecting the HMA layer to shear loads. The applied load can be either monotonic or

dynamic cycles. The shearing cycles mimic the typical thermal gradients in France. The shear is provoked by the horizontal displacement of the moving part. The opening and closing speed of the moving part varies between 0.05 and 0.22 in/hr (1.3 to 5.5 mm/hr).

The measuring system is composed of an ultrasonic transmission (US) system, force transducers, strain gauges and temperature probes. The force transducers can vary the speed of opening and closing of the gap below the HMA overlay. The amplitude of the opening plate can be varied for different test conditions. The US system can measure the energy transmitted by an ultrasonic wave train applied through the test sample. This wave train goes through the area where the cracking should appear (near the vertical section crossing the pre-cracking gap). The force transducers and the US provide a damage characterization of the HMA overlay. It can be used as an indication of the cracking resistance of the material.

The proposed apparatus was validated by comparing the results given by the fissurometer for mixtures with different cracking mitigation techniques to their performance from test sections built on the French highway RN 20. As a result, the researchers concluded that the four evaluated techniques were classified with the fissurometer in reverse order for the top two techniques when compared to their field observations at the experimental test sections on RN 20. The researchers relate the difference in resistance to reflective cracking between laboratory and field back to the basis of the fissurometer apparatus that simulates only thermal shrinkage without considering the effect of the traffic.

5.4 TECHNICAL UNIVERSITY OF VIENNA, AUSTRIA

In 1993, Tschegg et al. from the Technical University of Vienna, Austria developed a new testing device to characterize the mode I type of fracture in HMA mixtures (59). The device is called the wedge splitting method. The test device measures the load-displacement curve of a cubical or cylindrical HMA sample and provides information to completely characterize the fracture behavior of the tested specimens. Crushed and natural gravel HMA mixtures were tested to initiate the validation of this test method.

The principle of the testing method is shown schematically in Figure 5.7.a. Cubical (or prismatic) specimens are placed on a narrow linear support in a compression testing machine. The specimen has a rectangular groove with a starter notch at the bottom of the groove. Two load transmission pieces are placed in the groove. A wedge split is formed by inserting a wedge. Wedge, starter notch and linear support area are in the same vertical plane. The wedge transmits a force F_M from testing machine to the specimen. The slender wedge exerts a large horizontal force component F_H and a small vertical force component F_V on the specimen. The horizontal component splits the specimen similar as in a bending test. The force F_M is determined with a load cell in the testing machine. Knowing the wedge angle (approximately 5-10°), the force F_H in the horizontal direction which causes splitting of the specimen is calculated. The vertical force component F_V is small and does not influence the result if the wedge angle is small enough. The load application rate is 0.05 in/min (1.3 mm/min). Figure 5.7b shows the schematic load-deformation curve for a brittle and a ductile material.

Splitting must take place during stable crack propagation until complete separation of the specimen. This is possible with a stiff loading system only (wedge-loading system – testing machine). The wedge loading part is extremely stiff, i.e., it stores little deformation energy. Therefore, such experiments can be performed with usual mechanical spindle driven machines or hydraulic machines under strain or stroke controls together with the described loading device.

In order to reduce friction between wedged and the load transmission pieces, roll bodies (e.g. roller bearings) have been introduced in between. Displacement gauges are mounted on both ends of the starter notch in order to measure the displacement on the line of force application (crack opening displacement).

Different specimen shapes may be used in the above described method and are shown schematically in Figure 5.8. The Force F_M and the displacement δ can be registered during the test using an electronic device. The area under the load-displacement curve corresponds to the necessary energy to split the sample. Dividing this energy by the fracture area (plain projection of the area under the applied load), yields the specific fracture energy of the material (G_F). The G_F is a property of the material and does not depend on the specimen shape and size. Figure 5.9 shows the typical three charts obtained through this test:

- Horizontal force versus displacement curve at any give temperature
- Maximum vertical force versus temperature curve
- Fracture energy versus temperature curve

Characteristic load-deformation diagrams were performed for crushed and natural gravel HMA mixtures and the results are shown in Figure 5.10. The tests were performed at three temperatures: 8°C, -0.5°C, and -21°C. The six diagrams clearly show

that the deformation and the fracture behavior of the materials is changing with temperature. The slope of the curves is determined by the elasto-plastic behavior of the material. A steep and linear curve implies a high modulus of elasticity and little plastic deformation. On the other hand, a pronounced deviation from the linear behavior indicates a low modulus of elasticity and high deformation. The post-peak behavior characterized the fracture process. If the curve decreases quickly as shown in Figure 5.10.c, little energy is consumed for the crack propagation, and brittle fracture is observed. Contrary to this behavior, Figure 5.10.a shows a ductile fracture. In this case, the horizontal force approaches zero only at high values of the displacement. It is also shown that at low temperatures the crushed gravel withstand higher horizontal forces than the natural gravel.

Figure 5.11 shows the test results for the maximum splitting force and the specific fracture energy as a function of the testing temperatures. Figure 5.11.a shows that for temperatures between -21°C and $+8^{\circ}\text{C}$ the crushed stone has higher values of maximum splitting force. Figure 5.11.b shows that the specific fracture energy varies between 200 and 1100 N/m. At -21°C there is no significant difference between both mixtures. Between -5°C and $+5^{\circ}\text{C}$, the specific fracture energy for the crushed gravel mixture exhibit a pronounced maximum which is about 2.5 times higher than that of natural gravel. At $+8^{\circ}\text{C}$ the crushed gravel specific fracture energy is about twice of that of natural gravel.

The researchers concluded that the maximum splitting force is not an appropriate parameter to differentiate between HMA mixes since two different mixes can have the same maximum splitting force and different fracture behavior. On the other hand, the

specific fracture energy was recommended as a more reliable testing parameter to differentiate between various mixes. This parameter can better describe the fracture behavior of the material.

5.5 LABORATORY OF PUBLIC ROADS OF AUTUM, FRANCE

In 1993, Dumas and Vecoven (60) summarized the results and findings of 210 shrinkage-bending tests performed on various kinds of reflective cracking mitigation techniques. The shrinkage bending test used in this study was developed in 1988 to assess the efficiency of anticracks systems. The test simulates at the same time the pavement thermal contraction and the heavy traffic loads at a constant temperature (5°C).

The shrinkage-bending test shown in Figure 12 consists of an HMA overlay or a combination of HMA overlay and a cement treated base that are placed on top of two steel plates. One plate is fixed and the other is forced to move at a constant speed. The traffic loads are simulated by applying a vertical sinusoidal cycling load with a frequency of 1 Hz and a vertical movement of 7.9×10^{-3} inch (0.2 mm). Consequently, the test simulates concurrently both modes I and II type of fracture mechanics failures. The test is performed as follows.

- The thermal shrinkage of pre-cracked pavement is simulated by the opening of the movable plate (average speed 0.024 inch/hr).
- The action of a traffic axle is simulated by a cyclic loading at a frequency of 1 Hz monitored by the deflection set to 0.079 in (0.2 mm).
- The test sample is 23.6×2.8×2.8 inch (60×7.0×7.0 cm).
- The speed at which a crack open and close is 0.04 inch/hr (1 mm/hr).

The measurements during the test consist basically of a visual determination of the crack initiation time and length, crack propagation time and length, and breaking time of the sample. Such information is used to determine the crack speed at any of these

stages. The breaking time is considered as the efficiency of the reflective cracking mitigation technique.

Figure 5.13 shows the initiation time of the crack, its propagation speed in the first centimeter and the breaking time for two different HMA overlay mixtures.

Table 5.3 shows the test results of a 2.4 inch (6 cm) AC 0/10 overlay on top of a fabric interlayer, a rich-binder HMA mix, and a Stress Absorbing Membrane Interlayer (SAMI). It was concluded that the paving fabrics delays the crack initiation time, while the rich HMA mix slows down the crack propagation. The behavior of the SAMI is more similar to that of the paving fabrics.

5.6 UNIVERSITY COLLEGE OF DUBLIN, IRELAND

In 2002, Gibney et al. (61) assessed the resistance to reflective cracking of a variety of HMA mixtures that are used in Ireland using an accelerated simulative wheel tracking test in accordance with the British Standard (BS) 598 (62). The device is capable to simulate top-down and bottom-up cracking in the HMA layer on top of concrete slabs. This test simulates the modes I and II fracture mechanics type of failures.

Figure 5.14 shows the two mechanisms of reflective cracking that can be examined with the device: 1) overall deterioration and cracking of the underlying concrete slab on either side of a joint position and 2) differential movement of the underlying slab. The effect on the overlay in the first mechanism is such that cracks will start at the bottom of the overlay and propagate upwards to the surface. This will be referred to as “bottom-up” cracking. Conversely the effect of the second mechanism on the overlay will be that cracks will first appear at the point of highest tension force, on the surface and propagate downwards.

The test set-up to examine bottom-up cracking is of the form of a simply supported beam as shown in Figure 5.15. The ends of the specimen are supported on narrow timber blocks while the span of the specimen is underlain by foam (representing a weak foundation). Metal plates of 0.5 inch (10 mm) thick are placed above the foam support to mimic the concrete layer and a joint of 0.5 inch (10 mm) is provided under the centre of the specimen. The set-up is constrained within a metal mold which is 12×12×5.1 inch (305×305×130 mm) deep. The testing specimens are 5.5×11×2.0 inches (140×280×50 mm). This was chosen to allow a reasonable span of test duration for the different mixes (i.e. between approximately 20 minutes and 8 hours). The length of the specimen allows clearance for the specimen to deform naturally and avoid constraint against the ends of the mold. Foam spacers are placed at each end to prevent horizontal “slip” of the specimen (61).

The test set-up to examine top-down cracking is of the form of a cantilever beam and is shown in Figure 5.16. The testing specimens are 5.5×10.2×2.0 inches (140×260×50 mm) and are supported on one side on a rigid timber block with a timber clamping mechanism above. This mechanism is omitted from the photograph in Figure 5.16 for clarity but is shown in the line diagram. The cantilever end is supported on foam. Steel plates, 0.5 inch (10 mm) thick, are again used to represent the concrete layer and a joint of 0.5 inch (10 mm) is provided between the timber and foam supports. The timber clamping mechanism prevents uplift during the test and a screw is fixed through the clamping mechanism to prevent horizontal movement of the specimen (61).

In both test set-ups the travel speed of the wheel is fixed at 21 cycles per minute in accordance with the requirement of BS 598 (62). Thus the rest period between wheel

passes is short and the effect of variation in rest period on the mixtures is not examined. A cantilever arm is used to apply a normal load of 520 ± 5 N to the specimen. A test temperature of 25°C was used. During testing the loaded wheel travels over the specimen until failure occurs. Failure is taken as being the instant when a crack progresses through the full depth of the specimen. Depending on the type of test performed, the test result can be the number of wheel passes to produce either the bottom-up or the top-down failure. Throughout the test the deformation of the slabs over the central 200 mm is recorded at 10 mm intervals.

5.7 UNIVERSITY OF ILLINOIS, UNITED STATES

In 2001, Dempsey developed and evaluated an Interlayer Stress Absorbing Composite (ISAC) for mitigating the reflective cracking in HMA overlays (63). The ISAC system consists of a low stiffness geotextile as the bottom layer, a viscoelastic membrane layer as the core, and a very high stiffness geotextile for the upper layer. The effectiveness of the ISAC layer to control reflective cracking was evaluated in a laboratory pavement section with an HMA overlay placed on a jointed PCC slab constructed and tested in an environmental chamber. A mechanical device was used to simulate thermal strain in the PCC slab. The testing was conducted at -1.1°C and strain in the overlay was monitored using a sensitive LVDT device. Performance of ISAC was evaluated by comparing the cycles to failure of an ISAC treated overlay with a control section without ISAC and with two commercially available products. The base isolation properties of the ISAC system were demonstrated in the laboratory evaluation studies. The laboratory evaluation studies indicated that the ISAC system vastly outperformed the control section and the two commercial products tested. Several years of field

performance data have shown that the ISAC system is highly effective for mitigating reflective cracking in HMA overlays used on both airport and highway pavement systems.

The laboratory testing equipment consisted of a one fixed box section and a second horizontally movable box section on roller as shown in Figure 5.17. A mechanical device is used to simulate thermal strain in the slab by opening and closing the joint at an extremely slow rate. The force required to pull and push the slab back to its original position is monitored using a load cell placed between the slab and a hydraulic ram. Propagation of cracking in the overlay is also visually monitored. This test simulates the modes I and II fracture mechanics type of failures.

The test sample is a 6 inch wide and 90 inch long (15×225 cm) pavement section and 2.7 inch (6.8 cm) thick PCC slab, ISAC layer, and 2.5 inch (6.35 cm) of HMA was placed on top of the two box sections. The movable box section is attached to a hydraulic ram that can open and close the PCC slab joint very slowly to simulate seasonal or daily temperature variations (load frequency 0.041 mm/min). A load cell placed between the movable box section and the hydraulic ram indicates the force exerted by the hydraulic ram as it opens and closes the PCC slab joint. An LVDT device is located between the fixed and movable box sections to indicate their relative movement. The testing device is placed into an environmental chamber that is held constant during testing. Figure 5.18 shows the strain in an HMA overlay as a function of test cycles in pavement control section (HMA overlay on top of a PCC) and Figure 5.19 shows the strain in the HMA overlay as a function of test cycles in an ISAC pavement surface. The HMA overlay without ISAC completely split apart after 7 cycles.

5.8 AERONAUTICAL TECHNOLOGICAL INSTITUTE (ATI), BRAZIL

In 2003, Montestruque et al. presented an innovative laboratory test method to study the effect of a polyester geogrid interlayer on the performance of a non-cracked HMA layer on top of a cracked HMA layer (64). The laboratory evaluation was carried out using a dynamic fatigue test that was performed on prismatic beams resting on an elastic foundation (steel plates). This system was conceived to simulate a cracked pavement after rehabilitation with the load applied at two critical conditions: on bending and on shearing. Figure 5.20 shows the testing device.

The test specimen consists of an HMA beam of 18×6×3 inch (460×150×75 mm) resting on a steel base plate with a pre-crack gap. The beam is simply supported and the load actuator applies the loading at the center of the beam. The test is conducted for a crack opening (gap) of 0.078, 0.24 and 0.35 inch (2, 6 and 9 mm). The geogrid is placed on the crack tip between the HMA sample and the steel plate. A sinusoidal load is applied in the vertical axis with a loading frequency of 20 Hz. The position of the load is changed in relation to the crack to produce either bending or shearing as shown in Figures 5.21 and 5.22. The sinusoidal load is applied by hydraulic equipment through a steel plate with dimensions of 1.6×3.0 inch (40×75 mm), generating pressures of 80, 62 and 47 psi. Between the steel and the asphalt beam, a rubber was installed in order to minimize the concentration of stresses related to the stiffness of the steel plate.

The horizontal movements of the reflective cracks opening and the plastic deformation during the load application cycles are measured using the displacement Crack Activity Meter (CAM) which is installed in the steel plate. CAM is fixed by screws embedded within the asphalt concrete. A clip gage is used to record the pre-crack

opening during the test. The central part of the beam is white painted for an easier visual observation of the crack propagation.

The factor of effectiveness of geogrid ($FEG = N_{f(\text{with geogrid})} / N_{f(\text{without geogrid})}$) represents the beneficial effect of the geogrid and is calculated as follows:

$$N_f = \frac{1}{c_f} \quad (5.1)$$

$$c_f = \frac{1}{N_{f(B)}} + \frac{2}{N_{f(s)}} \quad (5.2)$$

where, c_f is the fatigue consumption, $N_{f(B)}$ represents the fatigue life of the beam with the load in the bend mode and $N_{f(s)}$ the fatigue life in the shear mode. Table 5.4 shows the calculated FEG values for the various beams evaluated by Montestruque et al. (64).

5.9 FLORIDA ATLANTIC UNIVERSITY, UNITED STATES

In 2004, Sobhan et al. (65) evaluated the effects of reinforcing an HMA overlay with stiff geogrids as a means to mitigate reflective cracking when placed on PCC joints. The primary objectives of this study were: 1) to evaluate the growth propagation of the reflective cracks under cycling loads, and 2) to assess the effects of placement location of the geogrid within the overlay on the propagation of reflective cracks. A new test was proposed by researchers to achieve the objectives and it is described as follows.

Figure 5.23 shows the schematic representation of the proposed test setup which simulates the mode I type of failure. HMA slab specimens of 18×6×7.5 inch (450×150×190 mm) representing the overlay were prepared in a detachable steel mold using roller compaction techniques developed in the laboratory. A cylindrical steel roller provided a kneading compaction to the HMA overlay and simulated the field compaction

practices as closely as possible. Such compaction technique allowed for compacting HMA beams reinforced with geogrids or other materials. After de-molding, and 24 hours before testing, two plywood pieces are attached at the bottom of the specimen (with 0.4 inch gap in between) by means of a tack coat to present the joints of the underlying concrete pavement. Then, the specimen was placed on the rubber foundation for testing.

Two types of test were conducted in the study:

- Static tests: these included series of test on unreinforced specimens with monotonically increasing loads in order to evaluate the ability of the test set up to successfully simulate the initiation and propagation of the reflection cracking, to determine the static load bearing capacity, and to develop various failure criteria. The load is applied in the center of the specimen. The HMA overlay is placed over a neoprene rubber foundation having a pre-crack or joint of 10 mm. Such pre-crack caused the cracking initiation.
- Cyclic tests: these included series of cyclic/fatigue tests on both unreinforced and geogrid reinforced specimens, conducted using a sinusoidal loading waveform at various constant amplitudes of 222, 444, 888, 1110 and 1332 N, and at a constant frequency of 2 Hz. The load is applied in the center of the specimen. The HMA overlay is placed over a neoprene rubber foundation having a pre-crack or joint of 10 mm. Such pre-crack caused the cracking initiation.

The data acquisition included time and load and deformation which were continuously recorded for all loading cycles to failure. In addition, continuous digital video data focused on the zone of the simulated concrete joint during the progress of the test was recorded for analyzing crack propagation.

The test setup was used by Sobhan et al. (65) to evaluate the performance of HMA overlays with two geosynthetic materials: the Tensar Biaxial Geogrid (BX 1500) and the Amoco Petrogrid (4582). Three failure criteria based on the observed length of crack propagation were established.

- Initial Crack, C_{if} : the load or number of cycles at which a reflective crack is first visible.

- Mature Crack, C_{mf} : the load or number of load cycles it takes for the reflection crack to propagate half of the overly depth.
- Terminal Cracking, C_{tf} : The load or number of load cycles it takes for the crack to advance to the top of the overlay.

These observed criteria for seven static tests conducted on the HMA overlay system revealed that the average C_{if} value is about 1,110 N. The results showed that for the unreinforced specimens, the formation of reflection cracks during the early stages and additional secondary cracks (cracks developing near the joint of the loaded area on both sides) near failure stages are clearly observed. In the case of reinforced specimens, although the crack initiation was clearly evident, the presence of geogrids restricted or diverted the cracks remarkably well. The secondary cracks for this case appeared near failure stages. For these cases, failure was defined when the specimens reached one million cycles. For geogrids placed at the middle, the cracks initiated early, but after reaching approximately the middle of the overlay, the rate of propagation was severely restricted due to the presence of the geogrids.

The beneficial effect of the geogrid was quantified by calculating a Fabric Effectiveness Factor (FEF) that is defined as a function of the number of cycles to crack corresponding to any particular load ratio as follows.

$$FEF = \frac{C_{1f(reinforced)}}{C_{1f(unreinforced)}} \quad (5.3)$$

It was found, at the same load ratio, the slabs having geogrids embedded at the bottom showed better resistance to reflection cracking compared to specimens in which the geogrids was simply attached to the bottom with a tack coat. Additionally, it was

found that geogrid embedded at mid-height was more effective than geogrid embedded at the bottom of overlay.

5.10 POLYTECHNIC UNIVERSITY OF MADRID, SPAIN

In 2006, Gallego and Prieto (66) presented the Wheel Reflective Cracking (WRC) device for testing the reflective cracking resistance of HMA overlays. A schematic representation and a picture of the WRC are shown in Figures 5.24 and 5.25, respectively.

The base temperature of $5\pm 1^{\circ}\text{C}$ was chosen to simulate the low-temperature distress mechanism and for running the test. However, the test can be performed in a range of temperatures between 0°C and 20°C .

As shown in Figures 5.24 and 5.25, the WRC test comprises a supporting system of four trapezoidal frames and two chasses. Each chassis is supported at one end by the trapezoidal frames by means of a horizontal shaft allowing it to rock and, at the other end, it rests on a rocker that simulates the relative vertical movement between the borders of the crack or the pavement joint. Both chasses are set 0.4 inch (10 mm) apart, a distance simulating the joint or crack in the deteriorated pavement on which the asphalt overlay is installed.

The temperature-change distress mechanism is simulated using a system of sliding plates. The specimen is stuck by a synthetic adhesive to two plates (Figure 5.26), then placed inside the apparatus and screwed down fast. During the test, one of the plates remains immobile while the other is displaced horizontally by the action of the tensile force applied to one end at a speed ranging from 0.001 to 50 $\mu\text{m/hr}$. This method is chosen to simulate the progressive widening of the crack as a result of the effect of the

temperature changes causing the concrete pavement slabs to contract, making joints and cracks open up.

Deflection is simulated by placing a prism-shaped rubber block under the rocker support (Figure 5.27). As a result, independently of the effect of the rocker on the centre of the specimen, a vertical displacement occurs caused by the strain in the rubber block. This equipment allows different magnitudes of deflection to be simulated by varying the hardness or thickness of the rubber blocks used, to which end different heights of rocker support are available.

During the test, the vertical deflection in the center of the test specimen, the vertical length of the crack, and the relative movement between the borders of the crack are measured. Also, a measure of the time to failure can be performed. The researchers suggested the failure criteria when a relative movement of 0.2 mm occurs between the crack edges.

5.11 REGIONAL LABORATORY OF PONTS ET CHAUSSSES, FRANCE

In 2004, Tamagny et al. (67) evaluated the capabilities and effectiveness of the MEFISTO device designed to determine the anti-reflective cracking behavior of various materials. The MEFISTO device is used to study the efficiency of anti-reflective cracking methods by simulating fatigue cracking in HMA overlays.

The MEFISTO test consists of subjecting the sample to a sinusoidal loading with a frequency of 10 Hz, applied with one or two columns close to the center of the beam, plus a monotonous horizontal loading (Figures 5.28 and 5.29). However, since the machine is still under development, it has not been yet possible to test such combined modes of loading, imposing vertical and longitudinal dynamic displacements at the same

time. Instead only vertical loading or horizontal loading modes have been tested independently.

The MEFISTO has two side connections of metal plates which allow the device frames to act as knee-joints with negligible flexural stiffness and zero imposed horizontal displacements. The test beam is 2×2×26 inch (50×50×650 mm). During the specimen compaction a 0.4 inch (10 mm) wide pre-crack is made in the center of the beam. The test is conducted at 5°C and the applied vertical load is 1.9 kips (8.5 kN).

The device has the capability of measuring the applied vertical and horizontal forces and the displacement in the center of the beam as shown in Figures 5.28. During the test, the dissipated energy as a function of the number of cycles until failure is calculated. Failure is defined as the moment when the crack has completely crossed the beam thickness. It is also possible to visually measure the crack length as a function of number of load cycles until the specimen fails.

The MEFISTO test produces a fatigue crack in the central part of the HMA sample, starting from the notch end that is submitted to traction and then growing upwards with time. Figure 5.30 shows a typical test results from the MEFISTO test. The amplitude of the vertical load is monitored with respect to the number of loading cycles as well as the crack expansion as a percentage of the sample thickness.

5.12 TEXAS TRANSPORTATION INSTITUTE OVERLAY TESTER, UNITED STATES

In 2003, Zhou et al. from the Texas Transportation Institute (TTI) upgraded the TTI overlay tester that has been widely used to evaluate the effectiveness of different geosynthetic materials since it was designed by Lytton et al. in late 1970's (68).

The apparatus is shown in Figure 5.31 consists of two steel plates, one fixed and the other movable horizontally to simulate the opening and closing of joint or crack in the old pavements beneath an overlay. A beam sample is spanned across the crack and epoxied to the horizontal surface platens with half of the length of the specimen resting on each platen. The moveable platen is opened and closed within a preset amount (between 0.0001 and 2 mm). For most applications this value is computed based on project specific information such as the slab length and anticipated temperature variation. Each sample is painted white in the areas where cracking was most likely to occur. This technique enhanced the visibility and measurement of cracks during the testing phase.

The TTI overlay tester was upgraded to be fully computer-controlled system with special programs. The test data including time, displacement, and force, are automatically recorded and saved as Excel file. The sample size of the upgraded TTI overlay tester has been reduced to 150 mm long by 75 mm wide by 38 through 50 mm high, making the overlay tester more practical and easier to handle samples from the Suprepave Gyrotory Compactor (SGC) or field cores. Figures 5.32 shows the upgraded TTI overlay tester. The upgraded system can be conducted in controlled displacement mode under the following conditions.

- Temperature: 0 – 35 °C
- Opening displacement: 0 – 2 mm
- Loading rate: 24 hours (or more) per cycle – 10 seconds per cycle
- Loading type: the loading is applied in a cyclic triangular waveform with constant magnitude.

The main output of the overlay tester is the reflective cracking life of an HMA mix which is the number of cycles to completely break the sample. Researchers found

that this value is a good indicator of reflective cracking resistance of asphalt mixtures and has a good correlation with the change of load (68, 69).

A typical relationship between load and time (number of load cycles) during testing is illustrated in Figure 5.33. The observation of results from many overlay tests showed that this plot has three distinct phases for the crack propagation (69).

- *Phase I: Crack initiation and steady propagation.* In this phase the load and displacement have similar shapes. As the displacement increases, the load increases too. For the first cycle, the load reaches its maximum value before the displacement arrives at the maximum displacement indicating the crack initiation at the bottom. After the first cycle, the load decreases rapidly as the crack starts to propagate through the specimen. However, both load and displacement reach the maximum values at the same time. In this stage, the cracking is steadily and slowly propagated to the top surface.
- *Phase II: Late crack propagation.* Phase II is the late stage of crack propagation, which is monitored as a saddle-shaped load. The saddle-shaped load indicates that the crack has partially gone through the whole cross section of the specimen. In fact, the first peak load is associated with the minor adhesion as the specimen gap is closed and the two halves of the specimen bond together. Then, the load rapidly decreases just after breaking the weak adhesion bonds. With the increasing opening displacement, more loading is needed to break the remaining parts of the specimen. Corresponding to the maximum displacement, there is another peak load. With the continuing cyclic loading, the crack will totally break the specimen and the second peak load will disappear. This indicates the onset of Phase III.
- *Phase III: Specimen failure.* As described above, the crack has propagated completely through the specimen in this phase. The maximum load induced by the minor adhesion occurs well before the maximum displacement.

Based on the above discussion, the reflective cracking life of asphalt mixtures, thus, can be defined by the number of cycles corresponding to the onset of Phase II or Phase III. From the conservative point of view, the onset of Phase II should be used to define the reflective cracking life. Using the evaluation scheme described above, the reflective cracking life of the specimen was determined to be four cycles (10 sec/cycle).

5.12.1 Variability of Upgraded Overlay Testing

The first step in evaluating the overlay tester concept, especially with the recommended small sample size (Superpave gyratory compacted – SGC cores instead of HMA slabs), was to determine the repeatability of the test. In general, the smaller the specimen, the more variable the test results can be. Since the upgraded overlay tester was using a small specimen, there was concern about its repeatability. Thus, two types of TxDOT mixtures, Type D and CMHB-C using PG64-22 asphalt binder, were selected to make six identical specimens (6 in [150 mm] diameter by 2.25 in [57 mm] high) for each mixture. All the specimens were molded using the SGC. Then, the specimens were cut to be 1.5 in (38 mm) high using a double blade saw; after that, 1.5 in (38 mm) was trimmed from each side of the specimens (Figure 5.34). The air void content of each specimen was controlled within 7 ± 0.5 percent after trimming the specimens. Finally, six overlay tester specimens for each mixture were glued to the overlay tester plates. The testing was conducted at room temperature (77 °F [25 °C]) and the opening displacement was set to 0.025 in (0.63 mm).

Figure 5.35 shows the reflective cracking lives of six identical Type D specimens. An average reflective cracking life of 140 cycles was found with a corresponding standard deviation and coefficient of variation of 11.7 and 8.3 percent, respectively. Generally speaking, the coefficient variation of asphalt mixtures is around 10 to 25 percent. These results clearly indicated that the overlay testing is a repeatable test.

On the other hand, The CMHB-C mixture showed a poor resistance to reflective cracking under the overlay tester with each of the specimens failing after only two cycles. Therefore, this mixture was excluded from the repeatability analysis.

The test results for the TxDOT type D mixture were used to provide an estimation of the minimum number of replicates needed to perform the test. Figure 5.36 shows the relationship between the number of specimens and the specified tolerance. It can be seen that the average reflective cracking life of two specimens, for Type D mix, will be within ± 12 percent of the “true” reflective cracking life of asphalt mixture with 95 percent reliability.

Based on the results of this analysis, it was recommended to use at least three replicates of the HMA mixture to get an error of less than 10 percent.

5.12.2 Sensitivity of Upgraded Overlay Testing

The sensitivity of the upgraded overlay tester to material properties and test conditions were also investigated. The parameters investigated in this project included test temperature, opening displacement, air voids, asphalt performance grade, and asphalt content. The TxDOT type D mixture from US281 in the Fort Worth District was used for this analysis. The optimum asphalt content was 5.1 percent. It should be noted that only one parameter was variable in this sensitivity test and the others were kept the same. The detailed results are presented as follows.

Influence of temperature on reflective cracking life

A PG76-22 SBS modified binder was used to mold six identical specimens at 4 percent air void content. Overlay testing was conducted at 77 °F (25 °C) and 50 °F (10 °C) and for an opening displacement of 0.025 inch (0.63 mm). At each temperature, three replicates were used. The averaged reflective cracking life presented in Figure 5.37 showed a significant influence for the temperature on the reflective cracking life of the

HMA mix. Therefore, it was concluded that the overlay testing is sensitive to temperature.

Influence of opening displacement on reflective cracking life

Similar to the previous test, a PG76-22 SBS modified binder was used to mold six identical specimens at 4 percent air void content. Overlay testing was conducted at 77 °F (25 °C) and for two opening displacements: 0.025 inch (0.63 mm) and 0.035 in (0.89 mm). At each opening displacement, three replicates were used. The averaged reflective cracking life presented in Figure 5.38 indicated that overlay testing results are sensitive to the opening displacement. The reflective cracking life of HMA mixes decreased with the increase of opening displacement.

Influence of asphalt content on reflective cracking life

A PG64-22 binder was used to mold three replicate specimens at each of the three asphalt binder contents: 4.2, 5.1 (optimum), and 6.1 percent. The overlay testing was conducted at 77 °F (25 °C) and 0.025 inch (0.63 mm) opening displacement. The averaged reflective cracking life presented in Figure 5.39 showed a significant increase in the reflective cracking life of the HMA mix with the increase of asphalt content. The results were consistent with the traditional flexural beam fatigue test results.

Influence of asphalt performance grade on reflective cracking life

The data from Figures 5.38 and 5.39 showed that an increase from a PG of 64 to 76 resulted in a drop in reflective cracking life from 90 to 33 indicating a poorer reflective cracking resistance for the stiffer asphalt binder.

Influence of air voids on reflective cracking life

Figure 5.40 shows the influence of air voids content on reflective cracking life with a better reflective cracking resistance for higher air voids. The researchers related this behavior to most possibility the generation of denser and stronger specimens when reducing air voids from 7.4 to 4.2 percent. Therefore, specimens with lower air voids content would have higher stiffness and higher strength as well. However, thermal reflective cracking simulated by the overlay tester is a different scenario. If temperature dropping is kept constant, the denser mixture with higher modulus will suffer a higher thermal stress. Inversely, although its strength is lower, the thermal stress induced within the specimen with higher air void content will be lower, too. When the thermal stress induced within a specimen is higher than its strength, a crack will occur. Whether or not a specimen with lower air void content is resistant to thermal reflective cracking depends on both its stiffness and strength.

5.12.3 Validation of Upgraded Overlay Tester

The validation of the upgraded overlay tester was composed of three steps. First, the effectiveness of the overlay tester on characterizing reflective cracking resistance of asphalt mixtures was discussed. Field cores with known reflective cracking performance were used for this validation. Then, the potential application of the overlay tester to evaluate the fatigue cracking resistance of asphalt mixtures was investigated. Finally, cores taken from MnRoad were tested to check the potential of the overlay tester on characterizing the low temperature cracking resistance of asphalt mixtures.

The validation of the TTI Overlay Tester was performed based on the performance of various projects around Texas. Since 2000, the TTI small overlay tester

has been successfully employed to characterize the reflective cracking resistance of different asphalt mixtures with known reflective cracking performance in the field. Reflective cracks quickly appeared in new overlays placed on US175, US84, SH3, SH6, and IH10 throughout the state. Cores taken from these poorly performing pavements were tested in the overlay tester and the results were compared with those of cores from the Special Pavement Studies 5 (SPS5) section on US175 near Dallas. This overlay was placed over a stabilized base and had no reflective cracks after 10 years in service. All of these good and poor performing cores were used to validate the TTI overlay tester concept. The HMA mixes tested by the overlay tester covered TxDOT type C mixes with PG76-22 tire-rubber, type D mixes with PG64-22, and type D mixes with 30 and 75 percent recycled asphalt concrete. Several cores were taken from the various projects and tested in the overlay tester. Also, a detailed condition survey was conducted in each of the project to assess the condition of the pavement. Therefore, the mechanisms of failure as well as the layer subjected to either reflective cracking or to a good performance were identified. This information was used to validate the capabilities of the TTI overlay tester to assess the reflective cracking performance of the HMA overlay.

In summary, the test results of the overlay tester were consistent with the field performance, and the poor crack resistant HMA mixes were differentiated from the good crack resistant mixes. The evaluated case studies also confirmed the overlay tester as a rapid performance-related tool to evaluate the reflective cracking resistance of asphalt mixtures. The overlay tester results on the known field performance cores taken from different highways showed that asphalt mixtures performed very well when the reflective cracking life (from the overlay tester) is larger than 300. Thus, the researchers proposed

the preliminary pass/fail criterion on reflective cracking resistance to be 300 cycles at 77 °F (25 °C) and 0.025 in (0.64 mm) opening displacement. When a rich bottom layer is used, the proposed reflective cracking life in the overlay tester should be at least 750 cycles.

The TTI OT was also validated using MnRoad Cores. For this purpose, it was used to evaluate the low temperature cracking resistance of asphalt mixtures from MnRoad. Three representative test cells (15, 18, and 20) at MnRoad were selected for evaluation. Table 5.5 presents the asphalt mixture information and field performance of the three cells. Two 6-inch (150 mm) diameter cores from each cell were taken from the mid-lane of the driving lane (6 feet offset) and tested under the overlay testing.

Although the cores are composed of different layers, only the top HMA layer was tested under the overlay tester since it is the critical layer for low temperature cracking. The overlay tester was conducted at a temperature of 77°F (25 °C) with an opening displacement of 0.025 in. The overlay tester results (Table 5.5) are found to be consistent with the observed field cracking performance of asphalt mixtures. The results also indicated that both asphalt content (cells 15 and 18) and asphalt binder PG (cell 15, 18, and 20) had influence on crack resistance, which is consistent with the results of the conducted sensitivity study.

5.13 FEDERAL UNIVERSITY OF RIO GRANDE DO SUL, BRAZIL

In 1994 the State Roads Department (DAER/RS) constructed the traffic simulator called UFRGS-DAER/RS (Figure 5.41) that was designed by the Mechanical Engineering Department at the Federal University of Rio Grande do Sul (UFRGS) in Brazil (70).

The traffic simulator dimensions are 49.2 ft (15 m) long, 8.2 ft (2.5 m) wide and 14.1 ft (4.5 m) high with a weight around 22 tons. The tires are mounted on a dual wheel system on the loading carriage. The system is controlled with a computer that controls the travel speed and wandering. The path of the tires can be varied in range of ± 1.3 ft (0.4 m) from centerline. The loads are hydraulically applied and can vary from 9.2 to 22.5 kips (63 to 155 MPa). The tire pressures can be varied from 81 to 100 psi (0.56 to 0.73 MPa). Wheel load and tire pressure are controlled within a tolerance of $\pm 2\%$. The test wheels travel at 3.7 mph (6 km/h) over a 23 ft (7.0 m) pavement. Loads are applied in one direction and normally distributed around the wheel path.

From March 2003 to February 2005, the traffic simulator was used on two full-scale pavement sections to evaluate the resistance to reflective cracking of HMA overlays (70). The experiment was carried out in an outdoor full-scale pavement testing facility in the UFRGS Campus.

The test pavement was 53 feet long (16.2 m) by 10.5 feet (3.2 m) wide. The pavement was longitudinally divided in two sections. In one of the sections the overlay consisted of HMA with conventional binder (Brazilian designation CAP 20), while in the other the overlay was made of asphalt rubber (AR). Figure 5.42 shows the cracked areas

in both sections and the location of instrumentation embedded during pavement construction.

Figure 5.43 shows the pavement structures. It may be seen that the sole difference between both sections is the type of HMA mix (CAP 20 or AR) used in the 2 inch (50 mm) thick overlay. The HMA overlays were placed on top of a 1.6 inch (4.0 cm) pre-cracked HMA layer, on top of an 11.8 inch (30 cm) granular base course, on top of a 20 inch (50.0 cm) clayey soil subgrade. The cracked layer consisted of a new dense graded HMA layer which was laid and compacted in situ.

An already failed old HMA layer was represented by sawing cracks in the newly compacted HMA layer on top of the granular base according to the pattern shown in Figure 5.44. Cracks were 1.6 inch (4.0 cm) deep and 0.2 inch (0.5 cm) wide simulating severe fatigue cracking. Four cracking areas of 4 feet (1.2 m) long by 2.7 feet (0.8 m) wide each were sawn, alternating with uncracked areas, in each test section. Cracks were filled with clayey soil in order to prevent crack sealing by the tack coat applied before overlay setting. An axle load of 22.5 kip with a tire pressure of 91.3 psi was applied using the UFRGS-DAER/RS traffic simulator.

During the testing process three types of measurements were conducted:

- Environmental measures: rainfall, air temperature and sun radiation were continuously recorded in a meteorological station built in the pavement test facility. Pavement temperatures were also recorded every time that deflections and strains were measured.
- Structural response: surface deflections were measured at seven locations along each test section, before and during trafficking. Deflections were measured under axle loads of 18, 22, and 26 kips (82, 100, and 120 kN) with tire inflation pressures of 80, 100 and 120 psi (0.56, 0.69 and 0.84 MPa), respectively. Deflection basins were also measured with a road surface deflectometer, in order to obtain back-calculated pavement and subgrade moduli.

- Pavement performance measurements: included cracking and rutting data. Rutting was measured using a profilograph. To eliminate initial surface irregularities from the rut depth data, profiles obtained before trafficking were used as references. A manual procedure was used to record and measure cracking. Different color sprays were used each time a crack survey was performed, as shown in Figure 5.45. Then, cracks were mapped using a square metal grid, 1.0 by 1.0 m, with a mesh opening of 0.10 m. Afterwards, a cracking severity index, given by the ratio of cracking total length to trafficked area was computed.

Figure 5.46 shows the cracking evolution in both the AR and the CAP 20 HMA sections. The asphalt rubber overlay outperformed the conventional asphalt concrete by delaying reflection cracking. During testing, the first cracks appeared in the conventional asphalt concrete (AC) overlay after 14,000 cycles of the 22 kip axle load. The cracks seen in the HMA layer underneath the neat binder section propagated through the HMA overlay, and after 98,000 loadings the crack density was 220 cm/m². On the other hand, the asphalt-rubber HMA overlay showed its first crack after 123,000 loading cycles of the 22 kip axle load. The reflected cracks in the asphalt-rubber HMA showed up 5 to 6 times loading cycles after the cracks of the conventional dense-graded HMA overlay.

5.14 SUMMARY OF LABORATORY TEST METHODS

Table 5.6 summarizes the review of the various laboratory test methods used to evaluate the resistance of HMA mixtures to reflective cracking.

Chapter 6 – SUMMARIES AND RECOMMENDATIONS

In 2006, the Nevada DOT initiated a three-phase research study to identify the promising techniques to mitigate reflective cracking in HMA overlays: a) Phase I: Review of literature and the performance of the various techniques in Nevada, b) Phase II: Identify analysis models and laboratory tests, and c) Phase III: field verification of the selected techniques. This chapter summarizes the findings of Phase I and Phase II of this research and presents the recommendations for Phase III.

6.1 SUMMARY OF PHASE I FINDINGS

Table 6.1 summarizes the literature review of the current and previous efforts outside Nevada on the mitigation of reflective cracking in HMA overlays.

Table 6.2 summarizes the general results of the review of the long-term field performance of NDOT projects with different techniques to reduce the impact of reflective cracking on HMA overlays. It should be noted that all treatments had either 0.375" or 0.75" open graded friction course on top. In general, the long-term effectiveness of the treatments experienced by NDOT was significantly hampered by the existence of severe alligator cracking on the projects prior to the application of these treatments. Therefore, it is recommended that projects experiencing severe alligator cracking as classified by the NDOT pavement distress manual should be subjected to either re-construction or full depth reclamation.

6.1.1 Recommendations of Phase I

The research effort documented in the Phase I of the study was directed toward identifying an effective method to eliminate the propagation of the cracks from the old surface layer through the new HMA overlay. Several techniques showed promising

results but none of the reviewed methods was able to completely stop reflective cracking. Even though, under Nevada's conditions the cold in-place recycling of a minimum 2.0 inches and overlaying with a minimum 2.5 inches of dense grade HMA mix was proven to be effective in stopping reflective cracking for at least 5 years, it may not be the most cost effective rehabilitation technique for every highway pavement. Therefore, based on the literature and performance reviews, it is recommended to further investigate the stress relief course technique. It should be noted that the stress relief course experienced by NDOT was not specifically designed or checked for its reflective cracking resistance and only consisted of a 1-inch of the typical Type II (1" max size) dense graded HMA mix placed between the existing HMA and the overlay. This study revealed promising performance for the stress relief course when specifically designed to resist reflective cracking. Additionally, for a good overall performance, the stress relief course needs to be coupled with an overlay mix with good resistance to reflective cracking.

6.2 SUMMARY OF PHASE II FINDINGS

The research effort of Phase II was directed toward identifying an analytical model(s) and laboratory or field test(s) that can be used to predict the resistance of HMA overlays to reflective cracking and predict their long-term performance.

6.2.1 Analysis Models

Based on the review of the currently available analytical models to predict the resistance of HMA overlays to reflective cracking, three design methods were identified and summarized.

- Virginia Tech Simplified Overlay Design Model
- Asphalt Rubber Association Overlay Design Model
- The New AASHTO model for Reflective Cracking

The Virginia Tech Simplified Overlay Design Model (45) consist of a simple regression equation for predicting the number of cycles in ESALs (W_{180}) to produce the crack reflection to the pavement surface as a function of: thickness and resilient modulus of HMA overlay ($H_{overlay}$ [mm], $E_{overlay}$ [MPa]), thickness and resilient modulus of existing HMA layer (H_{HMA} [mm], E_{HMA} [MPa]), thickness and resilient modulus of base layer (H_{base} [mm], E_{base} [MPa]), and resilient modulus of subgrade layer ($E_{subgrade}$ [MPa]). The total number of load repetitions is defined as the sum of the number of load repetitions for crack initiation and the number of load repetitions for crack propagation.

$$\log W_{180} = \frac{1}{10^4} \left(255H_{overlay} + 2.08E_{overlay} + 45.3H_{HMA} + 8.73E_{HMA} \right) \\ 1.37H_{Base} + 6.93E_{Base} + 1.49E_{subgrade} \quad (6.1)$$

Equation 6.1 clearly shows that the overlay mix with a higher stiffness will withstand a higher number of load repetitions. However, it should be noted that a stiffer mix may be brittle thus more susceptible to reflective cracking.

The Asphalt Rubber Association Overlay Design Model (53) consists of a mechanistic relationships and statistically based equations for designing HMA overlays on top of HMA pavements. The proposed models are based on a finite element model that closely approximates actual field phenomena of dense-graded HMA and gap-graded asphalt rubber-AR (wet process) overlay mixes. However, other HMA mixes used for overlays may also be calibrated and used through the proposed method using the relevant mix properties. The overlay design program is available from the Rubber Pavements Association in the form of an EXCEL spreadsheet that estimates the thickness of a PG70-10 or an AR HMA overlay mix for the specified level of reflective cracking for a wide range of traffic loading. The expected design level of cracking, the thicknesses and the

elastic moduli of the existing pavement layers, and the modulus of the HMA overlay are inputs for the EXCEL spreadsheet. The moduli may be backcalculated or determined in any reasonable manner, as long as they represent the in situ conditions in the field.

The reflective cracking models incorporated in the new AASHTO Mechanistic-Empirical Pavement Design Guide (MEPDG) are strictly based on empirical observations without any rigorous mechanistic-empirical analysis (55). The empirical models consider the development of distresses in the overlay as well as the continuation of damage in the existing pavement structure. The proposed MEPDG overlay design procedure allows for two types of reflective cracks: a) reflective cracks that exist on the surface prior to overlay placement and b) those that develop in the existing surface after overlay placement.

An overlay design was conducted for three different HMA overlay mixes using the three identified overlay design methods. The overlay mixes were manufactured using different aggregate gradations from the Sloan pit in Southern Nevada and a PG76-22NV polymer modified asphalt binder. The overlay was designed for 7,075,000 ESALs over the 20 years analysis period. Table 6.3 shows the material properties of the various pavement layers used in the analysis. It should be noted that the fatigue characteristics of the various mixes can only be incorporated in the Asphalt Rubber Association Overlay Design Method. Table 6.4 shows the required overlay thicknesses for the design ESALs according to all three design methods.

The data in Table 6.4 show that for the same design ESALs, a thicker overlay thickness is required for the T2C mix followed by the CT mix followed by the NRM mix when designing using the Virginia Tech method. On the other hand, the opposite was

found when designing using the Asphalt Rubber Association method where a thinner overlay thickness is required for the T2C mix followed by the CT mix followed by the NRM mix to reach the same selected percentage of cracking. The AASHTO MEPDG design method resulted in a 12 inch overlay thickness to reach 100% reflected cracking after 20 years design period regardless of the type of the overlay mix.

In a summary when only the stiffness of the overlay mix is considered, a thinner overlay thickness was found for the stiffer mix whereas, when both the stiffness and the fatigue characteristic of the mix are considered, the overlay thickness was depended on the interaction between the two material properties. On the other hand, when the material properties of the overlay mix are not considered a unique and thick overlay thickness was found.

6.2.2 Laboratory Tests

This task reviewed the laboratory tests that have been used to evaluate the resistance of HMA mixtures to reflective cracking. Laboratory tests are typically used to evaluate the resistance of the HMA mixtures to reflective cracking during the mix design stage.

None of the reviewed laboratory test methods has undergone field validation except the TTI Overlay Tester which showed consistency between the mixtures' test results and their corresponding field performance. The Overlay Tester was able to differentiate between the poor crack resistant and the good crack resistant HMA mixes. Additionally, the overlay tester results on the known field performance cores taken from different highways showed that asphalt mixtures performed very well when the reflective cracking life (from the overlay tester) is larger than 300. Thus, the researchers proposed

the preliminary pass/fail criterion on reflective cracking resistance to be 300 cycles at 77°F (25°C) and 0.025 inch (0.64 mm) opening displacement. When a rich bottom layer is used, it was proposed that the reflective cracking life in the overlay tester should be at least 750 cycles.

6.2.3. Recommendations of Phase II

The assessment of the three identified design models illustrated the following advantages for Asphalt Rubber Association method:

- Consider the overlay mixture material properties such as the stiffness as determined by the dynamic modulus test and the fatigue characteristic as determined by the flexural beam fatigue test at constant strains and various temperatures.
- Allow for the selection of the desired percent of cracking at the end of the design life.

Consequently, it is recommended to validate the Asphalt Rubber Association Overlay Design Model under Nevada's mixes and conditions.

It is recommended to use the TTI Upgraded Overlay Tester to evaluate typical NDOT mixtures along with their actual field performance to develop performance criteria that can be used at the design stage of the overlay mixture.

6.3 OVERALL RECOMMENDATIONS

Based on the findings of the Phase I and Phase II of the study it is recommended to evaluate the stress relieve courses under Nevada's conditions. Therefore the following recommendations are made:

- Review the current state highway agencies' (SHA) specifications for stress relieve courses (SRC).
- Use the TTI Upgraded Overlay Tester to evaluate mixtures in the Laboratory for reflective cracking resistance.
- Use the Asphalt Rubber Association Overlay Design Model to design the required overlay thickness.

6.4 REVIEW OF STRESS RELIEF COURSES (SRC) SPECIFICATIONS

Following the overall recommendations, the SHA specifications for SRC were reviewed and are summarized in the following section.

6.4.1 Arizona Department of Transportation

The Arizona Department of Transportation (ADOT) defines the Stress absorbing membrane interlayer (SAMI) as a furnishing of asphalt-rubber, tack coat, and a cover material of mineral aggregate (71).

6.4.1.a Asphalt Rubber

The asphalt rubber shall be a mixture of asphalt cement and rubber. The asphalt binder should have a performance grade (PG) conforming AASHTO Provisional Standard MP1.

The rubber gradation for the SAMI shall meet the requirements shown in Table 6.5 when tested in accordance with Arizona Test Method 714.

The rubber shall have a specific gravity of 1.15 ± 0.05 . Additionally, the rubber shall be free of wire or other contaminating materials and shall contain not more than 0.1 percent fabric. Calcium carbonate, up to 4 percent by weight of the granulated rubber, may be added to prevent the particles from sticking together. The asphalt rubber shall contain a minimum of 20 percent ground rubber by the weight of the asphalt cement and shall conform to the requirements in Table 6.6.

6.4.1.b Mineral Aggregates

Aggregates for cover material shall be of clean sand, gravel or crushed rock and shall be free from lumps or balls of clay and shall not contain calcareous or clay coatings,

caliche, synthetic materials, organic matter or foreign substances. The aggregates shall meet the requirements in Table 6.7.

6.4.1.c Construction Requirements

The asphalt rubber shall be placed on a previously cleaned surface. After cleaning and prior to the application of the SAMI, the existing pavement surface shall be treated with a tack coat with the following conditions.

- Ambient air temperature and pavement surface temperature are both above 65°F.
- Pavement is dry.
- Wind conditions are such that a satisfactory SAMI can be achieved.
- All construction equipment such as asphalt rubber distributor, aggregate spreader, haul trucks with aggregate material, and rollers are in position and ready to start placement operations.

Distributor trucks shall be so designed, equipped, maintained and operated that bituminous material at even heat may be applied uniformly on variable widths of surface up to 15 feet at readily determined and controlled rates of 0.03 to one gallon per square yard, with uniform pressure, and with an allowable transverse variation from any specified rate not to exceed 10 percent or 0.02 gallons per square yard, whichever is less. The maximum deviation from the specified rate shall not exceed 0.05 gallons per square yard.

The hot asphalt-rubber mixture shall be applied at the rate of approximately 0.55 ± 0.05 gallons per square yard (based on a unit weight of 7.75 pounds per gallon of hot asphalt-rubber). Cover material (aggregate) shall be immediately and uniformly spread over the freshly applied asphalt-rubber at the rate of approximately 0.014 cubic yards per square yard. Cover material shall be precoated with 0.40 to 0.60 percent asphalt cement,

by weight of the aggregate, and shall have a minimum temperature of 250 °F at the time of application.

At least three pneumatic rollers shall be provided to accomplish the required rolling. The first pass shall be made immediately behind the spreader and if the spreading is stopped for any reason, the spreader shall be moved ahead so that all cover material may be immediately rolled. The rolling shall continue until a minimum of four complete coverages have been made.

Traffic of all types shall be kept off the stress-absorbing membrane until it has had time to set properly. The minimum traffic free period shall be three hours. Sweeping shall be completed and all excess cover material removed prior to the placement of any subsequent layers of asphaltic concrete. If the asphalt-rubber membrane has been subjected to traffic, a tack coat shall be applied at the rate of approximately 0.06 gallons per square yard prior to placement of the asphaltic concrete.

6.4.2 California Department of Transportation

The California Department of Transportation (CALTRANS) defines an Asphalt-rubber membrane interlayer (SAMI-R) as an asphalt rubber chip seal that is overlaid with conventional dense graded asphalt mixture (AC) or a gap graded hot mix (RAC-G) (72). SAMI-R is a low modulus (nonstructural) layer that is used to retard and minimize reflective cracking in overlays placed on it, and to minimize further infiltration of surface water through the pavement structure.

No fog seal or sand should be applied over a SAMI-R because this could interfere with bonding of the overlay. SAMI-R may be applied to any type of rigid (PCC) or asphalt pavement, and have proved very effective at minimizing reflection of PCC joints.

However, according to the Caltrans Maintenance Manual, if the surface irregularities (rutting in AC or faulting of PCC) exceed 12.5 mm then either a leveling course should be placed or grinding and crack filling are required prior to placing SAMI-R.

SAMIs are used under corrective maintenance overlays and are a pavement rehabilitation tool. A SAMI-R would not be included as part of new construction. Design of the asphalt rubber binder is the same as for chip seal. Determination of appropriate binder and cover aggregate application rates is also the same.

6.4.2.a Asphalt Rubber

Typically the AR-4000 is used as a base asphalt binder. The asphalt rubber shall conform to the requirements in Table 6.8.

6.4.2.b Mineral Aggregates

The standard chip size for Caltrans asphalt rubber seals is 9.5 mm. The 12.5 mm chips are used by Caltrans only where ADT is less than 5,000 per lane.

6.4.2.c Construction Requirements

To construct a chip seal, the hot asphalt rubber binder is sprayed on the roadway surface at a rate determined by the Engineer. The binder is immediately covered with a layer of hot pre-coated chips that must be quickly embedded into the binder by rolling before the membrane cools. Best results are achieved with clean nominal 9.5 to 12.5 mm single-sized chips. Lightweight aggregates may be substituted to minimize windshield breakage by loose chips in areas where traffic is heavy or fast.

Pre-coating the aggregate with asphalt cement improves adhesion by removing surface dust and “wetting” the chips. Caltrans requires that the aggregate chips be

delivered to the job site precoated and hot. To further aid chip retention after the chips have been embedded and swept, a fog seal of asphalt emulsion (diluted 1:1 with water) is sprayed over the chips at a typical rate of 0.14 to 0.27 liter/m². A light dusting of sand, 1 to 2 kg/m² is then applied as blotter as directed by the Engineer. According to Caltrans standard special provisions for asphalt rubber seal coat, the application rates for asphalt rubber chip seals are shown in Table 6.9.

However, the exact rate is to be determined by the Engineer. There are a number of factors that can affect the asphalt rubber binder and cover aggregate application rates including:

- Surface texture of the existing pavement: severely aged, oxidized and open-textured surfaces will absorb more binder than newer tighter surfaces.
- Traffic volumes: typically use smaller chips for higher volumes to reduce potential for vehicle damage by loose chips. Binder application rates can be increased for low traffic volume areas.
- Seasonal temperature ranges: thicker membranes may be used in areas with cool climates.
- Aggregate size: large stone requires more asphalt rubber binder (thicker membrane) to achieve 50 to 70 percent embedment.
- Aggregate gradation: single-sized materials require more asphalt.

6.4.3 Florida Department of Transportation

The Florida Department of Transportation (FDOT) specification indicates that an asphalt rubber membrane interlayer is composed of a separate application of asphalt rubber binder covered with a single application of aggregate (73).

6.4.3.a Asphalt Rubber

The asphalt-rubber binder is a mixture of a PG-graded asphalt binder and ground tire rubber. The asphalt binder shall be graded in accordance to the AASHTO M-320. Three types of binders are identified: PG 64-22, PG 67-22 and PG 76-22.

The ground tire rubber shall be produced from tires by an ambient grinding method. The entire process shall be at or above ordinary room temperature. The rubber shall be sufficiently dry so as to be free flowing and to prevent foaming when mixed with asphalt cement. Also, it should be substantially free from contaminants including fabric, metal, mineral, and other non-rubber substances. Up to 4% (by weight of rubber) of talc or other inert dusting agent, may be added to prevent sticking and caking of the particles. The physical properties of the ground tire rubber shall meet the following requirements:

- Specific Gravity: 1.10 ± 0.06 .
- Moisture Content: Maximum 0.75%.
- Metal Contaminants: Maximum 0.01%.
- Gradation: Table 6.10.

Additionally, the asphalt-rubber should meet the specification shown in Table 6.11. The chemical composition of the ground tire rubber shall be determined in accordance with ASTM D297 and shall meet the following requirements:

- Acetone Extract: Maximum 25%.
- Rubber Hydrocarbon Content: 40 to 55%.
- Ash Content: Maximum 8% (10% for Type A).
- Carbon Black Content: 20 to 40%.
- Natural Rubber: 16 to 45%.

6.4.3.b Mineral Aggregates

The aggregate size No. 6 (0.75 inch aggregate size) shall be used and shall meet the requirements of Section 901 of the FDOT Standard Specifications.

6.4.3.c Construction Requirements

The existing pavement should be cleaned prior to the application of the asphalt rubber binder. The asphalt rubber binder should be applied only under the following conditions:

- Air temperature is above 50°F and rising.
- Pavement is absolutely dry.
- Wind conditions are such that cooling of the asphalt rubber binder will not be so rapid as to prevent good bonding of the aggregate.

The asphalt rubber binder shall be applied at the rate of 0.6 to 0.8 gal/yd² or as directed by the Engineer. Immediately after application of the asphalt rubber binder, the cover material (aggregate) should be spread uniformly at a rate of 0.26 and 0.33 ft³/yd². The application of the asphalt rubber binder and the application of the cover material should not be separated by more than 300 feet, unless approved by the Engineer.

In order to ensure maximum embedment of the aggregate, the entire width of the mat should be covered immediately by the traffic rollers. For the first coverage, a minimum of three traffic rollers should be provided in order to accomplish simultaneous rolling in echelon of the entire width of the spread.

6.4.4 Iowa Department of Transportation

The Iowa Department of Transportation (IDOT) only specifies the SAMI's for being placed under an unbounded Portland cement concrete (PCC). Such SAMI consists of a 1-inch nominal aggregate size HMA overlay (74).

The asphalt binder shall be a PG58-28. The mixture shall meet the following characteristics:

- 300,000 design ESAL.
- 3/8 inch (9.5 mm) nominal aggregate size gradation.
- The air voids target is 3.0%.
- No maximum film thickness restriction.
- No minimum filler/bitumen ratio restriction.
- Aggregate shall be Type B with no percent crushed particle requirements and gradation shall fall below the restricted zone.

The only performance test specified to the mixture is the Tensile strength ratio (TSR). The contractor shall run AASHTO T 283 during production. The test results shall satisfy 80% TSR when compared to the dry strength of specimens prepared with asphalt binder containing the anti-strip additive.

6.4.5 Massachusetts Department of Transportation

The Massachusetts Department of Transportation (MDOT) specifies the SAMI as the application of hot, rubberized asphalt and immediately embedding aggregate therein by spreading and rolling according with these specifications (75).

6.4.5.a Asphalt Rubber

The asphalt cement for the asphalt-rubber mixture shall be AC-10 or AC-20. If AC-10 is used, the SAMI shall be overlaid within ten days. The granulated rubber shall be a vulcanize rubber product from the ambient temperature processing of pneumatic tires. The granulated rubber type shall meet the gradation in Table 6.12.

The percent of asphalt-rubber shall be $23 \pm 2\%$ by the total weight of asphalt cement plus granulated rubber. The temperature of the asphalt shall be between 347°F and 428°F at the time of addition of the vulcanized rubber. The asphalt and the rubber shall be mixed together in a blender unit and reacted in a distributor for a period of time determined as required by the engineer. The temperature of the rubberized asphalt mixture shall be above 320 °C during the reaction period.

After the reaction between the asphalt and rubber has occurred, the viscosity of the hot rubberized asphalt mixture may be adjusted for spraying and “wetting” of the cover material by the addition of a diluent. The diluent shall comply with the

requirements of ASTM D369, Grade #1 fuel oil and shall not exceed 7.5 percent by volume of the hot asphalt rubber mixture.

Viscosities shall be run on each blended load of rubberized asphalt rubber using a Haake field viscometer. One viscosity prior to the induction of the diluent and one after the induction of the diluent blended into the asphalt and rubber mixture. The viscosity of the final product shall be in the range of 2 to 3 Pascal-seconds.

6.4.5.b Mineral Aggregates

The aggregate shall conform the requirements of M2.01.0 of the standard specifications for crushed stone. The percentage of wear as determined by the Los Angeles Abrasion Test (AASHTO T 96) shall be a maximum of 30.

6.4.5.c Construction Requirements

Prior to the application of the rubberized asphalt, the entire pavement surface to be treated shall be cleaned by sweeping, blowing and other methods until free of dirt and loose particles.

The rubberized asphalt mixture shall be applied at a temperature of 284°F to 338°F at a rate of 2.75 ± 0.25 liters/m². Transverse joints shall be constructed by placing building paper across and over the end of the previous rubberized asphalt application. Longitudinal joints shall be overlapped from 100 to 150 mm.

The application of the aggregate shall follow as close as possible behind the application of the hot rubberized asphalt which shall not be spread further in advance of the aggregate spread that can be immediately covered.

The dry aggregate should be pre-coated with 0.5 to 1.0% of AC-20 and shall be spread uniformly by a self-propelled spreader at a rate directed by the engineer, generally

between 15 and 20 kg per square meter. Prior to application the aggregate shall be pre-heated to a temperature between 248°F to 302°F.

Rolling shall be immediately following the spread of aggregate. There shall be at least three complete passes by the pneumatic tired rollers to embed the aggregates particles firmly into the rubberized asphalt, followed by an additional pass of the steel roller.

The rubberized asphalt surface should be overlaid immediately following completion of sweeping. If traffic must travel over the SAMI, it shall be allowed to cool and speed controlled as not to exceed 25 miles per hour.

6.4.6 Texas Department of Transportation

The Crack attenuating mixture (CAM) is a pavement layer composed of a hot compacted mixture of aggregate and asphalt binder mixed in a mix plant. It is not allowed to use reclaimed asphalt pavement (RAP) in the CAM mixture (76).

6.4.6.a Asphalt Binder

It is specified to use a conventional PG-graded asphalt binder based on AASHTO M-320 according to the contract requirements.

6.4.6.b Mineral Aggregates

The mineral aggregate shall meet the properties specified in Table 6.13. The coarse aggregate stockpiles must have no more than 20% material passing the No. 8 sieve. The fine aggregate consist of manufacture sands. Natural sands are not allowed. Fine aggregate stockpiles must meet the gradation requirements in Table 6.14. The fine aggregate shall be supplied free from organic impurities. If 10% or more of the fine aggregate stockpile is retained on the No.4 sieve, test the stockpile and verify that it

meets the requirements in Table 6.13 for coarse aggregate angularity and flat and elongated particles. Lime shall be added as mineral filler at a rate of 1% by weight of the total dry aggregate.

6.4.6.c Tack Coat

A base PG-graded binder should be used with a minimum high-temperature grade of PG58.

6.4.6.d Mixture Design

The mixture shall be designed according to the Superpave design procedure given in Tex-204-F, Part IV. The target laboratory density should be 98.0% at $N_{des} = 50$. The engineer will approve the target asphalt percentage based on acceptable results from the Hamburg Wheel and Overlay tests. The mixture gradation specification and volumetric properties of the mixture are shown in Table 6.15. The mixture design properties are shown in Table 6.16. Additives such lime or antistripping liquid can be added to the mixture if required.

6.4.6.e Construction Requirements

Prepare the surface by removing raised pavement markers and objectionable material such as moisture, dirt, leaves and other loose materials. Remove vegetation from pavement edges. Place the mixture to meet the typical section requirements and produce a smooth, finished surface with a uniform appearance and texture. Offset longitudinal joints of successive courses of hot mix by at least 6 inch. Place mixture so longitudinal joints on the surface coincide with lane lines, or as directed. Ensure all finished surface will drain properly. Place mixture within the compacted lift thickness shown in Table 6.17 unless otherwise shown on the plans.

Place the mixture when the roadway surface temperature is equal or higher than temperatures listed in Table 6.18 unless otherwise approved. The surface shall be cleaned before applying the tack coat. The tack coat rate shall be between 0.04 to 0.10 gal. of residual asphalt per square yard of surface area. Apply a thin, uniform tack coat to all contact surfaces of curbs, gutter, and structures. The mixture shall be compacted to achieve a maximum in-place air voids value of 4.0%.

6.4.7 Utah Department of Transportation

The Utah Department of Transportation (UDOT) specification covers the materials and construction requirements for producing and placing a reflective cracking relief bituminous mixture. Such stress absorbing membrane interface is a highly elastic, impermeable hot mix interlayer that is designed to reduce reflective cracking for underlying pavements. The SAMI should be placed in one lift and covered with an HMA overlay (77).

The reflective crack relief bituminous mixture shall meet the general requirements specified for a HMA mixture, except as modified herein.

6.4.7.a Asphalt Binder

The asphalt binder should meet the requirements of AASHTO MP-1 with a PG high temperature of 64 °C or higher and a PG low temperature of -34 °C or lower as required to meet the Hveem stability and the flexural beam fatigue mix requirements, in addition to the following requirements in Table 6.19.

6.4.7.b Blended Aggregate

The blended aggregate shall consist of natural sands and crushed fines. The aggregate gradation should meet the ranges specified in Table 6.20. The blended

aggregate sand equivalent should have a minimum value of 45% as determined by AASHTO T 176.

6.4.7.c Mixture Design

The mixture design should use fifty gyrations ($N_{\max} = 50$) for gyratory compaction. The mixture should be aged for beam testing for 4 hours at 135 °C in accordance to AASHTO PP2-99 Section 7.2 (mechanical property testing), prior to compact the beams. The volumetric properties of the SAMI should meet the specifications in Table 6.21.

6.4.7.d Construction Requirements

Immediately prior to applying the SAMI, thoroughly clean the surface of all vegetation, loss materials, dirt, mud, visible moisture and other objectionable materials. Fill the joints that are larger than 0.5 inch wide as determined by the engineer. Prior to the placement of the SAMI, fill large surface deformities (greater than 3 inch deep and 4 feet in diameter) with approved mix. During the placement of the SAMI, fill smaller pavement deformities, with the reflective crack bituminous mixture.

A tack coat should be applied between the HMA layer and the SAMI at typical rates of 0.02 to 0.04 gallons per square yard (undiluted tack). The SAMI should not be placed when the temperature is below 50°F. To reduce the occurrence of blisters, do not place the SAMI on a wet surface or within 24 hours of rain.

The SAMI should be placed in an average thickness of 1 inch with a tolerance of $\pm 1/4$ inch. The longitudinal joints should be overlapped by at least 6 inch to eliminate construction joints over the existing longitudinal joints. The SAMI should not be heated above 350°F.

The compaction operations should start promptly after placement of the SAMI. Only steel wheel rollers in static mode are allowed for compaction of the mixture. The density of the SAMI should be within $97 \pm 2\%$ of the maximum specific gravity as determined by AASHTO T 209.

The SAMI should be covered with the binder course within five days after placement. It should be opened to traffic or covered with the HMA overlay after cooling to less than 140°F.

6.5 PROPOSED PLAN FOR PHASE III

Based on NDOT's positive experience with stress relief courses and the review of the states' specifications for stress relief courses, it is recommended to conduct an extensive laboratory evaluation for the Texas DOT and the UTAH DOT SRC designs using Nevada's materials during 2008. The following summarizes the major steps recommended to be completed in the Phase III of the NDOT study:

- Select two aggregate sources with different mineralogy and absorption: one in northern Nevada and one in southern Nevada.
- Identify three categories of binders to be used with each of the aggregate sources. All binders must meet the PG64-28 grade for the northern part and the PG76-22 grade for the southern part.
 - Polymer modified asphalt binder
 - Tire rubber terminal blend asphalt binder
 - Crumb rubber asphalt binder
- For each combination of aggregate source and asphalt binder conduct a mix design according to the TxDOT and UDOT stress relief courses.
- Evaluate the mechanical properties of the SRC mixes in the laboratory in terms of their dynamic modulus, fatigue resistance, rutting resistance using the RLT, thermal cracking resistance using the TSRST, reflective cracking resistance using the TTI Upgraded Overlay tester, and moisture sensitivity.
- Conduct a Type 2C NDOT Hveem Mix design for each of the aggregate sources and the polymer modified asphalt binder.
- Evaluate the mechanical properties of the NDOT T2C mixes in the laboratory in terms of their dynamic modulus, fatigue resistance, rutting resistance using the

RLT, thermal cracking resistance using the TSRST, reflective cracking resistance using the TTI Upgraded Overlay tester, and moisture sensitivity.

- Optimize the gradation of the NDOT T2C HMA mixes.

Based on the results of the laboratory evaluation, recommendations will be made for constructing field test sections with SRC mixes in 2009. The overlay thickness will be designed using the Rubber Pavements Association Overlay Design Model. Field mixtures from the SRC and overlay mixes will be collected during construction from behind the paver and evaluated for asphalt binder content and gradation. Additionally, the field mixtures will be evaluated in terms of their dynamic modulus, fatigue resistance, rutting resistance using the RLT, thermal cracking resistance using the TSRST, reflective cracking resistance using the TTI Upgraded Overlay tester, and moisture sensitivity.

The performance of the field test sections will be monitored and field cores will be sampled for evaluation in the TTI Overlay Tester. Based on the laboratory evaluation and the field performance the specifications for reflective cracking resistance will be adjusted and the most effective technique will be selected.

REFERENCES

1. Dempsey, B. J. (2002). "Development and Performance of Interlayer Stress-Absorbing Composite in Asphalt Concrete Overlays," *In Transportation Research Record 1809*, TRB, National Research Council, pp. 175-183.
2. Freeman T. E. (2002). "Evaluation of Concrete Slab Fracturing Techniques in Mitigating Reflective Cracking Through Asphalt Overlays," Report VTRC 03-R3, Virginia Transportation Research Council, Charlottesville, Virginia.
3. NCHRP Research Project 1-37A, Development of the 2002 Guide for the Design of New and Rehabilitated Pavement Structures, Currently underway.
4. Scofield, L. A. (1989). "The History, Development, and Performance of Asphalt Rubber at ADOT," Report Number AZ-SP-8902, Arizona DOT.
5. Way, G. B. (1999). "Flagstaff I-40 Asphalt-Rubber Overlay-Nine Years of success," Presented at the 78th Annual Meeting of the Transportation Research Board.
6. The I-40 in Flagstaff, Arizona, The successful Asphalt-Rubber project that inspires engineers from around the world. www.rubberpavements.org/newsletter/fall2003/.
7. Trevino, M., Dossey, T., McCullough, F., and Yildirim, Y. (2003). "Applicability of Asphalt Concrete Overlays on Continuously Reinforced Concrete Pavements." CTR Research Report 4398-1, Center for Transportation Research, Bureau of Engineering Research, The University of Texas at Austin.
8. Rahman, M., Scofield, L., and Wolf, T. (1989). "Paving Fabrics for Reducing Reflective Cracking," Report No. FHWA-AZ-8801, Arizona Transportation Research Center, Prepared for Arizona Department of Transportation.
9. Amini, F. (2005). "Potential Applications of Paving Fabrics to Reduce Reflective Cracking," Report No. FHWA/MS-DOT-RD-05-174, Jackson State University, Prepared for Mississippi Department of Transportation.
10. Woodside, A. R., McIlhagger, R., Woodward, W. D. H., and Clements, H. W. (1996). "Inhibiting Reflective Cracking," University of Arizona, Department of Civil Engineering and Engineering Mechanics, Tucson, AZ.
11. Woodside, A. R., Woodward, W. D. H., Clements, H. W., Sikich, J., and Russell, T. (1997). "The Use of Fabrics to Inhibit Reflective Cracking in Porous Asphalt," European Conference on Porous Asphalt, Madrid, Spain, Volume I, pp. 271-83.
12. Predoehl, N. H. (1989). "Use of Paving Fabric Test Installations in California," Final Report, California Department of Transportation, Translab, 1989.
13. Banasiak, D. (1997). "Fiberglass Mesh Reduces Reflective Cracking on California Highway," *Road & Bridges*, Vol. 35, Issue 3, pp.54.
14. FHWA (1982). "Report on Performance of Fabrics in Asphalt Overlays," Office of Highway Operation, Experimental Application and Evaluation Branch.
15. Shuler, S., and Hermelink, D. (2004). "Reducing Reflection Cracking in Asphalt Pavements," *Cracking in Pavements, Mitigation, Risk Assessment and Prevention*, Proceedings of the Fifth International RILEM Conference, France, pp. 451-458.
16. Gulden, W., and Brown, D. (1984). "Overlays for Plain Jointed Concrete Pavements," *Research Project No. 7502*, Office of Materials and Research, Georgia Department of Transportation.

17. Gulden, W., and Brown, D. (1985). "Treatments for Reduction of Reflective Cracking of Asphalt Overlays on Jointed-Concrete Pavements in Georgia," *In Transportation Research Record 1007*, TRB, National Research Council, Washington, D.C., pp. 26-36.
18. Brown, D. R., Jared, D., Jones, C., and Watson, D. (1997). "Georgia's Experience with Crumb Rubber in Hot-Mix Asphalt," *In Transportation Research Record 1583*, TRB, National Research Council pp. 45-51.
19. Mascunana, I. (1981). "An Evaluation of Engineering Fabric in Pavement Rehabilitation (IHD-21)," Final Report, Physical Research Report No. 88, Illinois Department of Transportation.
20. Buttlar, W. G., Bozkurt, D. and Dempsey, B. J. (1999). "Evaluation of Reflective Crack Control Policy," Final Report, Report No. ITRC FR 95/96-4, Illinois Transportation Research Center, Edwardsville, IL, p. 184.
21. Vespa, J. (2005). "An Evaluation of Interlayer Stress Absorbing Composite (ISAC) Reflective Crack Relief System," Final Report No. FHWA/IL/PRR 150, Illinois Department of Transportation, Bureau of Materials & Physical Research, IL.
22. Jiang, Y., and McDaniel, R. S. (1993). "Application of Cracking and Sealing and Use of Fibers to Control Reflective Cracking," *In Transportation Research Record 1388*, TRB, National Research Council pp. 150-159.
23. Rasoulilian, M., Becnel, B., and Keel, G. (2000). "Stone Interlayer Pavement Design," *In Transportation Research Record 1709*, TRB, National Research Council, pp. 60-68.
24. Glasgrid Pavement Reinforcement System. "System Overview," Tensar International Corporation.
25. 2006 Standard Specifications for Roads & Bridges Manual, *Section 507 Asphaltic Surface Treatment*, Louisiana Department of Transportation.
26. V.T. Barnhart (1989). "Field Evaluation of Experimental Fabrics to Prevent Reflective Cracking in Bituminous Resurfacing," Report No. R-1300. Materials & Technology Division, Michigan Transportation Commission, Lansing, Michigan.
27. Kidd, S. Q. (1990). "Paving Fabric and Asphalt Stress Absorbing Membrane Interlayers (SAMI)," Final Report, Report No. MSHD-RD-90-67-6, Mississippi State Highway Department Research and Development Division, Jackson, MS.
28. Maurer, D. A. and Malashekie G. J. (1989). "Field Performance of Fabrics and Fibers to Retard Reflective Cracking," *In Transportation Research Record 1248*, TRB, National Research Council, pp. 13-23.
29. Hughes, J. J., and Somers, E. (2000). "Geogrid Mesh for Reflective Crack Control in Bituminous Overlays," Final Report, Report No. PA 200-013-86-001, Pennsylvania Department of Transportation.
30. Morian, D. A., Oswalt, J., and Deodhar A. (2004). "Experience with Cold In-Place Recycling as a Reflective Crack Control Technique: Twenty Years Later," *In Transportation Research Record 1869*, TRB, National Research Council, pp. 47-55.
31. Cleveland G. S., Button J. W., and Lytton R. (2002). "Geosynthetics in Flexible and Rigid Pavement Overlay Systems to Reduce Reflection Cracking," Research Report 1777-1, Project Number 0-1777, Texas Transportation Institute.

32. Darling, J.R., and Woolstencroft, J.H. (2004). "Fiberglass Pavement Reinforcement Used in Dissimilar Climatic Zones for Retarding Reflective Cracking in Asphalt Overlays," *Cracking in Pavements, Mitigation, Risk Assessment and Prevention*, Proceedings of the Fifth International RILEM Conference, France, pp. 435-442.
33. Chen, D. H., Scullion, T., and Bilyeu, J. (2006). "Lessons Learned on Jointed Concrete Pavement Rehabilitation Strategies in Texas," *In Journal of Transportation Engineering*, ASCE, Volume 132, Issue 3, pp. 257-265.
34. Freeman, T. E. (2002). "Evaluation of Concrete Slab Fracturing Techniques in Mitigating Reflective Cracking Through Asphalt Overlays," Report VTRC 03-R3, Virginia Transportation Research Council.
35. Bischoff, D., and Toepel, A. (2003). "GlassGrid Pavement Reinforcement Product Evaluation," Final Report FEP-03-03, WisDOT Research study # WI-89-03, Wisconsin Department of Transportation.
36. Abu Al-eis, K. (2004). "Evaluation of the Interlayer Stress-Absorbing Composite (ISAC) to Mitigate Reflective Cracking in Asphaltic Concrete Overlays," Construction Report WI-09-04, Wisconsin Department of Transportation.
37. Makowski, L., Bischoff, D., Blankenship, P., Sobczak, D., and Haulter F. (2005). "Wisconsin Experiences with Reflective Crack Relief Projects," *In Transportation Research Record* 1905, TRB, National Research Council, pp. 44-55.
38. Vanelstraete A., and De Visscher J. (2004). "Long Term Performance on Site of Interface Systems," *Cracking in Pavements, Mitigation, Risk Assessment and Prevention*, Proceedings of the Fifth International RILEM Conference, France, pp. 699-706.
39. Tighe, S., Haas, R., and Ponniah, J.. (2003). "Life Cycle Cost Analysis of Mitigating Pavement Rehabilitation Reflection Cracking," *In Transportation Research Record* 1823, TRB, National Research Council, pp. 73-79.
40. Valtonen, J., and Hyypä, I. (2004). "Field Study of Repair Methods for Transversal Cracks," *Cracking in Pavements, Mitigation, Risk Assessment and Prevention*, Proceedings of the Fifth International RILEM Conference, France, pp. 555-562.
41. *Flexible Pavements Distress Identification Manual*, Nevada DOT, Materials Division, Carson City, Nevada.
42. Lewis, A., and Collins, D. (1999). "Cold In-Place Recycling: A Relevant Process for Road Rehabilitation and Upgrading," 7th Conference on Asphalt Pavements for Southern Africa.
43. Fernandez, George. *Data Mining using SAS Applications*. Chapman & HALL/CRC, Washington, D.C, 2003.
44. Kuelh, R., Design of Experiments: statistical Principles of Research Design and Analysis. Second Edition, 2000. pp175-222.
45. Elseifi, M., and Al-Qadi, I. (2003). "A Simplified Overlay Design Model Against Reflective Cracking Utilizing Service Life Prediction," Paper No. 03-3285 presented at the TRB 82nd Annual Meeting, Washington, D.C.
46. Jacobs, M. M., Hopman, P. C., and Molenaar, A. A. A. (1996). "Application of Fracture Mechanics Principles to Analyze Cracking in Asphalt Concrete." In Proceeding Annual Meeting of the Association of Asphalt Paving Technologists, AAPT, Vol. 65, Baltimore, MD, pp. 1-39.

47. Uzan, J (1997). "Evaluation of Fatigue Cracking," *In Transportation Research Record 1570*, TRB, National Research Council, Washington, D.C., pp. 89-95.
48. BRRC, Belgian Road Research Center (1998). "Design of Overlaid Cement Concrete Pavements Reinforced with Bitufor® traffic loading." Research report EP5035/3544, Brussels, Belgium.
49. Paris, P. C., and Erdogan, F. A. (1963). "Critical Analysis of Crack Propagation Laws," *In Transactions of the ASME, Journal of Basic Engineering, Series D*, No. 3.
50. Mobasher, B., Mamlouk, M. S., and Lin, H-M (1997). "Evaluation of Crack Propagation Properties of Asphalt Mixtures," *In Journal of Transportation Engineering*, ASCE, Vol. 123, No. 5, pp. 405-413.
51. Kanninen, M. F., and Popelar, C. H. (1985). "Advanced Fracture Mechanics," Oxford University Press, Inc., NY.
52. Ullidtz, P. (1987). *Pavement Analysis*. New York: Elsevier Science.
53. Sousa, J., Pais, J., Saim, R., Way, G., and Stubstad, R. (2001). "Development of a Mechanistic Overlay Design Method Based on Reflective Cracking Concepts," Final Report for Rubber Pavements Association, Consulpav International.
54. Claussen, A.I.M., Edwards, J.M., Sommer, P., and Ugé, P. (1977). "Asphalt Pavement Design. The Shell Method," *Proceedings, Fourth International Conference on the Structural Design of Asphalt Pavements*, Vol. 1, Ann Arbor, pp. 39-74.
55. *Guide for Mechanistic-Empirical Design of New and Rehabilitated Pavement Structures* (2004). Final Report, Part 3 Design Analysis, Ch 6, National Cooperative Highway Research Program, Transportation Research Board, National Research Council.
56. Grzybowska, W., Wojtowicz, J., and Fonferko, L. C. (1993). "Application of Geo-Synthetics to Overlays in Cracow Region of Poland," *Reflective Cracking in Pavements, State of the Art and Design Recommendations*, Proceedings of the Second International RILEM Conference, Liege, Belgium, pp. 290-298.
57. Livneh, M., Ishai, I., and Kief, O. (1993). "Bituminous Pre-Coated Geotextile Felts for Retarding Reflection Cracks," *Reflective Cracking in Pavements, State of the Art and Design Recommendations*, Proceedings of the Second International RILEM Conference, Liege, Belgium, pp. 343-350.
58. Di Benedetto, H, Neji, J, Antoine, J. P, and Pasquier, M. (1993). "Apparatus for Laboratory Study of Cracking Resistance," *Reflective Cracking in Pavements, State of the Art and Design Recommendations*, Proceedings of the Second International RILEM Conference, Liege, Belgium, pp. 179-186.
59. Tschegg, E. K, Stanzl- Tschegg, S. E., and Litzka, J. (1993). "New Testing Method to Characterize Mode I Fracturing of Asphalt Aggregate Mixtures," *Reflective Cracking in Pavements, State of the Art and Design Recommendations*, Proceedings of the Second International RILEM Conference, Liege, Belgium, pp. 263-270.
60. Dumas, Ph., and Vecoven, J. (1993). "Processes Reducing Reflective Cracking; Synthesis of Laboratory Tests," *Reflective Cracking in Pavements, State of the Art and Design Recommendations*, Proceedings of the Second International RILEM Conference, Liege, Belgium, pp. 246-253.

61. Gibney, A., Lohan, G., and Moore, V. (2002). "Laboratory Study of Resistance of Bituminous Overlays to Reflective Cracking," *In Transportation Research Record 1809*, TRB, National Research Council pp. 184-190.
62. British Standard Institution (1998). "Sampling and Examination of Bituminous Mixtures for Road and Other Paved Areas: Methods of Test for the Determination of Wheel Tracking Rate," British Standard 598, Part 110, London, England.
63. Dempsey, B. J. (2002). "Development and Performance of Interlayer Stress Absorbing Composite (ISAC) in AC Overlays". *In Transportation Research Record 1809*, TRB, National Research Council pp. 175-183.
64. Montestruque, G., Rodrigues, R., Nods, M., and Elsing, A. (2004). "Stop of Reflection Crack Propagation with the Use of Pet Geogrid as Asphalt Overlay Reinforcement," *Cracking in Pavements, Mitigation, Risk Assessment and Prevention*, Proceedings of the Fifth International RILEM Conference, Lomoges, France, pp. 231-238.
65. Sobhan, T., Crooks, T., Tandon, T., and Mattingly, S. (2004). "Laboratory Simulation of the Growth and Propagation of Reflection Cracks in Geogrid Reinforced Asphalt Overlays," *Cracking in Pavements, Mitigation, Risk Assessment and Prevention*, Proceedings of the Fifth International RILEM Conference, Lomoges, France, pp. 589-596.
66. Gallego, J., and Prieto, J. N. (2006). "Development of New Laboratory Equipment for the Study of Reflective Cracking in Asphalt Overlays," *In Asphalt Overlays and Infrastructure Distress*. CD-ROM. Transportation Research Board of the National Academies, Washington, D.C.
67. Tamagny, P., Wendling, L., and Piau, J. M. (2004). "A New Explanation of Pavement Cracking from Top to Bottom: The Visco-elasticity of Asphalt Materials," *Cracking in Pavements, Mitigation, Risk Assessment and Prevention*, Proceedings of the Fifth International RILEM Conference, Lomoges, France, pp. 425-432.
68. Zhou, F., Scullion, T., and Williammee, R. (2004). "Upgraded TTI Overlay Tester: A Simple Reflective Cracking Simulation Test," *In Pavement Management, Design, and Testing*. CD-ROM. Transportation Research Board of the National Academies, Washington, D.C.
69. Zhou, F., and Scullion, T. (2005). "Overlay Tester: A Rapid Performance Related Crack Resistance Test," Texas Transportation Institute, the Texas A&M University System, Report FHWA/TX-05/0-4667-2, Austin, Texas.
70. Núñez, P. W., Ceratti, J. A. P., Theisen, K. M., and Morhila, A. (2006). "Using APT to Compare the Efficiency of Overlay Materials Used in Brazil," *In Bituminous Materials, Pavement Management, International*. CD-ROM. Transportation Research Board of the National Academies, Washington, D.C.
71. Standard Specifications for Highway Construction (2000). Arizona Department of Transportation, ADOT, Sections 404, 410 and 1009. http://www.dot.state.az.us/Highways/cns/CNS_Stored_specs.asp.
72. Asphalt Rubber Usage Guide Division of Engineering Services (2003). California Department of Transportation, Caltrans, http://www.dot.ca.gov/hq/esc/Translab/pubs/Caltrans_Aspphalt_Rubber_Usage_Guide.pdf.

73. Standard Specifications for Highway Construction (2005). Florida Department of Transportation, FDOT, Sections 336, 341 and 916, <http://www.dot.state.fl.us/Specificationsoffice/2007BK/TOC.htm>.
74. Standard Specifications for Highway Construction (2006). Iowa Department of Transportation, IDOT, Sections 2303, 2310 and 4127. http://www.erl.dot.state.ia.us/OCT_2006/GS/frames.htm.
75. Standard Specifications for Highway Construction (1995). Massachusetts Department of Transportation (MDOT), Section 466, <http://www.mhd.state.ma.us/default.asp?pgid=content/publicationmanuals&sid=about>
76. Standard Specifications for Highway Construction (2004). Texas Department of Transportation TxDOT, CSJ 0353-04-090, Section 3141.
77. Standard Specifications for Highway Construction (2002). Utah Department of Transportation, UDOT, Section 02744S, <http://www.udot.utah.gov/download.php/tid=520/UDOT2002SpecsBasic.pdf>.

TABLES

Table 3.1 List of Selected NDOT Projects.

Contract	Route	County	Location	Treatment	DOC	AADT
2191	US095	NY	Southern NV	CIR	April 1990	5,500
2385	US093	EL	Northern NV	CIR	April 1990	5,250
2385	US093	EL	Northern NV	CIR	April 1990	5,250
2428	US050	EU	Northern NV	CIR	April 1991	1,900
2808	US050	WP	Northern NV	CIR	April 1997	2,950
2808	US050	EU	Northern NV	CIR	April 1997	2,950
2838	SR396	PE	Northern NV	CIR	April 1997	1,100
2935	SR360	MI	Southern NV	CIR	March 1998	800
2819	US095	NY	Southern NV	CIR	May 1997	5,550
2873	US095	NY	Southern NV	CIR	May 1998	5,550
2961	US006	ES	Southern NV	CIR	March 1999	2,000
3013	US095A	LY	Northern NV	CIR	May 2001	14,500
3025	US093	WP	Northern NV	CIR	June 2000	5,000
3025	US093	LN	Northern NV	CIR	June 2000	1,000
3025	SR208	LN	Northern NV	CIR	June 2000	1,000
2876	SR208	LY	Northern NV	CIR	June 2000	1,500
2761	SR443	WA	Northern NV	Reinforced Fabrics	June 1996	9600
2932	US095	MI	Southern NV	Reinforced Fabrics	Feb. 1999	2850
2980	US050	CH	Northern NV	Reinforced Fabrics	June 1999	1000
2980	US095	CH	Northern NV	Reinforced Fabrics	June 1999	4400
3006	IR080	HU	Northern NV	Reinforced Fabrics	March 2000	7200
3008	SR227	EL	Northern NV	Reinforced Fabrics	May 2000	10000
2723	US095	CL	Southern NV	Stress Relief course	May 1997	40000
3031	US395	WA	Northern NV	Stress Relief course	June 2000	15600
3048	SR157	CL	Southern NV	Stress Relief course	Nov. 2000	2700
3045	US050	EU	Northern NV	Stress Relief course	June 2001	1900
3162	US395	WA	Northern NV	Stress Relief course	June 2003	29100
2384	US095	CC	Northern NV	Mill & Overlay	April 1990	40,000
2384	US095	LY	Northern NV	Mill & Overlay	April 1990	5,500
2432	SR157	CL	Southern NV	Mill & Overlay	May 1991	2,700
2505	US095	MI	Southern NV	Mill & Overlay	June 1992	3,350
2651	US095	ES	Southern NV	Mill & Overlay	July 1994	2,000
2651	US095	ES	Southern NV	Mill & Overlay	July 1994	1,700
2651	US095	ES	Southern NV	Mill & Overlay	July 1994	1,700
2679	US095	ES	Southern NV	Mill & Overlay	Feb. 1996	6,750
3028	SR512	CC	Northern NV	Mill & Overlay	June 2000	7250
2070	SR160	NY	Southern NV	Mill & Overlay	May 2005	7500
2886	IR080	LA	Northern NV	Crack & Seat	June 1998	6,750
2889	IR080	EL	Northern NV	Crack & Seat	July 1998	10,800
2962	IR080	EL	Northern NV	Crack & Seat	May 1999	4,700
2999	IR080	EL	Northern NV	Crack & Seat	Dec. 1999	6,200
3021	IR080	WA	Northern NV	Crack & Seat	June 2000	23,000
2544	IR080	EL	Northern NV	Rubblized PCCP	June 1993	7000
2869	IR080	EL	Northern NV	Rubblized PCCP	April 1998	6550
2901	IR080	HU	Northern NV	Rubblized PCCP	Sep. 1998	7200
3088	IR080	PE	Northern NV	Rubblized PCCP	Sep. 1998	7700
3186	IR080	HU	Northern NV	Rubblized PCCP	Oct. 2003	6300
3186	IR080	LA	Northern NV	Rubblized PCCP	Dec. 2001	6300

Table 3.2a Pavement Distresses Summary of Selected NDOT Projects.

Treatment	Contract	County	Route	Location (North/South)	Date of Construction	Treatment Life	AADT	Pavement Distresses Before Treatment Application (Severity)						Pavement Distresses After Treatment Application (Severity/Time in Years to Develop)						
								Fatigue cracking Type		Transverse Cracks	Block Cracking Type			Fatigue cracking Type		Transverse Cracks	Block Cracking Type			
								A	B		A	B	C	A	B		A	B	C	
Cold In-Place Recycling (CIR)	CIR-A-1	2808a	WP	US050	N	1998	7	2,950	Sev	-	Mod	Min	-	-	-	-	Min/7	-	-	-
	CIR-A-2	2808b	EU	US050	N	1997	8	2,950	Min	Sev	Mod	-	-	Min	-	-	Min/2	-	-	-
	CIR-A-3	2838	PE	SR396	N	1999	6	1,100	-	-	Sev	Sev	Sev	Sev	-	-	Min/1	-	-	-
	CIR-A-4	2935	MI	SR360	S	1999	6	800	Sev	Mod	Min	Min	Mod	Mod	-	-	-	-	-	-
	CIR-B-1	2819	NY	US095	S	1998	7	5,550	-	Sev	Mod	-	Min	Min	Min/3	-	Min/2	-	-	-
	CIR-B-2	2873	NY	US095	S	1998	7	5,550	Min	-	Min	Min	Sev	Min	Min/7	-	Min/7	-	-	-
	CIR-B-3	2961	ES	US006	S	1999	6	2,000	Min	-	Min	Sev	Sev	Sev	-	-	-	-	-	-
	CIR-B-4	3013	LY	US095	N	1999	6	14,500	Min	-	Min	Mod	-	-	-	-	Min/6	-	-	-
	CIR-C-1	3025a	WP	US093	N	2003	2	5,000	Min	Min	Min	-	-	-	-	-	Min/1	-	-	-
	CIR-C-2	3025b	LN	US093	N	2001	4	1,000	Min	Mod	Min	Mod	Mod	Min	-	-	Min/1	-	-	-
CIR-C-3	3025c	LN	SR208	N	2001	4	1,000	Min	Min	Min	Mod	Mod	Min	-	-	Min/1	-	-	-	
CIR-C-4	2876	LY	SR208	N	2001	4	1,500	Min	-	Sev	Mod	-	Min	-	-	Min/1	-	-	-	
Reinforced Fabric (RF)	RF-1	2761	WA	SR443	N	1999	6	9600	Min	Sev	Mod	Sev	Mod	-	Min/5	-	Min/1	-	-	-
	RF-2	2932	MI	US095	S	1999	6	2850	Min	Min	Sev	-	-	-	-	-	-	-	-	
	RF-3	2980a	CH	US050	N	2000	5	1000	Min	Min	Sev	-	Min	Min	-	-	-	-	-	
	RF-4	2980b	CH	US095	N	2000	5	4400	Min	Min	Min	-	-	-	-	-	Min/3	-	-	-
	RF-5	3006	HU	IR080	N	2001	4	7200	Min	Min	Min	-	-	-	-	-	-	-	-	
	RF-6	3008	EL	SR227	N	2001	4	10000	Min	Min	Min	-	-	-	-	-	Min/2	-	-	-
Stress Relief Course (SRC)	SRC-1	2723	CL	US095	S	1997	8	40000	Mod	Sev	Mod	Mod	Min	-	-	-	-	-	-	
	SRC-2	3031	WA	US395	N	2000	5	15600	Min	Min	Mod	Sev	-	-	-	-	Min/5	-	-	
	SRC-3	3048	CL	SR157	S	2000	5	2700	Mod	-	Mod	-	-	-	-	-	Min/5	-	-	
	SRC-4	3045	EU	US050	N	2001	4	1900	Min	Mod	Mod	-	-	-	-	-	-	-	-	
	SRC-5	3162	WA	US395	N	2003	2	29100	-	-	Min	-	-	-	-	-	-	-	-	

Min Denotes "Minor", Mod Denotes "Moderate", Sev Denotes "Severe"

Table 3.2b Pavement Distresses Summary of Selected NDOT Projects (Continued).

Treatment	Contract	County	Route	Location (North/South)	Date of Construction	Treatment Life	AADT	Pavement Distresses Before Treatment Application (Severity)						Pavement Distresses After Treatment Application (Severity/Time in Years to Develop)						
								Fatigue cracking Type		Transverse Cracks	Block Cracking Type			Fatigue cracking Type		Transverse Cracks	Block Cracking Type			
								A	B		A	B	C	A	B		A	B	C	
Mill and Overlay (MOL)	MOL-A-1	2384a	CC	US095	N	1990	15	40,000	-	Sev	Min	Mod	-	-	Mod/1	-	Mod/1	-	-	-
	MOL-A-2	2384b	LY	US095	N	1993	12	5,500	Mod	Sev	Mod	Min	-	-	Min/4	-	Min/2	-	-	-
	MOL-B-1	2432	CL	SR157	S	1993	12	2,700	Mod	-	Mod	-	-	-	-	-	Min/5	-	-	-
	MOL-B-2	2505	MI	US095	S	1993	12	3,350	-	Sev	-	Mod	-	Sev	-	-	-	-	-	-
	MOL-C-1	2651a	ES	US095	S	1995	10	2,000	-	Mod	-	Mod	-	Min	-	-	-	Min/5	-	-
	MOL-C-2	2651b	ES	US095	S	1996	9	1,700	-	-	-	-	Sev	Sev	-	-	Min/5	-	-	-
	MOL-C-3	2651c	ES	US095	S	1996	9	1,700	Mod	-	Mod	Mod	Sev	Sev	Min/5	-	Min/5	-	-	-
	MOL-C-4	2679	ES	US095	S	1997	8	6,750	Mod	-	Min	Mod	Min	-	-	-	Mod/1	Min/6	-	-
	MOL-B-3	3028	CC	SR512	N	2000	5	7250	-	-	Mod	-	-	-	-	-	Min/3	-	-	-
MOL-C-5	3070	NY	SR160	S	2003	2	7500	Min	Min	Min	Mod	Mod	-	-	-	-	-	-	-	
Crack & Seat PCCP (CS)	CS-1	2886	LA	IR080	N	1998	7	6,750	-	-	-	-	-	-	Min/6	-	Min/4	-	-	-
	CS-2	2889	EL	IR080	N	1999	6	10,800	-	-	-	-	-	-	Min/4	-	-	-	-	-
	CS-3	2962	EL	IR080	N	1999	6	4,700	-	-	Min	-	-	-	Min/6	-	-	-	-	-
	CS-4	2999	EL	IR080	N	2001	4	6,200	-	-	-	-	-	-	Min/4	-	-	-	-	-
	CS-5	3021	WA	IR080	N	2001	4	23,000	-	-	-	-	-	-	Min/4	-	-	-	-	-
Rubblized PCCP (R)	RPCC-1	2549	EL	IR080	N	1996	9	7000	-	-	Min	-	-	-	Min/5	-	-	-	-	-
	RPCC-2	2869	EL	IR080	N	1999	6	6550	-	-	-	-	-	-	Mod/4	-	-	-	-	-
	RPCC-3	2901	HU	IR080	N	1999	6	7200	-	-	-	-	-	-	Min/6	-	-	-	-	-
	RPCC-4	3088	PE	IR080	N	2002	3	7700	-	-	-	-	-	-	-	-	-	-	-	-
	RPCC-5	3186a	HU	IR080	N	2005	0	6300	-	-	-	-	-	-	-	-	-	-	-	-
	RPCC-6	3186b	LA	IR080	N	2005	0	6300	-	-	-	-	-	-	-	-	-	-	-	-

Min Denotes "Minor", Mod Denotes "Moderate", Sev Denotes "Severe"

Table 3.3a Ranking of Selected NDOT Projects Based on Principal Component Analysis.

Trt.	Cont.	ID	Description of Treatment	AADT	DOC	Life	Loc.	Ranking ⁺					
								-1 [#]	+1 [#]	-1 [#]	+3 [#]	-1 [#]	+5 [#]
CIR	2808a	CIR-A-1	CIR 2.0" + 2.5" DGHMA* + 0.75" OGFC	2,950	1998	7	N	27	1	26	1	20	1
	2808b	CIR-A-2	CIR 2.0" + 2.5" DGHMA + 0.75" OGFC	2,950	1997	8	N	17 [†]	1	19 [†]	14 [†]	21	12 [†]
	2838	CIR-A-3	CIR 2.0" + 2.5" DGHMA + 0.75" OGFC	1,100	1999	6	N	33	2	35	2	32	5
	2935	CIR-A-4	CIR 2.0" + 2.5" DGHMA + 0.75" OGFC	800	1999	6	S	31	1	33	1	29	1
	2819	CIR-B-1	CIR 3.0" + 3.0" DGHMA + 0.75" OGFC	5,550	1998	7	S	24	1	27	13 [†]	26	13 [†]
	2873	CIR-B-2	CIR 3.0" + 3.0" DGHMA + 0.75" OGFC	5,550	1998	7	S	30	1	31	1	30	1
	2961	CIR-B-3	CIR 3.0" + 3.0" DGHMA + 0.75" OGFC	2,000	1999	6	S	36	1	38	1	35	1
	3013	CIR-B-4	CIR 3.0" + 3.0" DGHMA (AC-20P) + 0.75" OGFC	14,500	1999	6	N	16 [†]	1	18	1	18	1
	3025a	CIR-C-1	CIR 2.0" + 2.0" DGHMA (AC-20P) + chip seal	5,000	2003	2	N	8 [†]	3	NA	NA [§]	NA	NA
	3025b	CIR-C-2	CIR 2.0" + 2.0" DGHMA (AC-20P) + chip seal	1,000	2001	4	N	23	5	25	1	NA	NA
	3025c	CIR-C-3	CIR 2.0" + 2.0" DGHMA (AC-20P) + chip seal	1,000	2001	4	N	25	5	28	8	NA	NA
2876	CIR-C-4	CIR 2.0" + 2.0" DGHMA + 0.75" OGFC	1,500	2001	4	N	28	5	29	8	NA	NA	
RF	2761	RF-1	Cold milling 2.0" + fiberglass + 2.0" Type II DGHMA (AC-20P) + 0.75" OGFC	9,600	1999	6	N	37 [†]	6 [†]	37 [†]	8	34 [†]	7
	2932	RF-2	Cold milling 2.0" + fiberglass + 2.0" Type II DGHMA (AC-20P) + 0.75" OGFC	2,850	1999	6	S	21	1	22	1	23	1
	2980a	RF-3	Cold milling 2.0" + fiberglass + 2.0" Type II DGHMA (AC-20P) + 0.75" OGFC	1,000	2000	5	N	13	1	15	1	17	1
	2980b	RF-4	Cold milling 2.0" + fiberglass + 2.0" Type II DGHMA (AC-20P) + 0.75" OGFC	4,400	2000	5	N	9	1	9	2	8	3
	3006	RF-5	Cold milling 2.0" + fiberglass + 2.0" Type II DGHMA (AC-20P) + 0.75" OGFC	7,200	2001	4	N	10	1	10	1	NA	NA
	3008	RF-6	Cold milling 2.0" + fiberglass + 2.0" Type II DGHMA (AC-20P) + 0.75" OGFC	10,000	2001	4	N	7	1	7	4	NA	NA
SRC	2723	SRC-1	Cold milling 2.0" + 1" SRC + 2.0" Type II DGHMA (AC-30) + 0.375" OGFC	40,000	1997	8	S	32	1	32	1	28	1
	3031	SRC-2	Cold milling 2.0" + 1" SRC + 2.0" Type II DGHMA (AC-30) + 0.375" OGFC	15,600	2000	5	N	29	1	30	1	27	10
	3048	SRC-3	Cold milling 2.0" + 1" SRC + 2.0" Type II DGHMA (AC-30) + 0.375" OGFC	2,700	2000	5	S	14	1	16	1	16	2
	3045	SRC-4	Cold milling 2.0" + 1" SRC + 2.0" Type II DGHMA (AC-30) + 0.375" OGFC	1,900	2001	4	N	15	1	17	1	NA	NA
	3162	SRC-5	Cold milling 2.0" + 1" SRC + 2.0" Type II DGHMA + 0.375" OGFC	29,100	2003	2	N	4	1	NA	NA	NA	NA

⁺ Ranking from best to worst; i.e., the projects ranked as "1" had the best performance.

[#] -1: Previous year to construction, +1, +3, +5: one, three, and five years after construction.

[§] NA: Project is younger than the indicated long-performance year.

* Denotes "dense graded HMA"

[†] Considered as an outlier according to the "univar" statistical analysis. Therefore, not included in the calculation of the mean ranking of each treatment.

Table 3.3b Ranking of Selected NDOT Projects Based on Principal Component Analysis (Continued).

Trt.	Cont.	ID	Description of Treatment	AADT	DOC	Life	Loc.	Ranking ⁺					
								-1 [#]	+1 [#]	-1 [#]	+3 [#]	-1 [#]	+5 [#]
MOL	2384a	MOL-A-1	Cold milling 1.0" + 1.0" Type III DGHMA* (AC-10) + 0.75" OGFC	40,000	1990	15	N	19	12	21	12	24	12
	2384b	MOL-A-2	Cold milling 1.0" + 1.0" Type III DGHMA (AC-10) + 0.75" OGFC	5,500	1993	12	N	22	1	24	5	22	9
	2432	MOL-B-1	Cold milling 1.0" + 1.0" Type III DGHMA (AC-20) + 0.75" OGFC	2,700	1993	12	S	20	1	20	1	19	12
	2505	MOL-B-2	Cold milling 1.0" + 1.0" Type III DGHMA (AC-20) + 0.75" OGFC	3,350	1993	12	S	35	1	34	1	31	1
	2651a	MOL-C-1	Cold milling 1.5" + 1.5" Type II DGHMA (AC-20P) + 0.75" OGFC	2,000	1995	10	S	18	1	23	1	25	11
	2651b	MOL-C-2	Cold milling 1.5" + 1.5" Type II DGHMA (AC-20P) + 0.75" OGFC	1,700	1996	9	S	34	1	36	1	33	6
	2651c	MOL-C-3	Cold milling 1.5" + 1.5" Type II DGHMA (AC-20P) + 0.75" OGFC	1,700	1996	9	S	38	1	39	1	36	15
	2679	MOL-C-4	Cold milling 1.5" + 1.5" Type II DGHMA (AC-20P) + 0.75" OGFC	6,750	1997	8	S	3 ¹	5 ¹	3 ¹	6 ¹	4 ¹	6 ¹
	3028	MOL-B-3	Cold milling 1.0" + 1.0" Type III DGHMA (AC-20P) + 0.75" OGFC	7,250	2000	5	N	11	1	11	3	14	4
3070	MOL-C-5	Cold milling 1.5" + 1.5" Type II DGHMA (AC-20P) + 0.75" OGFC	7,500	2003	2	S	26	1	NA	NA ^{\$}	NA	NA	
Ranking for rigid techniques													
CS	2886	CS-1	CS 8" slabs + 1.5" leveling course + 4.5" Type II DGHMA (AC-20P) + 0.375" OGFC	6,750	1998	7	N	1	1	1	1	1	3
	2889	CS-2	CS 8" slabs + 1.5" leveling course + 3.5" Type II DGHMA (AC-20P) + 0.375" OGFC	10,800	1999	6	N	1	1	1	1	1	2
	2962	CS-3	CS 8" slabs + 1.5" leveling course + 4.75" Type II DGHMA (AC-20P) + 0.375" OGFC	4,700	1999	6	N	2	1	2	1	3	1
	2999	CS-4	CS 8" slabs + 1.5" leveling course + 3.5" Type II DGHMA (AC-20P) + 0.375" OGFC	6,200	2001	4	N	1	1	1	1	1	2
	3021	CS-5	CS 6" slabs + 1.5" leveling course + 3.5" Type II DGHMA (AC-20P) + 0.375" OGFC	23,000	2001	4	N	1	1	1	1	1	2
RPCC	2549	RPCC-1	Rubblizing + 1.5" leveling course + 5.0" Type II DGHMA + 0.375" OGFC	7,000	1996	9	N	3	1	3	1	7	4
	2869	RPCC-2	Rubblizing + 1.5" leveling course + 5.0" Type II DGHMA + 0.375" OGFC	6,550	1999	6	N	1	1	1	1	1	6
	2901	RPCC-3	Rubblizing + 1.5" leveling course + 7.0" Type II DGHMA (AC-20P) + 0.375" OGFC	7,200	1999	6	N	1	1	1	1	1	1
	3088	RPCC-4	Rubblizing + reinforced fabric & non-woven geotextile + 1.5" leveling course + 5.0" Type II DGHMA (AC-20P) + 0.375" OGFC	7,700	2002	3	N	1	1	1	1	NA	NA
	3186a	RPCC-5	Rubblizing + 2.0" leveling course + 4.5" Type II DGHMA (AC-20P) + 0.375" OGFC	6,300	2005	0	N	1	1	1	1	NA	NA
	3186b	RPCC-6	Rubblizing + 2.0" leveling course + 4.5" Type II DGHMA (AC-20P) + 0.375" OGFC	6,300	2005	0	N	1	1	1	1	NA	NA

⁺ Ranking from best to worst; i.e., the projects ranked as "1" had the best performance.

[#] -1: Previous year to construction, +1, +3, +5: one, three, and five years after construction.

^{\$} NA: Project is younger than the indicated long-performance year.

* Denotes "dense graded HMA"

¹ Considered as an outlier according to the "univar" statistical analysis. Therefore, not included in the calculation of the mean ranking of each treatment.

Table 3.4 Statistical Analysis of the Various Treatments Based on the PCA Rankings at One-year Before Treatment Construction and One-year After Treatment Construction for Flexible Pavements.

Treatment	No. of Projects Analyzed	1-year Pre-construction (-1)		1-year after Construction (+1)		Change in Relative Ranking
		Average	STD*	Average	STD*	
CIR-A	3	30	3	1	1	29
CIR-B	3	30	6	1	0	29
CIR-C	3	25	3	5	0	20
RF	5	12	5	1	0	11
SRC	5	19	12	1	0	18
MOL-A	2	21	2	7	8	14
MOL-B	3	22	12	1	0	21
MOL-C	4	29	9	1	0	28

* Standard deviation

Table 3.5 Statistical Analysis of the Various Treatments Based on the PCA Rankings at One-year Before Treatment Construction and Three-years After Treatment Construction for Flexible Pavements.

Treatment	No. of Projects Analyzed	1-year Pre-construction (-1)		3-year after Construction (+3)		Change in Relative Ranking
		Average	STD*	Average	STD*	
CIR-A	3	31	5	1	1	30
CIR-B	3	29	10	1	0	28
CIR-C	3	27	2	6	4	22
RF	5	13	6	2	1	11
SRC	4	24	8	1	0	23
MOL-A	2	23	2	9	5	14
MOL-B	3	22	12	2	1	20
MOL-C	3	33	9	1	0	32

* Standard deviation

Table 3.6 Statistical Analysis of the Various Treatments Based on the PCA Rankings at One-year Before Treatment Construction and Five-years After Treatment Construction for Flexible Pavements.

Treatment	No. of Projects Analyzed	1-year Pre-construction (-1)		5-year after Construction (+5)		Change in Relative Ranking
		Average	STD*	Average	STD*	
CIR-A	3	27	6	2	2	25
CIR-B	3	28	9	1	0	27
CIR-C	0	NA	NA	NA	NA	NA
RF	3	16	8	2	1	14
SRC	3	24	7	4	5	19
MOL-A	2	23	1	11	2	13
MOL-B	3	21	9	6	6	16
MOL-C	3	31	6	11	5	21

* Standard deviation

Table 3.7 Fixed Qualitative Factorial Analysis Based on the PCA Rankings at One-year After Treatment Construction.

Treatment	p-value ^(!)	Comment
Reflective Cracking Treatment (RCT) ^(*)	<0.0001 ^(#)	Highly Significant
Location (LOC)	<0.0001	Highly Significant
RCT*Location	<0.0001	Highly Significant
Traffic (Tr)	<0.0001	Highly Significant
RCT×Tr	<0.0001	Highly Significant
LOC×Tr	<0.0001	Highly Significant
RCT×LOC×Tr	<0.0001	Highly Significant

(*) The reflective cracking treatments are: Cold in-place recycling, reinforced fabrics, stress-relief course, mill and overlay, PCC rubblization and PCC crack and seat.

(!) A p-value lower than 0.05 indicates a significant treatment.

(#) If the probability value is <0.0001, it indicates a highly significant treatment.

Table 3.8 Fixed Qualitative Factorial Analysis Based on the PCA Rankings at Three-years After Treatment Construction.

Treatment	p-value ^(!)	Comment
Reflective Cracking Treatment (RCT) ^(*)	<0.0001 ^(#)	Highly Significant
Location (LOC)	<0.0001	Highly Significant
RCT*Location	<0.0001	Highly Significant
Traffic (Tr)	<0.0001	Highly Significant
RCT×Tr	<0.0001	Highly Significant
LOC×Tr	<0.0001	Highly Significant
RCT×LOC×Tr	<0.0001	Highly Significant

(*) The reflective cracking treatments are: Cold in-place recycling, reinforced fabrics, stress-relief course, mill and overlay, PCC rubblization and PCC crack and seat.

(!) A p-value lower than 0.05 indicates a significant treatment.

(#) If the probability value is <0.0001, it indicates a highly significant treatment.

Table 3.9 Fixed Qualitative Factorial Analysis Based on the PCA Rankings at Five-years After Treatment Construction.

Treatment	p-value ^(!)	Comment
Reflective Cracking Treatment (RCT) ^(*)	<0.0001 ^(#)	Highly Significant
Location (LOC)	<0.0001	Highly Significant
RCT*Location	<0.0001	Highly Significant
Traffic (Tr)	<0.0001	Highly Significant
RCT×Tr	<0.0001	Highly Significant
LOC×Tr	<0.0001	Highly Significant
RCT×LOC×Tr	<0.0001	Highly Significant

(*) The reflective cracking treatments are: Cold in-place recycling, reinforced fabrics, stress-relief course, mill and overlay, PCC rubblization and PCC crack and seat.

(!) A p-value lower than 0.05 indicates a significant treatment.

(#) If the probability value is <0.0001, it indicates a highly significant treatment.

Table 3.10 Fixed Qualitative-Quantitative Factorial Analysis Based on the PCA Rankings at One-year After Treatment Construction.

Effect	p-value ^(!)	Comment
Reflective Cracking Treatment (RCT) ^(*)	<0.0001 ^(#)	Highly Significant
PCA-1	0.1776	Not Significant
(PCA-1) ²	<0.0001	Highly Significant
RCT×PCA-1	<0.0001	Highly Significant
RCT×(PCA-1) ²	<0.0001	Highly Significant
R-Square	0.77	

(*) The reflective cracking treatments are: Cold in-place recycling, reinforced fabrics, stress-relief course, mill and overlay, PCC rubblization and PCC crack and seat.

(!) A p-value lower than 0.05 indicates a significant treatment. If the probability value is <0.0001, it indicates a highly significant treatment.

(#) If the probability value is <0.0001, it indicates a highly significant treatment.

Table 3.11 Fixed Qualitative-Quantitative Factorial Analysis Based on the PCA Rankings at Three-years After Treatment Construction.

Effect	p-value ^(!)	Comment
Reflective Cracking Treatment (RCT) ^(*)	<0.0001 ^(#)	Highly Significant
PCA-1	0.8130	Not Significant
(PCA-1) ²	<0.0001	Highly Significant
RCT×PCA-1	0.0002	Highly Significant
RCT×(PCA-1) ²	<0.0001	Highly Significant
R-Square	0.71	

(*) The reflective cracking treatments are: Cold in-place recycling, reinforced fabrics, stress-relief course, mill and overlay, PCC rubblization and PCC crack and seat.

(!) A p-value lower than 0.05 indicates a significant treatment. If the probability value is <0.0001, it indicates a highly significant treatment.

(#) If the probability value is <0.0001, it indicates a highly significant treatment.

Table 3.12 Fixed Qualitative-Quantitative Factorial Analysis Based on the PCA Rankings at Five-years After Treatment Construction.

Effect	p-value ^(!)	Comment
Reflective Cracking Treatment (RCT) ^(*)	<0.0001 ^(#)	Highly Significant
PCA-1	0.2576	Not Significant
(PCA-1) ²	< 0.0001	Significant
RCT×PCA-1	<0.0001	Highly Significant
RCT×(PCA-1) ²	<0.0001	Highly Significant
R-Square	0.71	

(*) The reflective cracking treatments are: Cold in-place recycling, reinforced fabrics, stress-relief course, mill and overlay, PCC rubblization and PCC crack and seat.

(!) A p-value lower than 0.05 indicates a significant treatment. If the probability value is <0.0001, it indicates a highly significant treatment.

(#) If the probability value is <0.0001, it indicates a highly significant treatment.

Table 4.1 Plane Strain Fracture Toughness (K_{Ic}) for Different HMA Mixtures (50).

Binder type	Temperature (°C)	Binder content (%)	Modulus (GPa)	K_{Ic} (MPa/m ^{0.5})
Asphalt cement (AC-20)	- 7	4	12.48	1.00
		5	17.65	1.17
		6	11.93	1.04
	- 1	4	7.10	0.77
		5	9.44	0.91
		6	6.62	0.90
Asphalt rubber (80% AC-20 + 20% reclaimed rubber by weight)	- 7	7	4.65	0.67
		8	3.85	0.80
		9	5.99	0.74
	- 1	7	3.87	0.60
		8	4.21	0.79
		9	4.79	1.06

Table 4.2 Statistical Coefficients for the ε_{VM} Model.

i	a_{1i}	a_{2i}	b_{1i}	b_{2i}
1	-1.038E-04	-1.446E-01	7.169E-03	1.314E-01
2	2.777E-01	-4.022E+00	9.773E-05	-6.36E-01
3	-1.173E+00	1.212E+01	-4.946E-01	7.069E00
4	1.281E+00	5.070E-01	3.923E-02	2.641E00
5	-5.160E-01	6.964E+00	3.265E-02	-1.287E00
6	-1.775E-01	2.385E+00	1.875E-03	-8.167E-01

Table 4.3 Minimum and Maximum Values for the Pavement Thicknesses and Moduli.

i	X_i	Minimum	Maximum
1	Thickness of the existing cracked layer (m)	0.10	0.25
2	Thickness of the granular layer (m)	0.2	0.40
3	Modulus of the overlay layer (MPa)	2000	10000
4	Modulus of the existing cracked layer (MPa)	2000	3500
5	Modulus of the granular layer (MPa)	150	450
6	Modulus of the subgrade layer (MPa)	50	150

Table 4.4 Traffic Information.

Year	ESALs*
1	172,565
3	554,780
5	992,375
10	2,384,235
15	4,336,390
20	7,074,390

* Truck factor = 0.912, annual growth rate = 7%, directional distribution factor = 50%, lane distribution factor =

90%

Table 4.5 HMA Overlay Dynamic Modulus at 70°F and 10 Hz.

Type of Mix	E_{overlay} , ksi (MPa)
T2C	790 (5,455)
CT	1,045 (7,205)
NRM	1,375 (9,485)

Table 4.6 HMA Overlay Thickness Using the New AASHTO Model.

RC (%)*	HMA overlay thickness (inch)	a ⁺	b ⁺	Time (years)	Traffic (ESALs)
5.0	2	5.00	-2.48	0.83	142,382
	4	6.50	-1.64	2.17	390,329
	8	9.50	-1.19	5.50	1,112,109
	10	11.00	-1.10	7.33	1,583,897
10.0	12	12.50	-1.04	9.23	2,137,788
	2	5.00	-2.48	1.13	196,153
	4	6.50	-1.64	2.63	479,910
15.0	8	9.50	-1.19	6.13	1,267,196
	10	11.00	-1.10	8.01	1,774,625
	12	12.50	-1.04	9.95	2,368,123
20.0	2	5.00	-2.48	1.32	229,999
	4	6.50	-1.64	2.91	536,776
	8	9.50	-1.19	6.52	1,366,568
	10	11.00	-1.10	8.44	1,897,188
20.0	12	12.50	-1.04	10.40	2,516,472
	2	5.00	-2.48	1.46	255,765

* Percent of cracks reflected, $RC = \frac{100}{1 + e^{a+bt}}$

⁺ $a = 3.5 + 0.75 \times h_{ac}$, $b = -0.688584 - 3.37302 \times (h_{ac})^{-0.915469}$, h_{ac} HMA overlay thickness.

Table 5.1 Results of the Bending Test under Repeated load.

Structure	Sample ID	Number of cycles to crack	Average	Standard deviation	Coefficient of variation
Without geotextile	1.A	890	952	57	6%
	2.A	990			
	3.A	1,010			
	4.A	920			
With geotextile	1.B	2,100	1,810	752	42%
	2.B	2,740			
	3.B	1,170			
	4.B	1,230			

Table 5.2 Results of the Shearing Test.

Structure	Sample ID	Maximum Shear Force (N)	Maximum Shear Stress (MN/m ²)
Without geotextile	1.C	1,237.4	0.21
	2.C	1,202.1	0.21
	3.C	1,661.7	0.28
	4.C	2,262.7	0.37
	5.C	2,086.0	0.37
	6.C	1,909.2	0.33
Average		1,726.5	0.30
Standard Deviation		401.8	0.068
Coefficient of Variation		23%	23%
With geotextile	1.D	1,173.8	0.20
	2.D	735.4	0.13
	3.D	827.3	0.15
	4.D	824.4	0.14
	5.D	586.9	0.11
	6.D	756.6	0.13
Average		819.1	0.14
Standard Deviation		178.4	0.029
Coefficient of Variation		22%	20%

Table 5.3 Comparison of Different Mitigation Techniques.

Anti-reflective cracking system	Crack initiation time (minutes)	Crack speed in the first centimeter (µm/min)	Breaking time (minutes)
Paving fabric	170	90	520
Rich binder mix	95	65	535
SAMI	155	85	580

Table 5.4 Geogrid effectiveness factor (FEG).

Pre-crack opening	Beam	$N_{f(B)}$ (Cycles)	$N_{f(s)}$ (Cycles)	C_f (Cycles ⁻¹)	N_f (Cycles)	FEG
3 mm	Without geogrid	79,884	93,290	3.40×10^{-5}	29,450	6.14
	With geogrid	490,491	573,560	5.53×10^{-6}	180,970	
6 mm	Without geogrid	68,690	77,710	4.03×10^{-5}	24,820	4.60
	With geogrid	329,393	346,400	8.81×10^{-6}	113,510	
9 mm	Without geogrid	63,020	72,920	4.33×10^{-5}	23,100	5.11
	With geogrid	340,702	364,530	8.42×10^{-6}	118,740	

Table 5.5 Three Test Cells of MnRoad: Asphalt Mixture and Cracking Performance.

Test Cell	Asphalt Type	Mix Design (Marshall)	Linear Feet of Cracking in Field	Overlay Tester Results
15	PG 64-22	75 blow	475	91
18	PG 64-22	50 blow	315	153
20	PG58-28	35 blow	100	500

Table 5.6 Summary of Laboratory Testing Methods for Reflective Cracking.

Testing device	Type of test	Failure mode	Geometry of specimens	Type of load	Test results	Findings	Schematic
Cracow University of Technology, Poland (56)	Bending or Shearing	I & II	Beams: 12×3×3 inch	<ul style="list-style-type: none"> - Static bending load: loading rate 0.47 in/min. - Repeated haversine bending load: 5 Hz. - Static shearing: loading rate 4×10^{-2} in/min. 	<ul style="list-style-type: none"> - Static bending: cracking time, max force & bending strength. - Dynamic bending: number of repetitions. - Static shear: max shear force & stress. 	The bending test under repeated load indicates that HMA overlays reinforced with geotextiles exhibited a greater resistance to the crack development. The shearing test showed that the presence of a geotextile diminished more than two times the adhesion between the asphalt layers.	
Technion-Israel Institute of Technology, Israel (57)	Wheel tracking device	I	Beams: 28×4×4 inch	- Cyclic wheel load.	<ul style="list-style-type: none"> - Number of wheel loading repetitions to failure. - Crack length versus number of repetitions and testing time. 	The evaluated geotextile fabric had a resistance to reflective cracking 4 times greater than other techniques.	
Geo-materials Laboratory, ENTPE, France - Fissurometer (58)	Uniaxial tension	I	Slabs	<ul style="list-style-type: none"> - Static: rate of 0.05 to 0.22 in/hr. - Cyclic uniaxial. 	- Measure of energy transmitted by an ultrasonic wave train.	A comparison between the fissurometer and field results from different cracking mitigation techniques showed that the device classified them in reverse order (opposite to field performance). It might be because the fissurometer only simulates thermal shrinkage.	

Table 5.6 Summary of Laboratory Testing Methods for Reflective Cracking (continued).

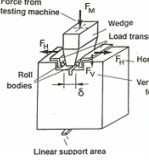
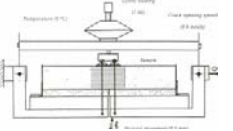
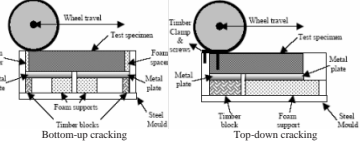
Testing device	Type of test	Failure mode	Geometry of specimens	Type of load	Test results	Findings	Schematic
Technical University of Vienna, Austria - Wedge splitting (59)	Splitting	I	Cubical or prismatic	- Static: loading rate 0.05 in/min.	- Horizontal force versus displacement. - Maximum vertical force versus temperature. - Fracture energy versus temperature.	The researchers concluded that the maximum splitting force is not an appropriate parameter to differentiate between HMA mixes since two different mixes can have the same maximum splitting force and different fracture behavior. On the other hand, the specific fracture energy was recommended as a more reliable testing parameter to differentiate between various mixes.	
Laboratory of Public Roads, France (60)	Biaxial	I & II	Beams: 24×2.8×2.8 inch	- Cyclic vertical load: 1 Hz. - Static horizontal load: 0.024 in/hr.	- Crack initiation time & length. - Crack propagation time & length. - Breaking time.	The test results of a 2.4 inch (6 cm) AC 0/10 overlay on top of a fabric interlayer, a rich-binder HMA mix, and a Stress Absorbing Membrane Interlayer (SAMI). It was concluded that the paving fabrics delays the crack initiation time, while the rich HMA mix slows down the crack propagation.	
University College of Dublin - accelerated simulative wheel tracking (61)	Wheel tracking device	I & II	Beams - Bottom-up 5.5×11×2.0 inch. - Top-down 5.5×10.2×2.0 inch.	- Cyclic wheel load: 21 cycles/min.	- Number of wheel loading repetitions versus crack length. - Deformation of the slabs over the central 8 inch throughout the test.	No tests were still performed.	

Table 5.6 Summary of Laboratory Testing Methods for Reflective Cracking (continued).

Testing device	Type of test	Failure mode	Geometry of specimens	Type of load	Test results	Findings	Schematic
University of Illinois, U.S.A (63)	Uniaxial tension	I	HMA layer on top of a PCC slab of 6×90×2.7 inch	- Cyclic uniaxial load: frequency 0.0016 in/min (triangular).	- Strain in HMA overlay as function of test cycles. - Crack length versus time	The Interlayer Stress Absorbing Composite (ISAC) had a much better performance than other commercial products when was tested in the proposed test device.	
Aeronautical Technological Institute, ATI, Brazil (64)	Bending or Shearing	I & II	Beams: 18×6×3 inch	- Sinusoidal load: loading frequency 20 Hz.	- Permanent strain versus number of load cycles. - Tensile stress versus crack length.	The HMA overlay reinforced with geogrid had a life up to 6 times higher than a HMA overlay without it.	N.A.
Florida Atlantic University, U.S.A (65)	Bending (single point of loading)	I	Beams: 18×6×7.5 inch	- Static - Cyclic (Sinusoidal) load: 2 Hz.	- The load value or number of repetitions to first reflected crack. - The load value or number of repetitions for crack propagation to half way of overlay. - The load value or number of repetitions for crack propagation to top of overlay.	At the same load ratio, the slabs having geogrids embedded at the bottom showed better resistance to reflection cracking compared to specimens in which the geogrids was simply attached to the bottom with a tack coat. Additionally, it was found that geogrid embedded at mid-height was more effective than geogrid embedded at the bottom of overlay.	
Polytechnic University of Madrid, Spain - Wheel Reflective Cracking device (66)	Biaxial	I & II	Beams: 12×12×2.4 inch	- Cyclic wheel load. - Static traction force: 0.001 to 50 μm/hr.	- Vertical length of the crack with time. - Vertical displacement with time - Relative movement between crack edges.	Three treatments were studied: HMA overlay without geotextile, and reinforced with two different types of geotextile. The overlay without reinforcing showed the worst performance.	

Table 5.6 Summary of Laboratory Testing Methods for Reflective Cracking (continued).

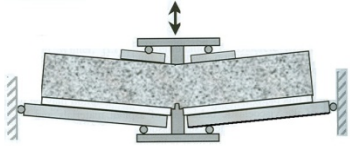
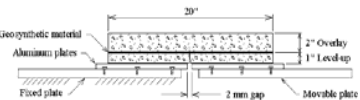
Testing device	Type of test	Failure mode	Geometry of specimens	Type of load	Test results	Findings	Schematic
Regional Laboratory of Pont et Chaussées, France - MEFISTO (67)	Biaxial	I & II	Beams: 2×2×26 inch	- Static (horizontal load) - Cyclic (vertical load): sinusoidal 10 Hz.	- Number of repetitions versus vertical force or dissipated energy. - Number of repetitions versus crack length.	No tests were performed.	
Texas Transportation Institute Overlay Tester (68)	Biaxial	I & II	Cores: 6-inch diameter Beams: 6×3×2 inch	- Triangular cyclic load: 10 seconds/cycle.	- Number of repetitions versus crack length. - Number of repetitions versus testing time.	The major findings of the extensive experimental work indicated that a very good repeatability for the device. It was found to be sensitive to the testing temperature, opening displacement, asphalt binder content and grade, and air voids. Also it showed consistency between the mixtures' test results and their corresponding field performance. The pass/fail criterion on reflective cracking resistance is 300 cycles at 77 °F (25 °C) and 0.025 in (0.64 mm) opening displacement. When a rich bottom layer is used, the reflective cracking life in the overlay tester should be at least 750 cycles.	

Table 6.1 Summary of Literature Review.

Treatment	Description	Performance
Cold in-place recycling	Remove and mill the upper layers of the existing pavement with specialized recycling equipment then mix with virgin materials to produce a strong flexible base course.	Promising performance for roads with up to 13,000 ADT and 200,000 annual equivalent single axle loads.
Glassgrid	Geosynthetic material consisting of connected parallel sets of intersecting ribs with openings of sufficient size.	Benefits in retarding or preventing reflective cracking are not clear. Field performance has varied from excellent to very poor. Concerns when used on rough surfaces.
Fabric interlayer	Geosynthetic comprised solely of textiles. A paving fabric interlayer provides the generally acknowledged functions of a stress-absorbing interlayer and a waterproofing membrane. The stress-related performance has been easily verified by the observed reductions of cracking in pavement overlays.	Effective when used for load-related fatigue distress. It did not performed well when used to delay or retard thermal cracking. Optimum performance highly associated with proper construction procedures. The key factor is proper tack-coat installation. In general, overlays reinforced with fabrics have shown better performance than unreinforced overlays under same conditions.
Asphalt rubber interlayer + thin overlay (about 1.5")	Asphalt rubber chip seal overlaid with conventional dense graded HMA or gap graded HMA.	Reduce and/or delay reflective cracking for a period of 5 years.
Stress absorbing membrane interlayer	A thin layer placed between an underlying pavement and an HMA overlay for the purpose of dissipating movements and stresses at a crack in the underlying pavement before they create stresses in the overlay. SAMIs consist of a spray application of rubber or polymer-modified asphalt as the stress-relieving material, followed by placing and seating aggregate chips.	Successful in reducing the rate of reflective cracking.
Crumb rubber overlay	Produced by adding ground tire rubber to HMA using the wet process.	Ranged from successful to devastating failures depending on percent of crumb rubber in mix.

Table 6.2 Summary of NDOT Reflective Cracking Mitigation Techniques Review.

Treatment	Description	Application Conditions		Performance
		Traffic	Pre-rehabilitation Pavement Condition	
Cold in-place recycling (CIR)	CIR of minimum top 2.0" of existing HMA materials and overlaying it with a minimum of 2.5" dense graded HMA mixture.	Up to 14,000 AADT.	No severe alligator cracking.	Stopped reflective cracking for 5 years after construction
Reinforced fabric (RF)	Cold milling 2.0" of existing HMA layer, placing fiberglass yarns, and overlaying with 2.0" Type II (1 inch maximum size) dense graded HMA.	Between 1,000 and 10,000 AADT.	No severe alligator cracking.	Retarded reflective cracking for at least 3 years after construction and reduced the rate of reflected transverse cracks 5 years after construction.
Stress relief course (SRC)	Cold milling 2.0" of existing HMA layer, placing a 1" stress relieve course and overlaying with 2.0" Type II (1" max size) dense graded HMA.	Up to 40,000 AADT.	NA	Stopped reflective cracking for 3 years after construction. Rate of reflected transverse cracks accelerated 5 years after construction.
Mill and overlay (MOL)	Cold milling 1.0" of existing HMA pavement and overlaying it by 1.0" HMA mixture manufactured with an AC-10 asphalt binder.	Up to 40,000 AADT.	NA	Reflected fatigue and transverse cracks 1 to 2 years after construction.
	Cold milling 1.0" of existing HMA pavement and overlaying it by 1.0" HMA mixture manufactured with an AC-20P asphalt binder.	Up to 4,000 AADT.	NA	Stopped reflective cracking for 3 years after construction. Minor reflected transverse cracks 5 years after construction.
	Cold milling 1.5" of existing HMA pavement and overlaying it by 1.5" HMA mixture manufactured with an AC-20P asphalt binder. (*)	Up to 2,000 AADT.	NA	Stopped reflective cracking for 3 years after construction. Minor reflected transverse cracks 5 years after construction. (*)

* This treatment was placed on pavements with a condition worse than the condition of the pavements where the other two mill and overlay treatments were applied.

Table 6.3 Pavement Layers Material Properties.

Layers		Thickness (inch)	Modulus at 70°F (ksi)	Fatigue characteristics*
HMA overlay	NDOT T2C	--#	790	$N_f = 1.3740 \times 10^{-5} \times \left(\frac{1}{\varepsilon}\right)^{4.4142} \left(\frac{1}{E_{overlay}}\right)^{2.0374}$
	CT	--#	1,045	$N_f = 6.5815 \times 10^{-5} \times \left(\frac{1}{\varepsilon}\right)^{4.3172} \left(\frac{1}{E_{overlay}}\right)^{2.0598}$
	NRM	--#	1,375	$N_f = 6.8745 \times 10^{-5} \times \left(\frac{1}{\varepsilon}\right)^{4.2395} \left(\frac{1}{E_{overlay}}\right)^{2.1470}$
Cracked HMA		4.0	360	N.A.
Unbound base		10.0	30	N.A.
Subgrade		--	12	N.A.

* N_f is the number of repetitions to failure, ε is the flexural strain in microns

to be designed according to all three reflective cracking design methods

Table 6.4 Overlay Design Thicknesses for 20 years Design Period.

HMA overlay mix	Overlay thickness (inches)					
	Virginia Tech	Asphalt Rubber Association % reflected cracking				AASHTO MEPDG (100% reflected cracks)
		0%	2%	5%	15%	
NDOT T2C	4.50	3.60	2.40	2.00	0.75	12.00
CT	4.00	4.90	4.00	3.00	1.00	12.00
NRM	3.25	15.25	12.50	9.25	3.25	12.00

Table 6.5 ADOT Rubber Gradation for SAMI (Type A).

Sieve size	Percent Passing
No. 8	100
No. 10	95-100
No. 16	0-10
No. 30	--
No. 50	--
No. 200	--

Table 6.6 Required Properties for the Asphalt-rubber.

Property	Specifications		
	Type 1	Type 2	Type 3
Grade of base asphalt cement	PG 64-16	PG 58-22	PG 52-28
Rotational viscosity: 350 °F, Pa.s	1.5 – 4.0	1.5 – 4.0	1.5 – 4.0
Penetration at 4°C, 200 g, 60 s (ASTM D5), minimum	10	15	25
Softening point (ASTM D 36), °F, minimum	135	130	125
Resilience, 77 °F (ASTM D 5329), % minimum	30	25	15

Table 6.7 Required Properties for the Mineral Aggregates.

Property	Test Method	Specifications	
Los on Abrasion	AASHTO T96	9% for 100 revolutions 40% for 500 revolutions	
% of carbonates	Arizona Test Method 238	Max. 30	
% fractured coarse aggregate particles	Arizona Test Method 212	Min. 70	
Flakiness Index	Arizona Test Method 233	Max. 25	
Bulk Oven Dry Specific Gravity	Arizona Test Method 210	2.30 – 2.85	
Gradation	Arizona Test Method 201	<i>Sieve Size</i>	<i>% Passing</i>
		3/8 inch	100
		¼ inch	0-15
		No. 8	0-5
		No. 200	0-2

Table 6.8 Laboratory Asphalt Rubber Binder Design Data.

Property	Minutes of Reaction					45 minutes Specifications Limits
	45	90	240	360	1,440	
Viscosity, Haake at 190°C, Pa.s, (10 ⁻³), or cP (*)	2,400	2,800	2,800	2,800	2,100	1,500-4,000
Resilience at 25°C, % Rebound (ASTM D 3407)	27	--	33	--	23	18 Minimum
Ring & Ball Softening Point, °C (ASTM D 36)	59.0	59.5	59.5	60.0	58.5	52-74
Cone Pen. at 25°C, 150g, 5 sec., 1/10 mm (ASTM D217)	39	--	46	--	50	25-70

(*) The viscosity test shall be conducted using a hand-held Haake viscometer or equivalent.

Table 6.9 Requirements for CALTRANS SAMI-R's Construction.

Chip Size (mm)	Asphalt Rubber Binder (l/m ²) rate	Aggregate rate (kg/m ²)
9.0, 12.5	2.5 – 3.0	15-22

Table 6.10 Gradations for Ground Tire Rubber.

Sieve size	% Passing		
	Type A	Type B	Type C
No. 16	-	-	100
No. 30	-	100	70-100
No. 50	100	40-60	20-40
No. 100	50-80	-	-

Table 6.11 FDOT Standard Specifications for Asphalt-rubber.

Binder Type	ARB 5	ARB 12	ARB 20
Rubber Type	A or B (*)	B or A (**)	C (or A or B) (**)
Min Ground Tire Rubber (by weight of asphalt binder)	5%	12%	20%
Binder Grade	PG 67-22	PG 67-22	PG 64-22
Minimum Temperature, °F	300	300	300
Maximum Temperature, °F	335	350	375
Minimum Reaction Time, minutes	10	15 (Type B)	30 (Type C)
Unit Weight at 60°F, lb/gal (***)	8.6	8.7	8.8
Minimum viscosity (****), Poise at 300 °F	4.0	10.0	15.0
* Use of Type B rubber may require an increase in the mix temperature in order to offset higher viscosity values.			
** Use of finer rubber could result in the reduction of the minimum reaction time.			
*** Conversions to standard 60°F are as specified in 300-9.3.			
**** FM5-548, Viscosity of Asphalt Rubber Binder by use of the Rotational Viscometer.			

Table 6.12 MDOT Standard Specifications for Asphalt-Rubber Gradation.

Sieve	Percent Passing
2.36 mm	100
2.00 mm	95-100
1.18 mm	-
600 µm	0-10
300 µm	0-5

Table 6.13 Aggregate Quality Requirements.

Property	Test Method	Requirement
Coarse Aggregate		
Deleterious material, %, max	Tex-217-F, part I	1.0
Decantation, % max	Tex-217-F, part II	1.5
Micro-Deval abrasion, % max	Tex-431-A	7
Los Angeles abrasion, % max	Tex-410-A	30
Magnesium sulfate soundness, 5 cycles, %, max	Tex-411-A	20
Coarse aggregate angularity, 2 crushed faces, %, min	Tex-460-A, Part I	95 ²
Flat end elongated particles @5:1, %, max	Tex-280-F	10
Fine Aggregate		
Linear shrinkage, % max	Tex-107-E	3
Combined Aggregate³		
Sand equivalent, %, min	Tex-203-F	45

¹ Not used for acceptance purposes. Used by the engineer as an indicator of the need for further investigation.

² Only applies to crushed grave.

³ Aggregates, without mineral fillers, or additives, combined as used in the job-mix formula (JMF)

Table 6.14 Gradation Requirements for Fine Aggregate.

Sieve Size	% Passing by Weight or Volume
3/8"	100
#8	70-100
#200	0-30

Table 6.15 Master Gradation Bands and Volumetric Properties.

Sieve Size	Fine Mixture (% passing by weight or volume)
2"	-
1 1/2"	-
3/4"	-
1/2"	-
3/8"	98.0-100.0
#4	70.0-90.0
#8	40.0-65.0
#16	20.0-45.0
#30	10.0-30.0
#50	10.0-20.0
#200	2.0-10.0
Property	Requirement
Binder Content	6.5% minimum
Design VMA2, % Minimum	16.0
Plant-Produced VMA, % Minimum	15.5

Table 6.16 Mixture Design Properties.

Mixture Property	Test Method	Requirement
Target laboratory-molded density, %	Tex-207-F	98.0
Tensile strength (dry), psi	Tex-226-F	85-200 ¹
Dust/asphalt ratio ²	-	0.0-1.6 max
Boil test ³	Tex-530-C	-
Hamburg Wheel Test Requirements		
High-Temperature Binder Grade	Test Method	Minimum # of passes @ 0.5" Rut Depth, Tested @ 122°F ⁴
PG 64 or lower	Tex-242-F	7,000
PG 70		15,000
PG 76 or higher		20,000
Overlay Tester Requirements		
Cycles to failure	Tex-248-F	750 cycles minimum

¹ May exceed 200 psi when approved and may be waived when approved.

² Defined as % passing #200 sieve divided by asphalt content.

³ Used to establish baseline for comparison to production results. May be waived when approved.

⁴ May be decreased or waived when shown on the plans or when directed.

Table 6.17 Compacted Lift Thickness and Required Core Height.

Mixture Type	Compacted Lift thickness (inch)		Minimum Untrimmed Core Height (inch) Eligible for Testing
	Minimum	Maximum	
Crack attenuation mixture (CAM)	1.0	2.0	0.75

Table 6.18 Minimum Pavement Surface Temperatures.

High Temperature Binder Grade	Minimum Pavement Surface Temperatures (°F)	
	Subsurface Layers or Night Paving Operations	Surface Layers Placed in daylight Operations
PG 64	45	50
PG 70	55	60
PG 66	60	60

Table 6.19 UDOT Specifications for Asphalt Binder.

Property	Test Method	Criteria
RTFO elastic recovery	ASTM D6084 Section 6.2	Min. 45% @ 25°C
Separation Test,	ASTM D5976 Section 6.1	Max. 6°C difference after 48 hr

Table 6.20 Aggregate Gradation for SAMI According to UDOT Specifications.

Sieve	% Passing
3/8 inch	100
No. 4	80-100
No. 8	60-85
No. 16	40-70
No. 30	25-55
No. 50	15-35
No. 100	8-20
No. 200	6-14

Table 6.21 UDOT Specifications for SAMI.

Property	Criteria
Air voids, %	0.5-2.5
Voids in the mineral aggregate (VMA)	Min 16.0 min
Hveem stability (AASHTO T 246) at 140°F, 100 mm molds, 50 gyrations	Min. 18.0
Flexural beam fatigue-AASHTO T321, 2000 μ strain, 10 Hz, 3 \pm 1 air voids at 15°C	Min. 100,000 cycles

FIGURES

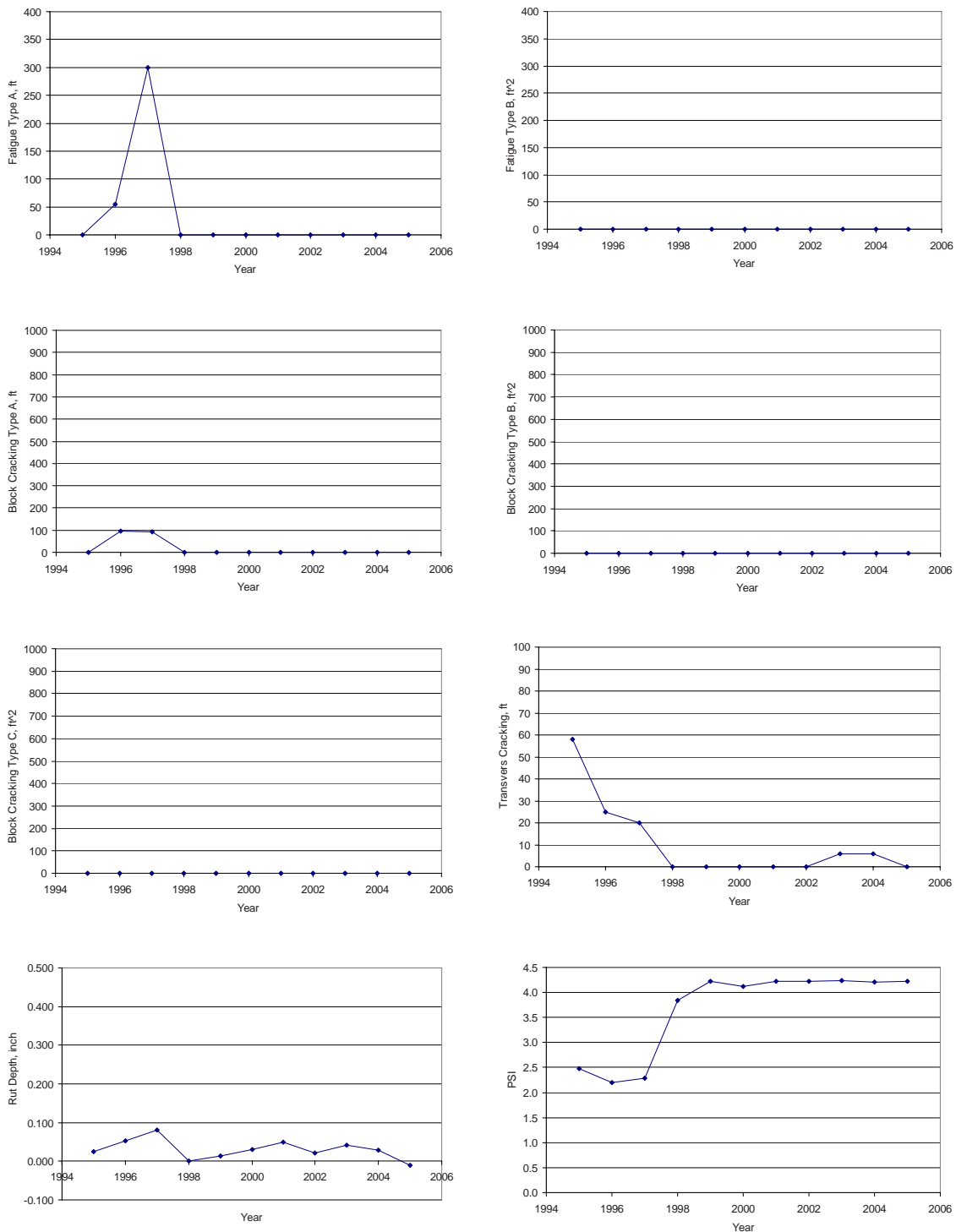


Figure 3.1: Performance data of contract 2808a on US050 from mileposts 0 to 3

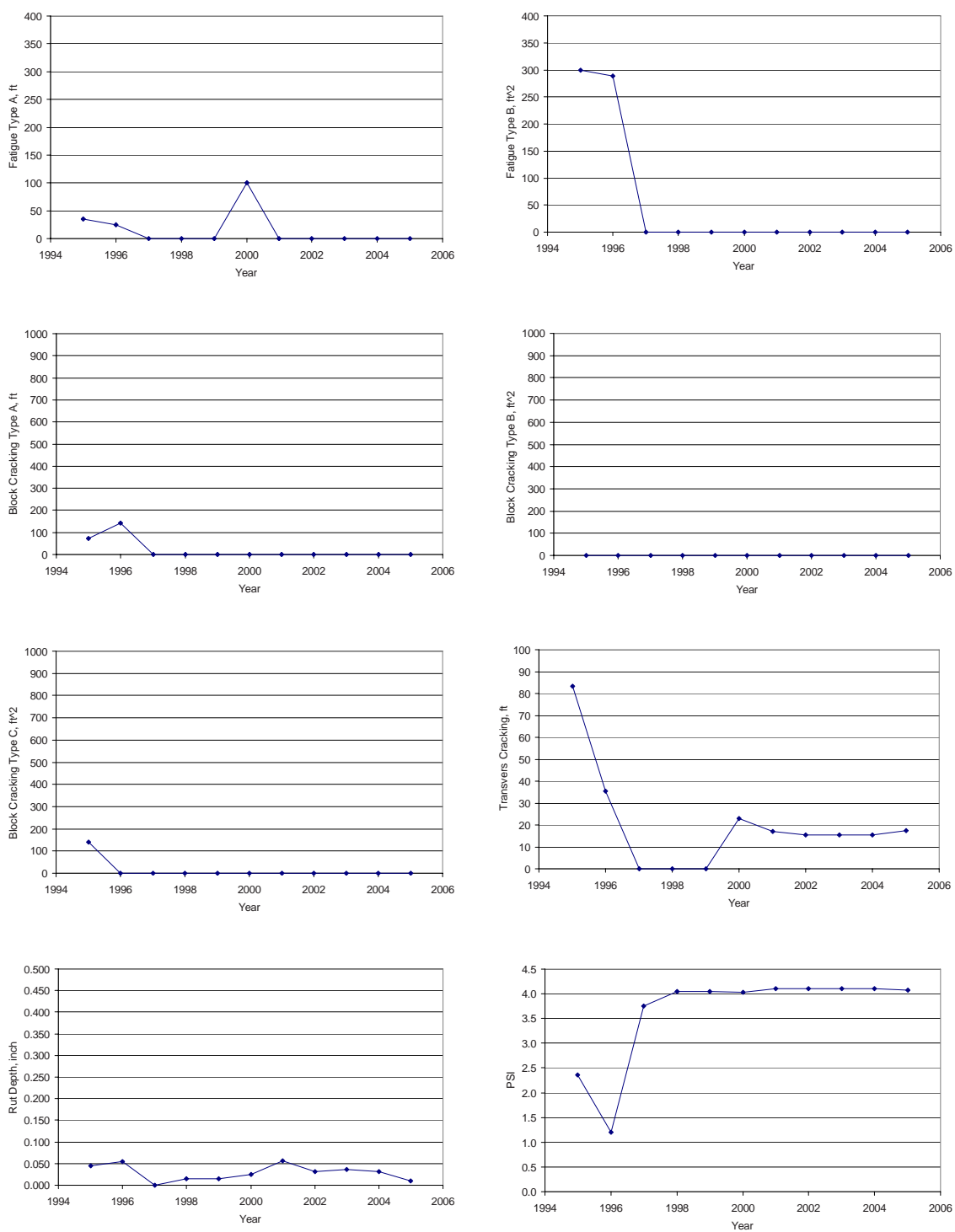


Figure 3.2: Performance data of contract 2808b on US050 from mileposts 38.04 to 47.39

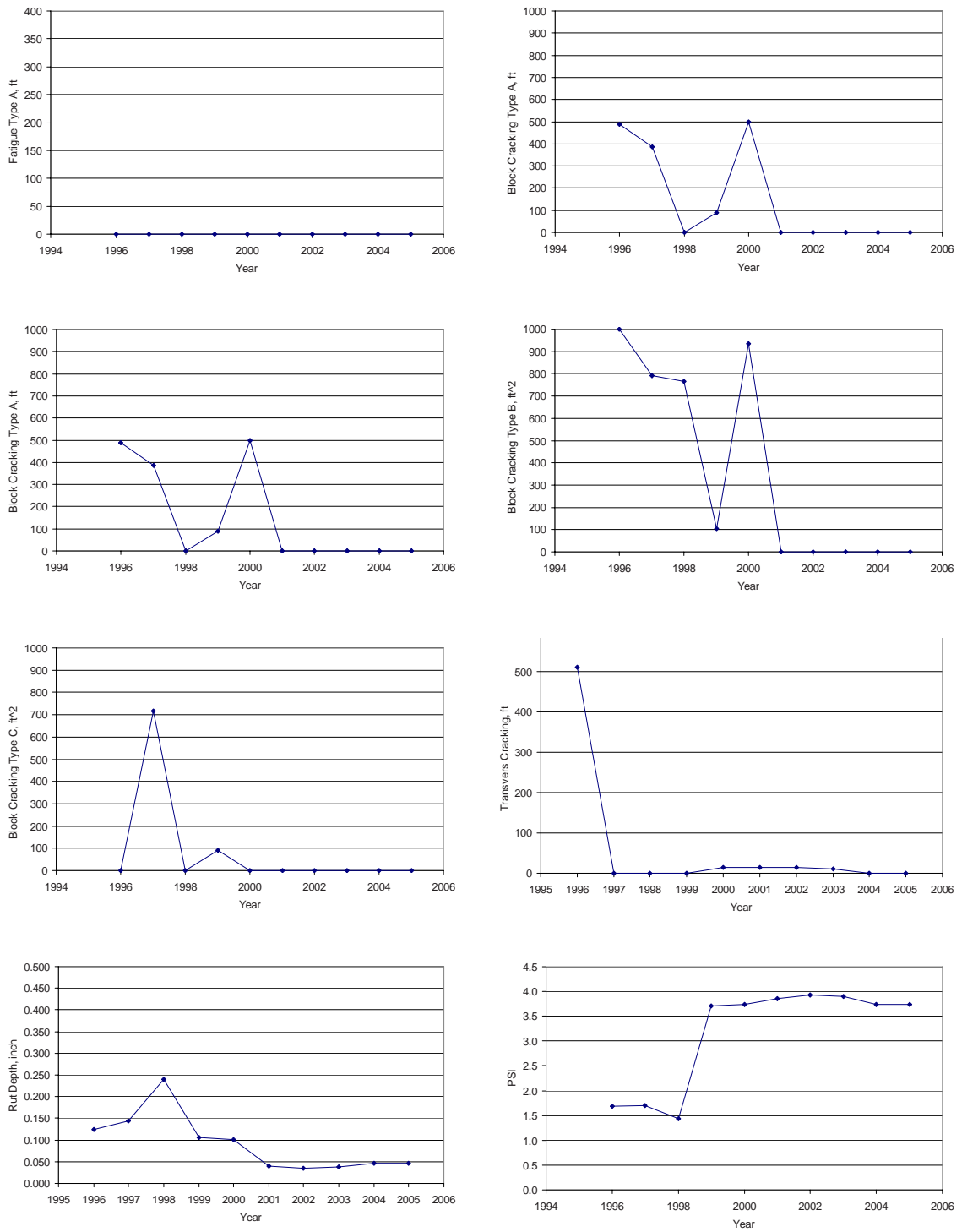


Figure 3.3: Performance data of contract 2838 on SR396 from mileposts 1.13 to 7.7

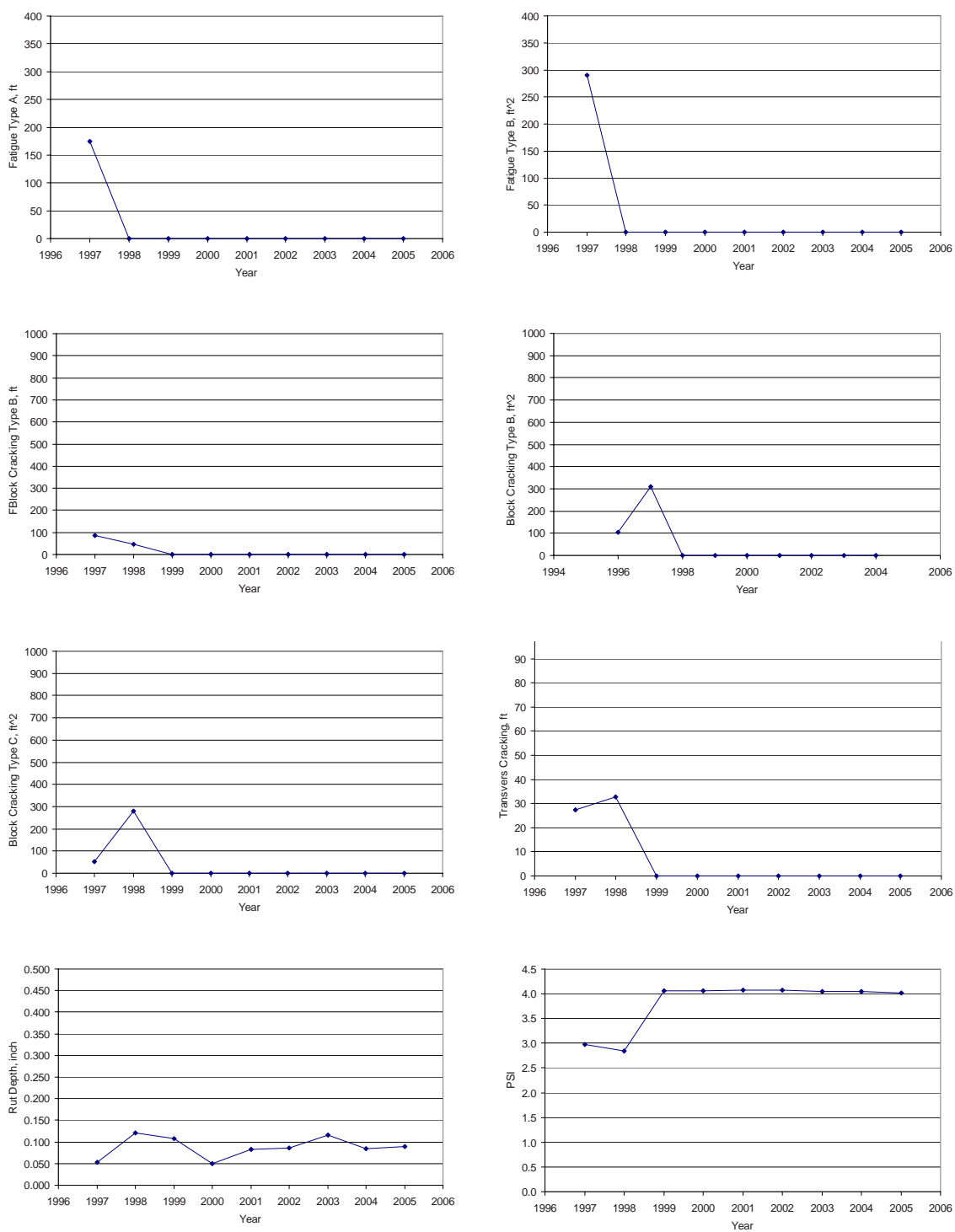


Figure 3.4: Performance data of contract 2935 on SR360 from mileposts 0 to 23.25

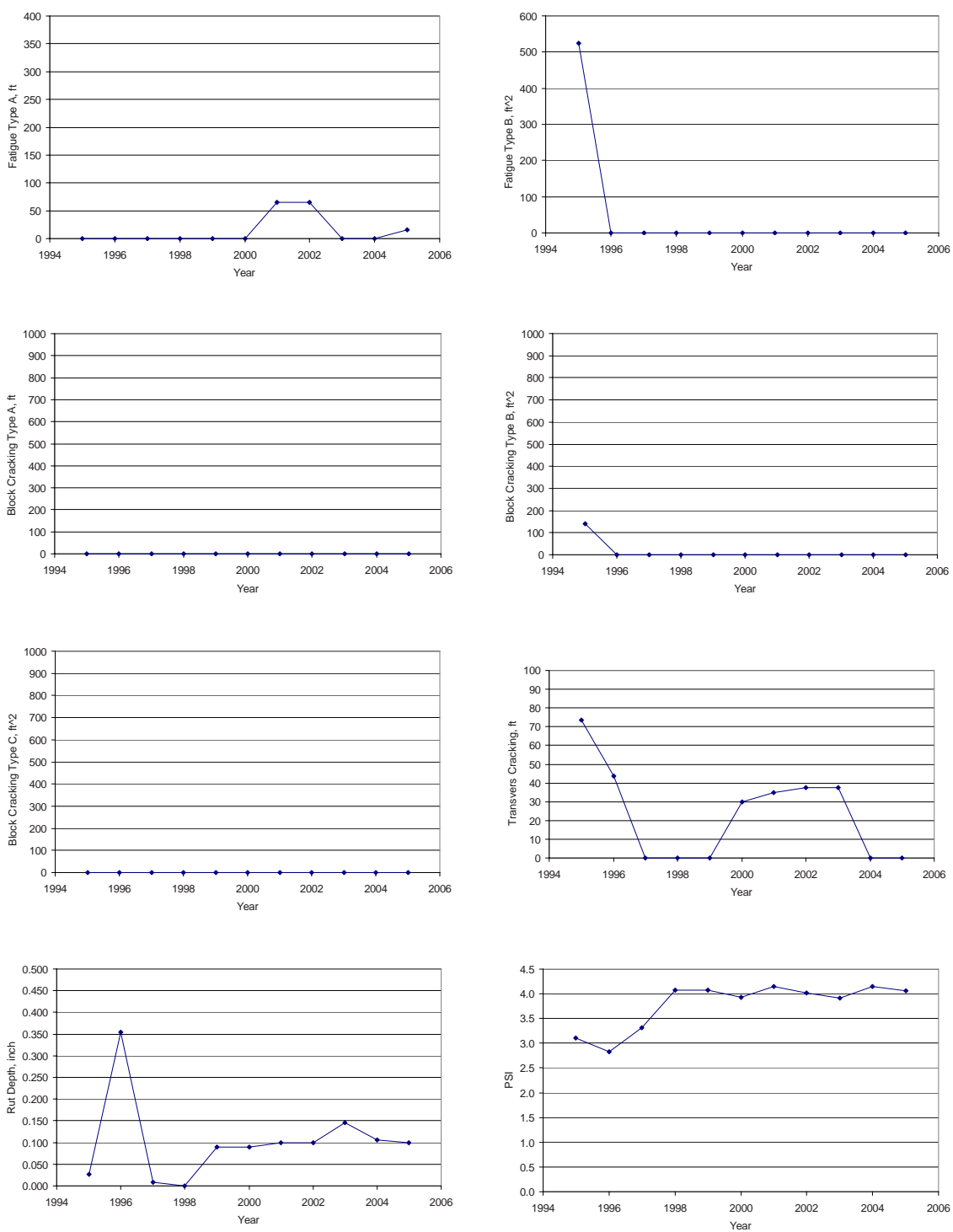


Figure 3.5: Performance data of contract 2819 on US095 from mileposts 6.98 to 14.38

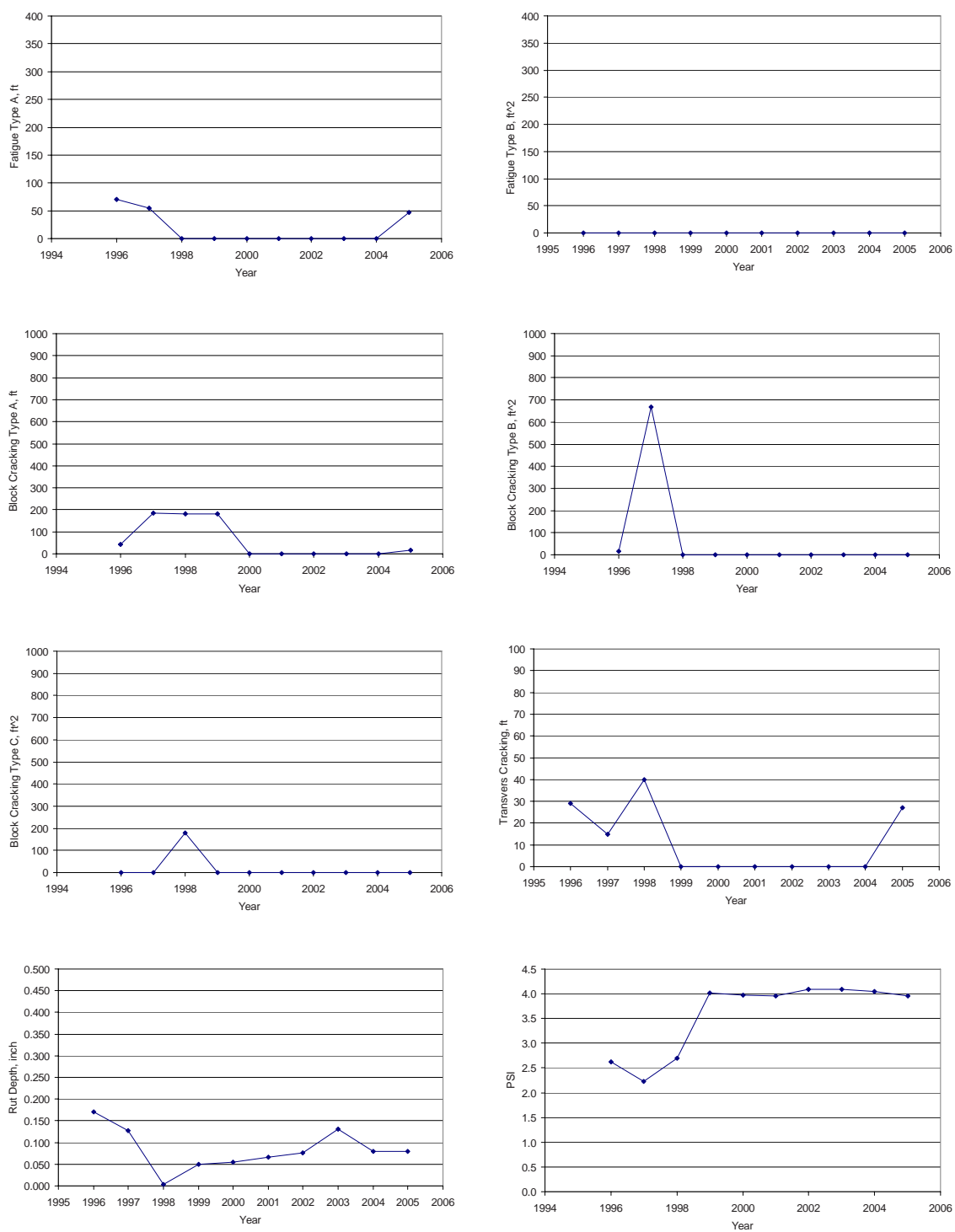


Figure 3.6: Performance data of contract 2873 on US095 from mileposts 56.24 to 72.00

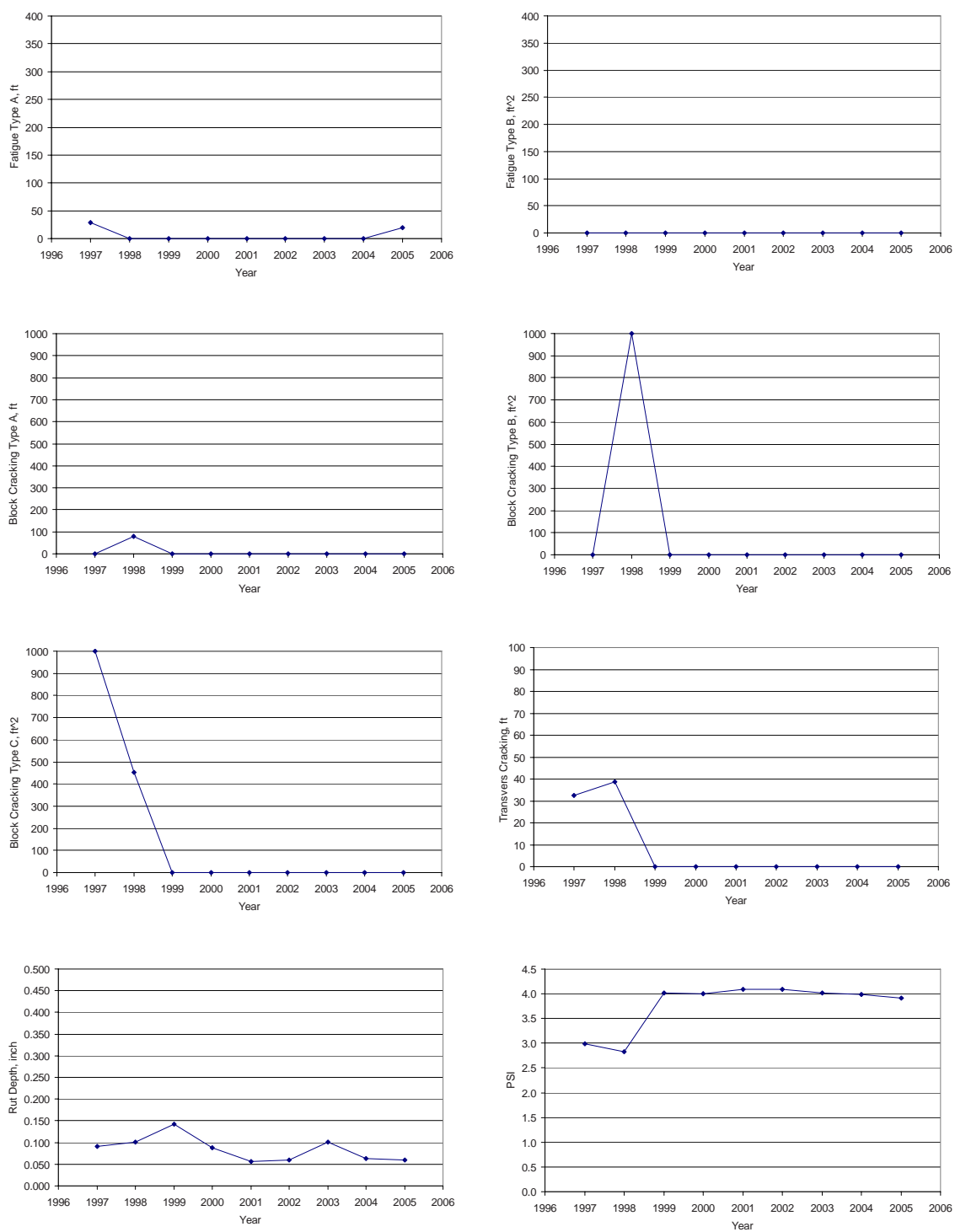


Figure 3.7: Performance data of contract 2961 on US006 from mileposts 18.87 to 43.99

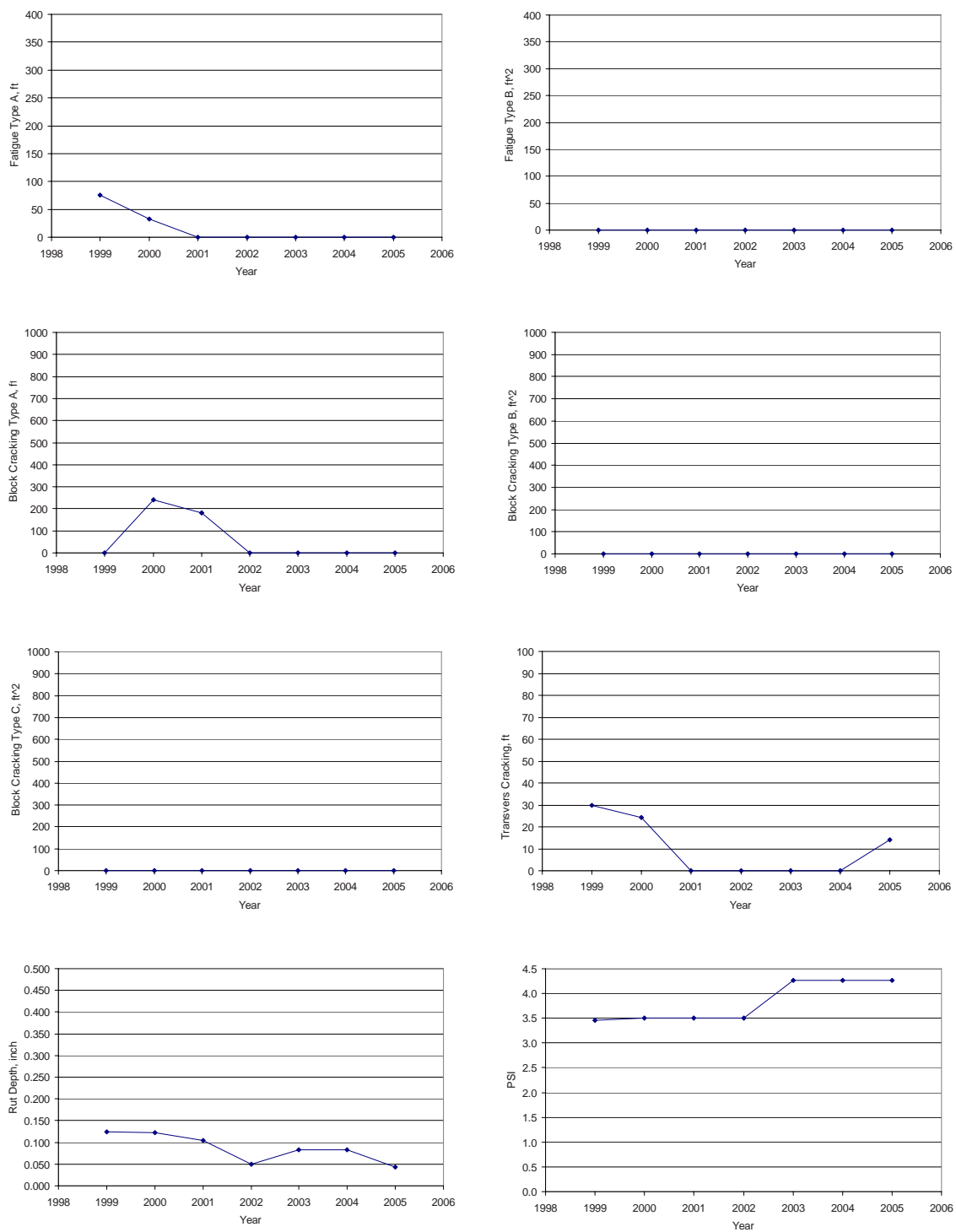


Figure 3.8: Performance data of contract 3013 on US095A from mileposts 24.55 to 44.18

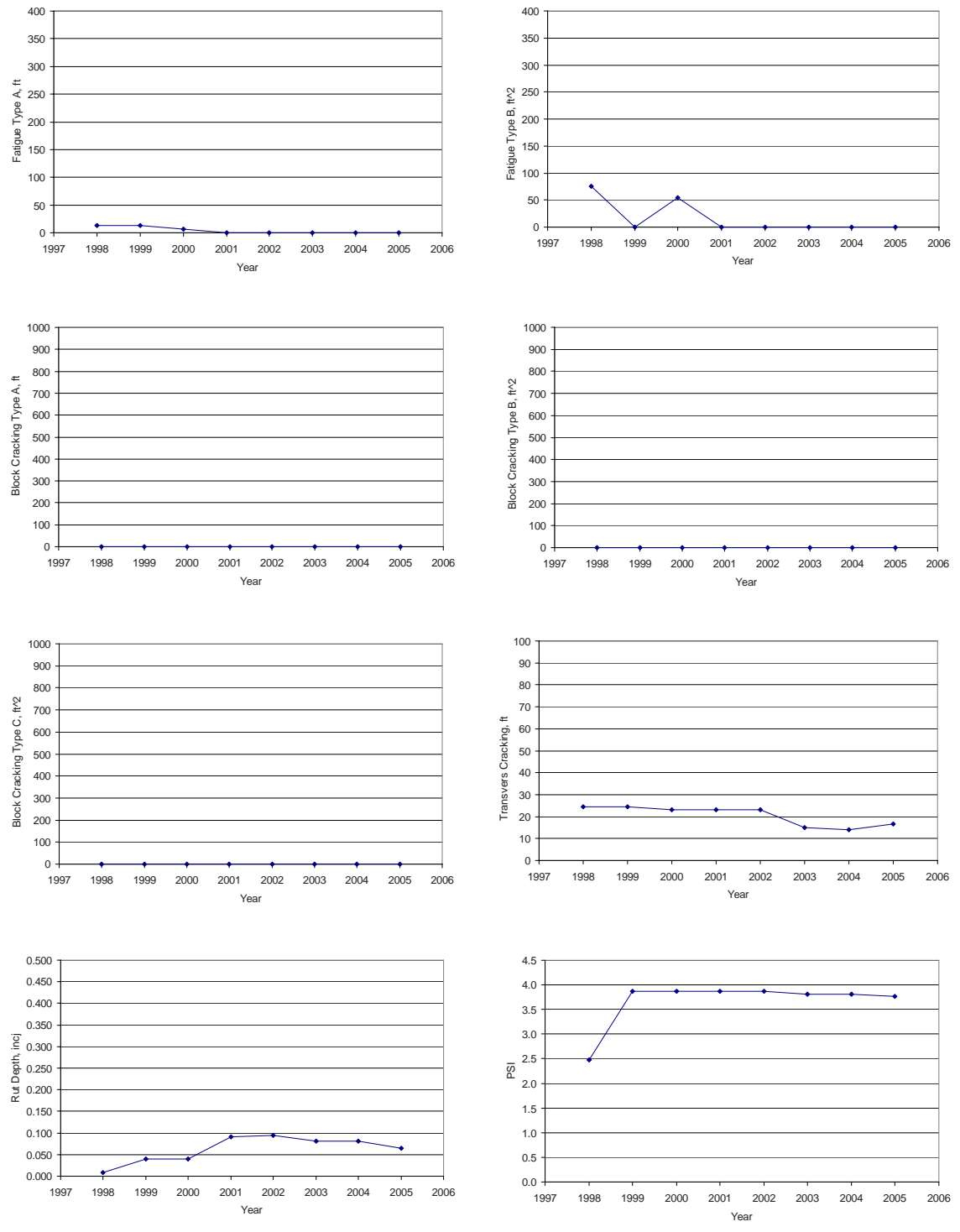


Figure 3.9: Performance data of contract 3025a on US093 from mileposts 0 to 11

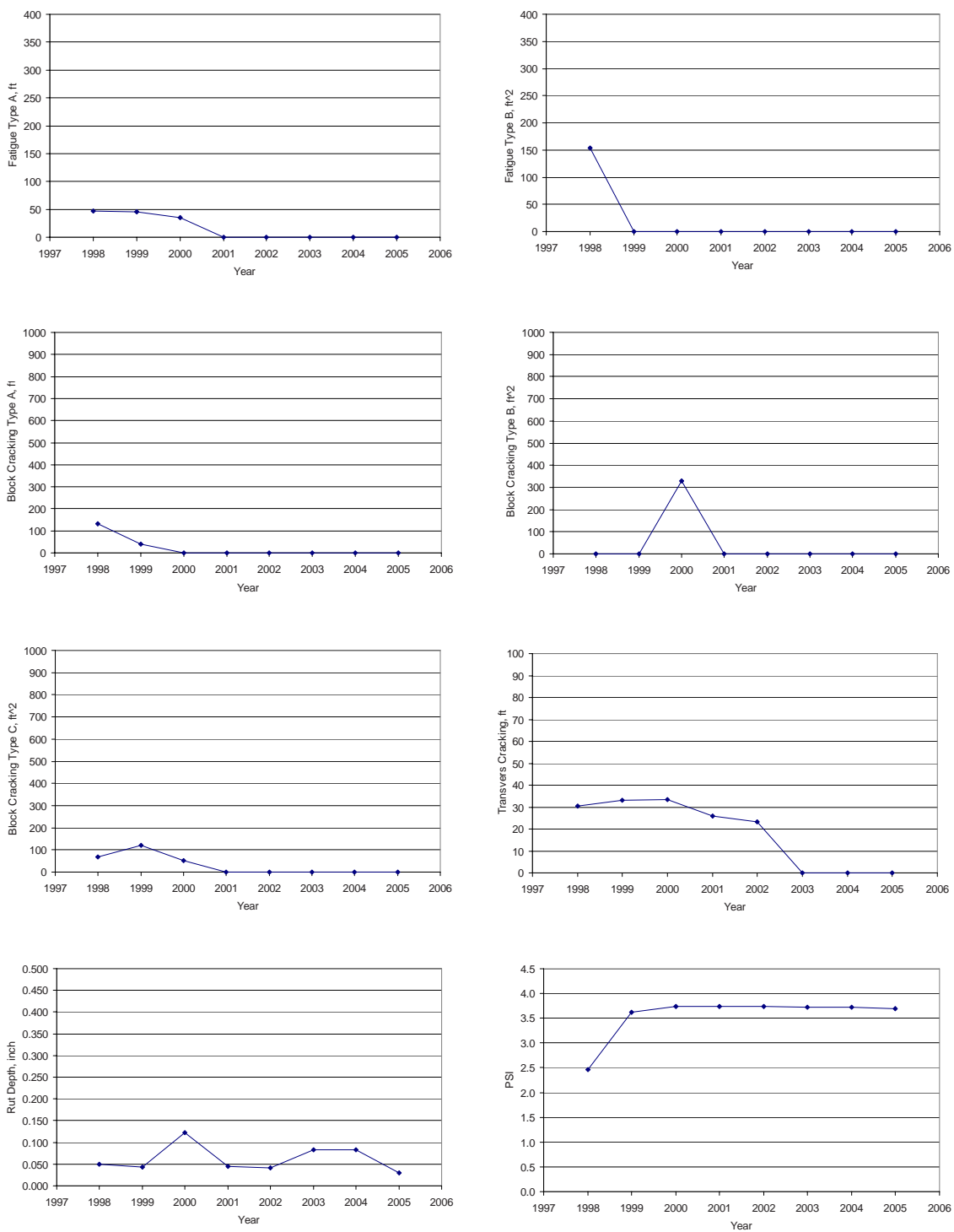


Figure 3.10: Performance data of contract 3025b on US093 from mileposts 109.33 to 131.55

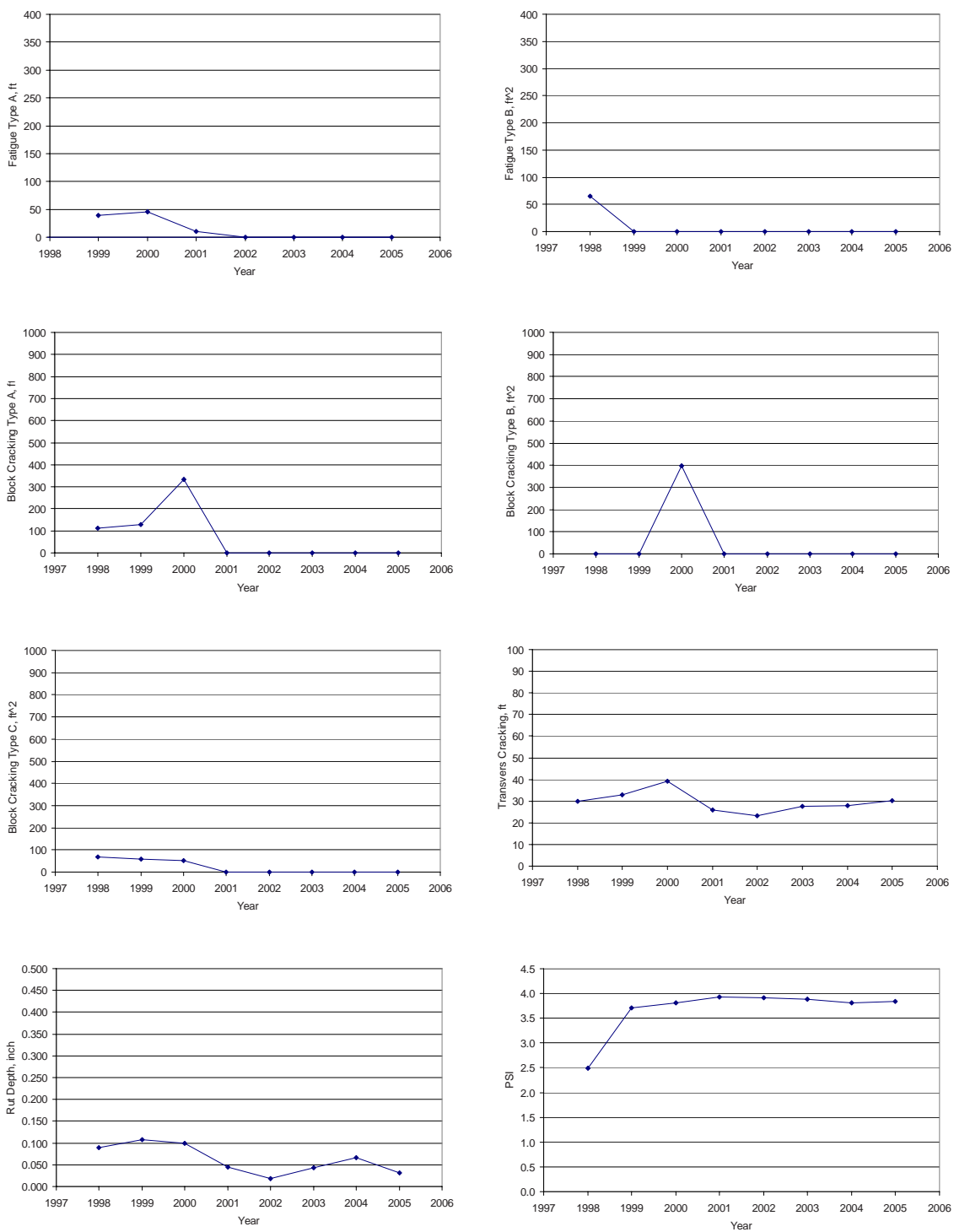


Figure 3.11: Performance data of contract 3025c on US093 from mileposts 147.45 to 172.4

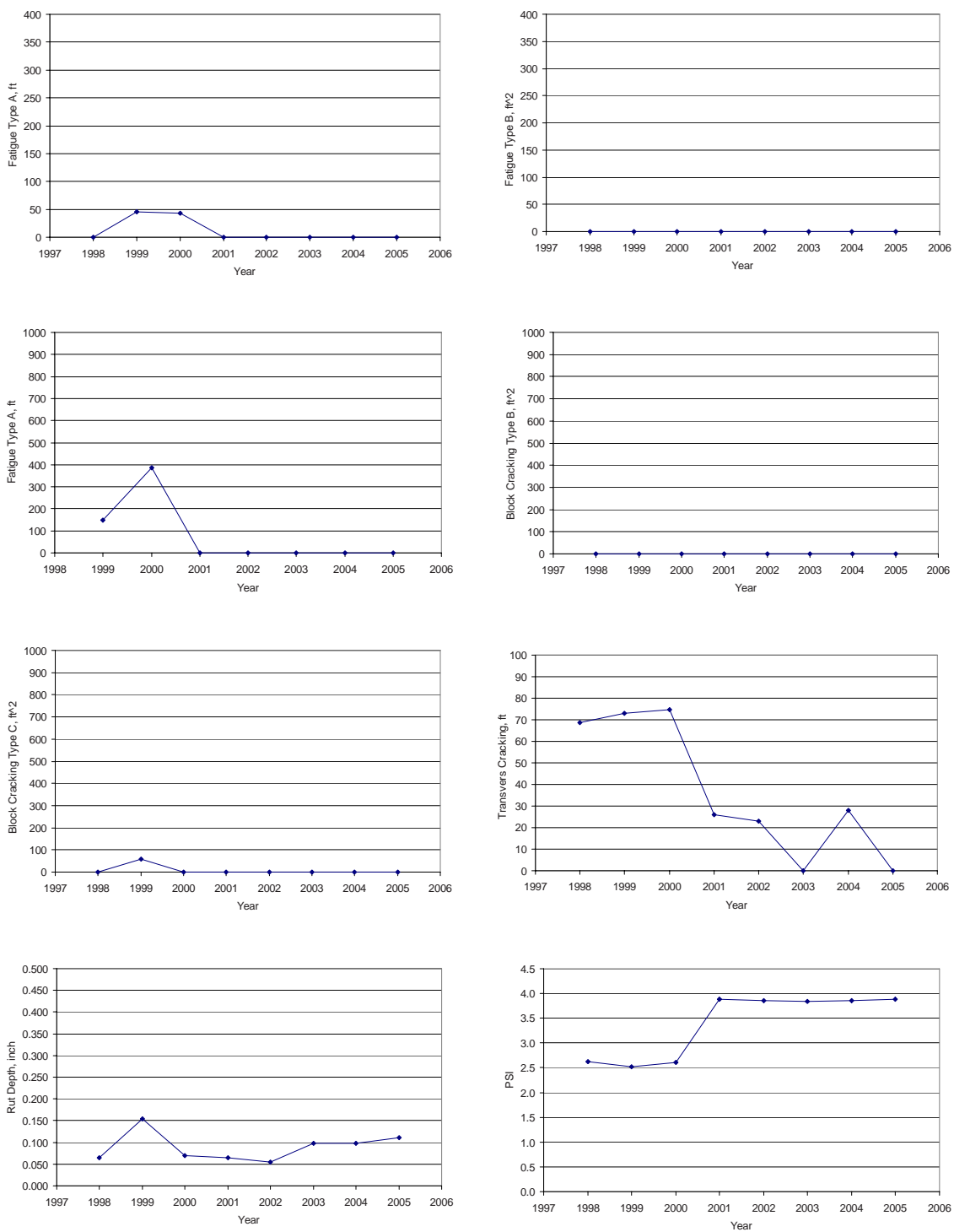


Figure 3.12: Performance data of contract 2876 on SR208 from mileposts 2.33 to 8.86

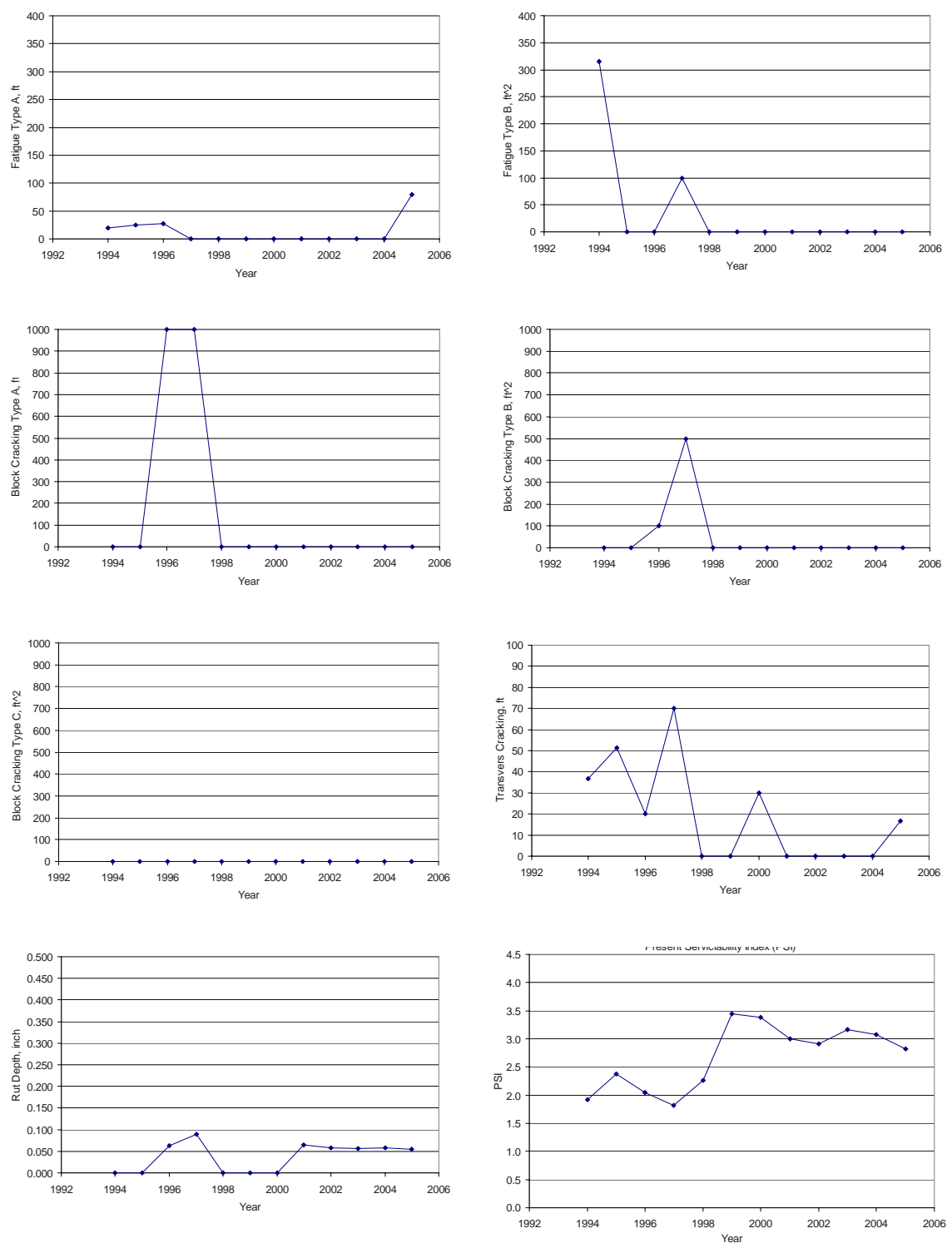


Figure 3.13: Performance data of contract 2761 on SR443 from mileposts 0.00 to 0.87

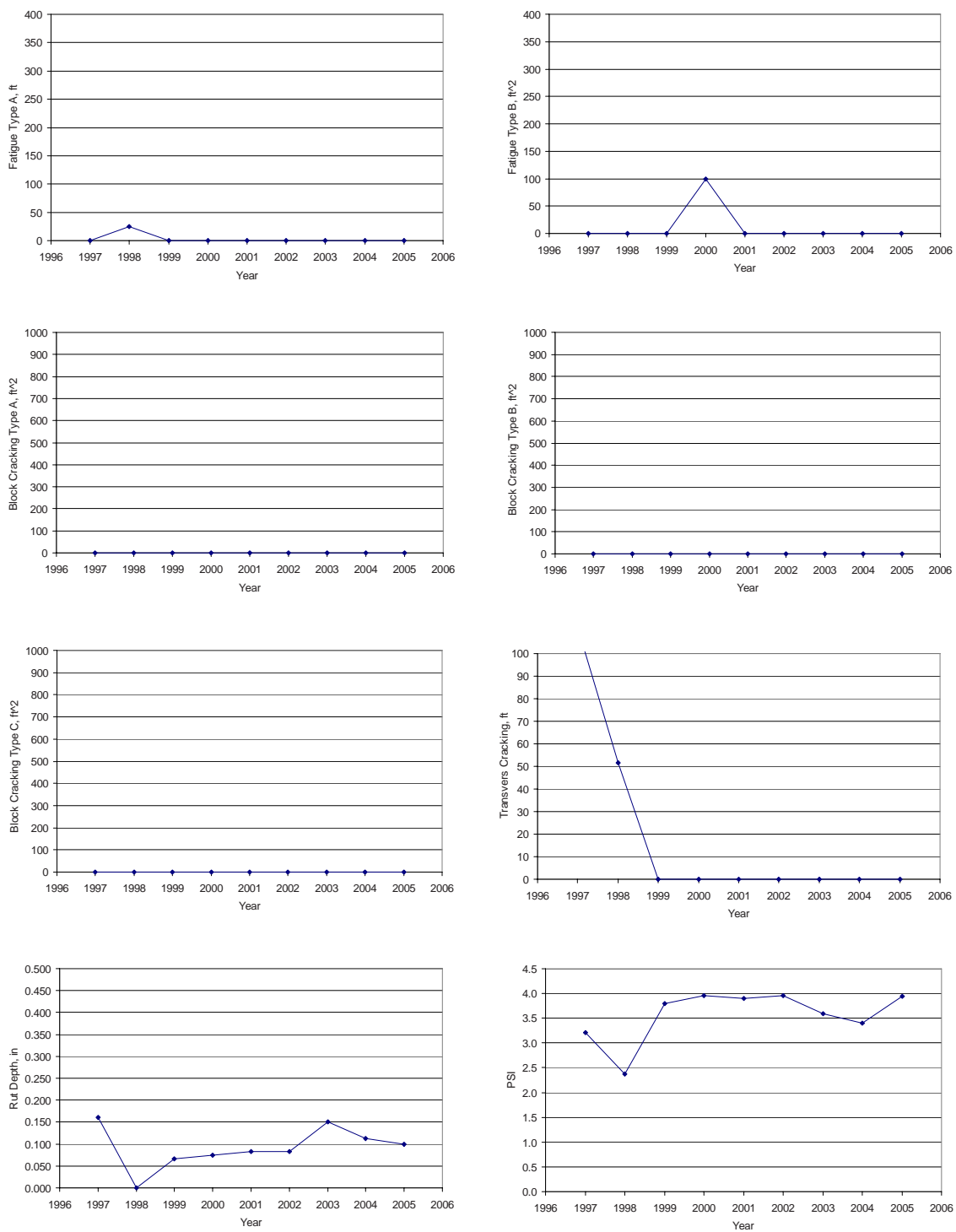


Figure 3.14: Performance data of contract 2932 on US095 from mileposts 49.24 to 50.41

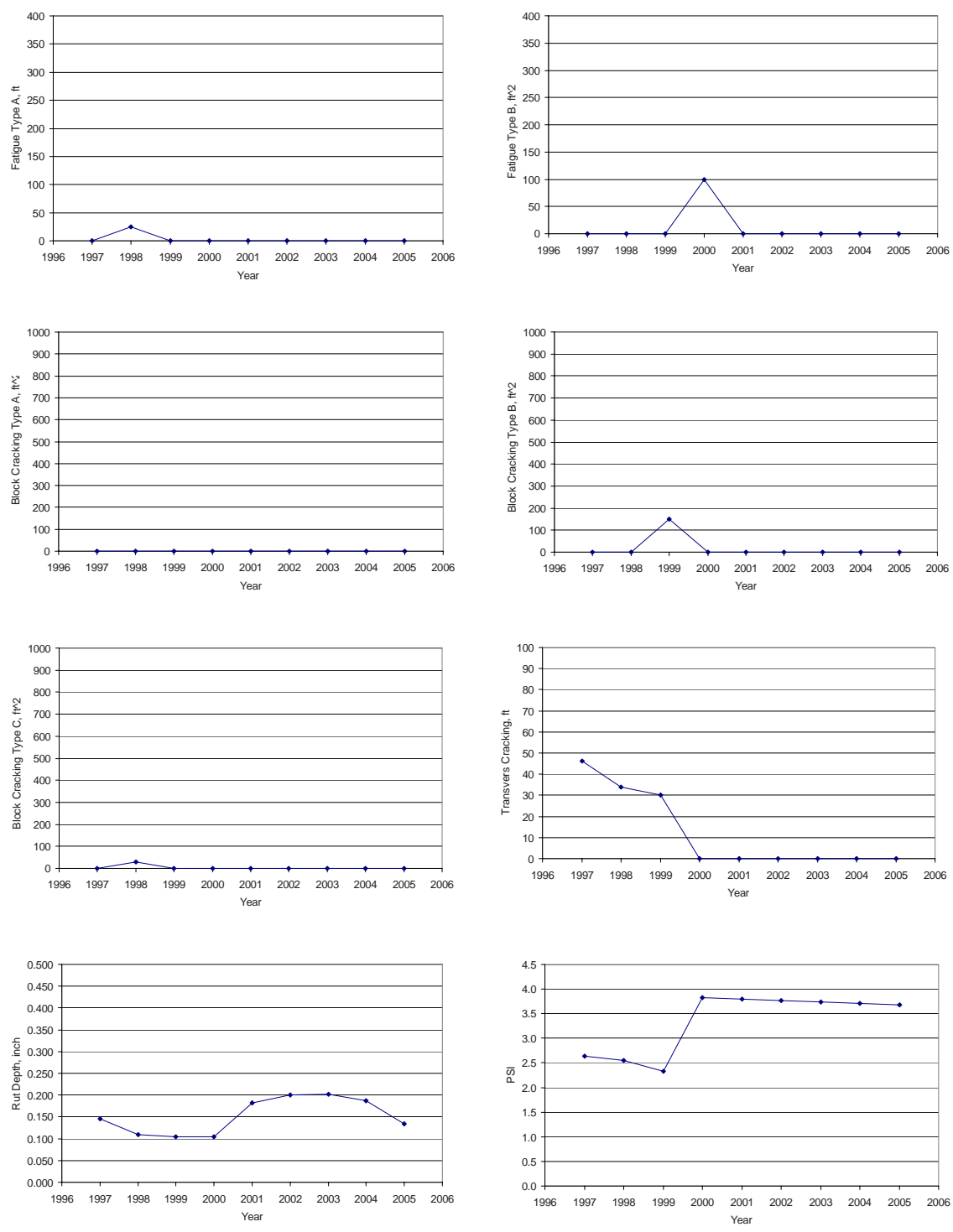


Figure 3.15: Performance data of contract 2980a on US050 from mileposts 19.4 to 21.14

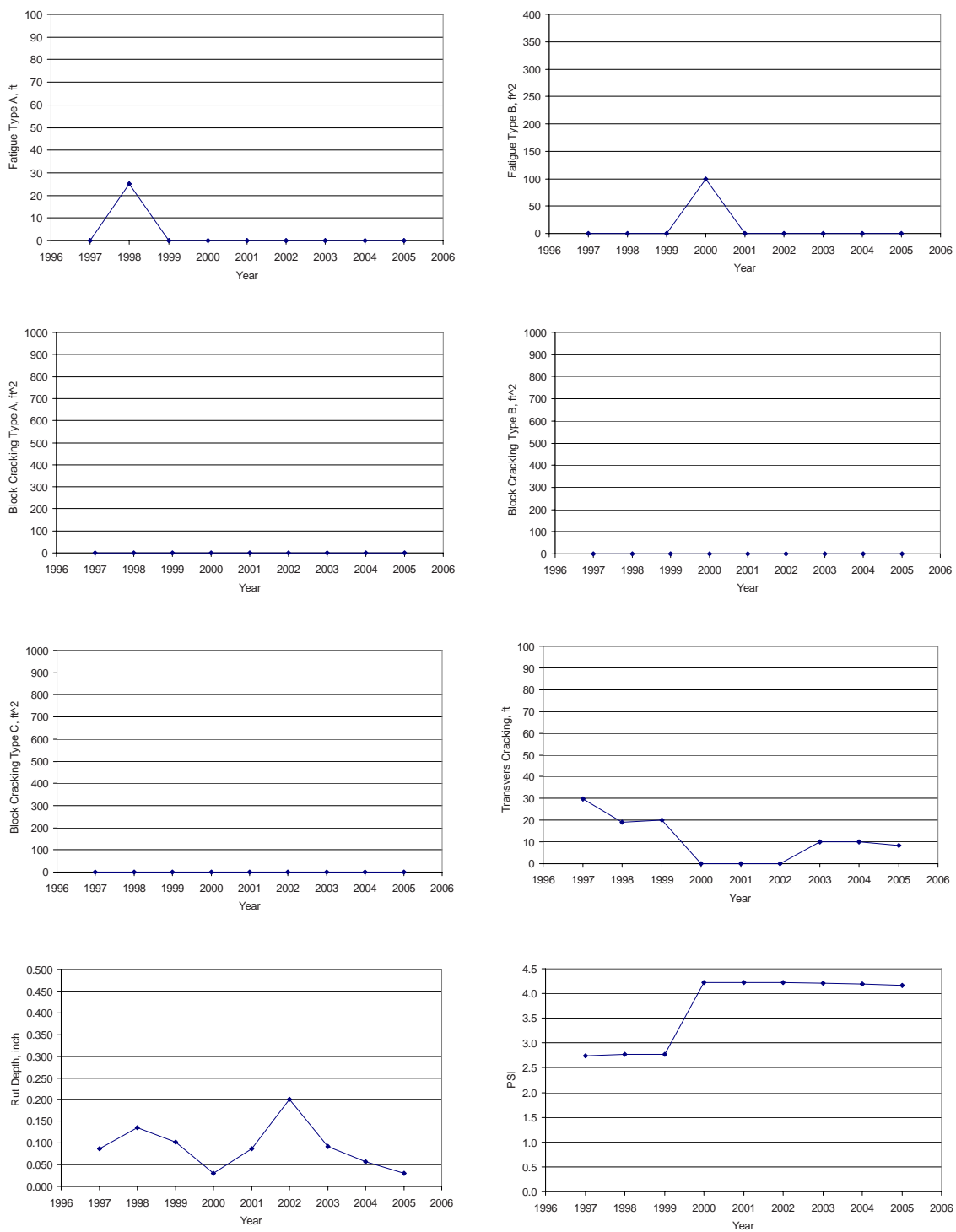


Figure 3.16: Performance data of contract 2980b on US095 from mileposts 26.19 to 28.22

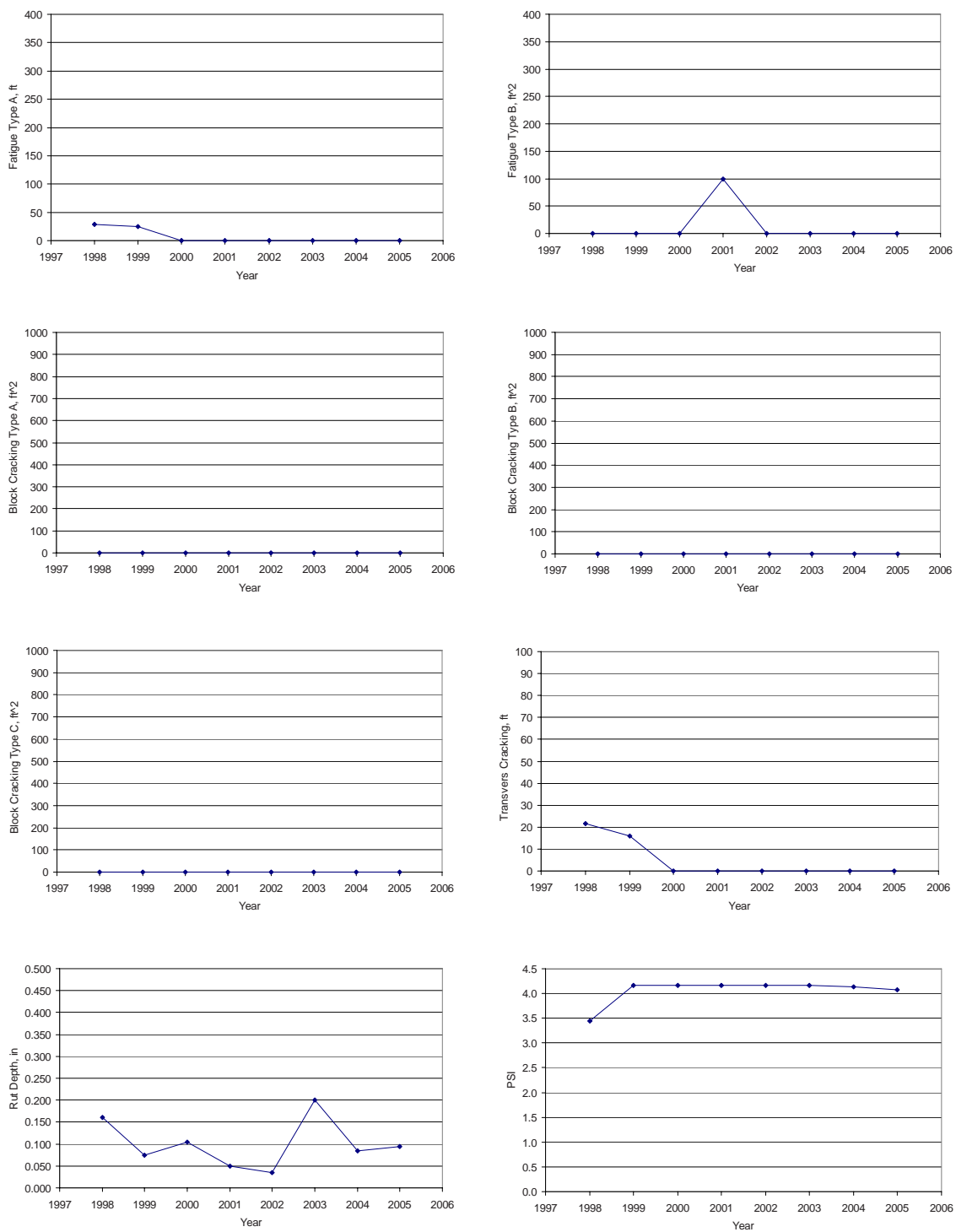


Figure 3.17: Performance data of contract 3006 on IR080 from mileposts 50.0 to 50.23

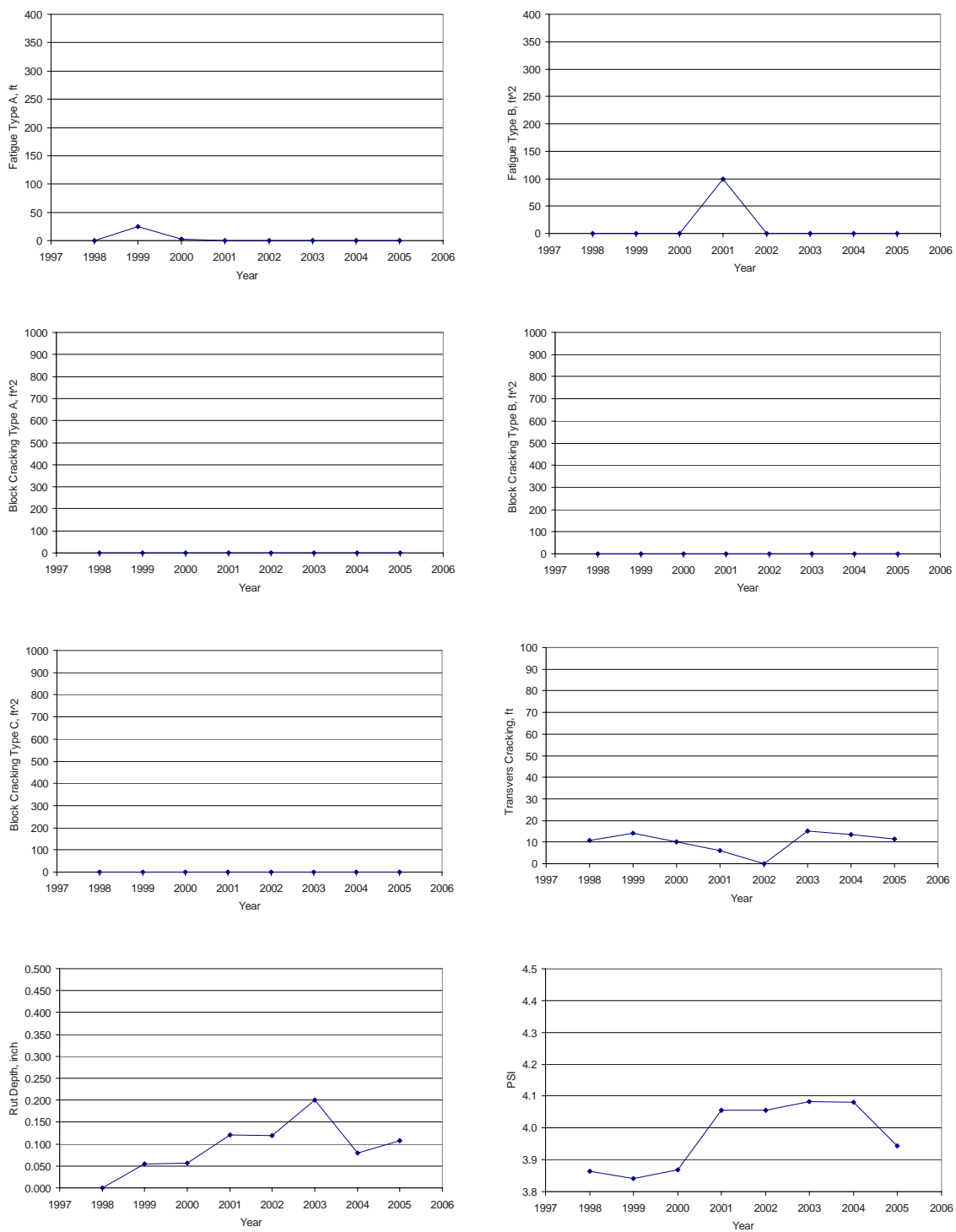


Figure 3.18: Performance data of contract 3008 on SR227 from mileposts 1.39 to 6.56

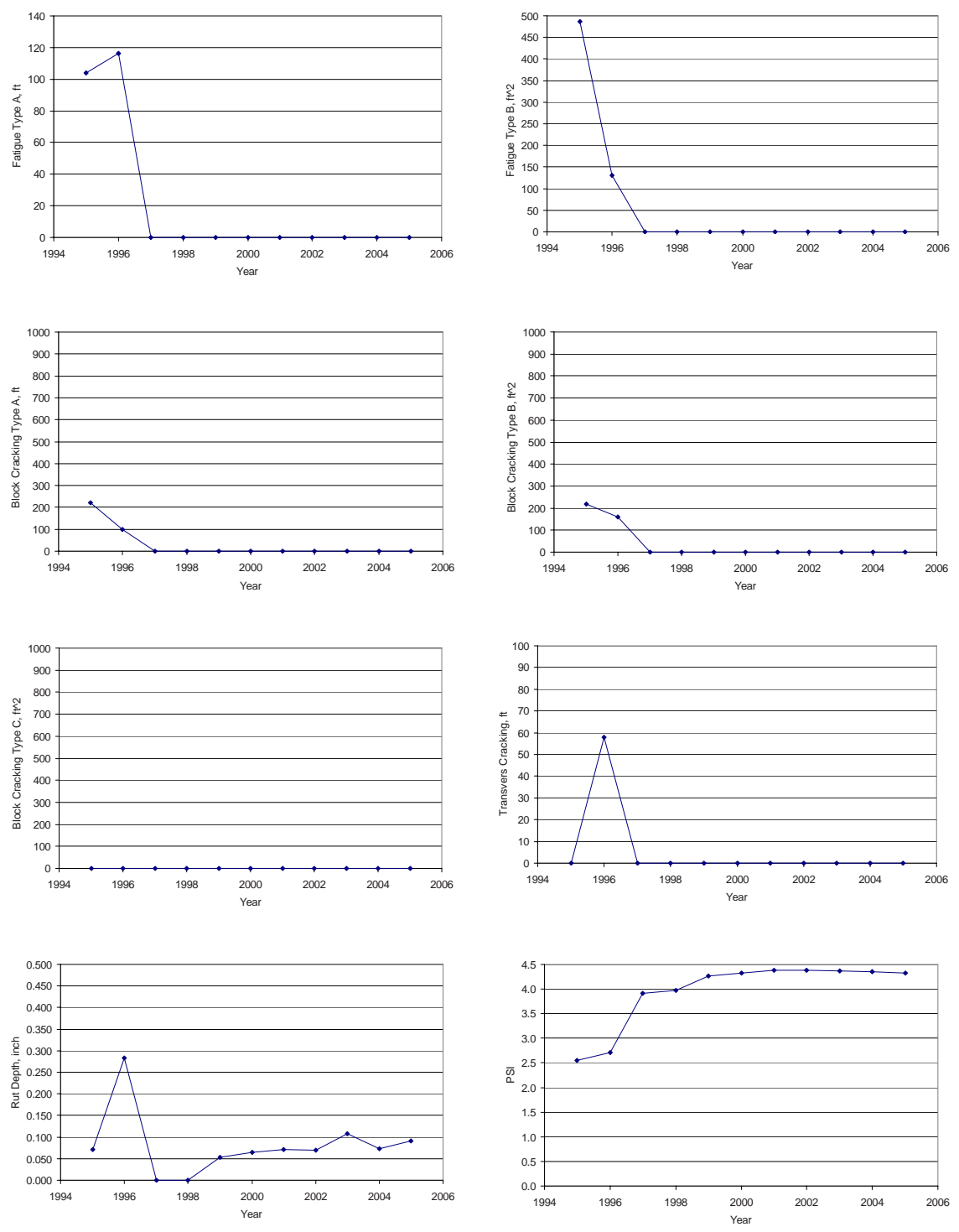


Figure 3.19: Performance data of contract 2723 on US095 from mileposts 96.89 to 117.5

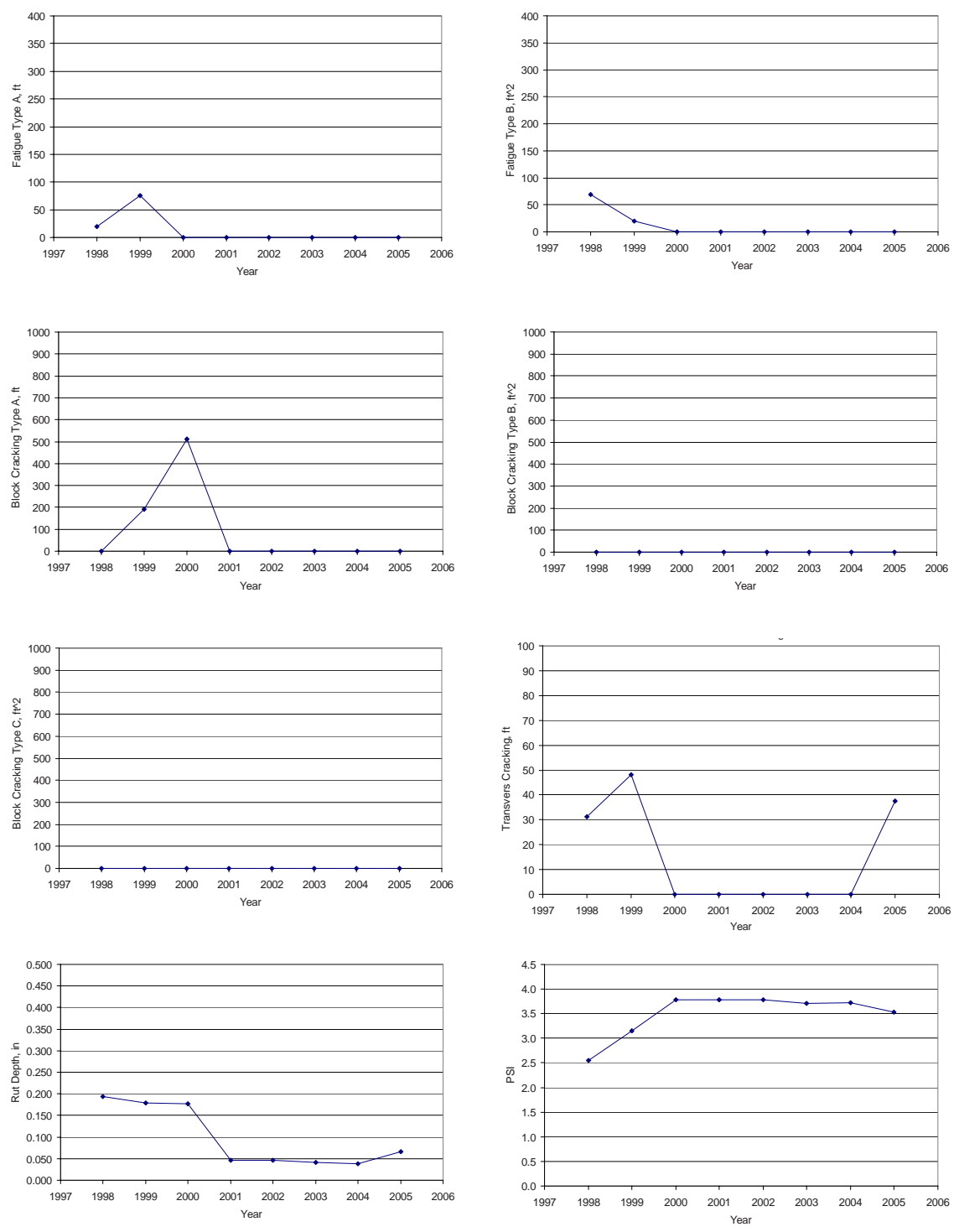


Figure 3.20: Performance data of contract 3031 on US395 from mileposts 25.21 to 29.24

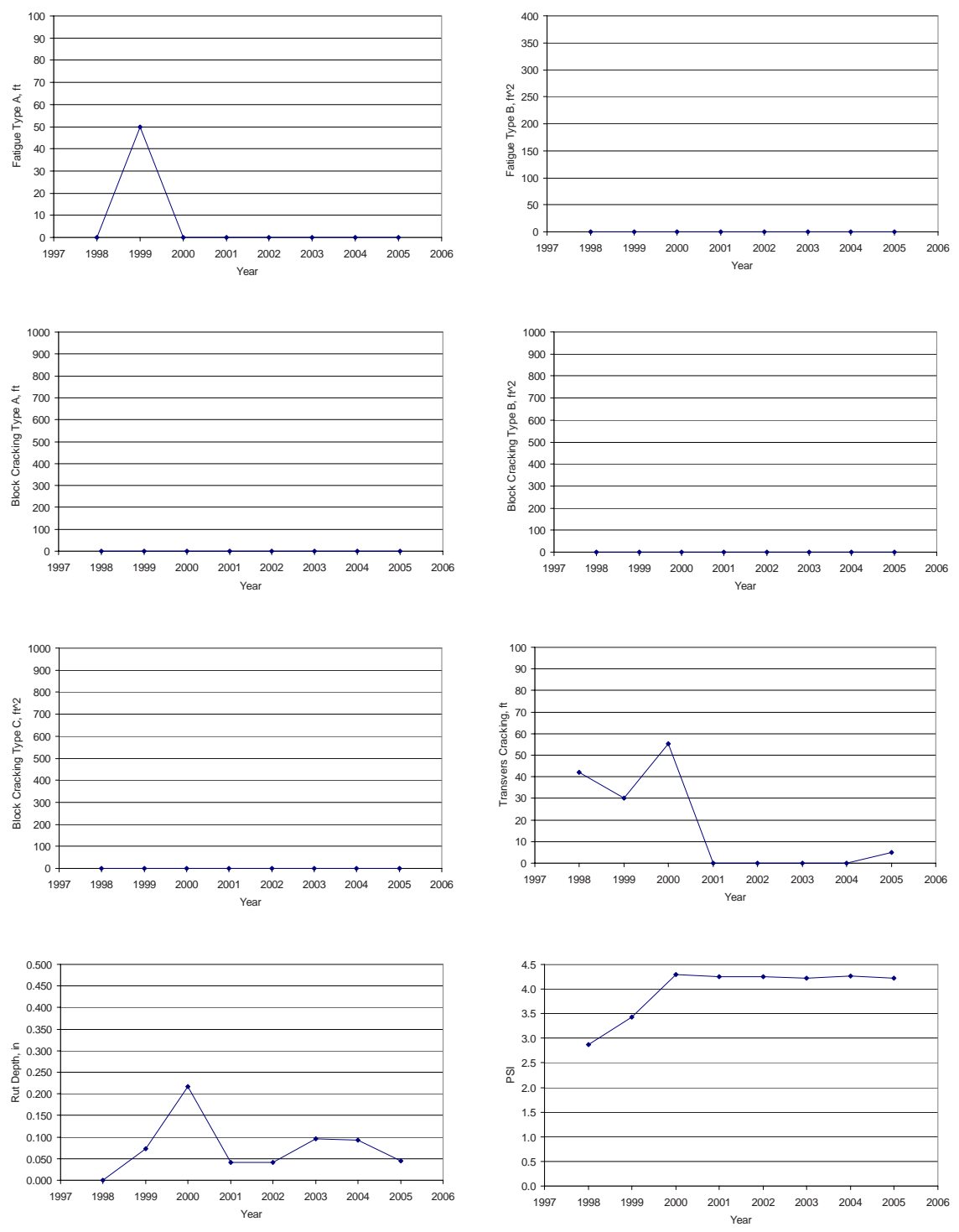


Figure 3.21: Performance data of contract 3048 on SR157 from mileposts 12.47 to 21.1

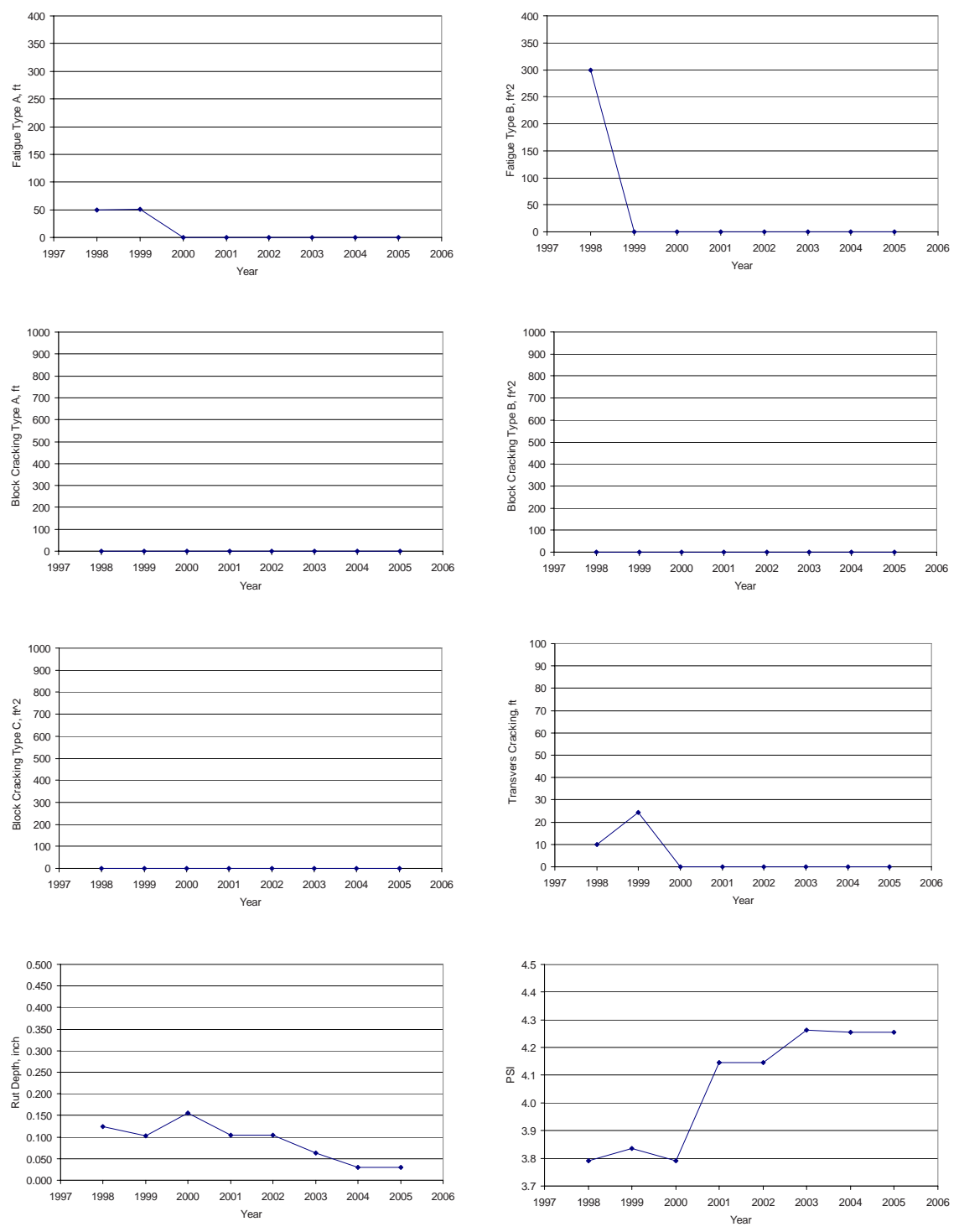


Figure 3.22: Performance data of contract 3045 on US050 from mileposts 36.81 to 37.38

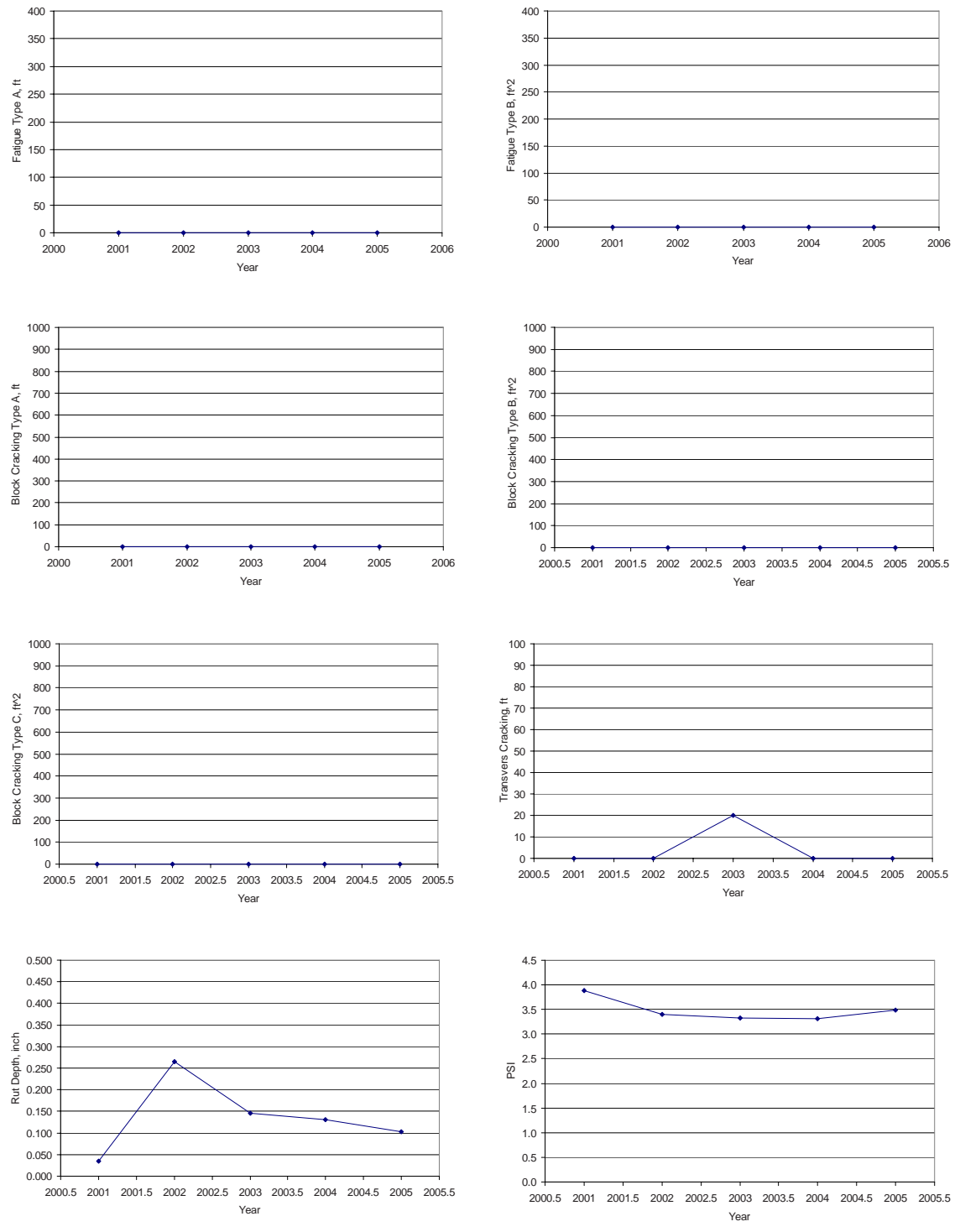


Figure 3.23: Performance data of contract 3162 on US395 from mileposts 17.37 to 19.4

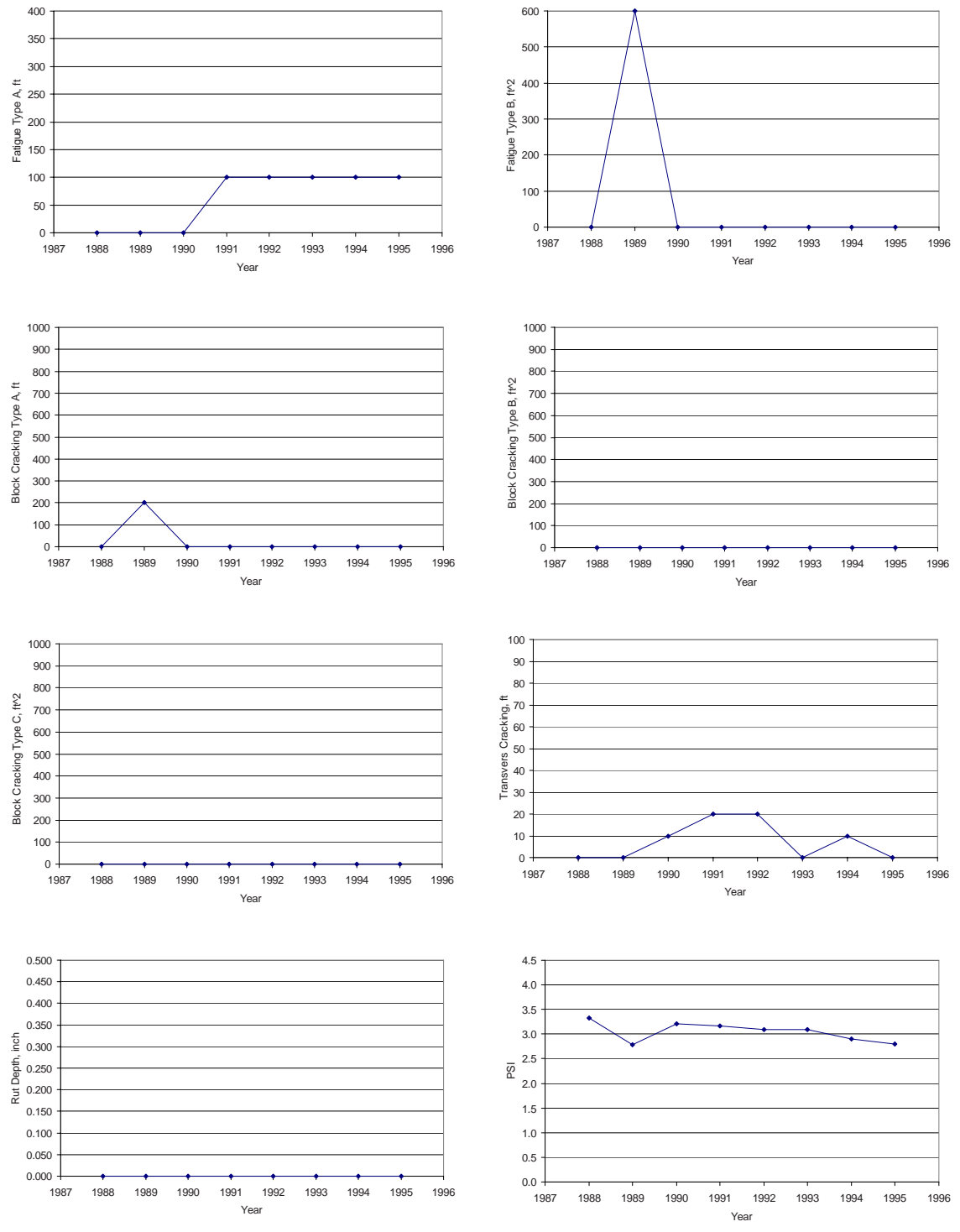


Figure 3.24: Performance data of contract 2384a on US095 from mileposts 14.81 to 16.6

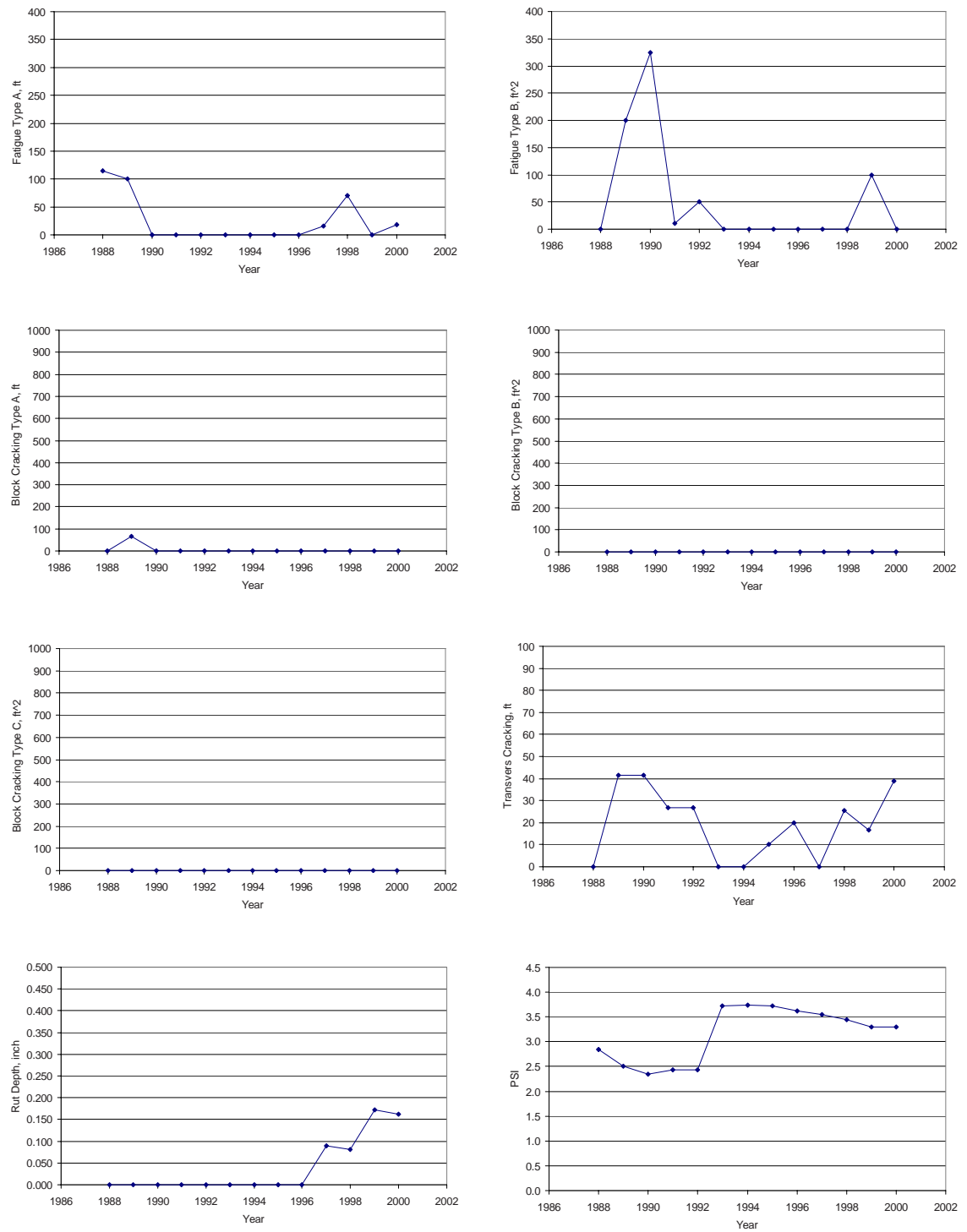


Figure 3.25: Performance data of contract 2384b on US095 from mileposts 0 to 2.74

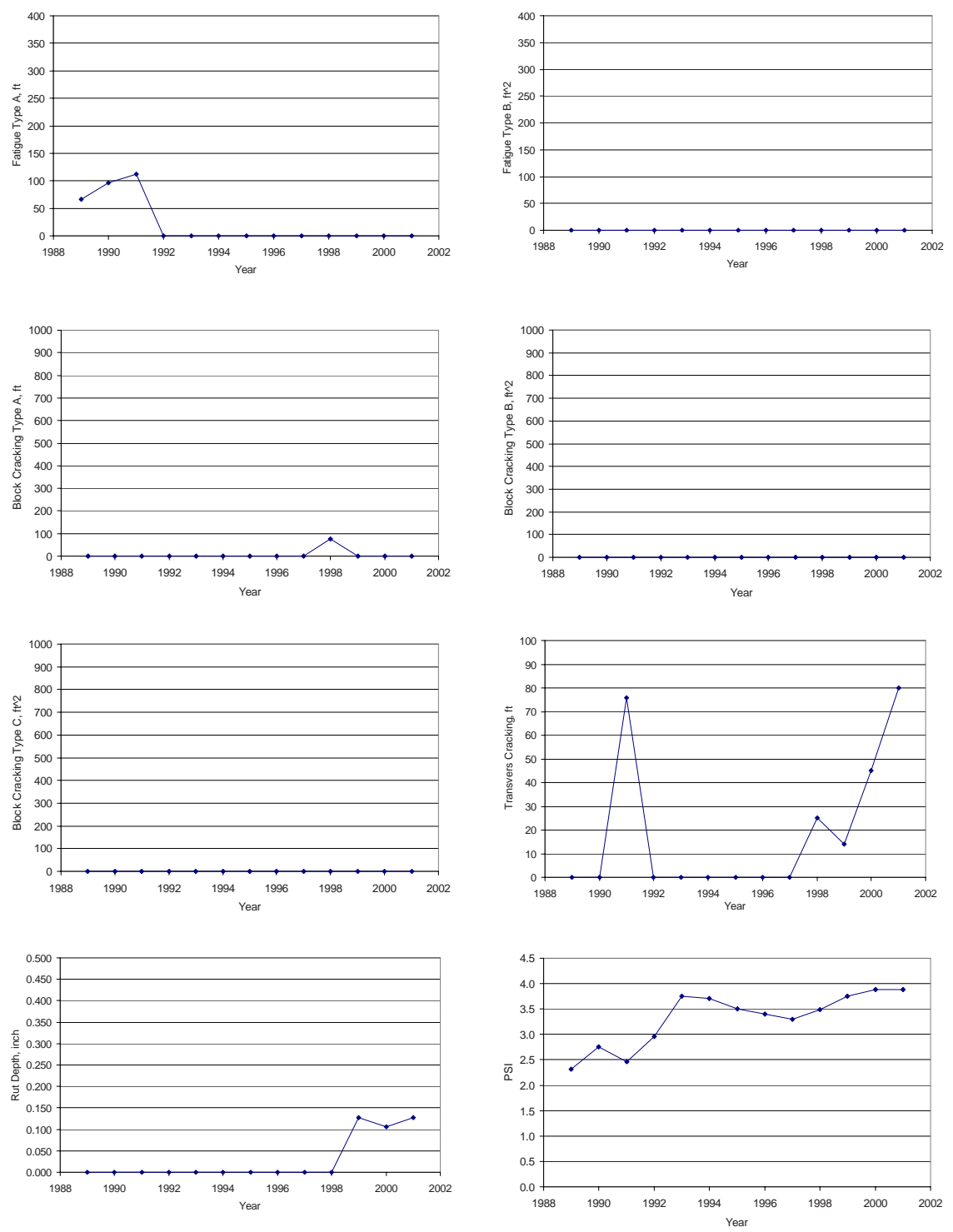


Figure 3.26: Performance data of contract 2432 on SR157 from mileposts 3.41 to 12.18

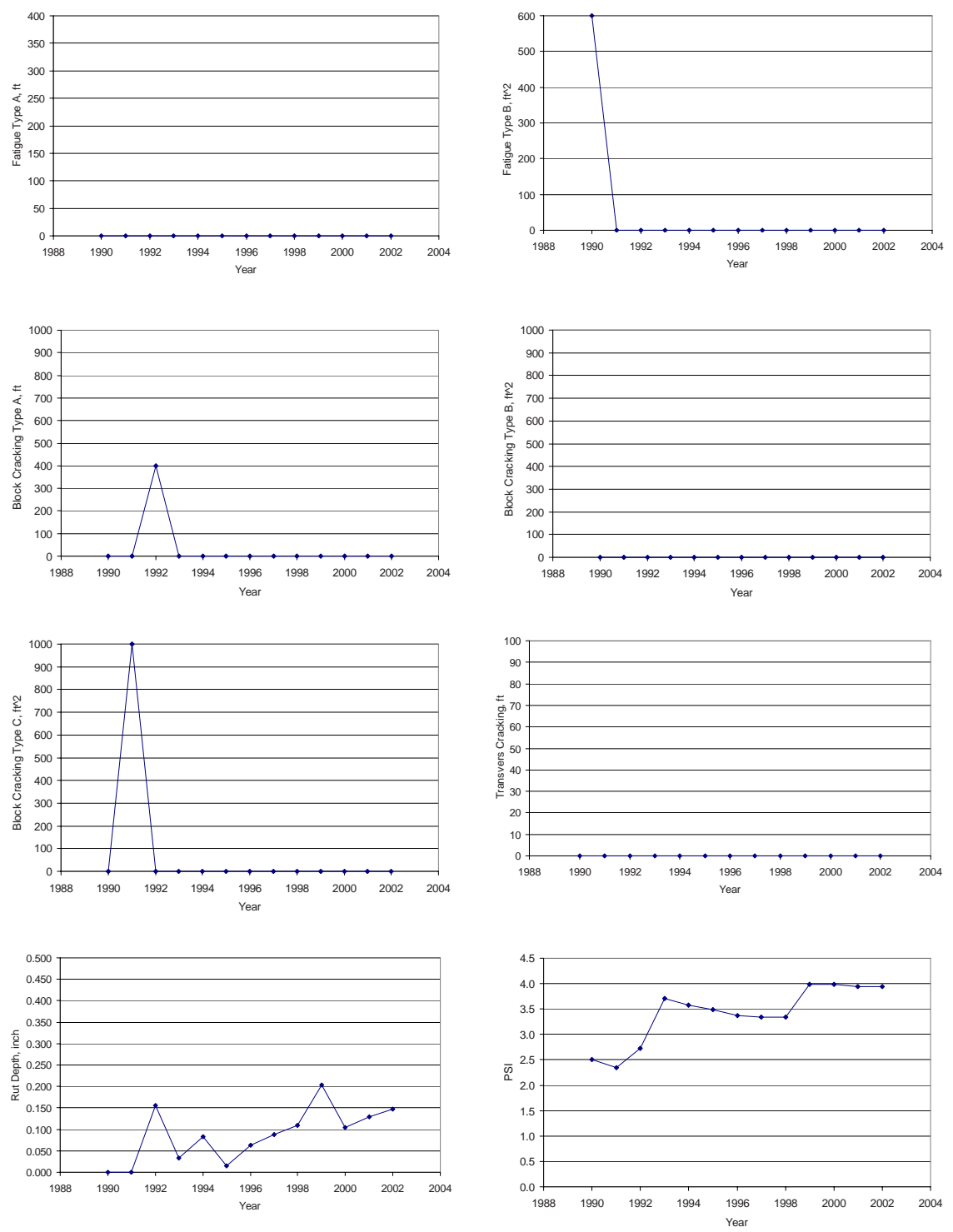


Figure 3.27: Performance data of contract 2505 on US095 from mileposts 62.54 to 64.01

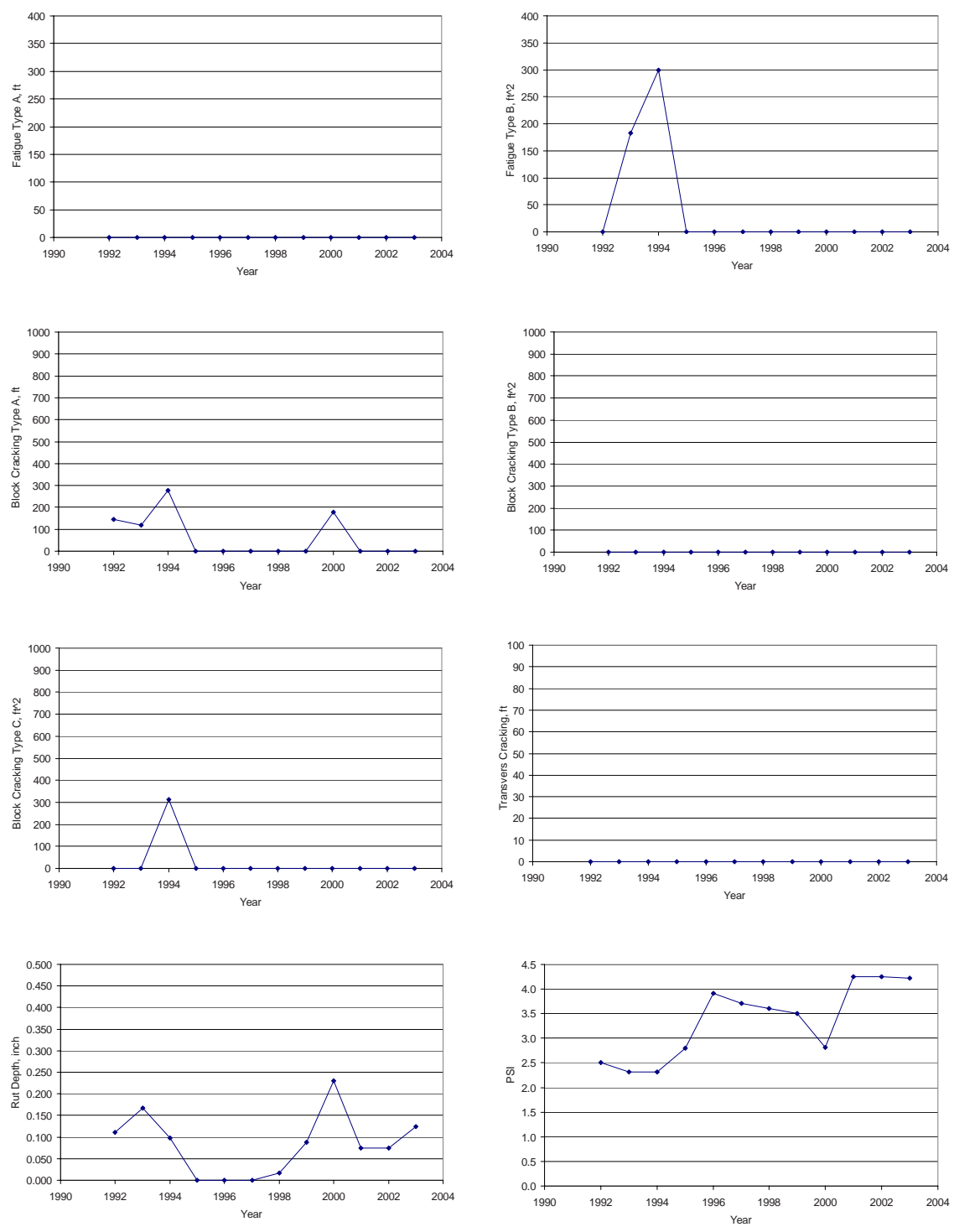


Figure 3.28: Performance data of contract 2651a on US095 from mileposts 12 to 15

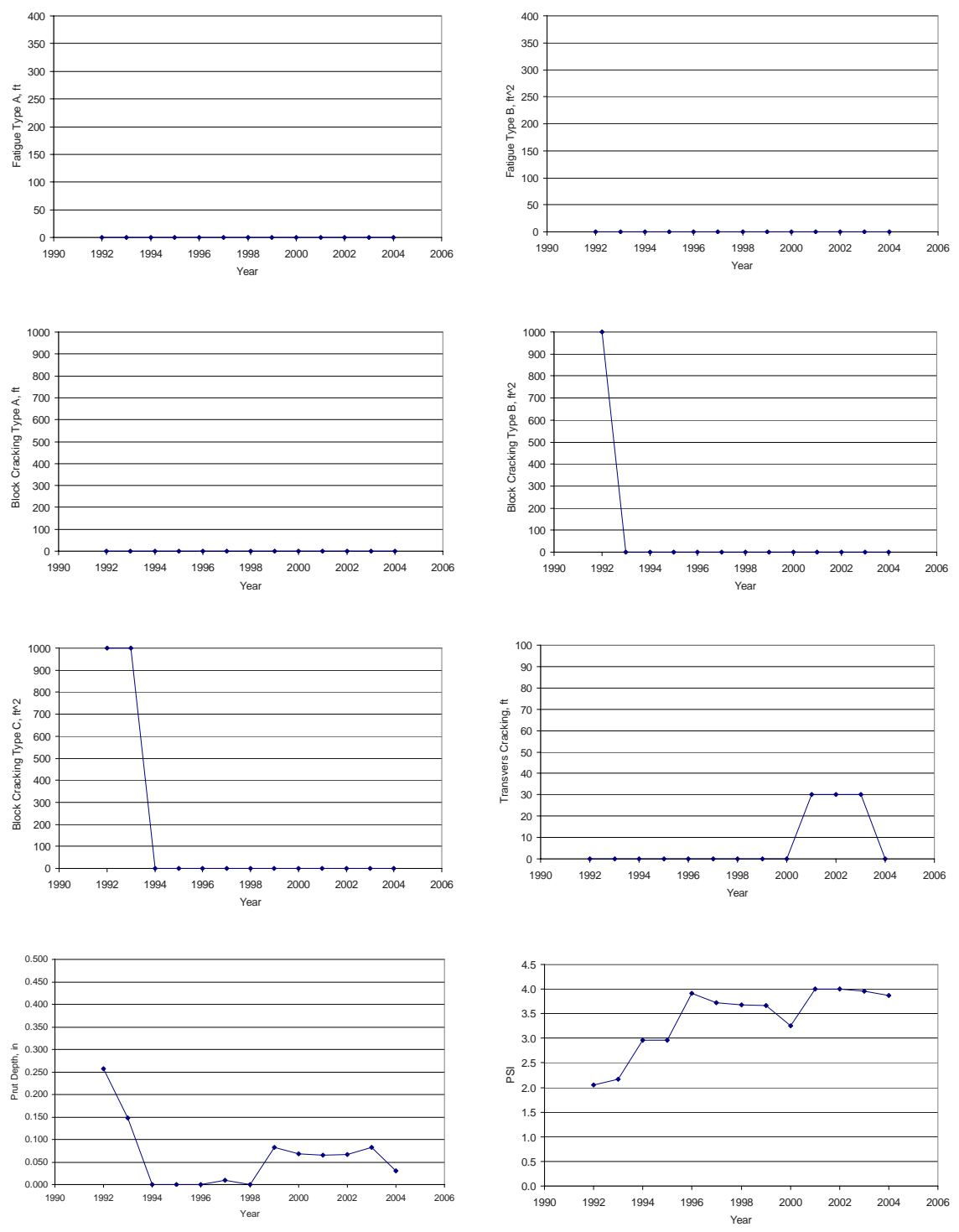


Figure 3.29: Performance data of contract 2651b on US095 from mileposts 43 to 44.8

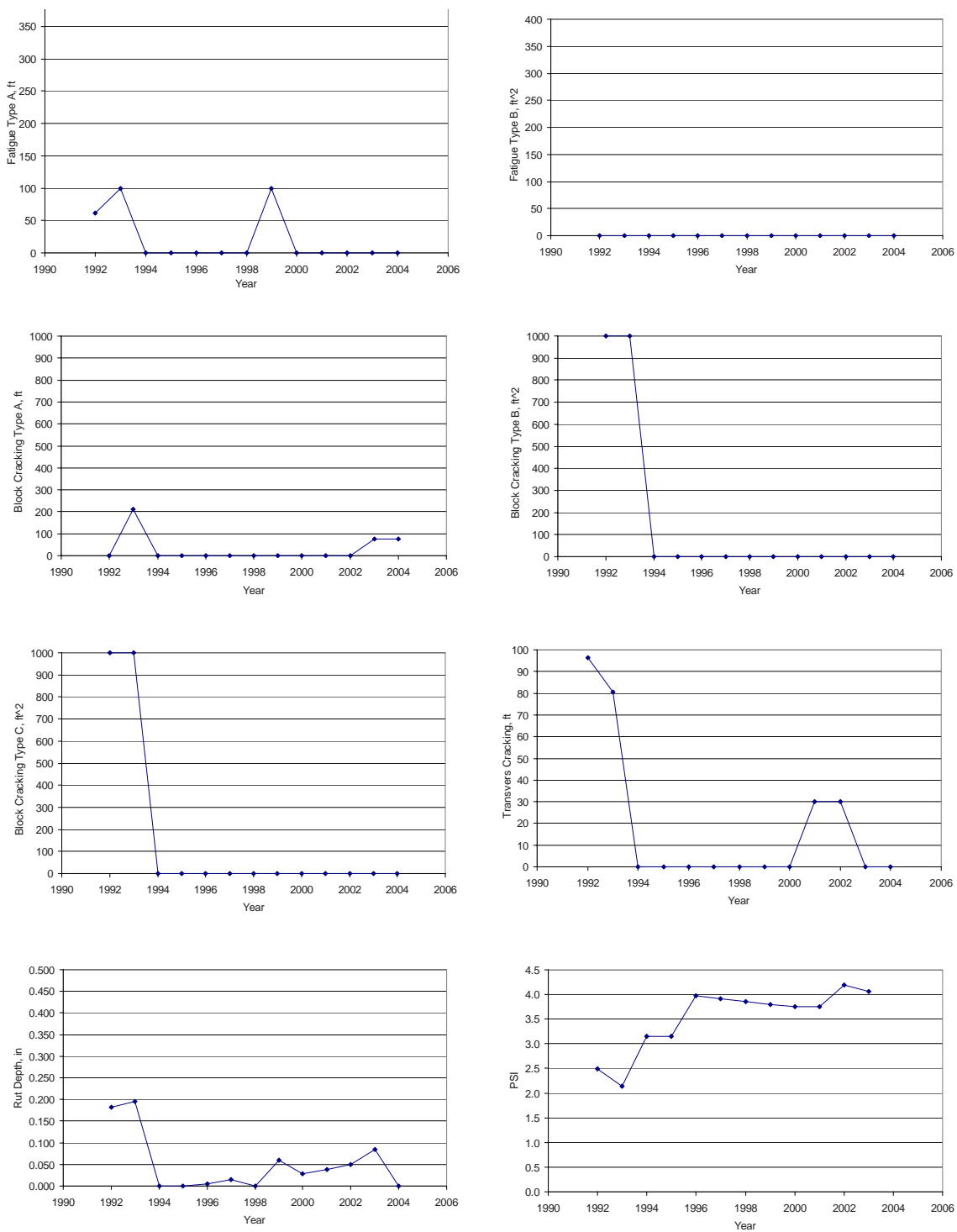


Figure 3.30: Performance data of contract 2651c on US095 from mileposts 32.88 to 39

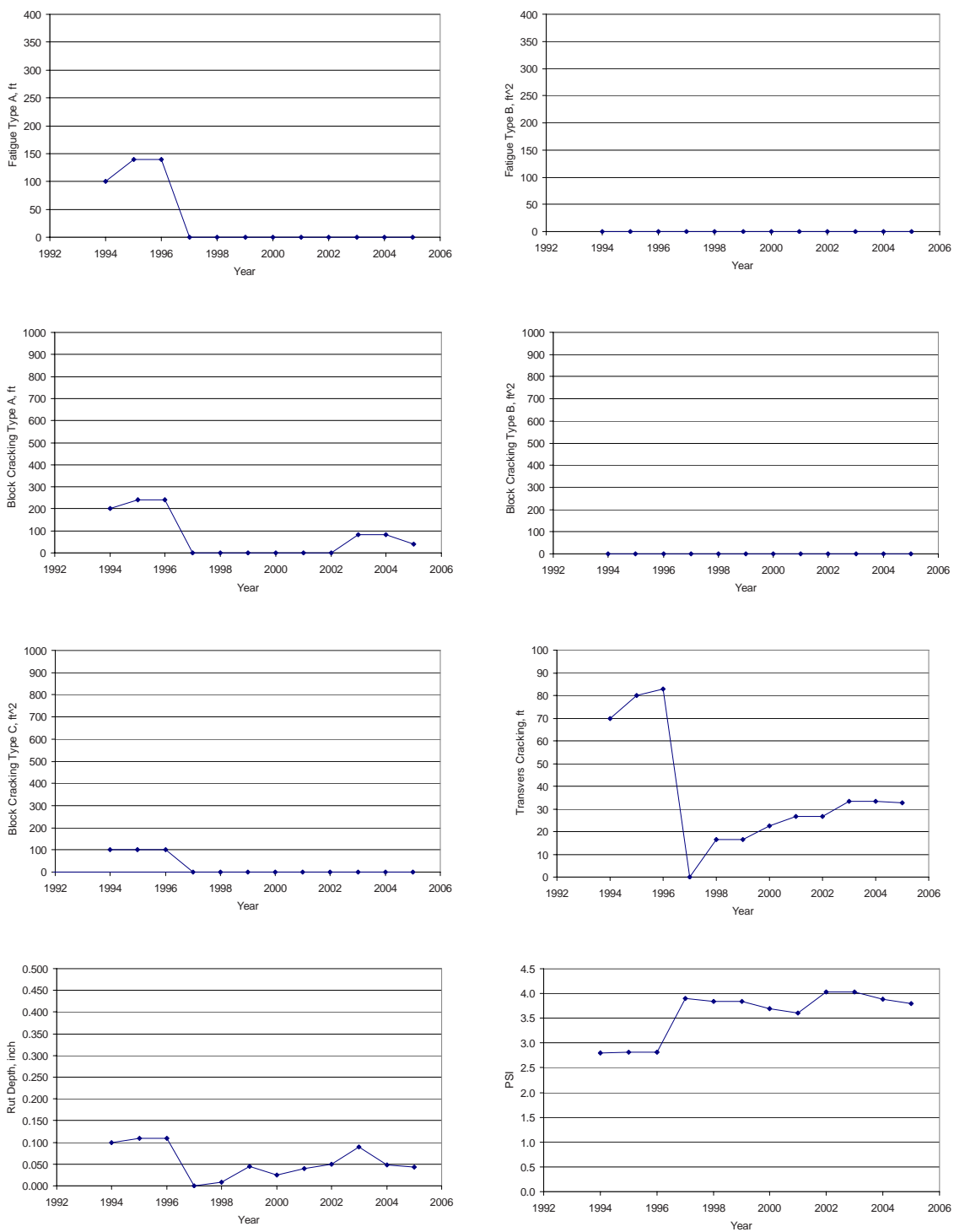


Figure 3.31: Performance data of contract 2679 on US095 from mileposts 19.96 to 32.88

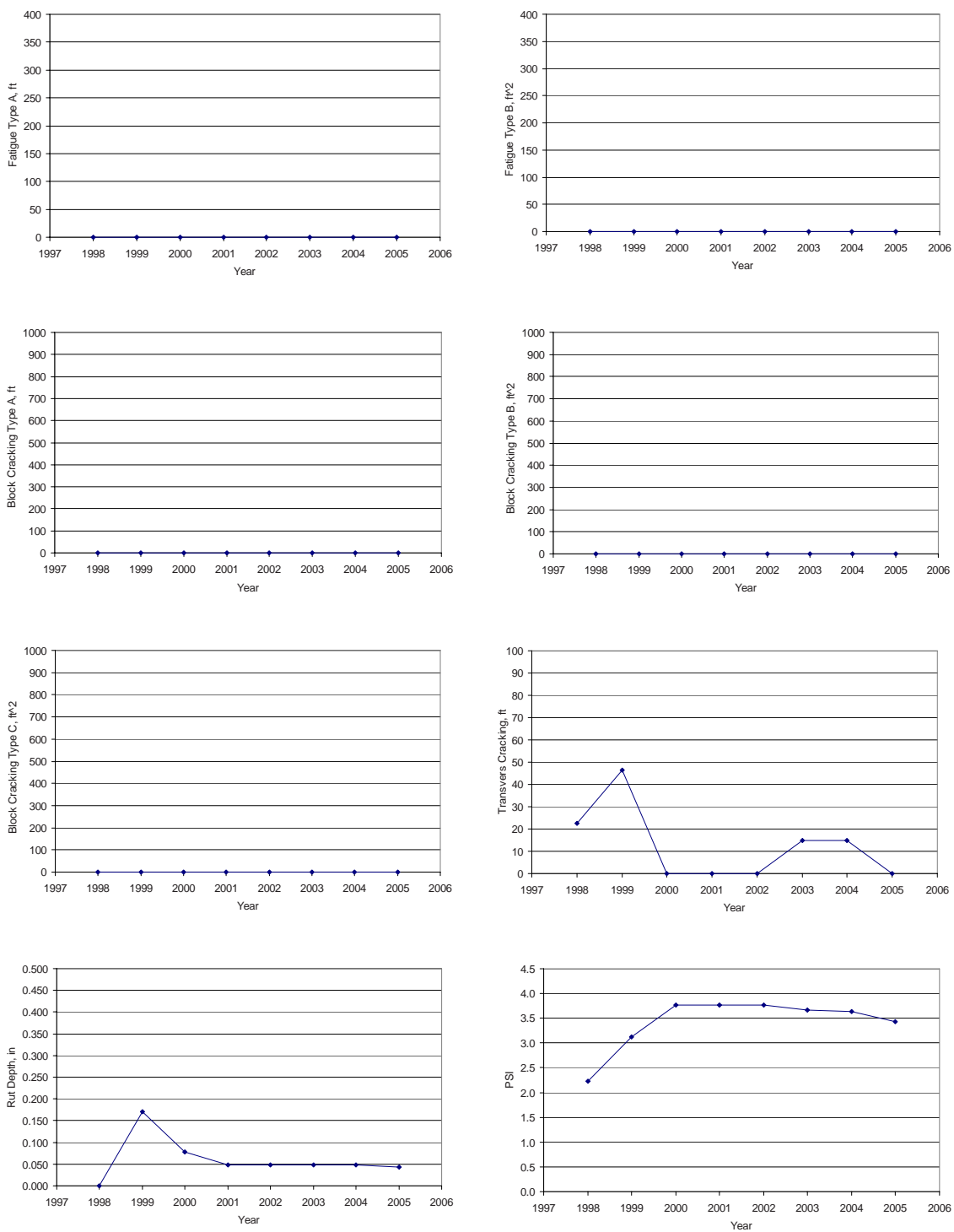


Figure 3.32: Performance data of contract 3028 on SR512 from mileposts 0 to 1.38

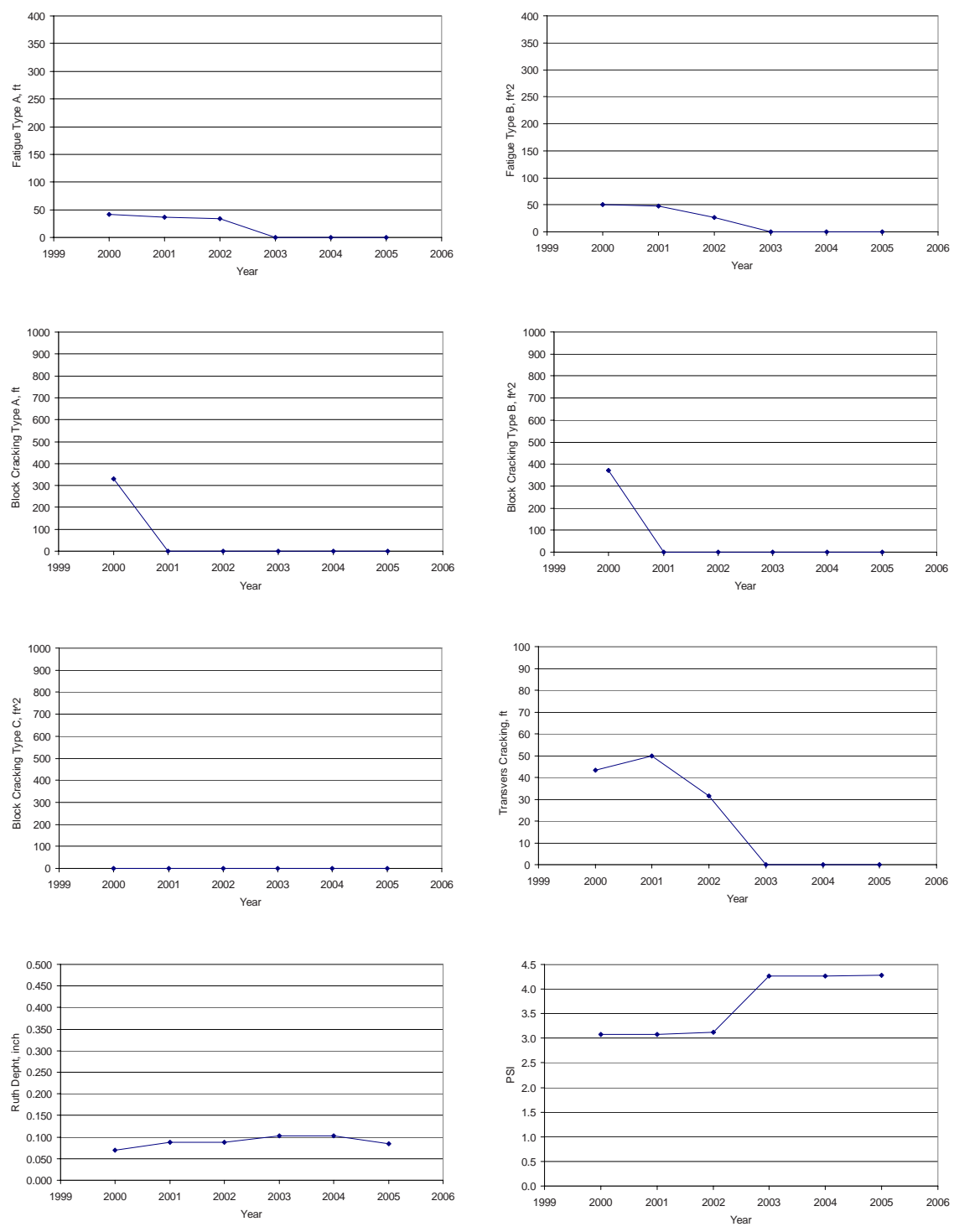


Figure 3.33: Performance data of contract 3070 on SR160 from mileposts SR 160

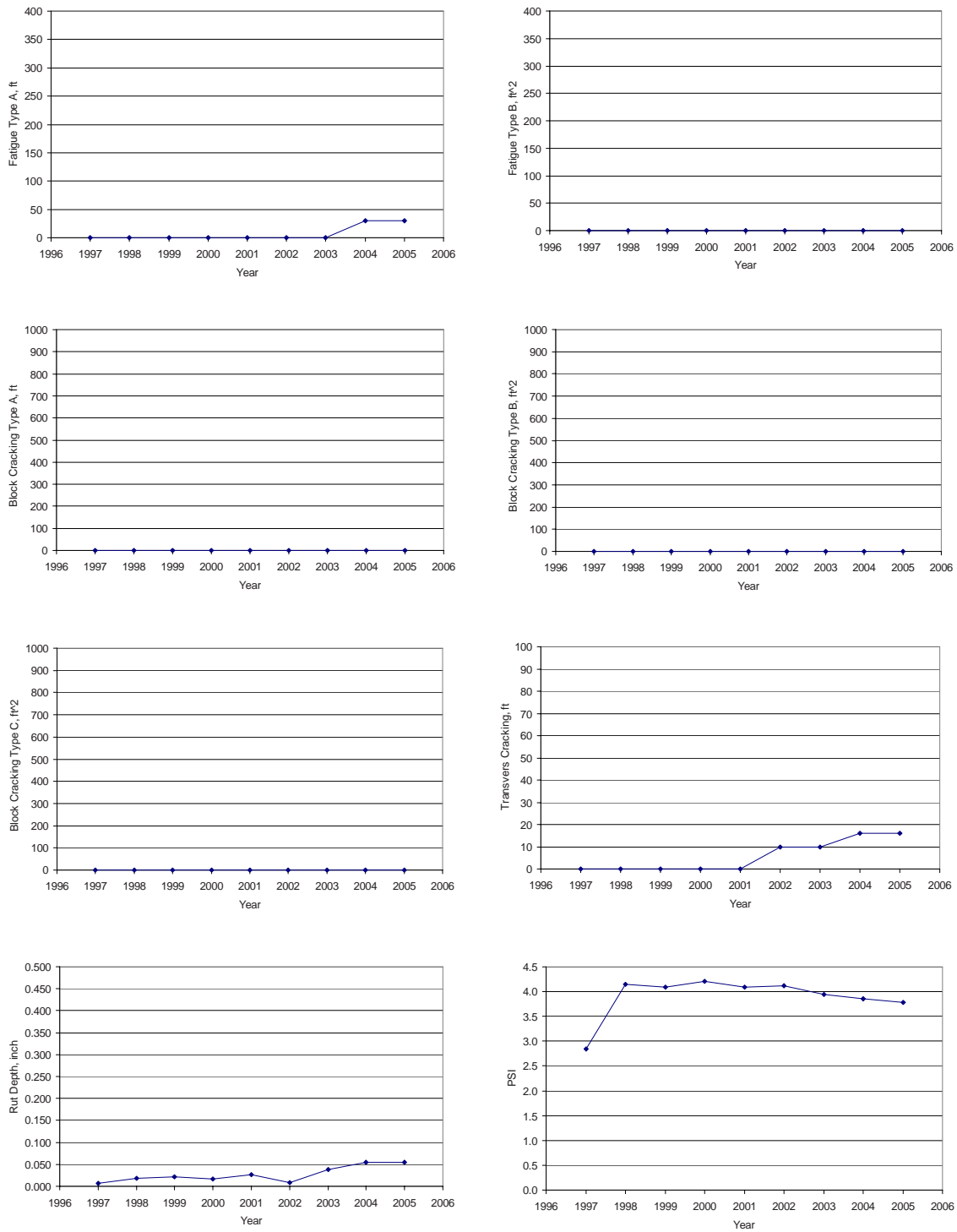


Figure 3.34: Performance data of contract 2886 on IR080 from mileposts 3.36 to 9.06

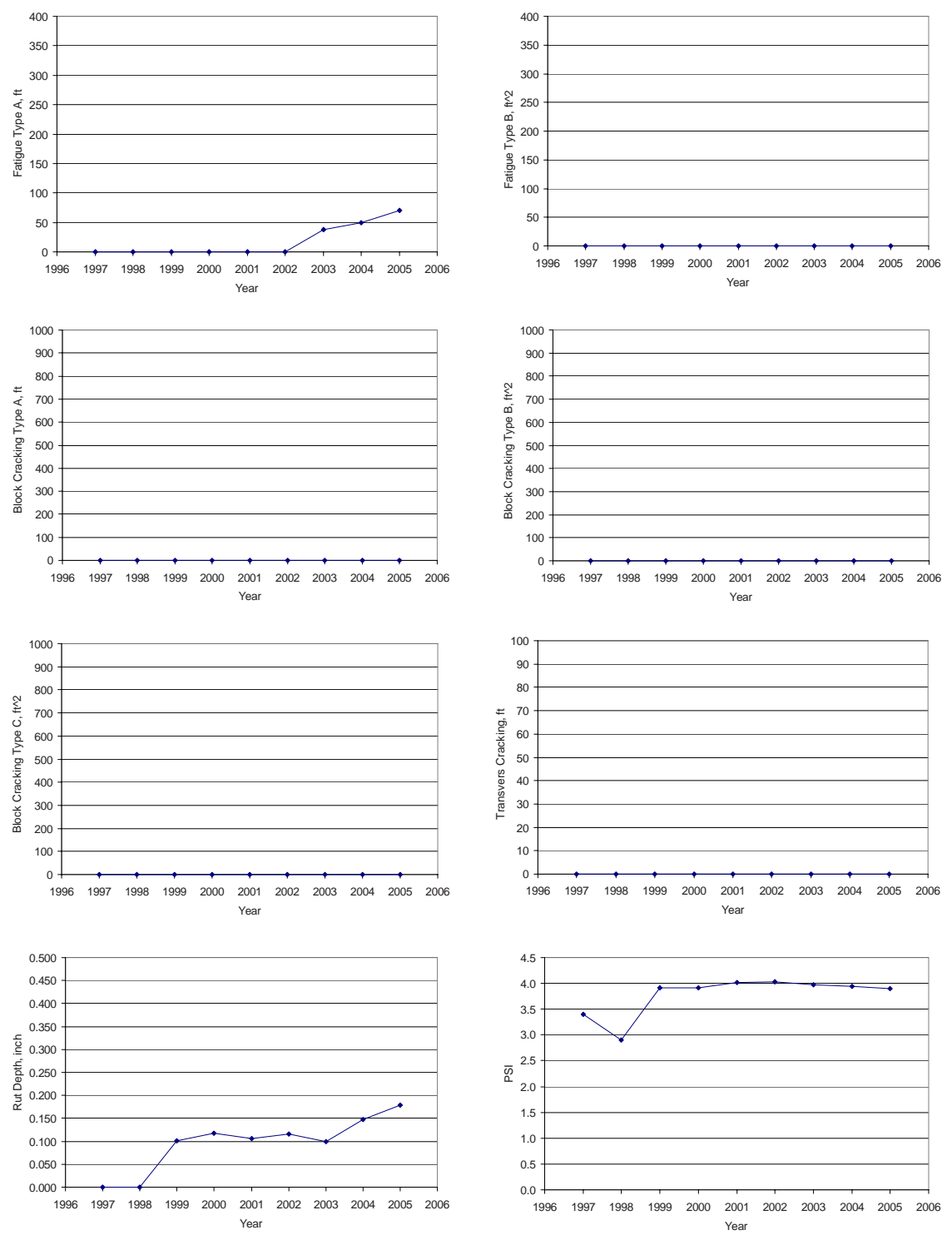


Figure 3.35: Performance data of contract 2889 on IR080 from mileposts 26.61 to 32

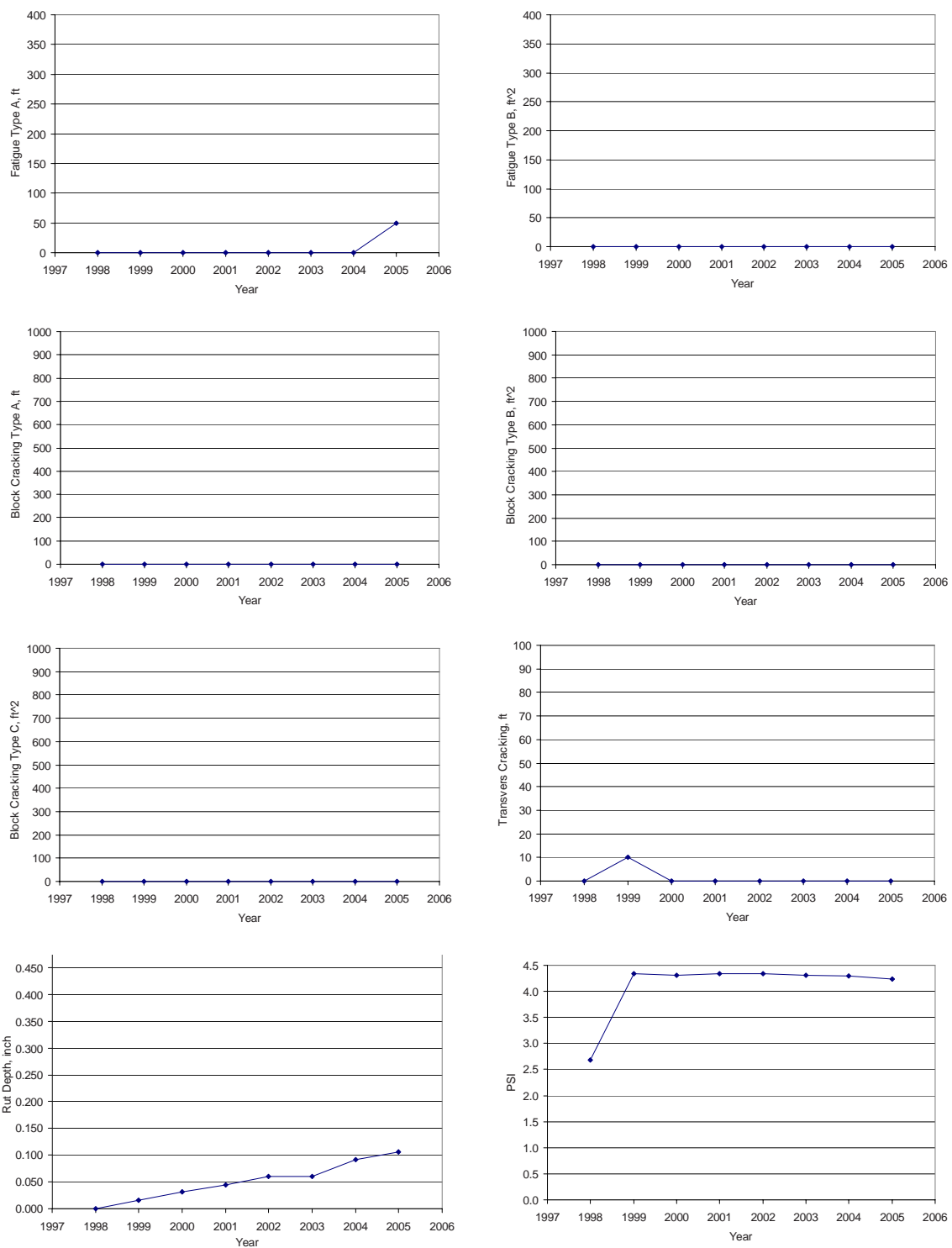


Figure 3.36: Performance data of contract 2962 on IR080 from mileposts 117.68 to 132.72

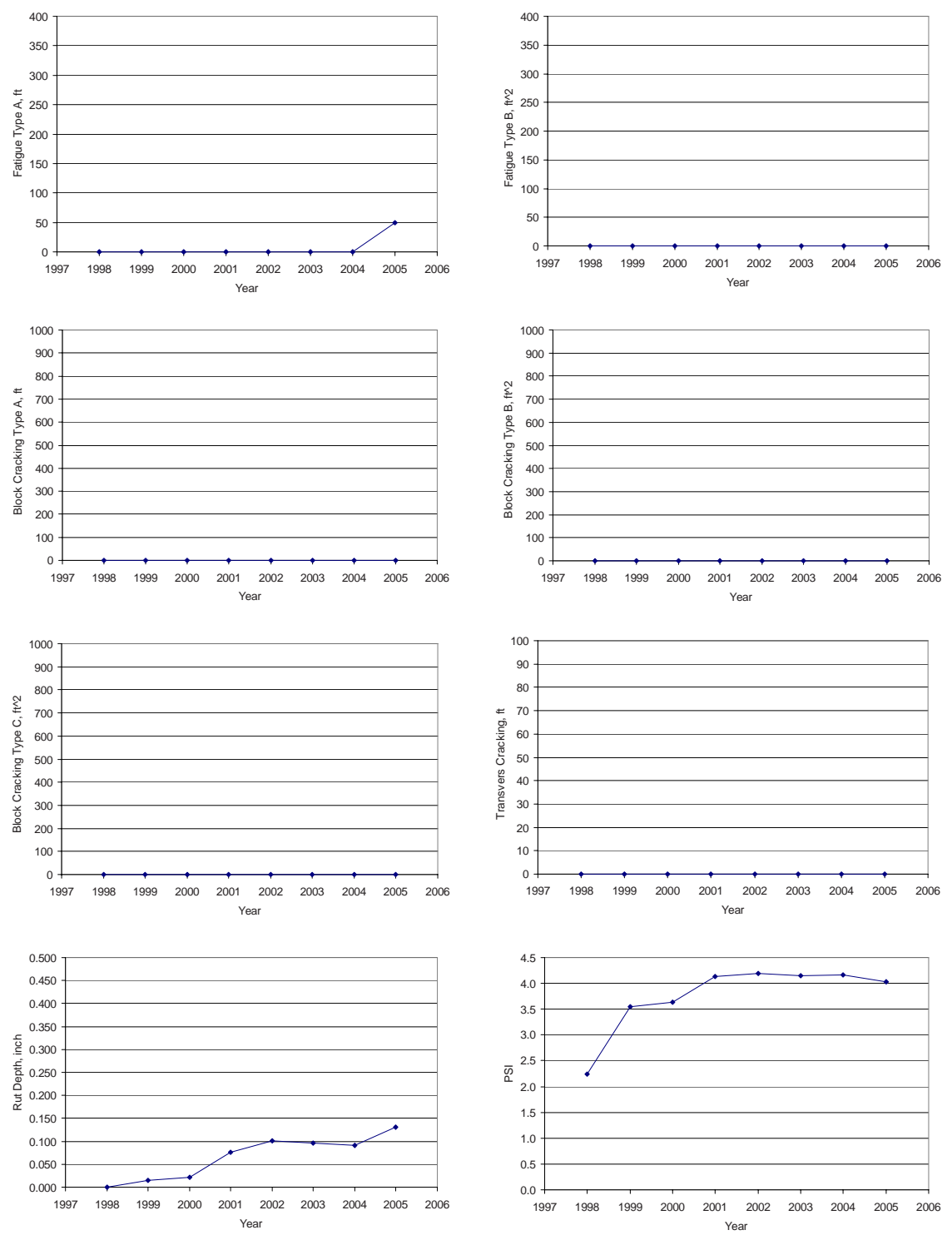


Figure 3.37: Performance data of contract 2999 on IR080 from mileposts 69.02 to 74.92

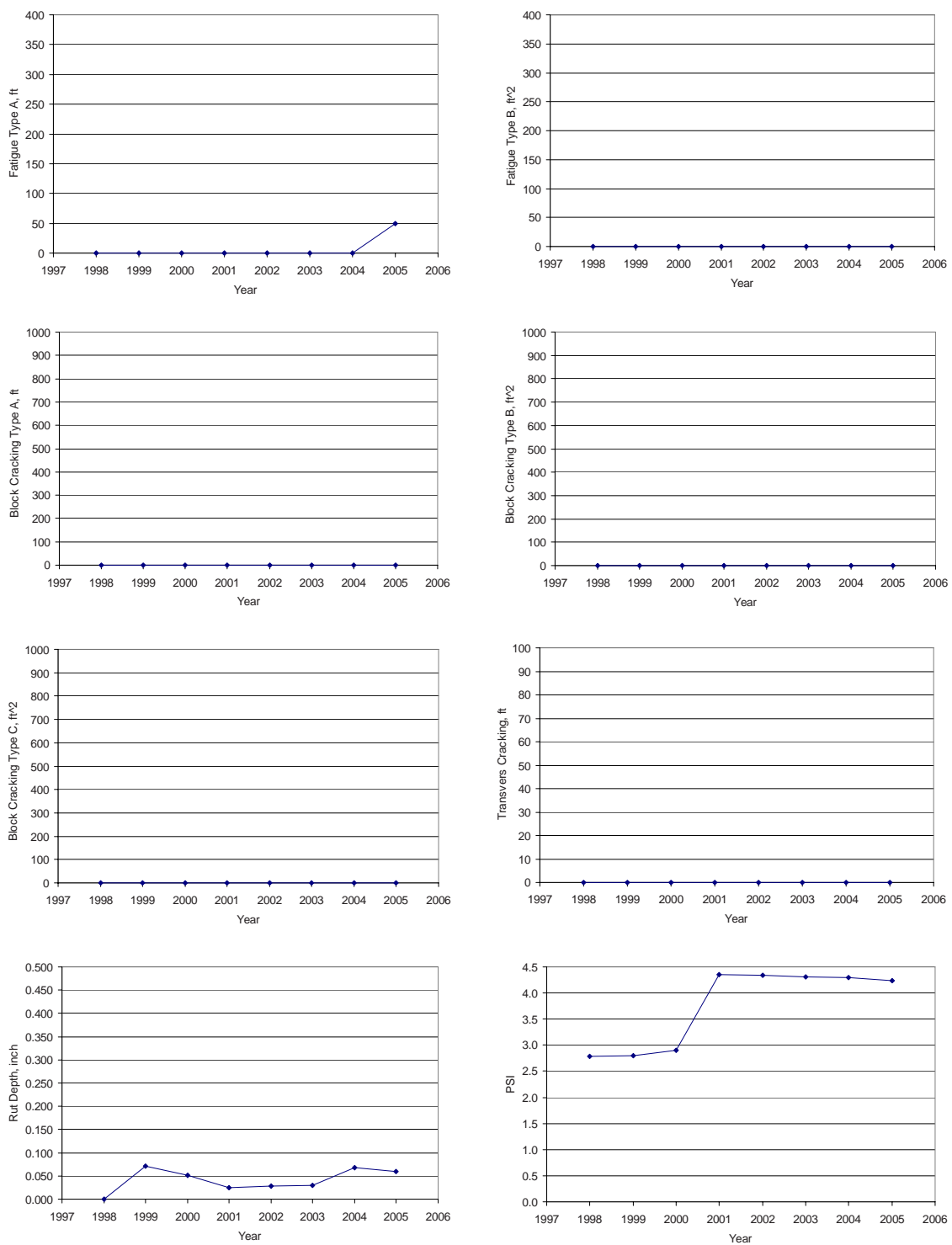


Figure 3.38: Performance data of contract 3021 on IR080 from mileposts 26.77 to 41.99

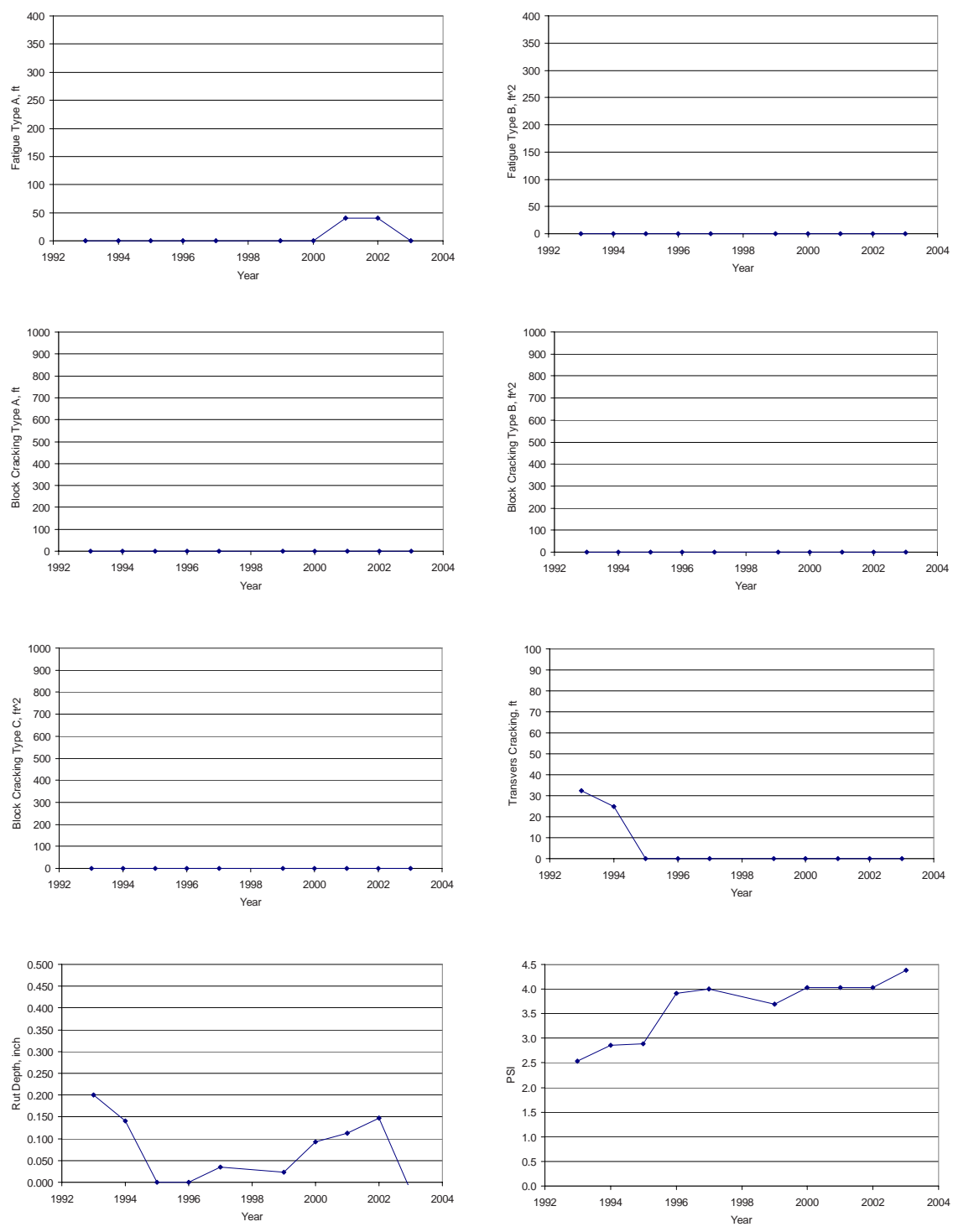


Figure 3.39: Performance data of contract 2549 on IR080 from mileposts 11.08 to 20

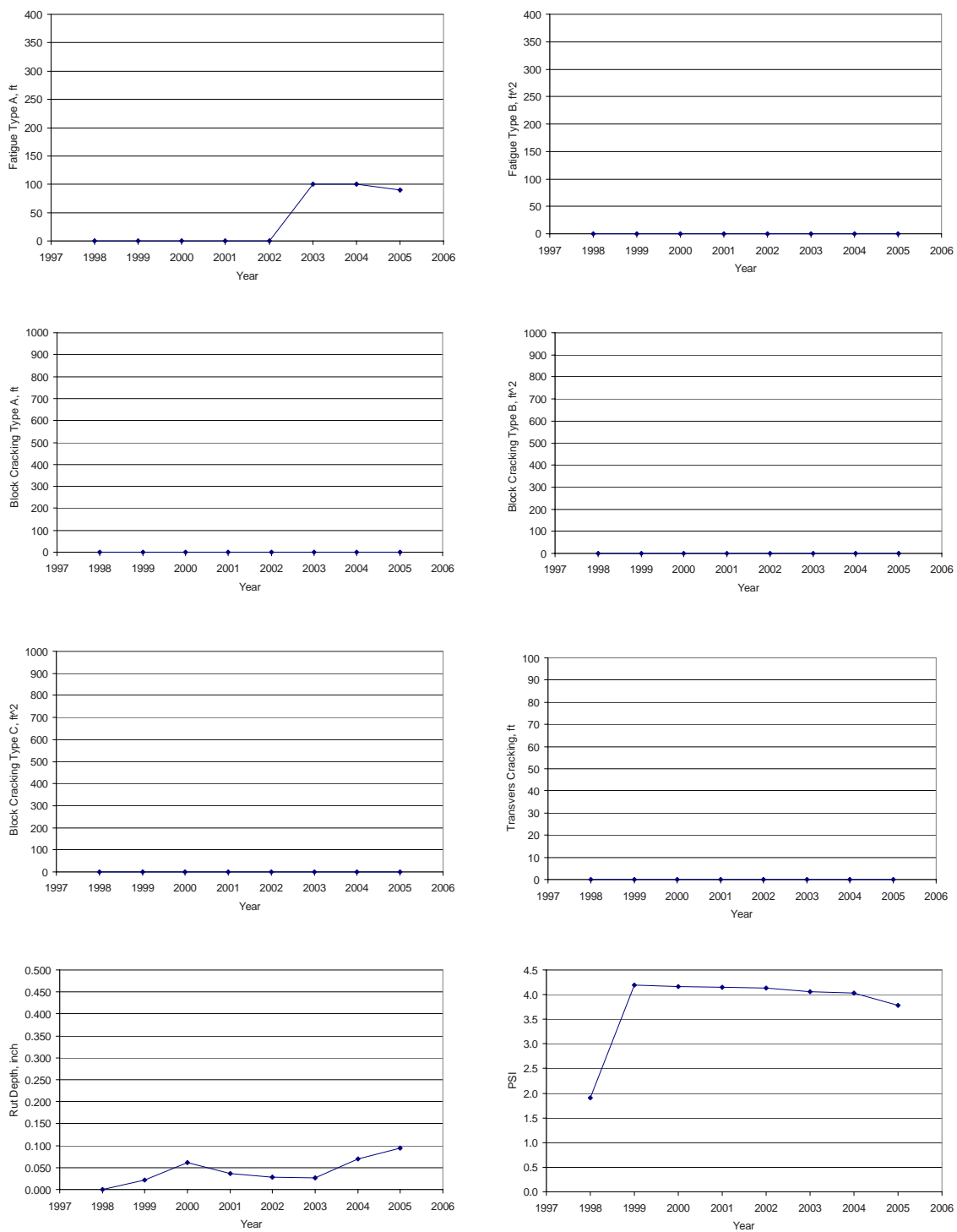


Figure 3.40: Performance data of contract 2869 on IR080 from mileposts 1.13 to 7.51

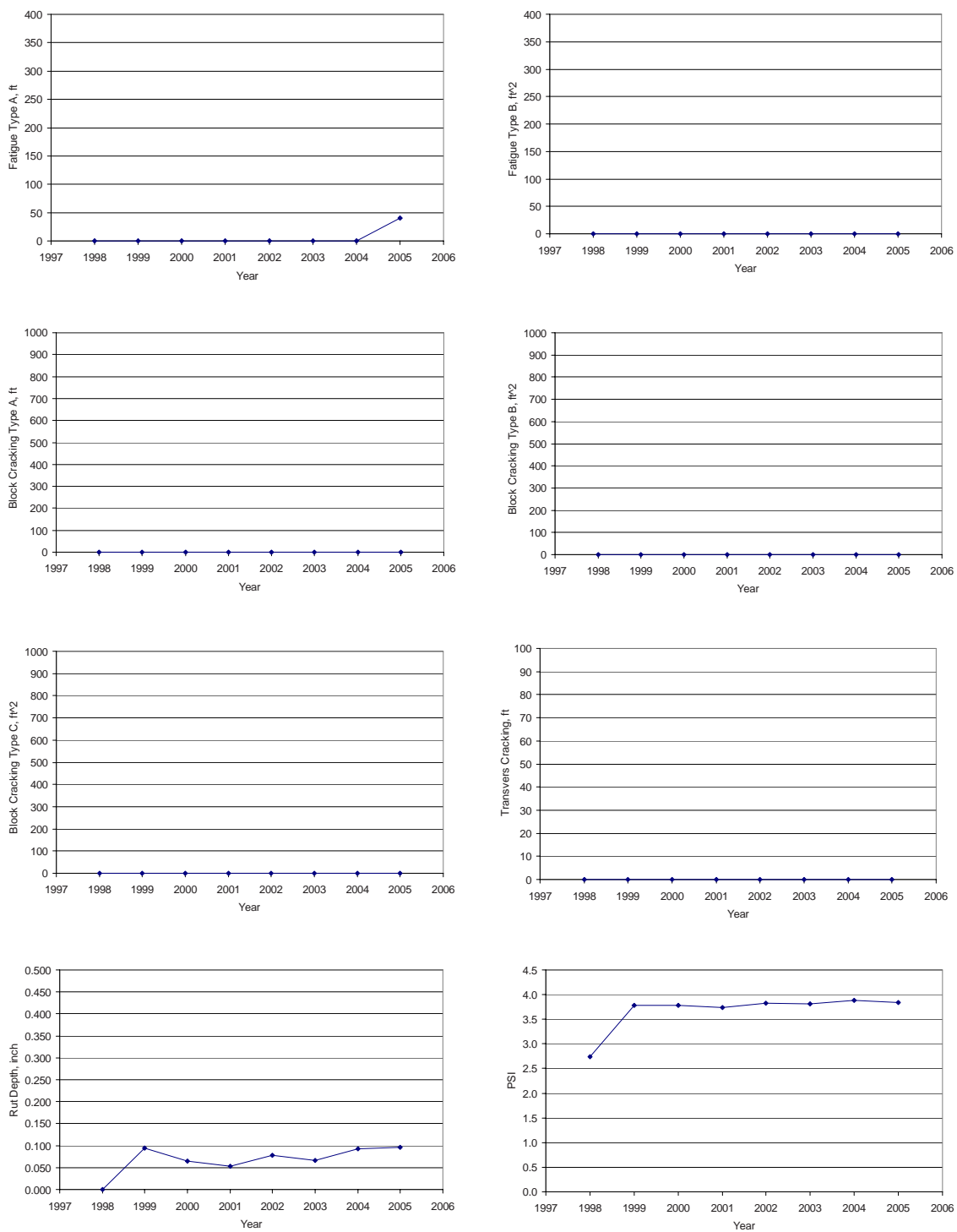


Figure 3.41: Performance data of contract 2901 on IR080 from mileposts 11.68 to 17.36

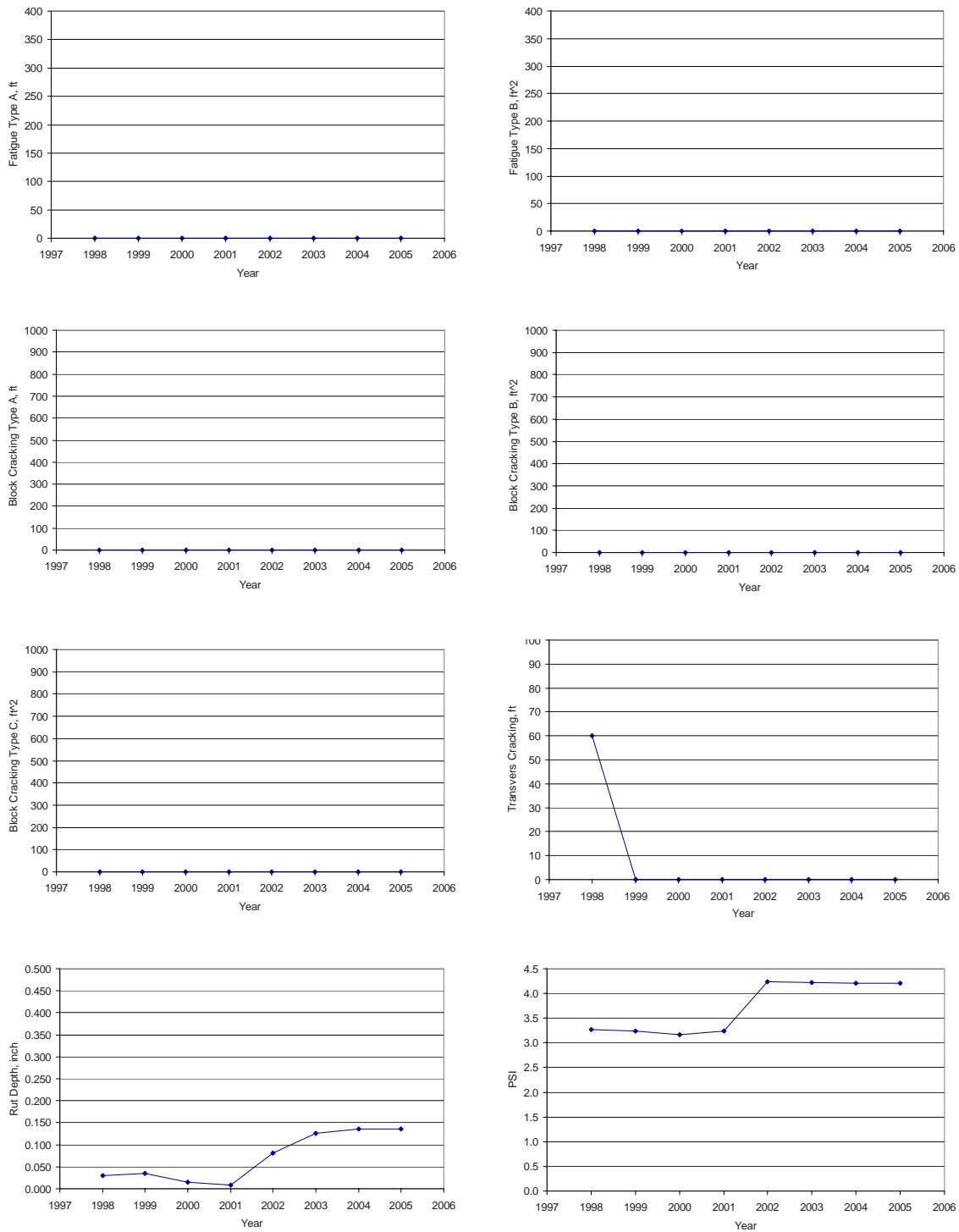


Figure 3.42: Performance data of contract 3088 on IR080 from mileposts 18.59 to 26.21

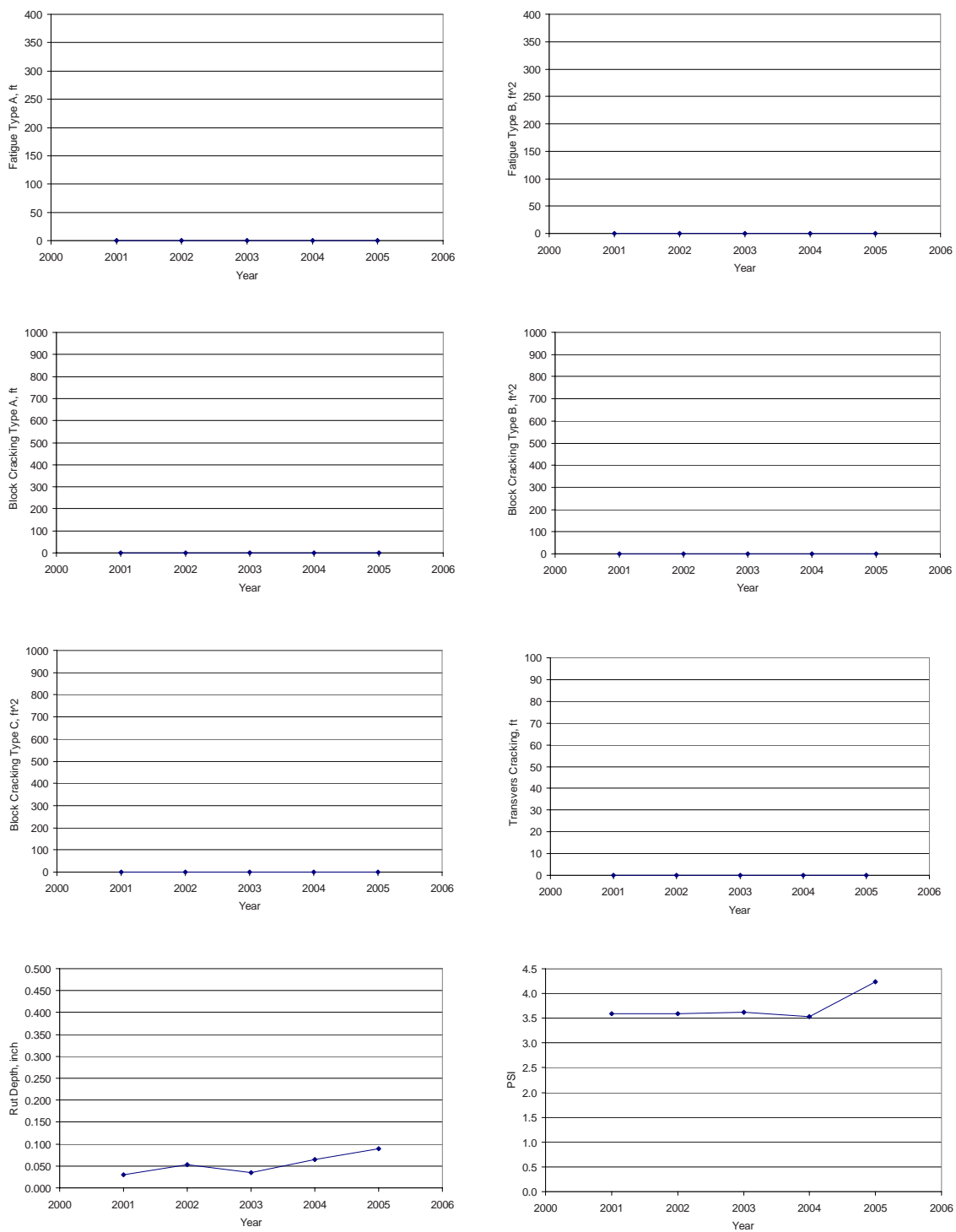


Figure 3.43: Performance data of contract 3186a on IR080 from mileposts 60.32 to 61.38

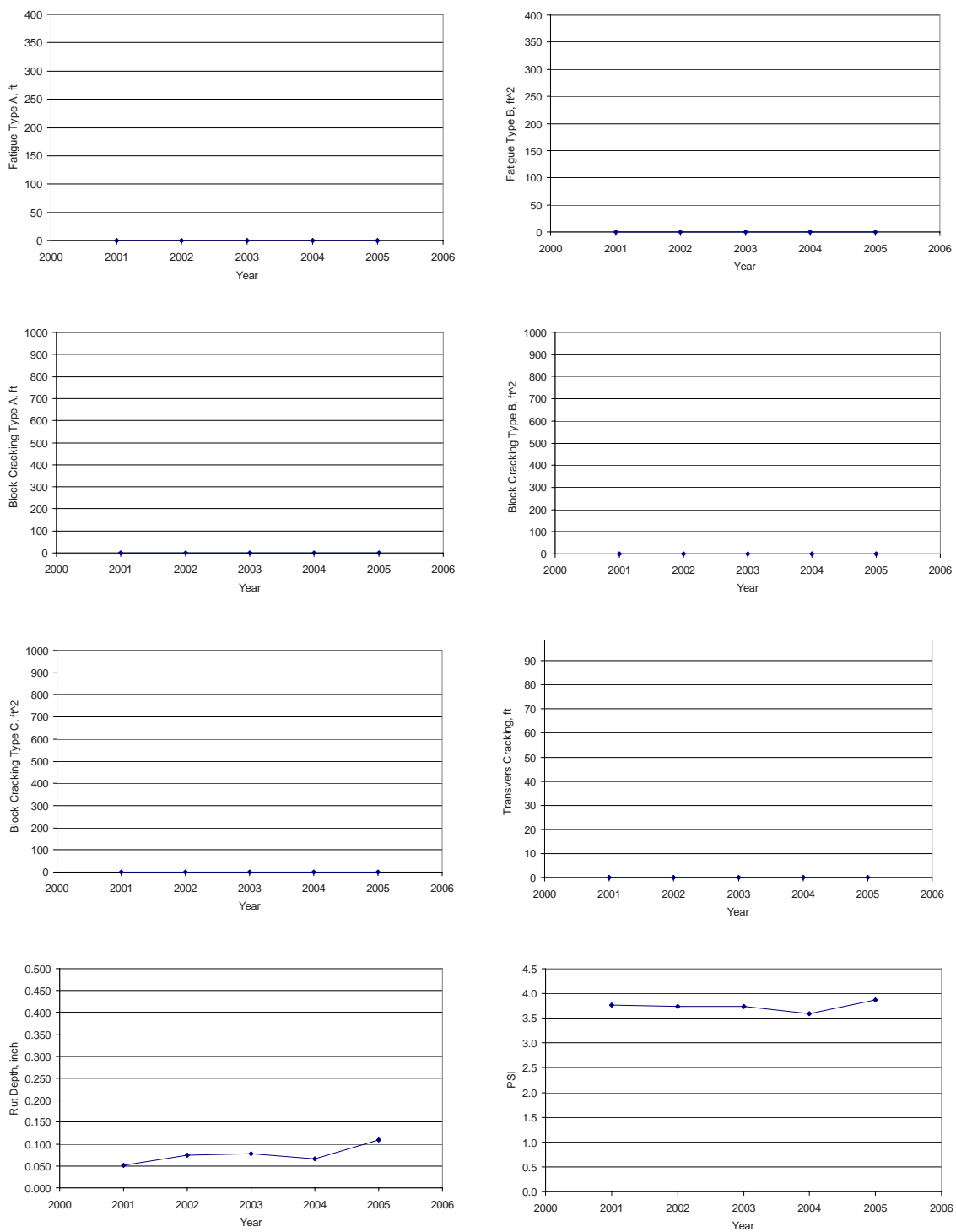


Figure 3.44: Performance data of contract 3186b on IR080 from mileposts 85.25 to 26.21

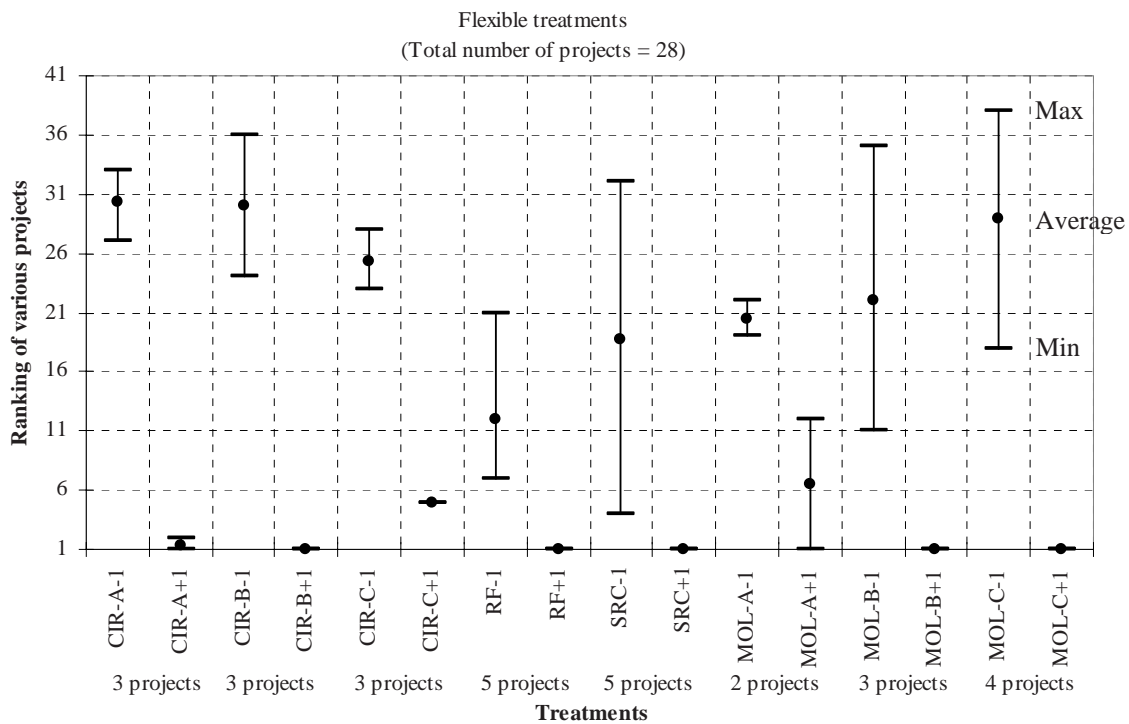


Figure 3.45: Comparison between the ranking of the various treatments at 1-year before treatment construction and 1-year after treatment construction.

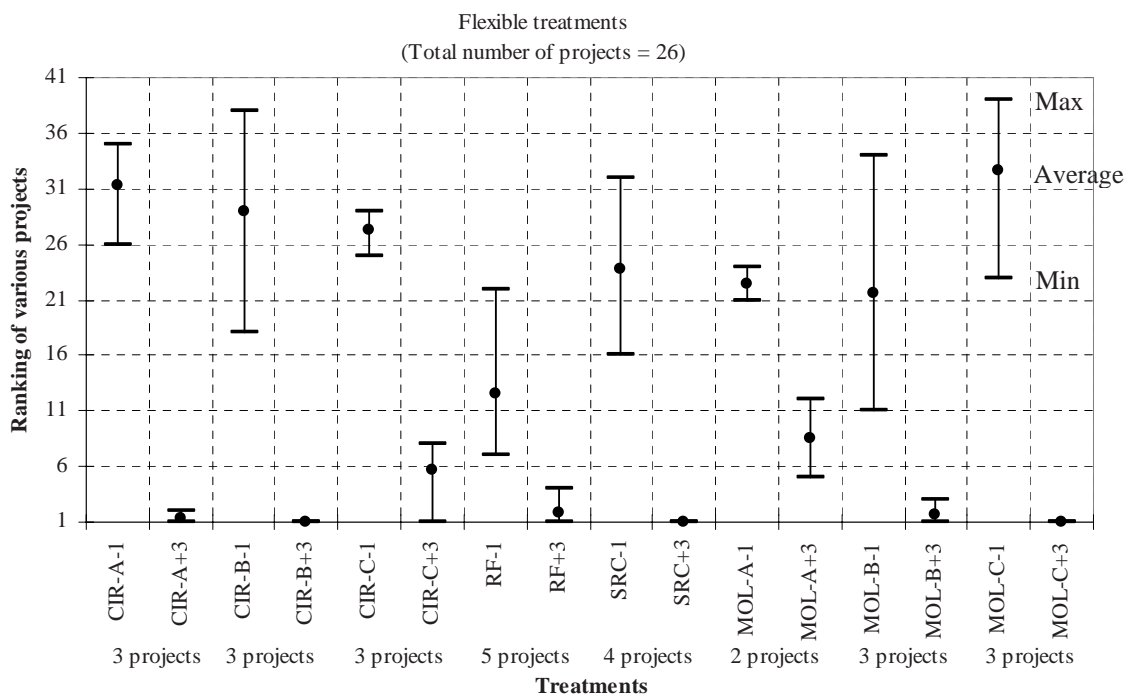


Figure 3.46: Comparison between the ranking of the various treatments at 1-year before treatment construction and 3-year after treatment construction.

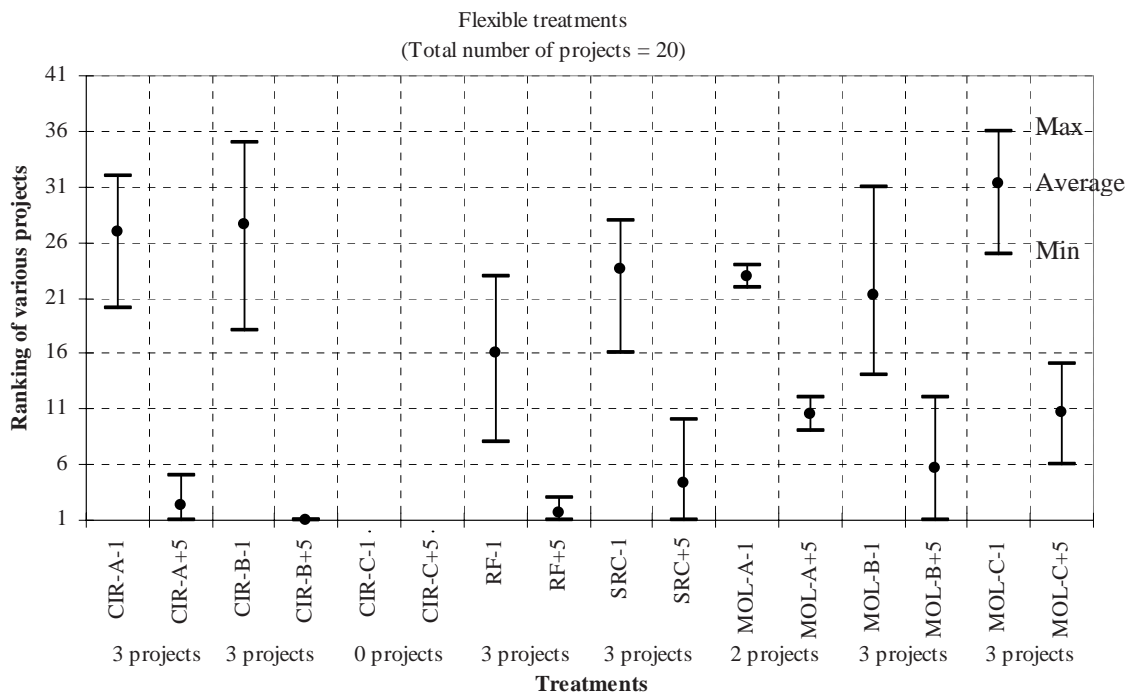


Figure 3.47: Comparison between the ranking of the various treatments at 1-year before treatment construction and 5-year after treatment construction.

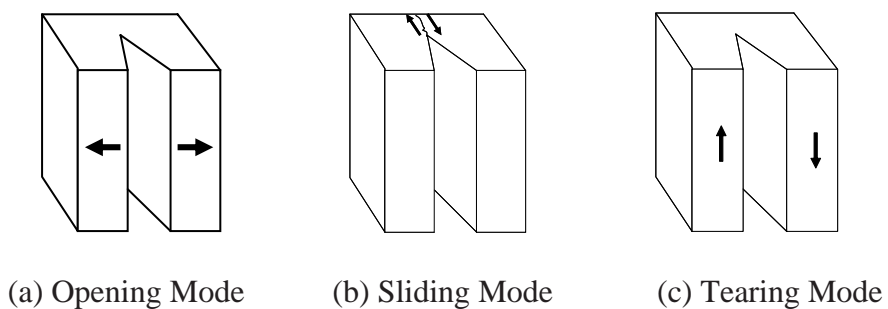


Figure 4.1 Fracture Modes

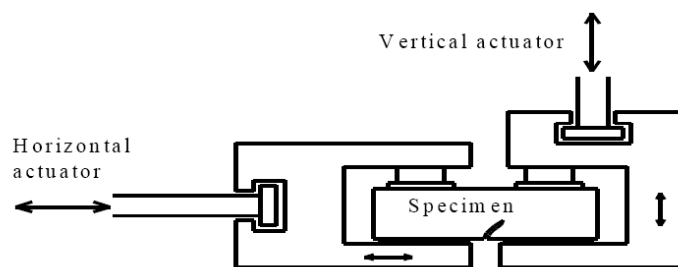


Figure 4.2 Schematic representation of reflective cracking device (RCD)



(a)



(b)

Figure 4.3 (a) Bottom platens of the reflective cracking device
 (b) Reflective cracking device with both (top and bottom) plates

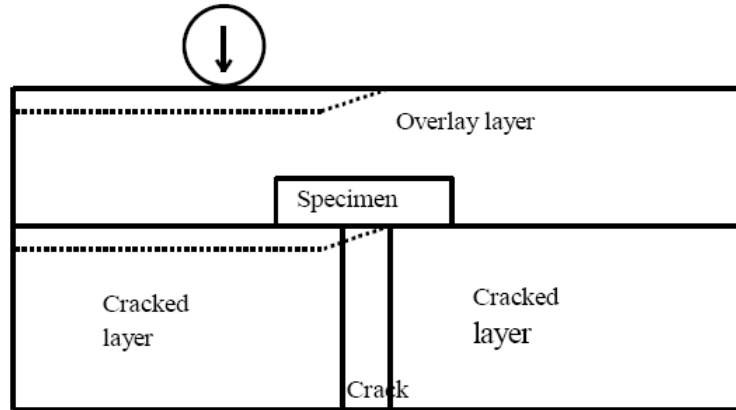


Figure 4.4 Representation of the overlay zone subjected to the reflective cracking

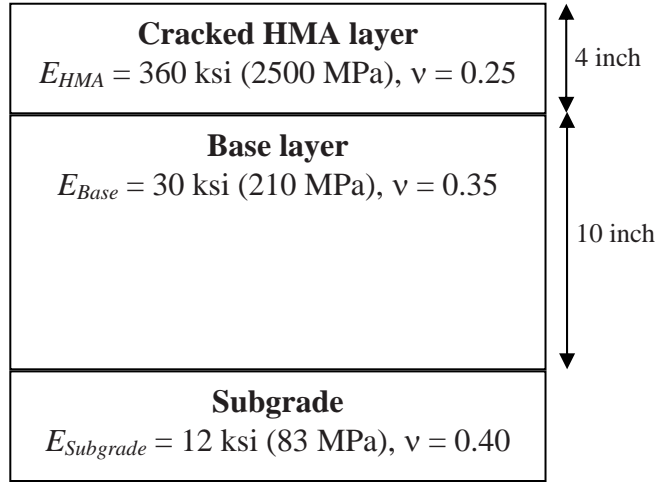


Figure 4.6 Existing HMA pavement structure

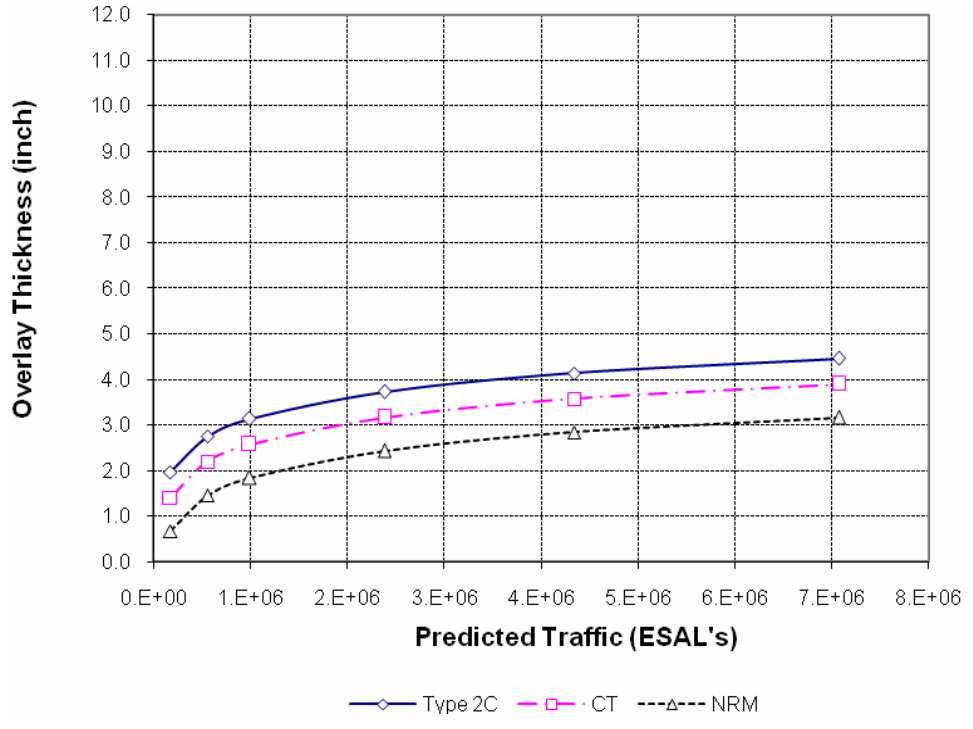


Figure 4.7 Required overlay thickness according to the Virginia tech method

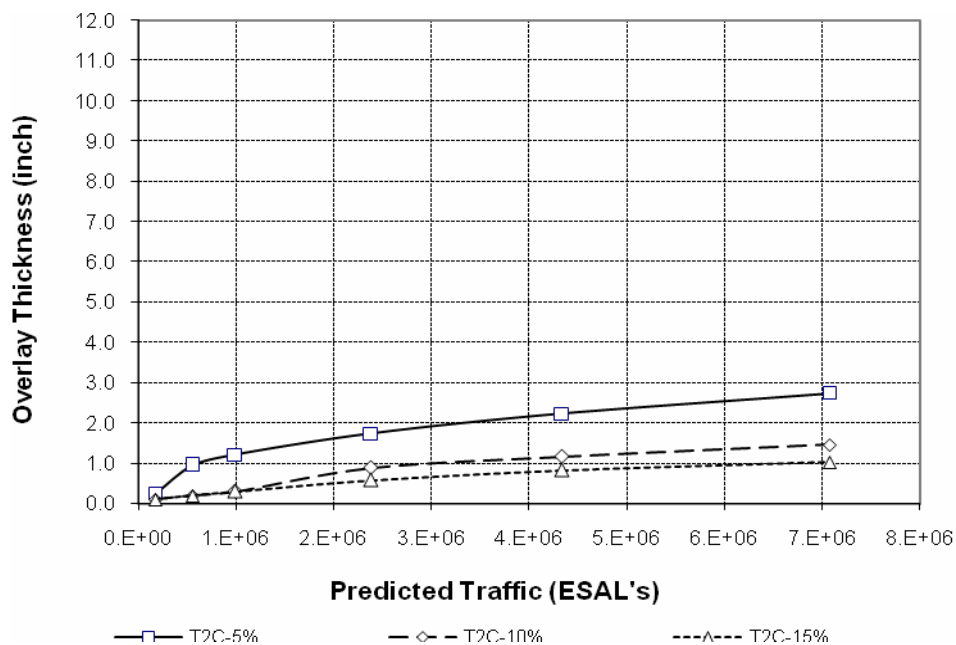


Figure 4.8 T2C required overlay thickness according to the asphalt rubber method

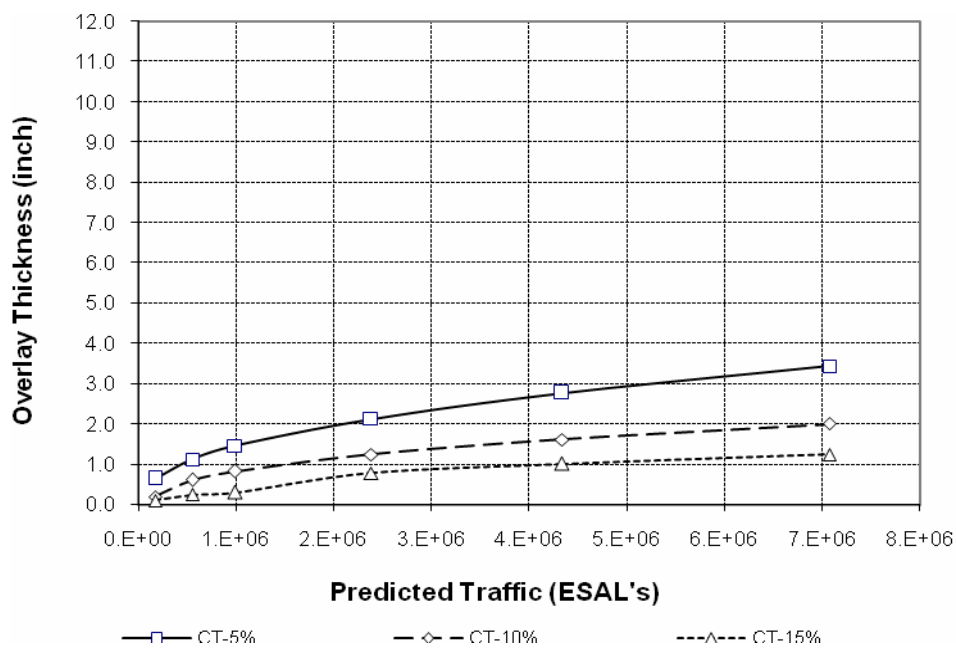


Figure 4.9 CT required overlay thickness according to the asphalt rubber method

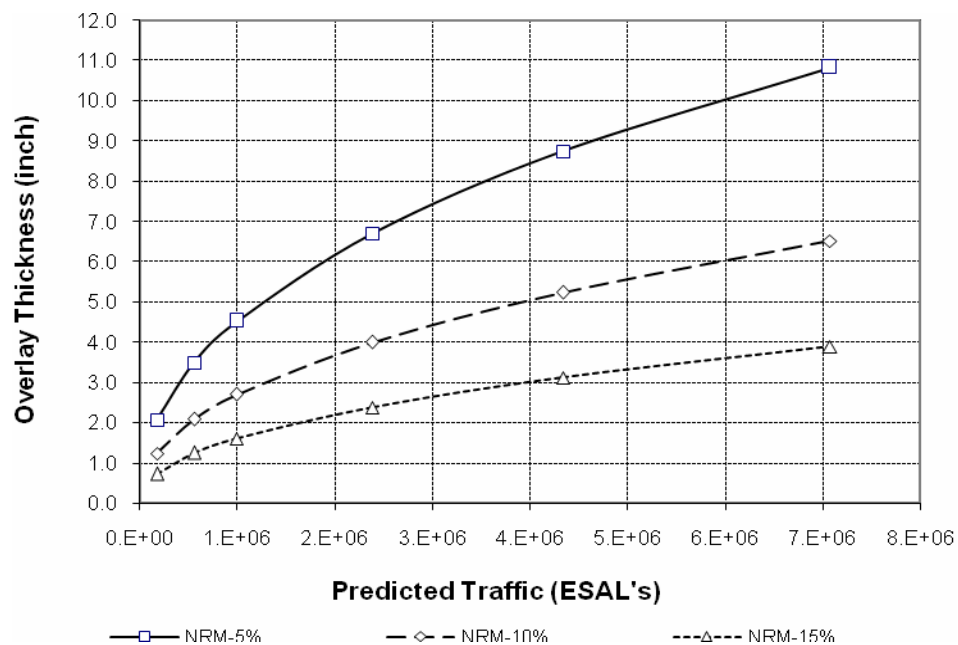


Figure 4.10 NRM required overlay thickness according to the asphalt rubber method

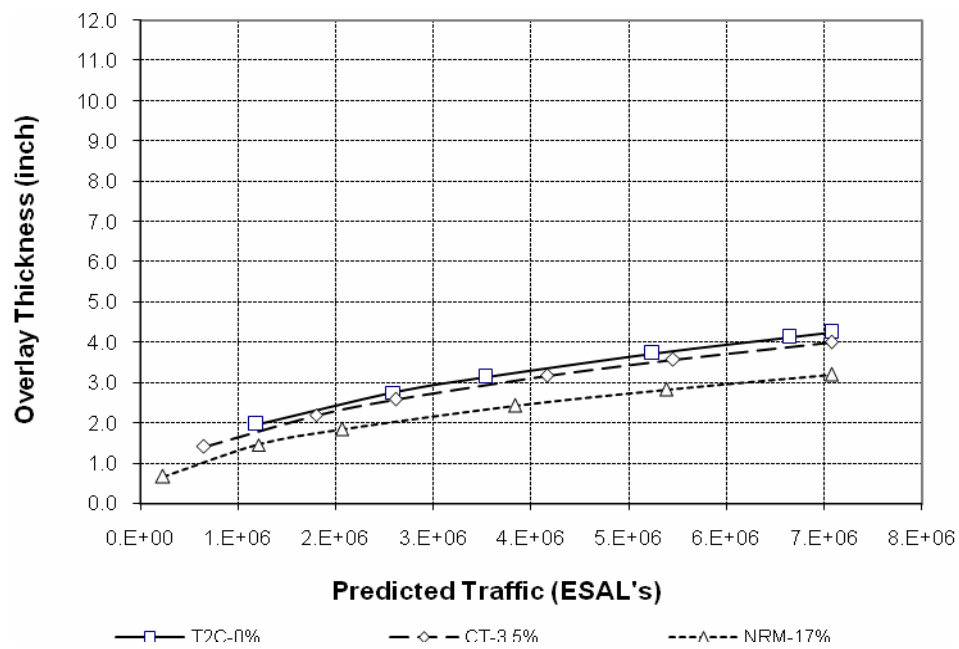


Figure 4.11 Overlay thickness according to the asphalt rubber method for selected percent cracking

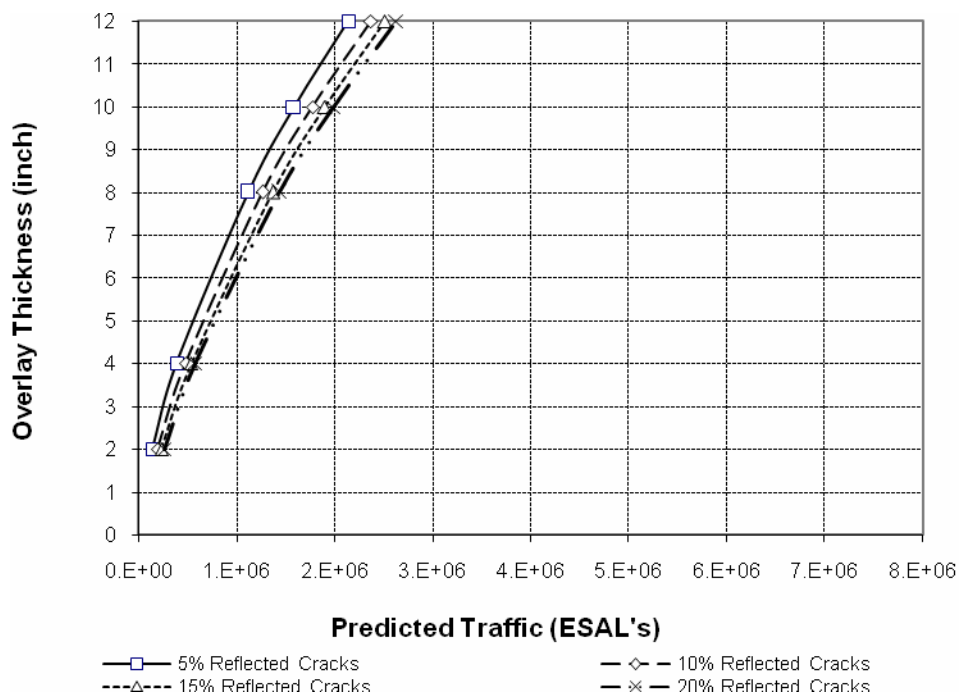


Figure 4.12 Required overlay thickness according to the new AASHTO method

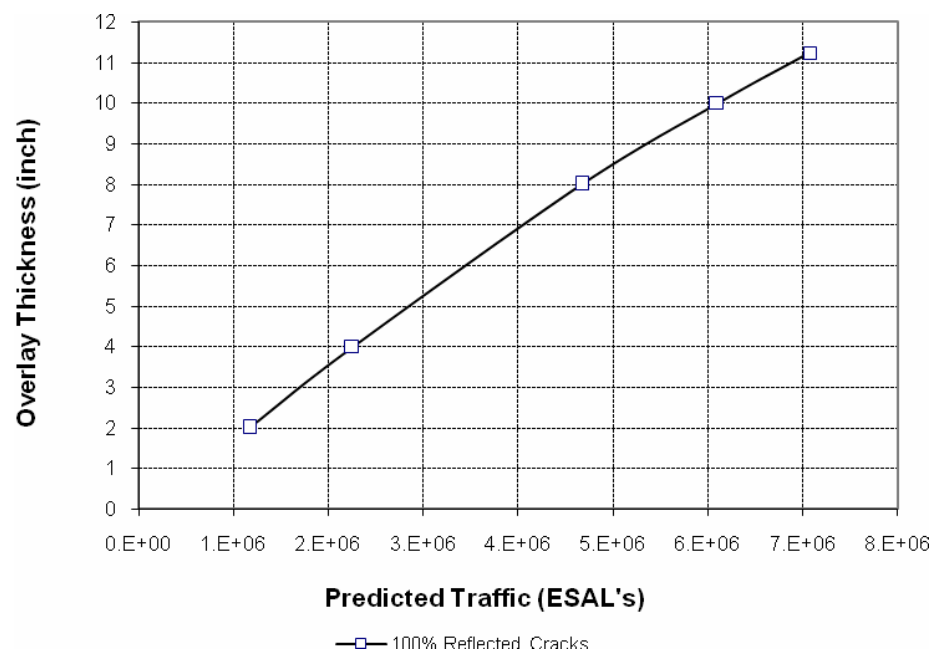


Figure 4.13 Required overlay thickness according to the new AASHTO method for 100% reflected cracks

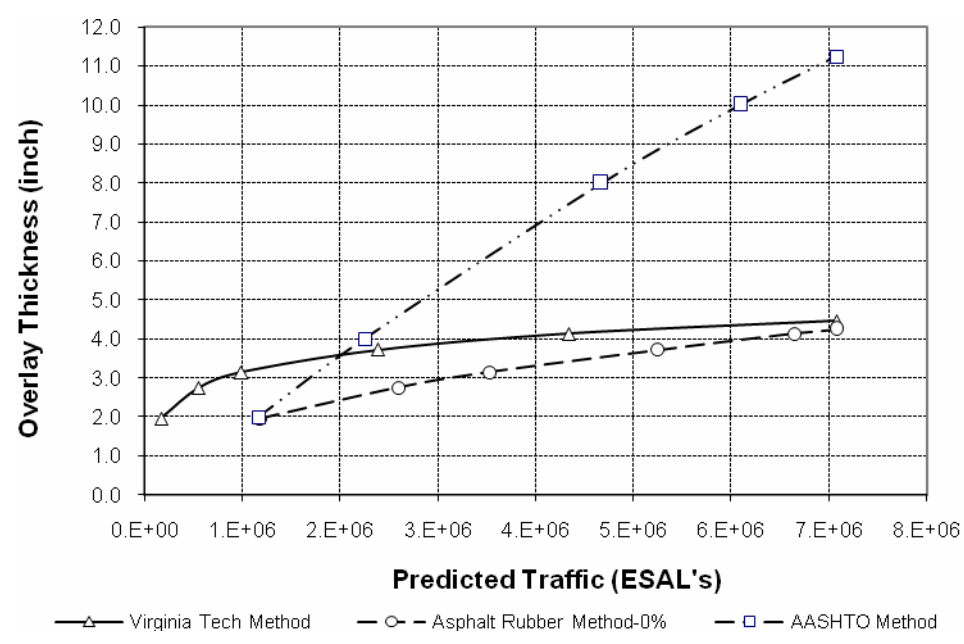


Figure 4.14 Required T2C overlay thickness using various analysis models

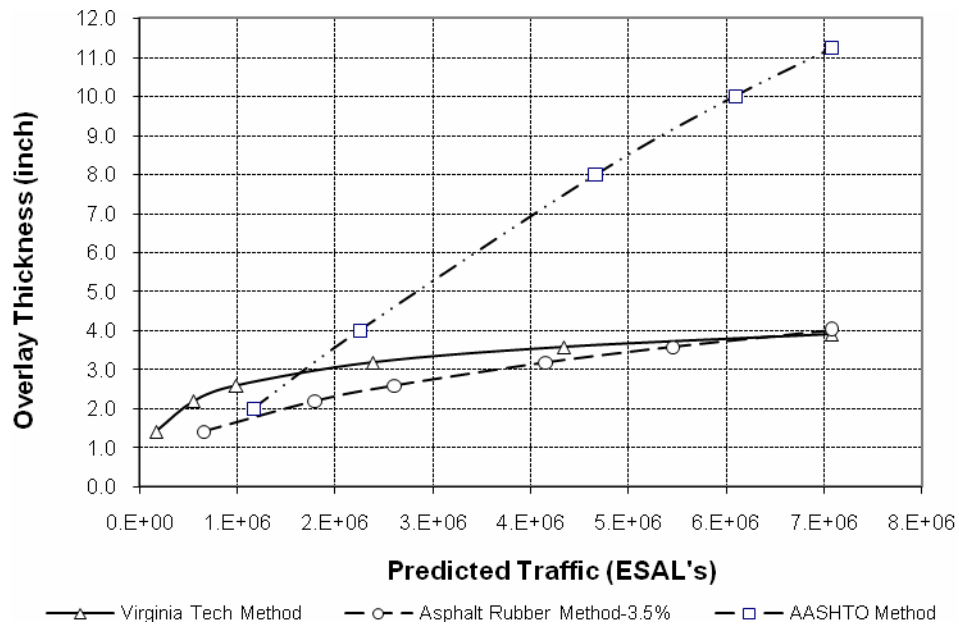


Figure 4.15 Required CT overlay thickness using various analysis models

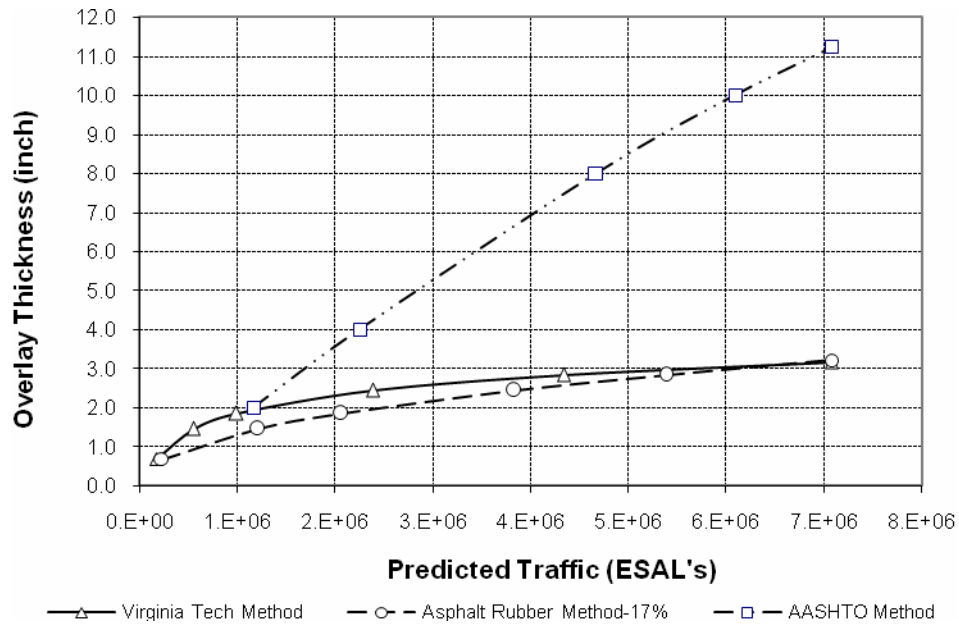


Figure 4.16 Required NRM overlay thickness using various analysis models

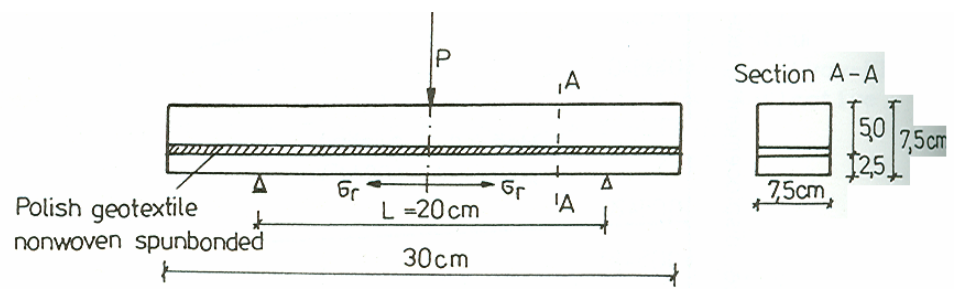


Figure 5.1 Bending test under static load – Cracow University of Technology

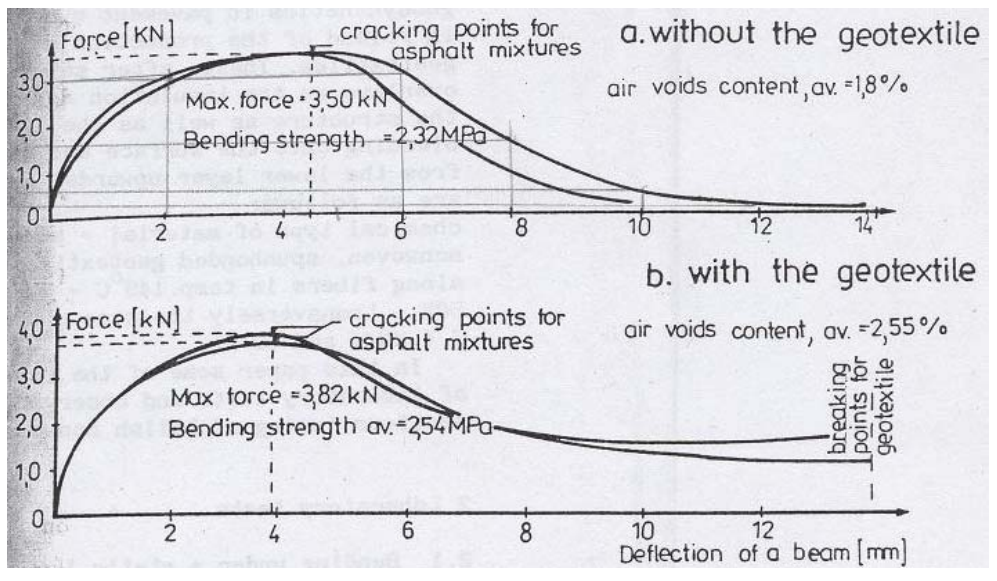


Figure 5.2 Results of the bending test under static load for HMA beams with and without geotextile at 20°C

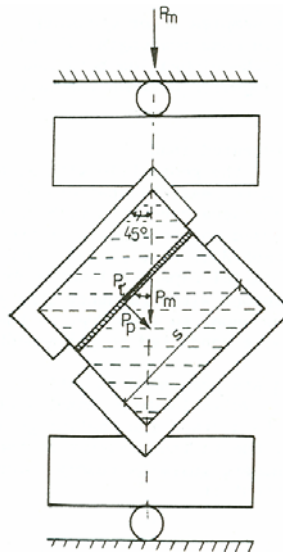


Figure 5.3 Shearing test – Cracow University of Technology

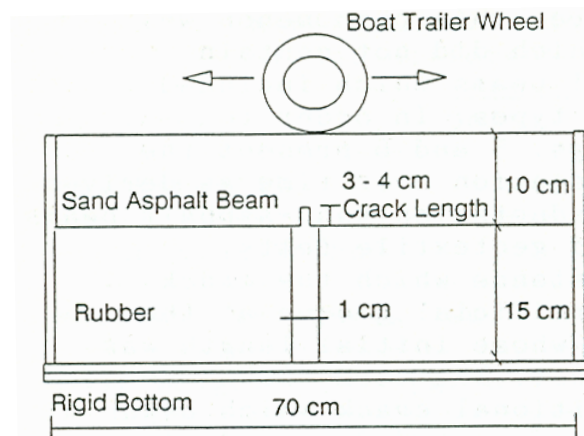


Figure 5.4 The laboratory wheel-tracking device

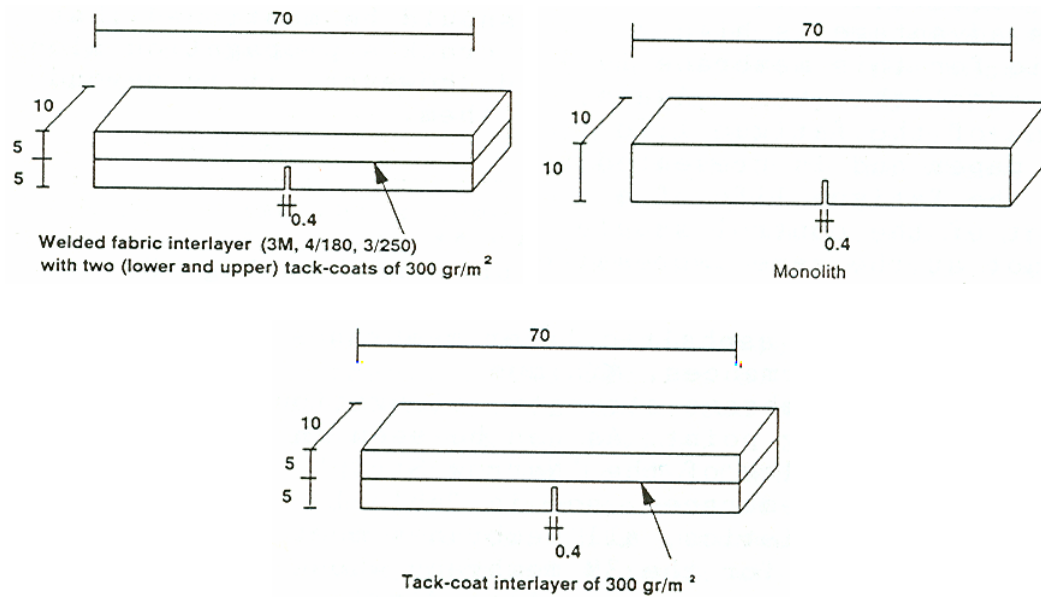


Figure 5.5 Beam specimens for the laboratory wheel-tracking device

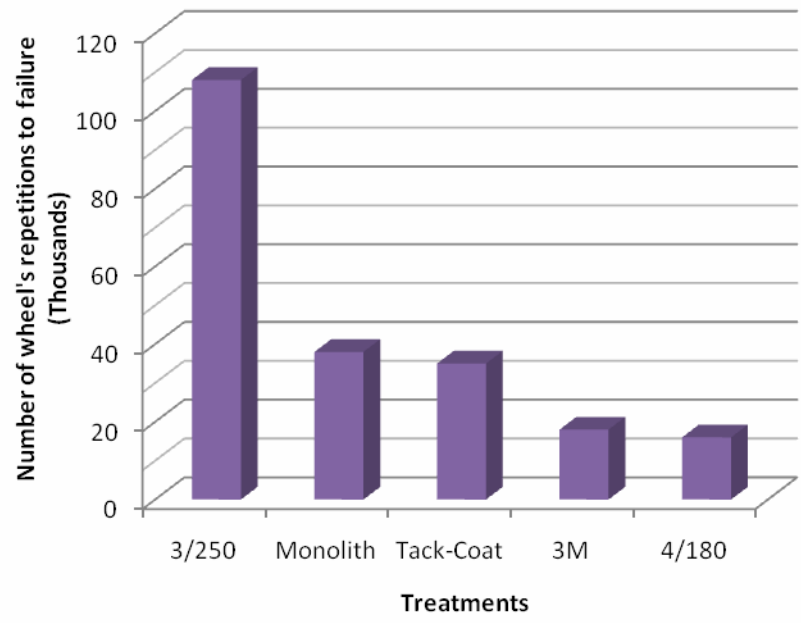


Figure 5.6 Summary of test results under the laboratory wheel-tracking device

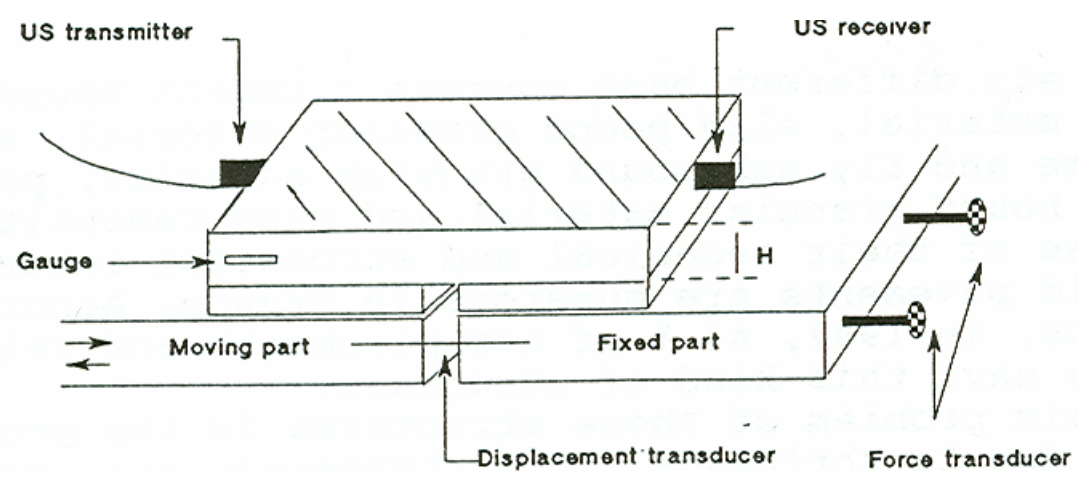


Figure 5.7 Fissurometer apparatus description

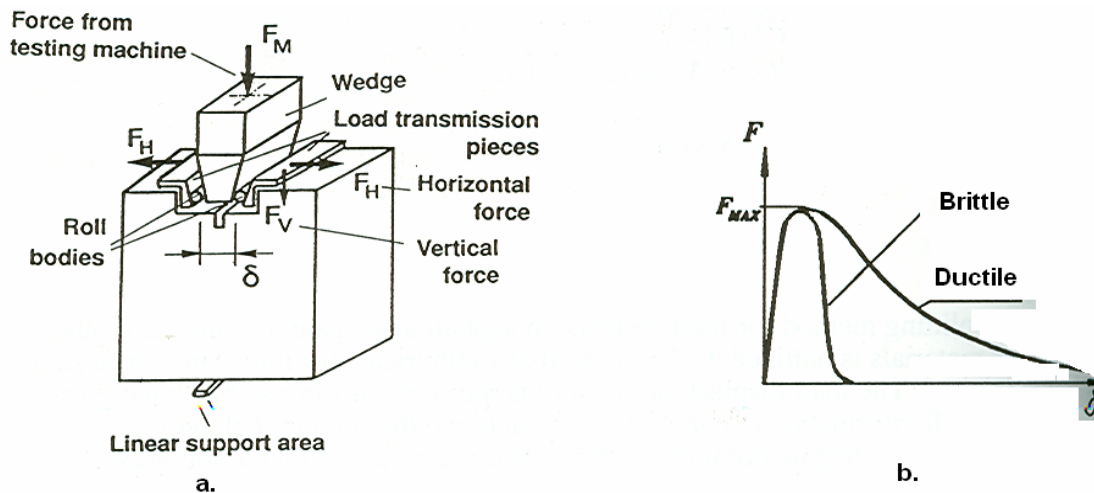


Figure 5.7 a. Principal of testing method (Tschegg 1986)
 b. Schematic load-deformation curve

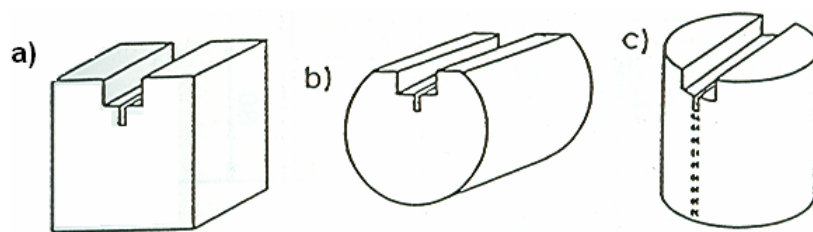


Figure 5.8 Specimen shapes for the wedge splitting test method (Tschegg 1986)

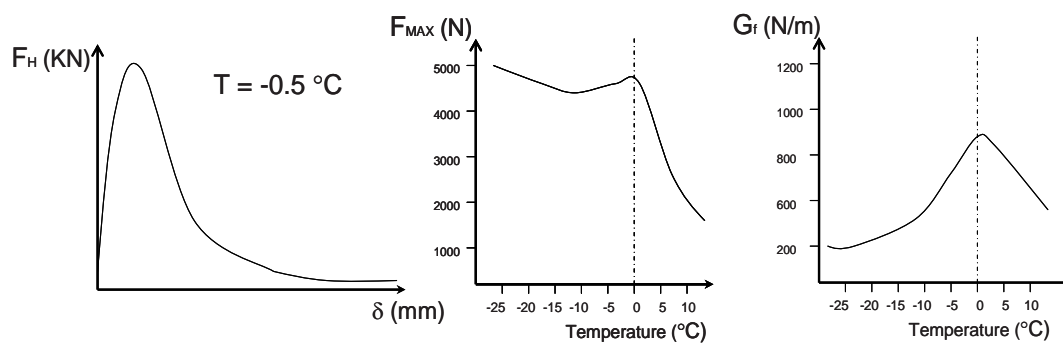


Figure 5.9 Typical results from the wedge splitting test method

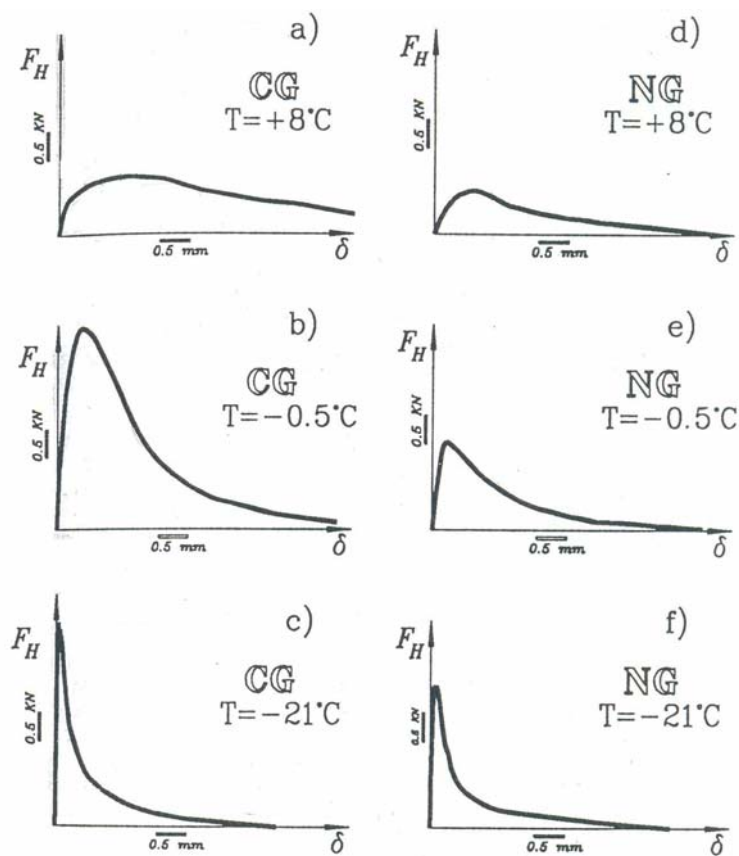


Figure 5.10 Load-displacement curves for gravel and crushed HMA mixtures

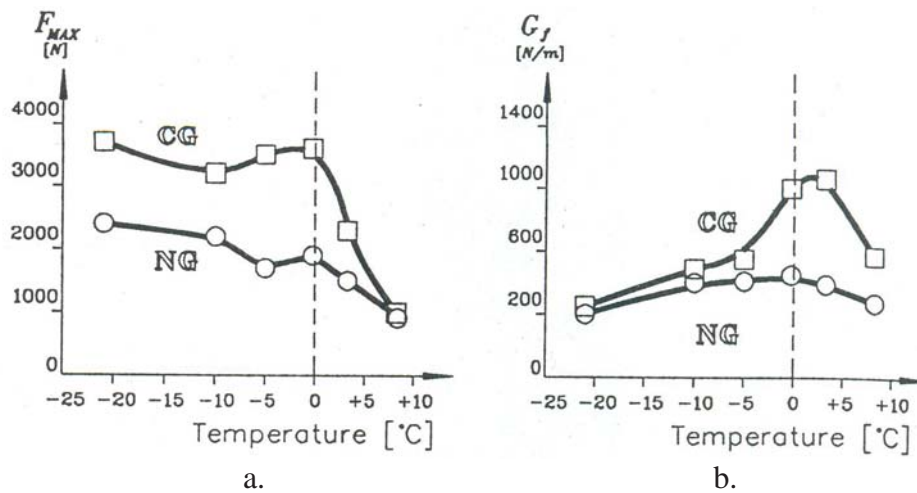


Figure 5.11 a. Maximum splitting force F_{max} versus test temperature
b. Specific fracture energy G_f versus test temperature

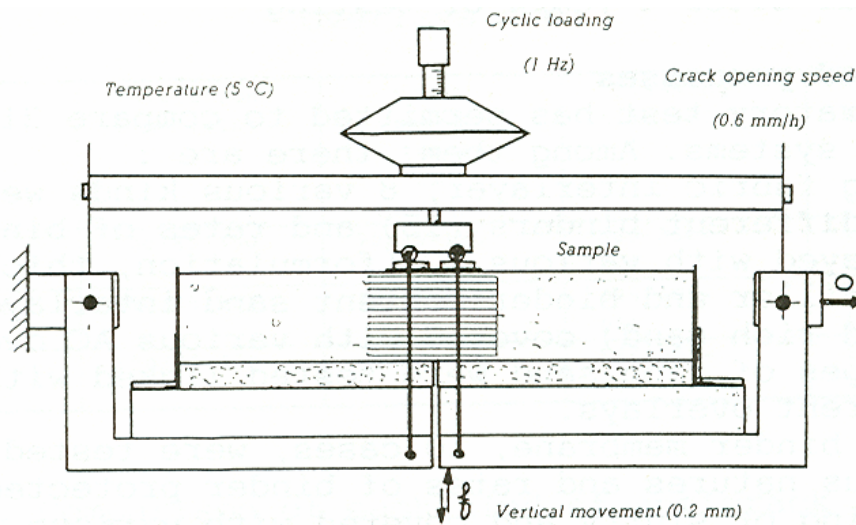


Figure 12 Shrinkage-bending test device for reflective cracking resistance

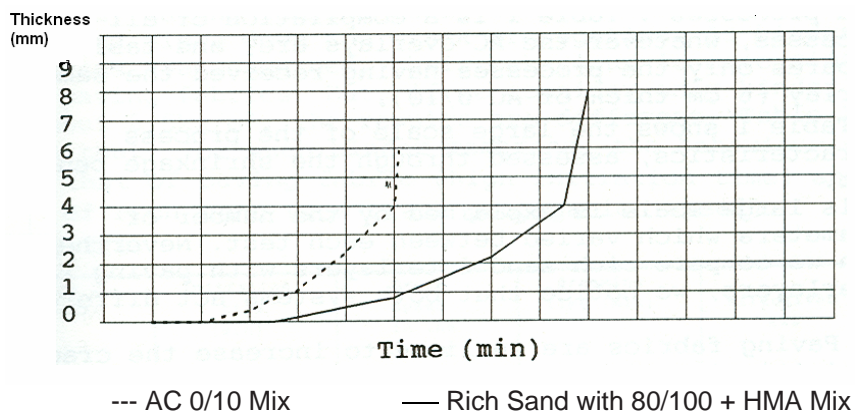


Figure 5.13 Test results example for shrinkage-bending test device

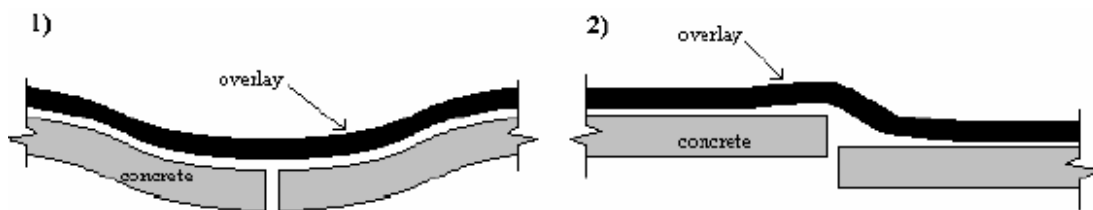


Figure 5.14 Mechanism of cracking of overlay

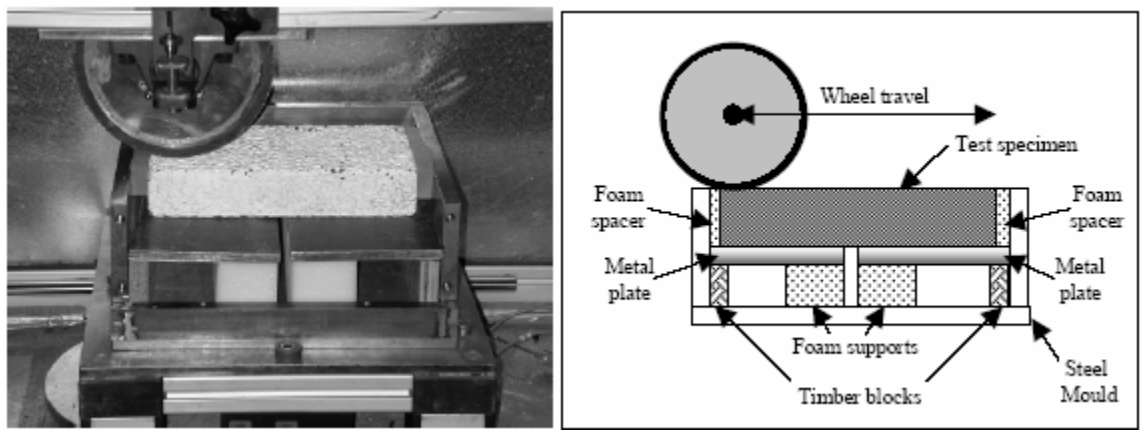


Figure 5.15 Test set-up for bottom-up cracking tests

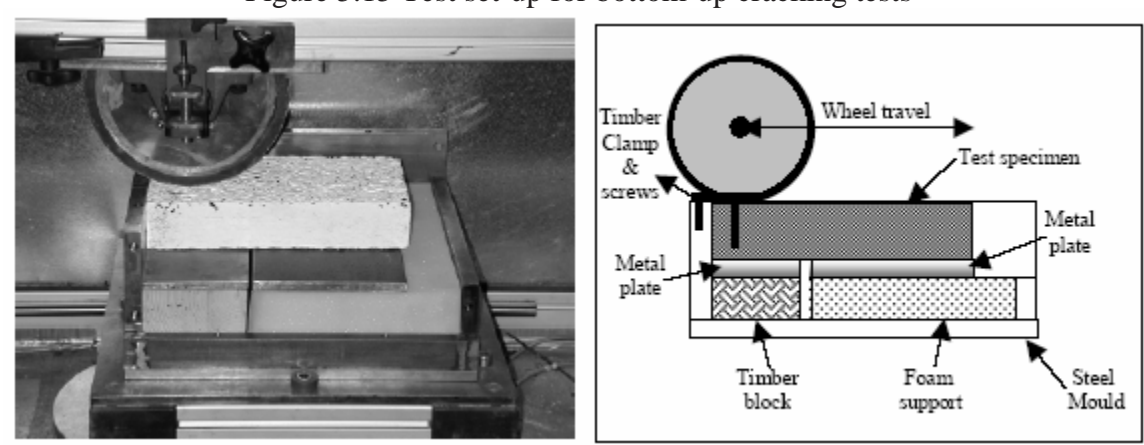


Figure 5.16 Test set-up for top-down cracking tests

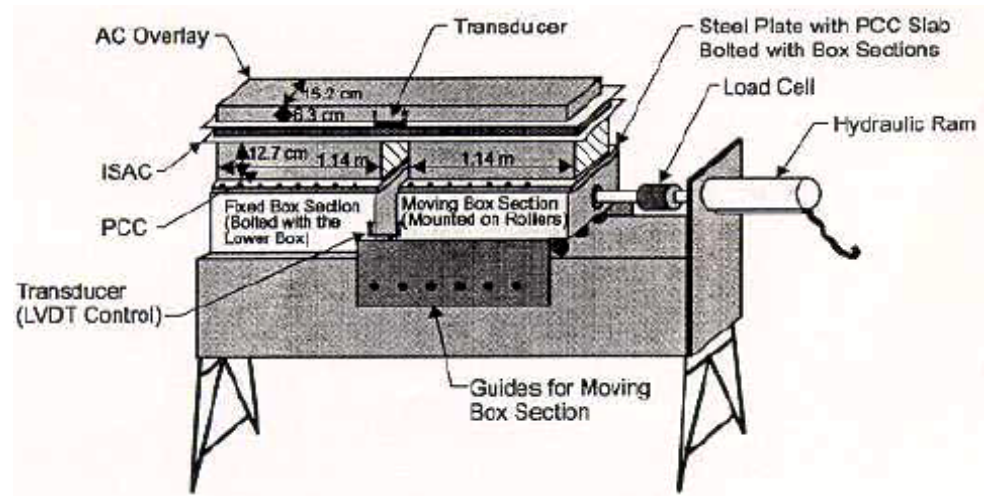


Figure 5.17 Testing equipment for ISAC system

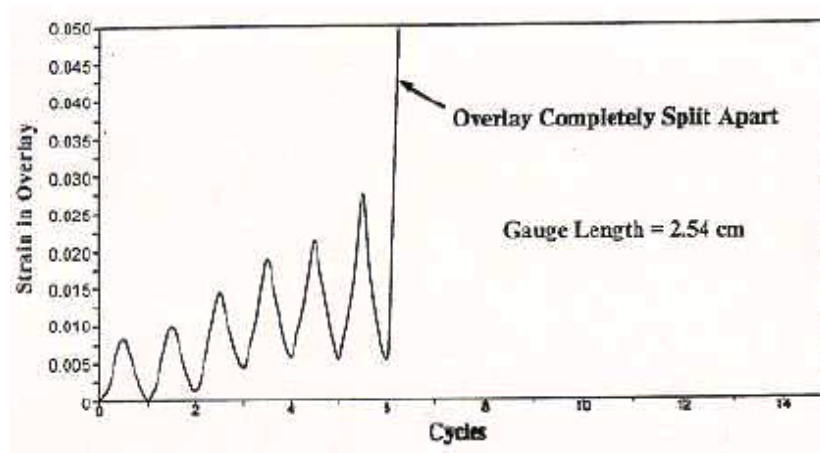


Figure 5.18 Strain in HMA overlay as function of test cycles – control section

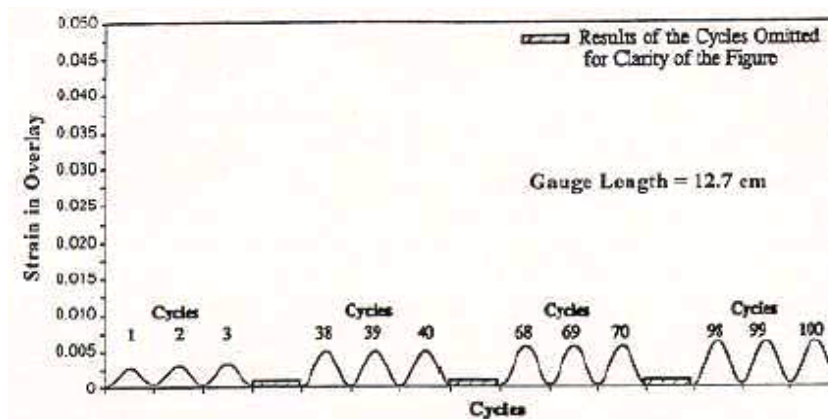


Figure 5.19 Strain in HMA overlay as function of test cycles – ISAC section

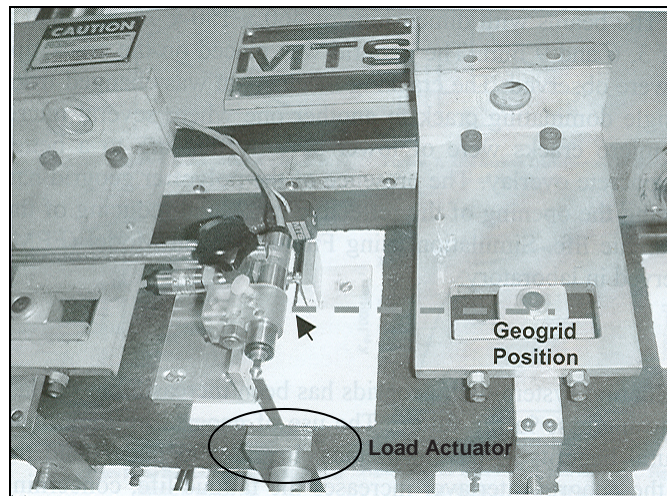
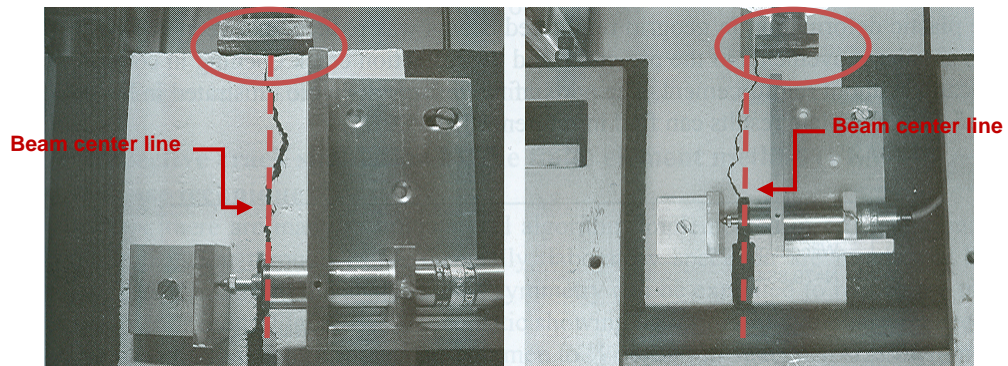


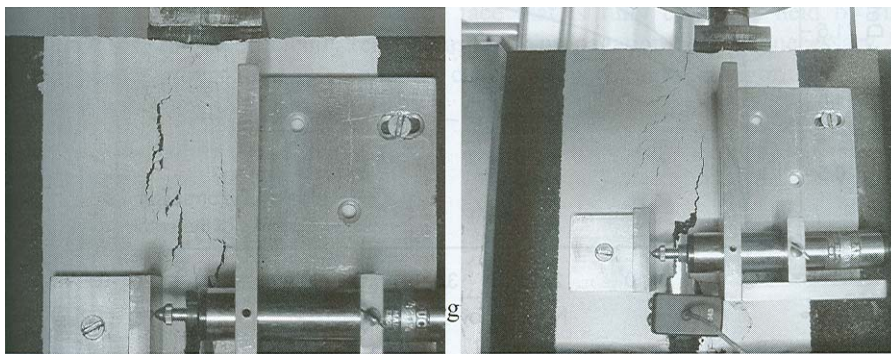
Figure 5.20 Instrumentation of fatigue test



a. Bending mode

b. Shearing mode

Figure 5.21 Cracking pattern at the end of test – beam without geogrid



a. Bending mode

b. Shearing mode

Figure 5.22 Cracking pattern at the end of test – beam with geogrid

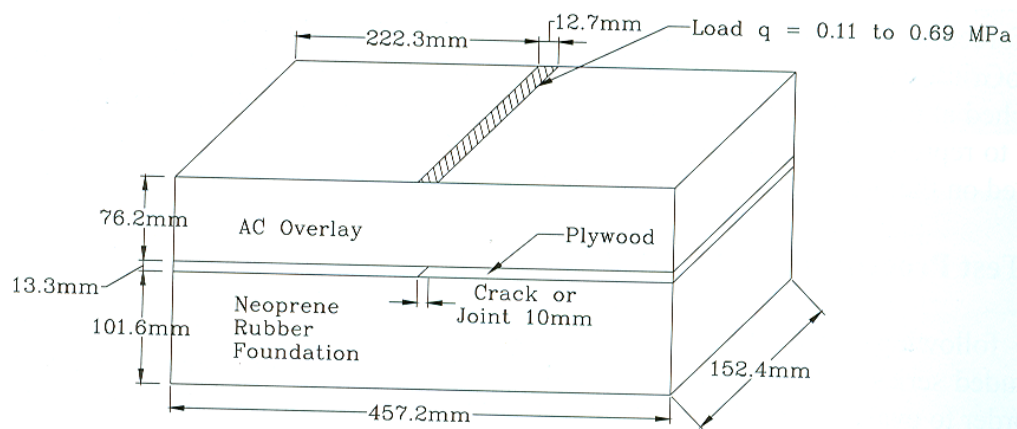


Figure 5.23 Schematic representation of the test setup

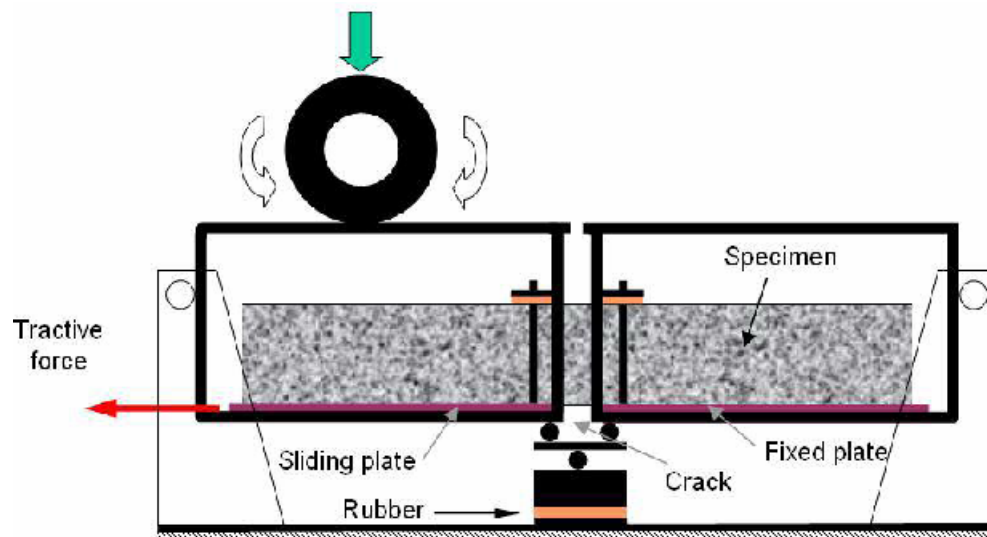


Figure 5.24 Schematic representation of WRC test



Figure 5.25 Wheel Reflective Cracking (WRC) equipment

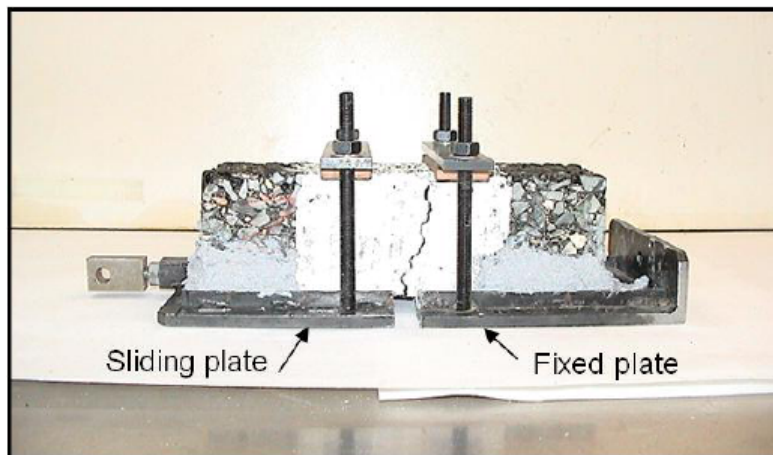


Figure 5.26 Wheel Reflective Cracking device test specimen in plates of adherence

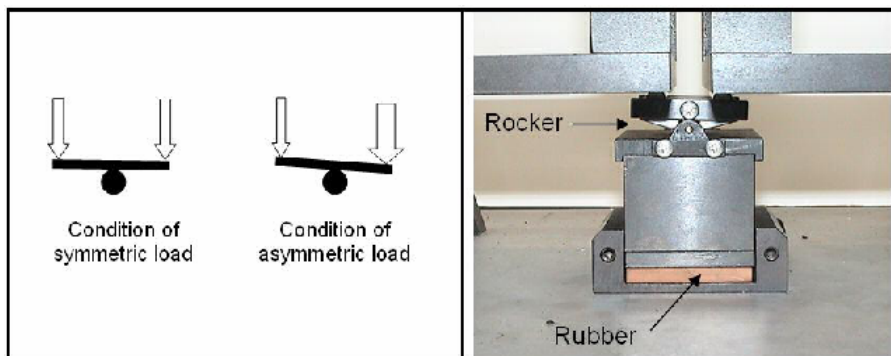


Figure 5.27 Mechanism simulating the relative vertical movement in the WRC

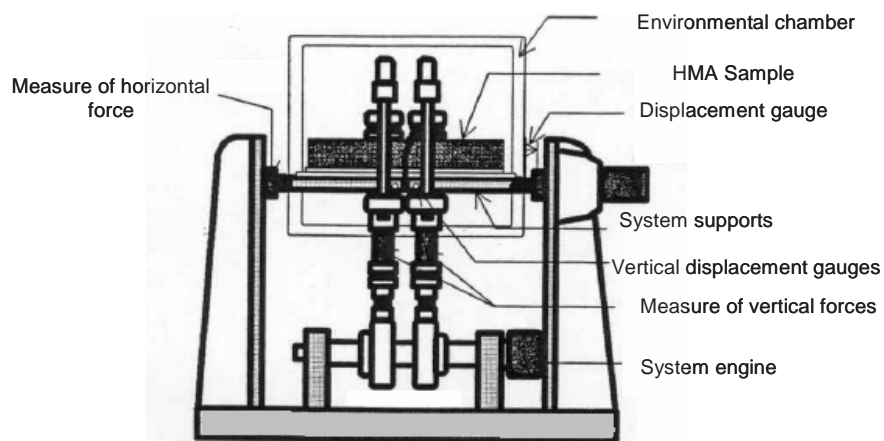


Figure 5.28 General scheme of the MEFISTO device

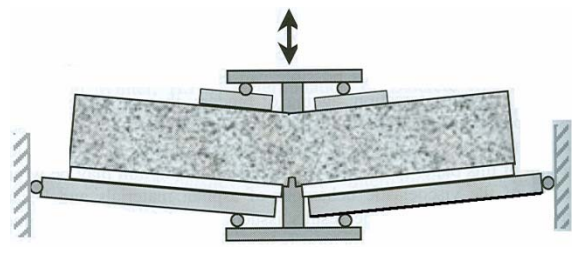


Figure 5.29 Schematic of MEFISTO device and testing sample (one column)

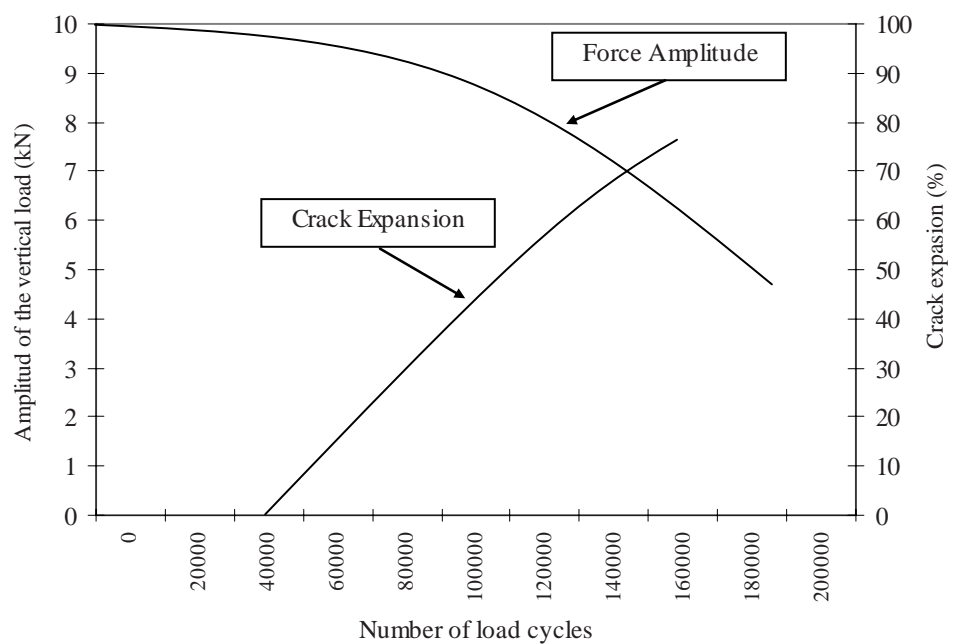


Figure 5.30 Typical test results from the MEFISTO device

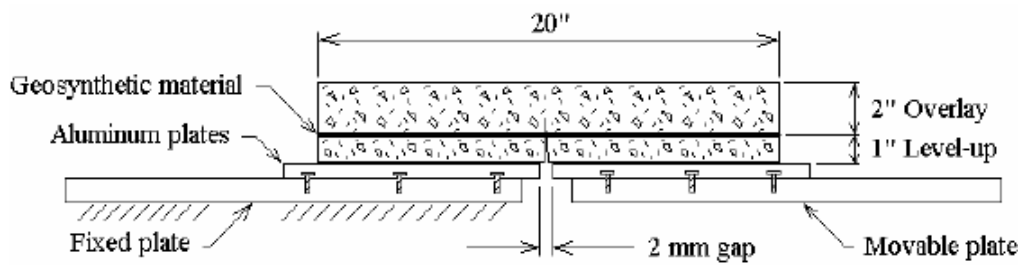


Figure 5.31 Concept of TTI overlay tester (after Cleveland et al. (68))

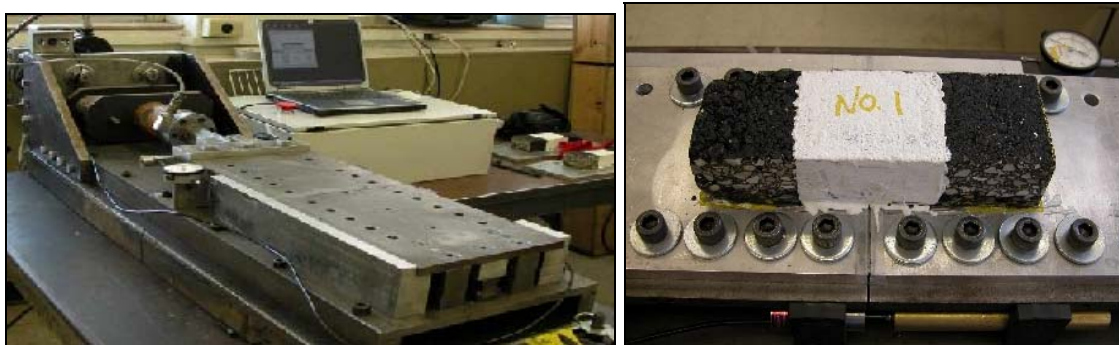


Figure 5.32 Upgraded TTI overlay tester

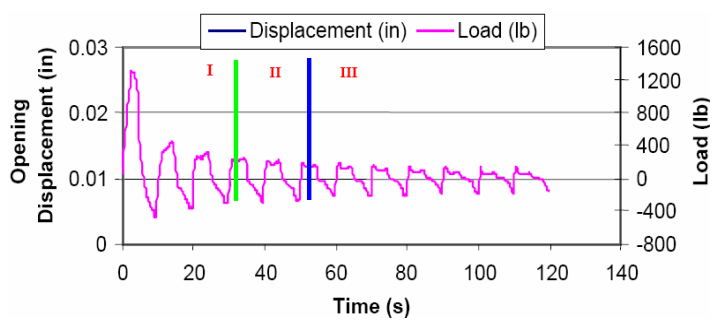


Figure 5.33 Typical TTI overlay tester result (each opening and closing is 10 sec.)



Figure 5.34 Upgraded overlay tester SGC sample

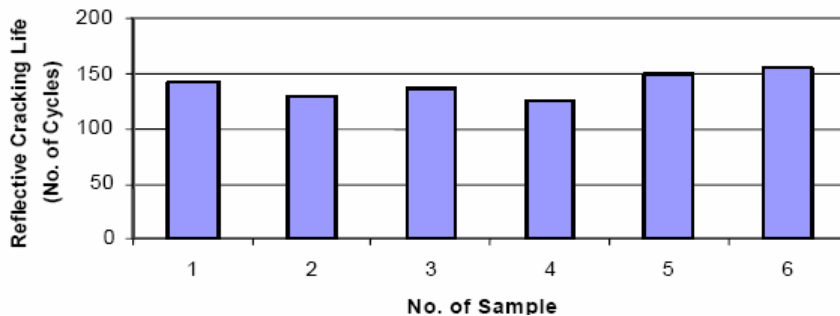


Figure 5.35 Repeatability of overlay testing on TxDOT type D mixture.

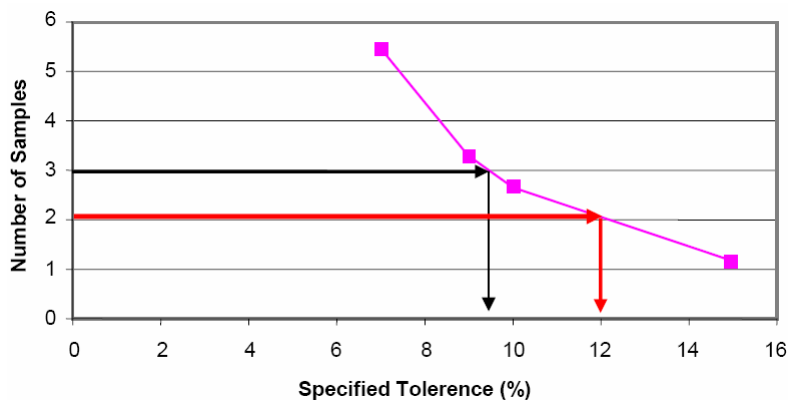


Figure 5.36 Relationship between number of specimens and specified tolerance of reflective cracking life for TxDOT type D mixture

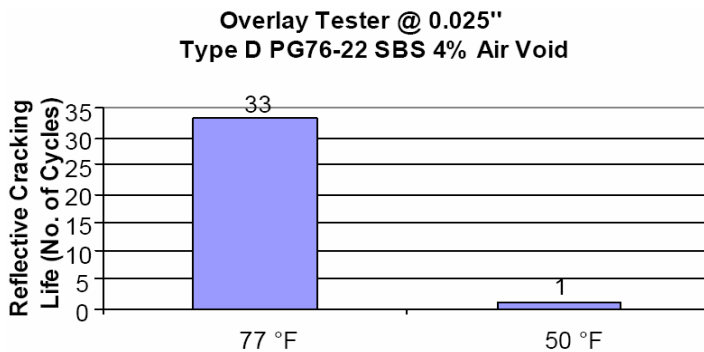


Figure 5.37 Influence of temperature on reflective cracking life

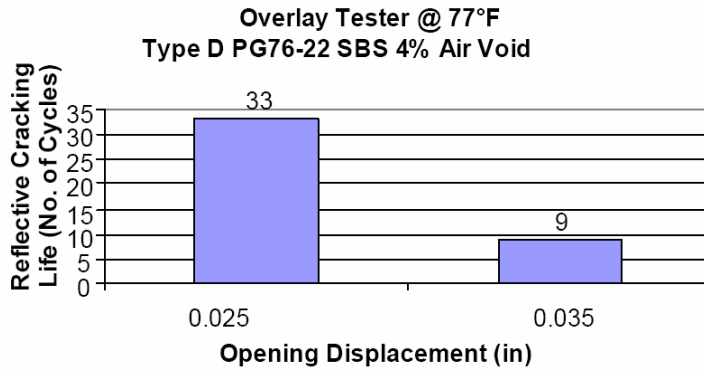


Figure 5.38 Influence of opening displacement on reflective cracking life

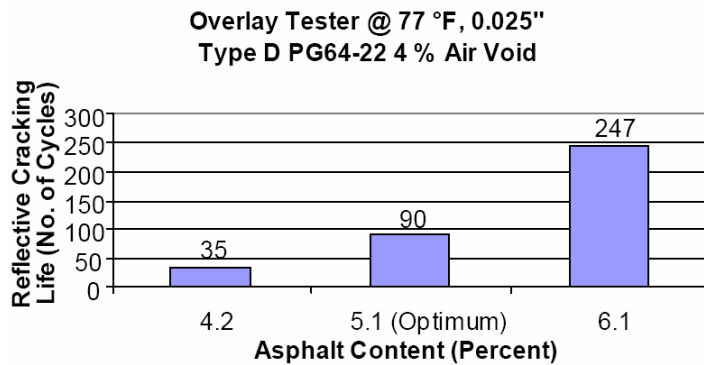


Figure 5.39 Influence of asphalt content on reflective cracking life

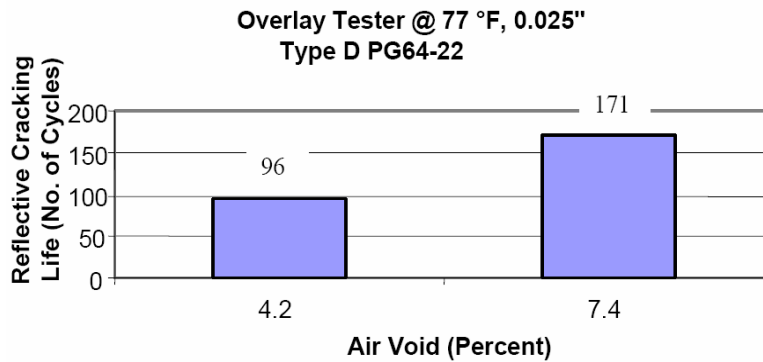


Figure 5.40 Influence of air voids on reflective cracking life



Figure 5.41 UFRGS-DAER traffic simulator from Brazil

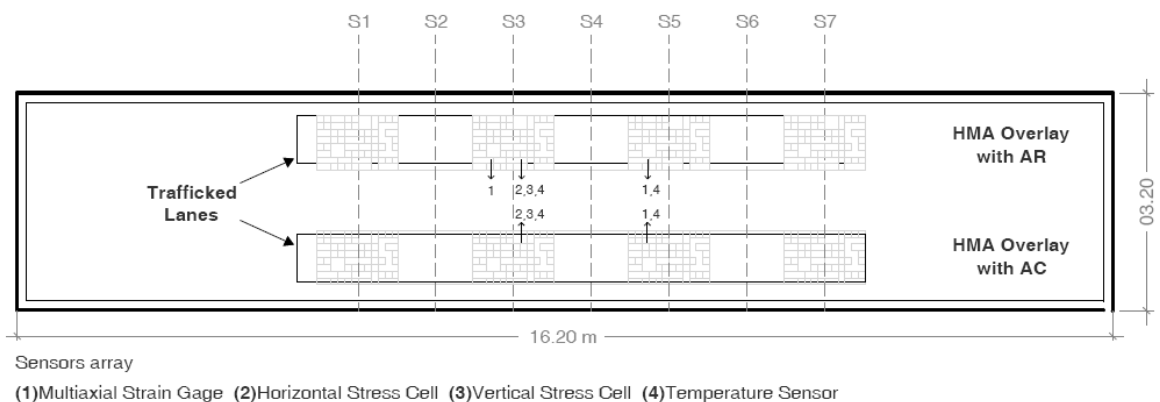


Figure 5.42 Test pavement showing cracked areas and instrumentation location

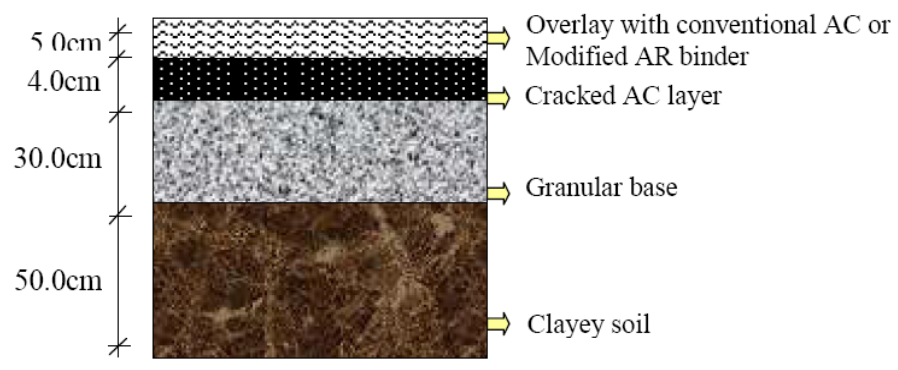


Figure 5.43 Test pavement sections

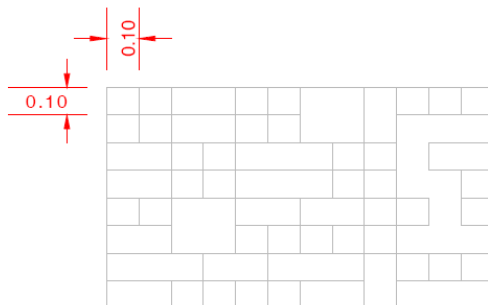


Figure 5.44 Failed HMA layer cracking pattern



Figure 5.45 Transverse cracks painted in different colors according to their appearance

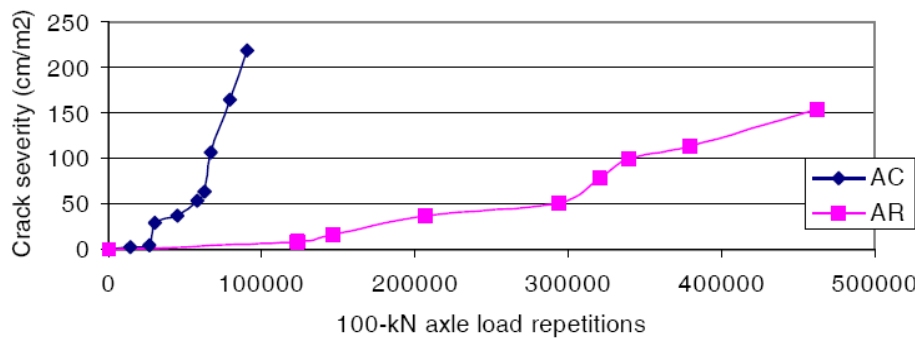


Figure 5.46 Cracking severity index evolution in both overlays

APPENDICES

APPENDIX A – Summary of Various Studies to Mitigate Reflective Cracking

Study Title	Researchers/Agency	Reference	Year	Evaluated Techniques	Findings
The History, Development, and Performance of Asphalt Rubber at ADOT	Scofield, L. A./Arizona DOT	5	1989	Asphalt rubber (AR)	AR has successfully been used as an encapsulating membrane to control pavement distortion due to expansive soils and to reduce reflective cracking in overlays on both rigid and flexible pavements.
Flagstaff I-40 Asphalt-Rubber Overlay-Nine Years of success	Way, G. B./ Arizona DOT	6	1999	Asphalt rubber (AR)	After 9 years of service, overlay was still nearly crack-free, with good ride, virtually no rutting or maintenance, and good skid resistance.
Paving Fabrics for Reducing Reflective Cracking	Rahman, M., Scofield, L., and Wolf, T/ Arizona Transportation Research Center	9	1989	Paving fabrics	Need for proper tack coat selection Caution regarding the use of Glassgrid on rough surfaces.
Potential Applications of Paving Fabrics to Reduce Reflective Cracking	Amini, F/ Jackson State University	10	2005	Paving fabrics	Proper installation procedures are critical for optimum performance. Field performance of overlays using fabric interlayers has generally been successful. Most effective in warm climates-southern states.
Inhibiting Reflective Cracking and Use of Fabrics to Inhibit Reflective Cracking in Porous	Woodside, A. R., McIlhagger, R., Woodward, W. D. H., and Clements, H. W./ Arizona University	11/12	1996/ 1997	Paving fabrics Stress absorbing membrane interlayer (SAMI).	Fabric structure and rate of spray of emulsion tack-coat had the most significant effect in the bitumen/fabric bond strength. SAMIs can reduce the likelihood of damage and the need for large reconstruction work. Extend pavement fatigue life.

Study Title	Researchers/Agency	Reference	Year	Evaluated Techniques	Findings
Asphalt					
Use of Paving Fabric Test Installations in California	Predoehl, N. H./ Caltrans	13	1989	HMA overlays	4.8 inches of overlay is required to reduce reflective cracking for 10 years.
Fiberglass Mesh Reduces Reflective Cracking on California Highway	Banasiak, D./ Caltrans	14	1997	Glassgrids + 7 inch HMA overlay	After 3 years, glassgrid reinforced the HMA overlay and retarded reflective cracking in an area of high tensile stress.
Report on Performance of Fabrics in Asphalt Overlays	FHWA	15	1982	Paving fabrics in HMA overlays	Fabric section (1.5 inch AC overlay + fabric) developed less than 2% reflection cracking in 1.25 years and 30% within 3.25 years while control section developed 10% cracking in 1.25 years and 50% within 3.25 years.
Reducing Reflective Cracking in Asphalt Pavements	Shuler, S., and Hermelink, D./Colorado State University	16	2004	Geotextile 90 lb Geotextile 120 lb Reinforcing fabric Fiberglass tape Crack sealer type ASTM D 3405 with routing original cracks Crack sealer type ASTM D 3405 without routing original cracks Crack sealer type ASTM D 3405 polymer modified	No treatments performed better than the control (HMA over milled surface directly) in the passing lane. Geotextile, paving fabric and crack sealer polymer modified ASTM D3405 performed better than control to reduce reflective cracking.
Overlays for Plain Jointed Concrete Pavements and Treatments for Reduction of Reflective Cracking of Asphalt	Gulden, W., and Brown, D/ Georgia DOT	17/18	1984/ 1985	HMA overlays over deteriorated PCC	20% of cracking area occurred in 6 years for a 6-inch HMA overlay compared to 2 years for a 4-inch HMA overlay. Reflective cracking appeared almost immediately after construction for a 2-inch overlay.

Study Title	Researchers/Agency	Reference	Year	Evaluated Techniques	Findings
Overlays on Jointed-Concrete Pavements in Georgia					
Georgia's Experience with Crumb Rubber in Hot-Mix Asphalt	Brown, D. R., Jared, D., Jones, C., and Watson, D./ Georgia DOT	19	1997	Crumb rubber mix (CRM)	After 4 years the section showed a large amount of transverse reflective cracking. Compared with the control mix, the CRM did not reduce rutting and was more than twice as expensive to place.
An Evaluation of Engineering Fabric in Pavement Rehabilitation (IHD-21)	Mascunana, I/ Illinois DOT	20	1981	Paving fabrics Fabricated interlayer membrane Asphalt rubber membrane interlayer	Treatments not effective in preventing the development of transverse reflective cracking on overlays with cement treated bases but longitudinal reflective cracking. Treatments effective in reducing transverse and longitudinal reflective cracking on overlays with bituminous base courses.
Evaluation of Reflective Crack Control Policy	Buttlar, W. G., Bozkurt, D. and Dempsey, B. J/ Illinois Transportation Research Center	21	1999	Non-woven paving fabrics	Performance monitoring indicated an increase in life spans by 1.1 and 3.6 years for paving fabric strip.
An Evaluation of Interlayer Stress Absorbing Composite (ISAC) Reflective Crack Relief System	Vespa, J./ Illinois DOT	22	2000	Interlayer Stress Absorbing Composite (ISAC)	The formation of reflective cracks and the subsequent deterioration of these cracks were delayed at ISAC treated joints and cracks.
Application of Cracking and Seating and	Jiang, Y., and McDaniel, R. S./Indiana DOT	23	1993	Cracking and seating before overlay Fiber reinforcement of the overlay mixture	Cracking and seating was successful to delay most of the reflected cracks for 5 years. The use of fibers in the overlay mixture further reduced

Study Title	Researchers/Agency	Reference	Year	Evaluated Techniques	Findings
Use of Fibers to Control Reflective Cracking					transverse cracks on cracked and seated sections.
Stone Interlayer Pavement Design	Rasoulia, M., Becnel, B., and Keel, G./ Louisiana DOT	24	2000	Stone interlayer or inverted pavement	Stone interlayer had significantly reduced the amount of reflective cracking. The life of the stone interlayer pavement system is increased to almost 5 times that of the standard soil cement pavement.
Glasgrid Pavement Reinforcement System. "System Overview	Tensar International Corporation	25	1994	Glassgrid	GlasGrid System showed benefits in retarding reflective cracking.
Field Evaluation of Experimental Fabrics to Prevent Reflective Cracking in Bituminous Resurfacing	V.T. Barnhart/Michigan Transportation Commission	27	1989	Paving fabric/rubberized asphalt composite membrane	Pavements with the Petrotac interlayer show considerably less recurrence of reflective cracking.
Paving Fabric and Asphalt Stress Absorbing Membrane Interlayers (SAMI)	Kidd, S. Q./ Mississippi DOT	28	1990	Paving fabrics Asphalt rubber interlayer system Single bituminous surface treatment	Asphalt rubber interlayer, in combination with a thin overlay (about 1 ½ inch), reduced and/or delayed reflective cracking over a lengthy period of time (about 5 years).
Field Performance of Fabrics and Fibers to Retard	Maurer, D. A. and Malashekie G. J./ Pennsylvania DOT	29	1989	Paving fabrics Fiber Pave reinforced asphalt membrane interlayer Bonifiber reinforced asphalt concrete	All treatments retarded cracks over the evaluation period, although the amount and rate of reduction varied.

Study Title	Researchers/Agency	Reference	Year	Evaluated Techniques	Findings
Reflective Cracking					
Geogrid Mesh for Reflective Crack Control in Bituminous Overlays	Hughes, J. J., and Somers, E./ Pennsylvania DOT	30	2000	Fabric/geogrid	None of the 3 paving fabric/geogrid types were found to be effective in preventing or retarding reflective cracking.
Experience with Cold In-Place Recycling as a Reflective Crack Control Technique: Twenty Years Later	Morian, D. A., Oswald, J., and Deodhar A./ Pennsylvania DOT	31	2004	Cold in-place recycling (CIR)	CIR provided resistance against reflective cracking between 2 and 3 times that exhibited by conventionally resurfaced control sections. The cost of CIR is one to two-thirds the cost of conventional HMA material while providing superior performance.
Geosynthetics in Flexible and Rigid Pavement Overlay Systems to Reduce Reflection Cracking	Cleveland G. S., Button J. W., and Lytton R./ Texas Transportation Institute	32	2002	Geosynthetics	Performance of geosynthetics in addressing reflection cracking in HMA overlays has ranged from highly successful to disastrous failures.
Fiberglass Pavement Reinforcement Used in Dissimilar Climatic Zones for Retarding Reflective Cracking in Asphalt	Darling, J.R., and Woolstencroft, J.H./Saint-Gobain Technical Fabrics, Canada	33	2004	Fiberglass	Fiberglass reinforcements are extremely strong and experience low elongations at ultimate strength and are able to reduce the rate of crack reflections significantly to that of non-reinforced overlay.

Study Title	Researchers/Agency	Reference	Year	Evaluated Techniques	Findings
Overlays					
Lessons Learned on Jointed Concrete Pavement Rehabilitation Strategies in Texas	Chen, D. H., Scullion, T., and Bilyeu, J./Texas DOT	34	2006	Crack-retarding grid Crack-retarding asphalt material Flexible base overlay with thin asphalt surfacing Arkansas open graded large stone AC interlayer	Crack-retarding grid (plastic geosynthetics) did not perform well in retarding reflective cracks. Crack-retarding asphalt material (Strata) performed well over 2 years of monitoring. Flexible base overlay with thin asphalt surfacing performed well. Arkansas open graded large stone AC interlayer mix performed well.
Evaluation of Concrete Slab Fracturing Techniques in Mitigating Reflective Cracking Through Asphalt Overlays	Freeman, T. E/Virginia Transportation Research Council	35	2002	Concrete slab fracturing	Fracturing and seating distressed concrete pavements effective in retarding the formation of reflective cracking through asphalt overlays on jointed plain concrete pavements. Fracturing technique was somewhat less successful in reinforced concrete pavements. Formation of reflective cracks appeared to be delayed for only about 3 years.
GlassGrid Pavement Reinforcement Product Evaluation	Bischoff, D., and Toepel, A/Wisconsin DOT	36	2003	GlasGrid Glass fiber mesh	Both products performed unsatisfactorily and were unable to prohibit or control reflective cracking effectively.
Evaluation of the Interlayer Stress-Absorbing Composite (ISAC) to Mitigate Reflective Cracking in Asphaltic Concrete Overlays	Abu Al-eis, K/Wisconsin DOT	37	2004	Interlayer Stress-Absorbing Composite (ISAC)	Due to the transverse bumps in the overlay, the overlay and the ISAC fabric were removed and the test section was repaved without the ISAC

Study Title	Researchers/Agency	Reference	Year	Evaluated Techniques	Findings
Wisconsin Experiences with Reflective Crack Relief Projects	Makowski, L., Bischoff, D., Blankenship, P., Sobczak, D., and Haulter F/Wisconsin DOT	38	2005	Modified asphalt mix interlayer	In one project, interlayer showed no impact on delaying reflection cracking within the first 3 years. Other projects showed an average 42% improvement in the time to the appearance of surface cracks compared with the control sections.
Long Term Performance on Site of Interface Systems	Vanelstraete A., and De Visscher J./Belgium Road Research Center, Belgium	39	2004	2 SAMI 3 Non-woven fabric 4 Geogrid 5 Steel nettings	6 Crack and seat and steel reinforcing nettings are both effective against reflective cracking. 7 Less reflective cracks were developed on sections with interface systems (SAMI, non-woven, grid, steel reinforcing nettings). 8 Projects with steel reinforcing nettings performed very well even after more than 10 years of repair.
Life Cycle Cost Analysis of Mitigating Pavement Rehabilitation Reflection Cracking	Tighe, S., Haas, R., and Ponniah, J./University of Waterloo, Canada	40	2003	9 Routing and sealing	10 Proper and timely crack treatment (routing and sealing) can result in extending life by 2 years and cost savings in the order of \$7,000/lane-km.
Field Study of Repair Methods for Transversal Cracks	Valtonen, J., and Hyyppa, I./Helsinki University of Technology, Finland	41	2004	Milling the form of a box, 1.5 m wide grid, leveling the old surface, hot milling and asphalt surfacing. Milling the form of a box, 0.75 m wide grid, leveling the old surface, hot milling and asphalt surfacing. Sawing a crack, filling the crack with hot modified bitumen, leveling the old surface, hot milling and asphalt surfacing. Sawing a crack, filling the crack with a band of modified bitumen, leveling the old surface, hot milling and asphalt surfacing. Hot milling, apply 1.5 m wide grid, and asphalt surfacing. Hot milling, apply 0.75 m wide grid, and asphalt surfacing.	After one year, traditional methods (crack filling and HMA overlay or mill and HMA overlay) were not successful. The best promising method to prevent the reflection of transverse cracks is to lay a grid on a "milled box.

Study Title	Researchers/Agency	Reference	Year	Evaluated Techniques	Findings
				Hot milling and asphalt surfacing.	

APPENDIX B – DOTs Standard Specifications for Highway Construction

Agency	Std Specs for Highway Construction Edition	Reflective Cracking Control System	Description
Alabama	2006	Geotextiles	Stress relieving membrane within pavement structure Used as strips over transverse or longitudinal joints Cracks exceeding 1/8" in width shall be filled with a rubberized joint sealer meeting the requirements of ASTM D 6690, for Type II sealant. Potholes shall be properly repaired as directed by Engineer.
Alaska	2004	Paving fabrics	Fill all potholes and cracks wider than 1/4 inch with an approved asphalt emulsion and sand slurry. Overlap transverse joints in the direction of paving. Apply 0.20 gallons/yd ² of additional asphalt sealant beneath all fabric joints.
Arizona	2000	Asphalt rubber stress absorbing membrane Crack sealing Joint sealing	Cover material shall be precoated with 0.40 to 0.60% AC by weight of aggregate. The AC shall meet the requirements of Section 1005. The end result shall be a dust-free material. Crack sealing: a. mixture of asphalt and 100% vulcanized granulated rubber. b. Premixed block material consisting of asphalt and 100% vulcanized granulated rubber. Joint sealant: a. mixture of asphalt and 100% vulcanized granulated rubber. b. mixture of asphalt, extender oil, and reclaimed high natural and ground vulcanized rubber. c. Premixed block material consisting of asphalt and 100% vulcanized rubber. d. Premixed block material consisting of asphalt and extender oil, reclaimed high natural and ground vulcanized rubber.
Arkansas	2003	NA	NA
California	2006	Reinforcing fabric	Shall be 100% polypropylene staple fiber fabric material, needle-punched, thermally bonded on one side
Colorado	2006	Joint and crack sealant Geosynthetics	Joint and crack sealant: fill cracks with a width greater than 1/8" and less than 1". Cracks shall be cleaned of loose and foreign matter to a depth approximately twice the crack width before applying hot poured sealant. Pavement surface shall be broomed clean immediately prior to beginning the crack reduction geotextile treatment using a self-propelled power broom. AC binder shall be applied to pavement surface at the rate of approximately 0.25 gallon/yd ² . Geosynthetic rolls shall be furnished with suitable wrapping to protect against moisture and extended ultraviolet exposure prior to placement.
Connecticut	2005	NA	NA

Agency	Std Specs for Highway Construction Edition	Reflective Cracking Control System	Description
Delaware	2005	NA	NA
District of Columbia	2005	Replace of bituminous materials and base	Removing and replacing the binder and surface courses in defective areas by: a. Cutting defective areas, b. Repair of cuts, c. Cutting to a neat line: The perimeter of all cuts and/or defective area repairs in asphalt roadways, alleys, sidewalks, gutters and other miscellaneous pavements which become part of the permanent roadway surface shall be cut to a neat line by means of power saw, and d. Compaction of bituminous materials to the specified compaction.
Florida	2005	Asphalt rubber membrane interlayer	Constructing an asphalt rubber membrane interlayer composed of a separate application of asphalt rubber binder covered with a single application of aggregate. Use Asphalt Rubber Binder ARB-20. Cover Material: Use Size No. 6 stone, slag, or gravel. Combine the materials as rapidly as possible for such a time and at such a temperature that the consistency of the binder approaches that of a semi-fluid material.
Georgia	2006	Asphalt rubber joint and crack seal Hot Asphalt-Rubber Seal Treatment for Stress-Relieving Interlayer Geogrid reinforcement Pavement reinforcement fabric	Filling (Type M) or sealing (Type S) joints and cracks in existing pavements with rubber asphalt mixtures. A polymer-modified asphalt rubber (PMAR) blend may be used in lieu of both Type M and Type S. The mixture pours readily and penetrates a 1/4" pavement joint or crack to a depth of at least 1". For Hot Asphalt-Rubber Seal Treatment for Stress-Relieving Interlayer follow specifications as included in the contract. For geogrid reinforcement follow specifications as included in the contract. Pavement reinforcement fabric properties: a. non-woven, heat-resistant material composed of polypropylene or polyester fibers, b. Can be saturated with asphalt cement, c. Can be placed smooth with mechanical devices and be without wrinkles, d. Can withstand the heat of asphaltic concrete mixes during paving operations, d. Can withstand normal field handling and construction operations without damage.
Hawaii	2006	Paving fabric	Surface Preparation: clean surface before applying AC, and cracks and joints with compressed air. Seal cracks and joints wider than 3/8" with sand slurry consisting of 20% CSS-1 emulsified asphalt, approximately 2% portland cement, and water. Clean potholes and other surface defects and fill with HMA pavement. Apply AC to cover area of paving fabric plus 3" on each side. Place fabric onto AC before it has cooled and lost its tackiness, with heat-bonded side up and minimum wrinkling/folding. Overlap fabric 6" at joints.
Idaho	2004	Geotextile	Shall be composed only of long chain polymeric filaments or yarns oriented into a stable network, which retains its relative structure, including selvages, during handling, placement, and design service life.

Agency	Std Specs for Highway Construction Edition	Reflective Cracking Control System	Description
			Only nonwoven geotextiles are acceptable
Illinois	2002	Reflective cracking control treatment	<p>Surface on which reflective crack control system is to be constructed shall be clean and dry. All base failures shall be repaired and all cracks, spalls, potholes or other depressions shall be sealed with an approved crack sealer or filled with mixture for cracks, joints and flange ways.</p> <p>Area reflective crack control treatment System A: area to be covered with fabric shall be sprayed uniformly with asphalt binder at a rate of 0.25 to 0.30 gal/yd² as directed by Engineer. Binder application shall be accomplished with a pressure distributor for all surfaces except, where the distributor does not have room to operate, hand spraying will be allowed.</p> <p>Area reflective crack control treatment System B: primer to be used with the waterproofing membrane shall be supplied by the manufacturer of the membrane and shall be compatible with the membrane.</p> <p>Area reflective crack control treatment System C: immediately prior to application of a tack coat, the surface shall be thoroughly cleaned by sweeping. When placed as a strip treatment, the strip shall be 24" wide. Also when placed as a strip treatment, a self-propelled distributor will not be required for applying the tack coat nor the asphalt-rubber, nor will a self-propelled spreader be required to place the cover aggregate.</p>
Indiana	2006	Seal cracking and joints	Sealing longitudinal and transverse cracks and joints in existing asphalt pavement. The steps to do that are: a. Routing and Filling Cracks and Joints, b. Sealing Cracks and Joints Cracks and joints shall be cleaned by blowing with compressed air or by other suitable means. Asphalt material shall be placed utilizing a "V" shaped wand tip. The cracks and joints shall be completely filled or over banded not to exceed 5".
Iowa	2006	Asphaltic overlay fabric	<p>Fabric placed under asphalt mixtures to provide waterproofing and delay reflective cracking. Shall be capable of withstanding installation stresses and shall not be damaged by temperatures common to asphalt mixtures</p> <p>Asphalt absorption shall be sufficient to produce good bond between overlay and overlaid surface when a tack coat of 0.20 to 0.25 gallon/yd² is used.</p>
Kansas	1990	NA	NA
Kentucky	2004	NA	NA
Louisiana	2004	Asphaltic surface treatment Paving fabric	Asphaltic surface treatment consist of a specified emulsion applied "cold" or modified asphalt material applied "hot", at the temperature range specified. Paving fabric shall conform to requirements in AASHTO M 288.
Maine	2002	Geotextiles	Shall have property values expressed as Minimum Average Roll Value (MARV) in

Agency	Std Specs for Highway Construction Edition	Reflective Cracking Control System	Description
			the weakest principal direction, which meet or exceed given values. Sampling and conformance testing shall be in accordance with ASTM D4354. Geotextile product acceptance shall be based on ASTM D4759. Geotextile storage and handling requirements shall be based on ASTM D4873.
Maryland	2001	Filling cracks in HMA pavements	Cleaning and filling cracks 1/8 to 1-3/4" wide in HMA pavement as specified in the Contract Documents or as directed by the Engineer. Distressed areas shall be repaired. Cracks more than 1-3/4" wide; and map, edge or alligator cracks requiring major repairs are not included in Specification
Massachusetts	1995	NA	NA
Michigan	2003	NA	NA
Minnesota	2005	NA	NA
Mississippi	2004	Cleaning and sealing of cracks	Joints and cracks to be sealed shall be cleaned by routing, sawing and/or sand blasting to the minimum dimensions specified. Other cleaning methods shall be approved by Engineer. Surface which is to receive the new joint sealing material shall be dry and free of all lubricants, tar, asphalt, discoloration and stain as well as all other forms of contamination.
Missouri	2004	Bituminous cracking crack sealing	This work consists of preparing and sealing all working transverse and longitudinal cracks in bituminous pavement as shown on the plans or as directed by engineer. The sealant shall be a single-component material in accordance with AASHTO M 301, except as herein modified.
Montana	2006	NA	NA
Nebraska	2007	Fabric reinforcement Crack sealing bituminous surface	Fabric reinforcement shall be applied immediately before the placement of the bituminous overlay. The materials and application method shall resist shoving and lifting during placement of the bituminous overlay. Sealant shall be a mixture of paving grade asphalt, vulcanized recycled rubber, and polymer modifier
Nevada	2007	Engineering fabrics	Pavement Reinforcing Fabric manufactured from polyester, polypropylene, or polypropylene-nylon material. Fabric shall be nonwoven.
New Hampshire	2006	Hot poured crack sealing	Crack sealing material to be covered by a 1" or less overlay shall cure a minimum of 45 days prior to the placement of bituminous pavement. Material covered by an asphalt pavement overlay shall be low modulus conforming to ASTM D 3405, modified. All cracks greater than 1/8" up to 3/4" in width shall be shaped with a power router to a dimension of 3/4" + 1/8" wide by 5/8" deep rectangular shape and treated unless otherwise directed. Cracks greater than 3/4" shall be treated but not routed.

Agency	Std Specs for Highway Construction Edition	Reflective Cracking Control System	Description
New Jersey	2001	Sawing and sealing of joints	<p>Sawing and Sealing Joints in HMA Overlays. Existing transverse joints that are offset at the longitudinal joint by more than 1", measured between the centers of the joints, require separate saw cuts terminating at the longitudinal joint. Overlays shall be saw cut over transverse cracks that are reasonably straight, at least 1/8" wide, and extend one full lane width.</p> <p>For overlays whose total thickness is 2 inches or less, the saw cut shall be 3/8 to 1/2" wide by 5/8" deep. For overlays whose total thickness is greater than 2", the saw cut shall be a T-shaped cut consisting of the saw cut specified in Item a above plus a 1/8" wide saw cut at the center.</p>
New Mexico	2002	NA	NA
New York	2006	NA	NA
N. Carolina	2006	NA	NA
N. Dakota	2006	Geotextile fabric	<p>Shall be a fabric consisting of polymeric filament or yarns such as polypropylene, polyethylene, polyester, polyamide, or polyvinylidene chloride. The filaments or yarns shall be formed into a stable network so they retain their relative position to each other.</p>
Ohio	2005	Sawing and sealing of asphalt concrete pavement joints	<p>Saw cutting and sealing finished surface of the asphalt concrete pavement and shoulders directly over and in line with transverse joints in the underlying portland cement concrete pavement.</p>
Oklahoma	1999	Fabric reinforcement for asphalt concrete pavement	<p>Surface should be cleaned and free of any material.</p> <p>Binder should be placed at no less than 290°F and a rate of 0.5 gal/yd².</p> <p>Fabric should be placed after application of the bituminous binder.</p>
Oregon	1999	Crack sealing flexible pavements Geotextile	<p>All sealant materials for crack repair of flexible pavements shall be approved by the Engineer before being incorporated into the work.</p> <p>Clean all cracks designated for sealing of loose and foreign matter.</p> <p>Seal the cracks from the bottom up in a neat manner, so that upon completion of the work, the surface of the sealant material is flush to 3/16" below adjacent pavement surface.</p> <p>Geotextile can be use under an overlay and should follow the requirements of table 02320-1.</p>
Pennsylvania	1994	Fiberized asphalt membrane Polymer modified asphalt joint and cracking	<p>Fiberized asphalt membrane: cleaning and sealing of longitudinal and transverse joints and cracks in existing pavement surfaces with a fiberized asphalt membrane prior to overlaying. Provide membrane having a width of 5" + 1" on concrete and bituminous pavement surfaces.</p> <p>Polymer modified asphalt joint and cracking: cleaning and sealing of longitudinal</p>

Agency	Std Specs for Highway Construction Edition	Reflective Cracking Control System	Description
			and transverse joints and cracks in existing pavement surfaces with polymer modified asphalt prior to overlaying.
Rhode Island	1999	Cleaning, routing, and sealing cracks in bituminous concrete pavement	Cracks Less than 1" in width. Poured joint seal material shall be an asphalt rubber compound, hot poured type, conforming to the requirements of AASHTO M173 and approved by the Engineer. Cracks 1" and over in width, bituminous concrete, Class I-2.
South Carolina	2000	NA	NA
South Dakota	2004	Asphalt concrete crack sealing	Routing equipment shall be mechanical, power driven, and capable of cutting a reservoir to the required dimensions. Equipment designed to plow the cracks to dimension will not be permitted. Cracks which are less than 3/4" in width or depth will require routing to a width and depth of 3/4 to 7/8". Cracks which are 3/4" or greater in width and depth will not require routing, but shall be thoroughly cleaned of foreign material to a depth equal to the width of the crack.
Tennessee	2006	NA	NA
Texas	2004	Fabric underseal	Furnish and place fabric underseal in a longitudinal, full-road-width application or over pavement joints. Prepare the surface by cleaning off dirt, dust, or other debris. Apply asphalt binder immediately after asphalt binder application, align the fabric and broom or roll it in place. Overlap transverse joints by minimum of 6". Overlap longitudinal joints by a minimum of 4".
Utah	2002	NA	NA
Vermont	2001	Bituminous crack filling	This work shall consist of furnishing and placing sealing compound in cracks of existing bituminous concrete pavement. Cracks 1/4" and wider shall be shaped with a power router and flame cleaned of all dirt, foreign material, and loose edges to a minimum depth of 3/4". All cracks may be cleaned with a hot compressed air lance instead of routing, if approved by the Engineer.
Virginia	2006	NA	NA
Washington	2002	NA	NA
West Virginia	2000	NA	NA
Wisconsin	2006	NA	NA

Agency	Std Specs for Highway Construction Edition	Reflective Cracking Control System	Description
Wyoming	2003	Crack sealing Paving fabric	Crack sealing consist of: a. Removing of existing material, b. routing, c. cleaning/drying, d. Sealing. Paving fabric applies to fabric membranes used for full coverage of the pavement or as strips over transverse and longitudinal pavement joints

APPENDIX C – PC1 Values Along with Measured Surface Cracks of NDOT Projects

Table C1 PC1 Values 1-year Before Rehabilitation and 1-year After Treatment Construction for Flexible Pavements.

Contract	Project ID	Fatigue cracking		Transverse Cracking (ft)	Block cracking			PC1 at -1	PC1 at +1
		Type A (ft)	Type B (ft ²)		Type A (ft)	Type B (ft ²)	Type C (ft ²)		
2808a	CIR-A-1	300	0	20	100	0	0	0.841196	-0.7828
2808b	CIR-A-2	50	300	35	110	0	0	0.313319	-0.7828
2838	CIR-A-3	0	0	0	400	750	700	1.728775	-0.67827
2935	CIR-A-4	150	300	35	100	300	300	1.464507	-0.7828
2819	CIR-B-1	0	530	75	0	150	0	0.79174	-0.7828
2873	CIR-B-2	50	0	40	190	675	190	1.291939	-0.7828
2961	CIR-B-3	40	0	40	100	1000	1000	2.485455	-0.7828
3013	CIR-B-4	75	0	30	225	0	0	0.227509	-0.7828
3025a	CIR-C-1	10	50	25	0	0	0	-0.4243	-0.62601
3025b	CIR-C-2	35	150	35	125	300	110	0.639205	-0.52148
3025c	CIR-C-3	50	150	10	300	400	50	0.802542	-0.52148
2876	CIR-D-1	50	0	75	400	0	50	0.953418	-0.52148
2761	RF-1	25	100	70	1000	500	0	2.545001	-0.46921
2932	RF-2	25	100	100	0	0	0	0.477578	-0.7828
2980a	RF-3	25	100	30	0	150	10	-0.0425	-0.7828
2980b	RF-4	25	100	20	0	0	0	-0.35866	-0.7828
3006	RF-5	25	100	21	0	0	0	-0.34821	-0.7828
3008	RF-6	25	100	10	0	0	0	-0.46319	-0.7828
2723	SCR-1	120	445	60	210	210	0	1.477647	-0.7828
3031	SCR-2	75	75	50	500	0	0	0.991769	-0.7828
3048	SCR-3	50	0	55	0	0	0	-0.00065	-0.7828
3045	SCR-4	50	300	25	0	0	0	0.020147	-0.7828
3162	SCR-5	0	0	20	0	0	0	-0.57374	-0.7828
2384a	MOL-A-1	0	600	20	200	0	0	0.43801	-0.15926
2384b	MOL-A-2	100	325	42	60	0	0	0.535849	-0.7828
2432	MOL-B-1	110	0	75	0	0	0	0.457102	-0.7828
2505	MOL-B-2	0	600	0	400	0	1000	1.752618	-0.7828
2651a	MOL-C-1	0	300	0	300	0	300	0.420265	-0.7828
2651b	MOL-C-2	0	0	0	0	1000	1000	1.730051	-0.7828
2651c	MOL-C-3	100	0	95	200	1000	1000	3.48055	-0.7828
2679	MOL-C-4	0	0	15	0	0	0	-0.62601	-0.52148
3028	MOL-B-3	0	0	48	0	0	0	-0.28106	-0.7828
3070	MOL-C-5	35	50	35	325	375	0	0.840768	-0.7828

